Thirteenth Edition

Photovoltaics International

THE TECHNOLOGY RESOURCE FOR PV PROFESSIONALS

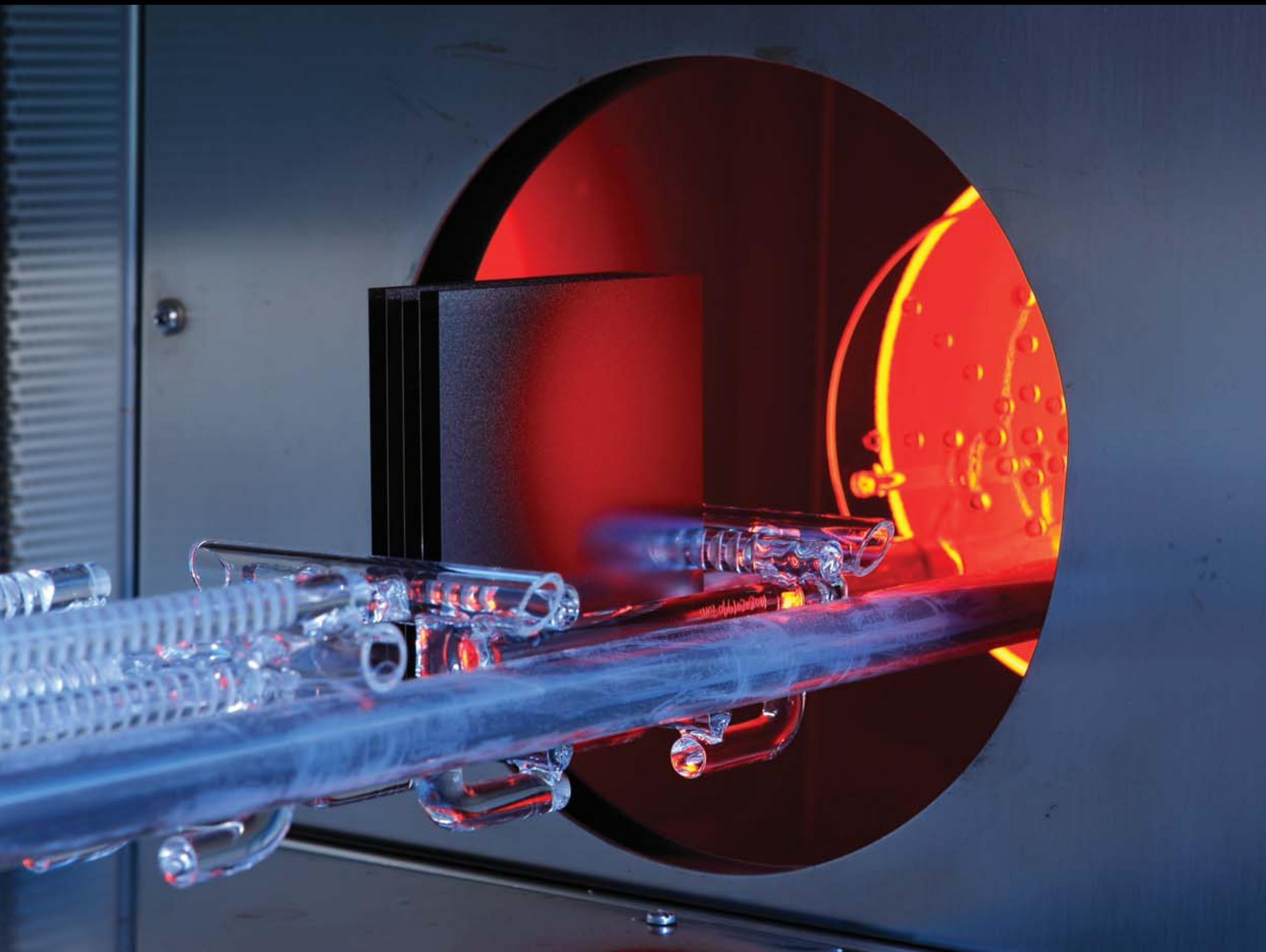

Wafering focus: wire sawing thermodynamics & polysilicon cost reduction

Atomic layer deposition of Al_2O_3: imec presents the passivation benefits

Motech Industries: influence of etch depth on cells' electrical properties

Fraunhofer IST: reactive magnetron sputtering of ZnO:Al

University of Toledo: polarized light metrology, part 2

PI Berlin: PV module degradation and quality assurance measures

Third Quarter, August 2011

www.pv-tech.org


GROWTH
BEGINS
HERE

Photovoltaics International

Published by:
Solar Media Ltd.,
Trans-World House, 100 City Road, London
EC1Y 2BP, UK
Tel: +44 (0) 207 871 0123
Fax: +44 (0) 207 871 0101
E-mail: info@pv-tech.org
Web: www.pv-tech.org

Publisher: David Owen

Managing Editor: Síle Mc Mahon

Design & Production: Daniel Brown
Production: Viki Hämmerle & Tina Davidian
Senior Editor, North America: Tom Cheyney
Senior News Editor: Mark Osborne
News & Features Editor: Emma Hughes
News & Projects Editor: Chris Whitmore
Sub-Editor: Steve D. Brierley
Commissioning Editor: Adam Morrison
Sales Director: David Evans
Account Managers: Adam Morrison, Graham Davie, Daniel Ryder, Gary Kakoullis, David Evans, Nick Richardson, Ben Irving, Peter Gibson & Martin Lehmann
Marketing & Operations Director: Joy-Fleur Brettschneider
Marketing & PR Executive: Laura Pleasants

Cover image shows a quartz carrier at ISFH transporting silicon wafers to the quartz tube of a $POCl_3$ and oxidation furnace to undergo phosphorus emitter diffusion and SiO_2 surface passivation. Image courtesy of ISFH/Ulf Salzmann.

Printed by Quentin Press
Photovoltaics International
Thirteenth Edition
Third Quarter 2011
Photovoltaics International is a quarterly journal published in February, May, August and November.

Distributed in the USA by Mail Right International, 1637 Stelton Road B4, Piscataway, NJ 08854.

ISSN: 1757-1197

USPS Information
USPS Periodical Code: 025 313

Periodicals Postage Paid at New Brunswick, NJ
Postmaster: Send changes to: Photovoltaics International, Solar Media Ltd., C/o 1637 Stelton Road, B-4, Piscataway, NJ 08854, USA

Foreword

The Time is Now!

Four years ago when we first started publishing the *Photovoltaics International* journal, this was our call to action. Looking back over the past four years, we have seen a dramatic increase in the adoption of solar PV technologies and I am proud that this publication has played such an essential role in presenting new technologies to the market.

Regular readers will know that we take guidance from our Editorial Advisory Board, a select group of individuals from leading PV technology companies, to help us select the very best technical papers for our journal. One of our founding members, Gerhard Rauter, former COO of **Q-Cells**, has left us and I would like to take this opportunity to thank him for all of his help and vision over the last four years. I would like to extend a warm welcome to Gary Yu, Senior Vice President of Operations for **Trina Solar**, who will be joining our board to offer ideas and direction for our future publications.

So it is appropriate that this milestone issue is our largest ever at 224 pages. We are also running our longest-ever technical paper on page 127, written by the **University of Toledo**, which provides 15 pages of technical data, research findings and suggestions for the future direction of polarized light metrology for thin-film manufacturing-scale processes.

We have always placed great import on the quality of our technical papers, and this is an emphasis that will continue to pervade our publications for the future. Over the years we have delivered many technology 'first looks' with our content, from wire-sawing issues to selective emitter developments, and from ion implantation to module degradation.

This issue is no different, and we are proud to feature some key themes in this edition. Award-winning research firm **imec** has provided us with two papers for our cell processing section. Page 92 features a detailed look at the atomic layer deposition (ALD) of Al_2O_3, and finds that the tool specifications are the critical factors in achieving good surface passivation results. Immediately following this paper on page 102, imec presents the benefits of adapting and applying IC manufacturing processes to the PV industry – one of several such similarly themed papers we have featured in this publication over the years.

Some other key themes of this issue are our polysilicon focus, which includes a look at opportunities for reducing polysilicon materials costs (p. 41), while throughput gains could be achievable by applying some thermodynamic considerations as outlined by **Argenta Consulting** on page 48. Testing and certification, two of the most crucial steps in the lifecycle of a PV module, are discussed by **PI Berlin** (p. 166) and **STS Certified** (p. 177), while in our market watch section, **SolarVision** takes a closer look at the likelihood of micro-grid systems encouraging the uptake of PV in developing countries.

As always, a very warm thank you to all of our authors, be they repeat scribes or new contributors. We are always on the lookout for new editorial submissions, and are currently planning our themes for 2012, so please get in touch if you have a topic you feel would be of interest to our readers.

The PV-Tech & *Photovoltaics International* team will be in attendance at this year's EU PVSEC in Hamburg, so do drop by our booth (B3G/C8) to sign up for our newsletter, purchase a subscription or technical annual, or to check out our new *Newscast* video channel, delivering a weekly video update of the industry's most exciting news topics.

See you there!

Síle Mc Mahon
Managing Editor
Photovoltaics International

Photovoltaics International

Photovoltaics International's primary focus is on assessing existing and new technologies for "real-world" supply chain solutions. The aim is to help engineers, managers and investors to understand the potential of equipment, materials, processes and services that can help the PV industry achieve grid parity. The Photovoltaics International advisory board has been selected to help guide the editorial direction of the technical journal so that it remains relevant to manufacturers and utility-grade installers of photovoltaic technology. The advisory board is made up of leading personnel currently working first-hand in the PV industry.

Editorial Advisory Board

Our editorial advisory board is made up of senior engineers from PV manufacturers worldwide. Meet some of our board members below:

Gary Yu, Senior Vice President, Operations

Mr. Yu served as Trina Solar's Vice President of Manufacturing since May 2007 and in July 2010 was promoted to the position of Senior Vice President of Operations. Mr. Yu has 17 years' manufacturing management experience in semiconductor-related industries. Before joining Trina Solar, he was Managing Director of Wuxi Lite-On Technology, an LED assembly company based in China. Prior to Wuxi Lite-On Technology, he served as a Director of Manufacturing for 1st Silicon Sdn. Bhd. in Malaysia, prior to which he worked at Macronix International, a semiconductor integrated device manufacturer in Taiwan. Mr. Yu has a master's degree in Industrial Engineering and Management from National Chiao Tung University in Taiwan and a bachelor's degree in Chemical Engineering from Tunghai University.

Takashi Tomita, Senior Executive Fellow, Sharp Solar

Takashi Tomita has been working at Sharp for 34 years and is widely recognised as a fore-father of the solar industry in Japan. He was responsible for setting up Sharp's solar cell manufacturing facilities in Nara and silicon production in Toyama. Takashi's passion for solar power has led him to hold numerous posts outside of his roles at Sharp, including: Vice Representative at the Japan Photovoltaic Industry Association; Committee Member of Renewable Energy Portfolio Standard of METI; Adviser Board Member of Advanced Technology of Nara; Visiting Professor of Tohoku University; Adviser of ASUKA DBJ Partners (JAPAN) and Adviser of Global Catalyst Partners (US).

Dr. Kuo En Chang, President of Solar Division, Motech Industries, Inc.

Dr. Kuo En Chang joined Motech in 1999 as Chief Technology Officer and became President of the Solar Division in 2008, with responsibility for all technology and manufacturing. Motech is the sixth largest solar cell producer in the world. Before Dr. Chang joined Motech Solar, he worked on secondary battery research at the Industrial Technology Research Institute (ITRI) for more than three years. Dr. Chang holds a Ph.D. degree in Metallurgical & Materials Engineering from the University of Alabama.

Professor Eicke R. Weber, Director of the Fraunhofer Institute for Solar Energy Systems ISE in Freiburg

Professor Eicke R. Weber is the Director of the Fraunhofer Institute for Solar Energy Systems ISE in Freiburg. Weber has earned an international reputation as a materials researcher for defects in silicon and III-V semiconductors such as gallium arsenide and gallium nitride. He spent 23 years in the U.S. in research roles, most recently as Professor at the University of California in Berkeley. Weber is also the Chair of Applied Physics, Solar Energy, at the University of Freiburg, and during his career has been the recipient of several prestigious awards including the Alexander von Humboldt Prize in 1994, and the German Cross of Merit on ribbon in June 2006.

Dr. Zhengrong Shi, Chief Executive Officer, Suntech

Dr. Zhengrong Shi is founder, CEO and Chairman of the board of directors of Suntech. Prior to founding Suntech in 2001, he was a Research Director and Executive Director of Pacific Solar Pty., Ltd., the next-generation thin-film technology company, before which he was a Senior Research Scientist and leader of the Thin Film Solar Cells Research Group in the Centre of Excellence for Photovoltaic Engineering at the University of New South Wales in Australia. Dr. Shi holds 11 patents in PV technologies and is a much-published author in the industry. His work has earned him such accolades as "Hero of the Environment" (TIME magazine 2007) and "Corporate Citizen of the Year" at the China Business Leaders Awards 2007. A member of the NYSE advisory board, Dr. Shi has a Bachelor's degree in optical science, a Master's degree in laser physics and a Ph.D. in electrical engineering.

Dr. Sam Hong, President and COO of Neo Solar Power

Dr. Hong has more than 30 years of experience working in the solar energy industry. He has served as the Research Division Director of Photovoltaic Solar Energy Division at Industry Technology Research Institute (ITRI), a research organization that serves to strengthen the technological competitiveness of Taiwan, and Vice President and Plant Director of Sinonar Amorphous Silicon Solar Cell Co., which is the first amorphous silicon manufacturer in Taiwan. In addition, Dr. Hong was responsible for Power Subsystem of ROCSAT 1 for the Taiwan National Space Program. Dr. Hong has published three books and 38 journal and international conference papers, and is a holder of seven patents. Dr. Hong was the recipient of Outstanding Achievement Award from the Ministry of Economic Affairs, Taiwan.

Dr. G. Rajeswaran, President and CTO of Moser Baer Photovoltaic Ltd

Raj served as President and CTO of Moser Baer Photovoltaic Ltd. from July 2007 until October 2008, since which time he has been Group CTO for all the Moser Baer business units and holder of the CEO function for launching new businesses. He spent 22 years with Eastman Kodak Company as the Vice President of Advanced Development & Strategic Initiatives, where he managed Kodak's Japan display operations including technology & business development in Japan, Taiwan, Korea and China. He has also served as Vice President and on the board of SK Display Corporation, and worked in technology development with Brookhaven National Laboratory. Raj has a Ph.D., an M.Tech. and a B.E. in electrical engineering. A much-published author, speaker and patent holder, Raj is a member of the Society for Information Display (SID) and has chaired several international conferences in the field of OLEDs.

Contents

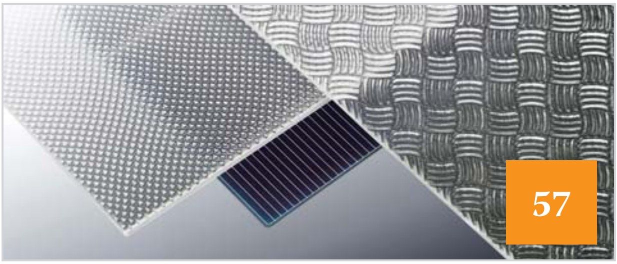

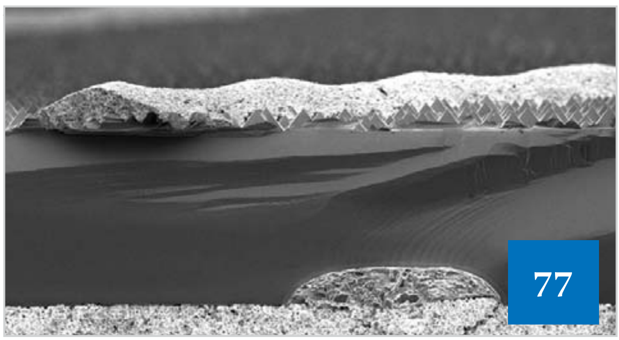

Contents

WE'LL GIVE YOU PLENTY OF SPACE TO SPREAD YOUR WINGS

Imec stands for groundbreaking research that leads to technological developments.
We also continue to be a world leader in nanotechnology. Something we can't achieve alone. This is where you come in. More than 1.850 of us are developing the technology of the future. We can use all the help we can get. Come and join us and we'll give you plenty of space to spread your wings.

Are you fascinated by renewable energy sources?

Do you want to join a leading research institute and drive its photovoltaics ambition?

Do you consider yourself an expert in photovoltaics?

Then we gladly invite you today to Hall B4G/booth C11 or www.imec.be/jobs to discuss our challenging opportunities and potential collaboration.

We are currently looking for, amongst others:

- Photovoltaics Experts
- Crystalline Silicon Solar Cell Principal Integration Researcher
- Crystalline Silicon Solar Cell Passivation Researcher
- Crystalline Silicon Solar Cell Diffusion Researcher
- Heterojunction Solar Cell Integration Specialist
- Postdoctoral Researcher for Silicon Nanowire Characterization

imec

www.imec.be/jobs

Contents

Fab & Facilities

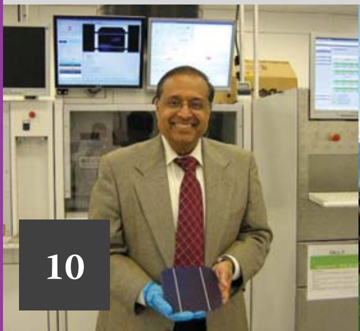

News

Bosch opens €530 million solar PV competence centre in Arnstadt, Germany

The Bosch Group has inaugurated its new €530 million photovoltaics competence centre in Arnstadt, Germany. The facility includes the company's solar energy division headquarters as well as R&D, PV cell and module production, and a training centre under one roof. Together with an adjacent ingot and wafer manufacturing plant, Bosch covers all the steps in the crystalline-silicon value chain at this location.

Construction on the 382,000m^2 site took place over two years. The company said it expects to create about 1000 new jobs by 2012, with 600 of those positions coming online this year.

The administration building façade features 620 slats integrated with ~4m × 0.5m thin-film solar modules, while semitransparent PV panels line the top floor's hallway ceiling. The overall installed power rating of the PV systems totals more than 1MW, which will provide ample electricity to meet the needs of the offices in the HQ complex.

The Arnstadt site is one of three locations where Bosch has made significant investments in its solar division, which is expected to top €1 billion in revenues this year.

Source: The Bosch Group

Bosch's new photovoltaics competence centre in Arnstadt, Germany.

Capacity News Focus

Kaco invests €30 million in new manufacturing facility

Kaco new energy is investing €30 million in a new manufacturing plant to ramp up capacity by 4GW. When completed, the 12,000m^2 site will be the German solar inverter manufacturer's fifth facility; it will primarily be used to produce three-phase inverters for Kaco's TL3 series.

Source: Kaco

Kaco's Powador TL3 series inverters will be produced at the company's new manufacturing facility.

Kaco believes the climate-neutral facility will allow flexible production, enabling quick response to fluctuating market conditions. A new testing plant has also been added to put the company's inverters through endurance tests.

To date, 30 new employees have been hired to man the near-fully-automated site, although this number could increase to 150 should the company meet its expansion targets. The location of the new facility was not disclosed.

MEMC opens new module manufacturing base in Ontario

Wafer manufacturer MEMC is to create 400 jobs by opening a new module production line in Ontario, Canada. Located in Newmarket on the outskirts of Toronto, the Flextronics-owned site will produce PV panels for the 60MW project pipeline of MEMC's subsidiary, SunEdison.

The decision to establish a module manufacturing site in Ontario, as opposed to Southeast Asia, where SunEdision and Flextronics have a pre-existing manufacturing partnership, was made in part to meet the 60% domestic content requirement necessary to be eligible for Ontario's feed-in-tariff (FiT). MEMC has not yet revealed the production capacity of the facility.

Spire begins expansion of advanced tech centre lab, adds new PV module equipment

Spire has begun the expansion of its Advanced Technology Center (ATC) Lab at its corporate headquarters in Bedford, MA, with updated equipment for customer evaluation and factory training. The new Spire systems installed include a larger format laminator and electroluminescence crack detection system, as well as next-generation assembler and simulator gear.

Source: Spire Solar

Spire has expanded its ATC lab with updated lamination and EL crack detection equipment.

Spire's ATC Lab includes a fully functioning PV module production line. Customers use the facility for the development and qualification of new and advanced crystalline-silicon and thin-film modules. The site also provides support for the development and qualification of new materials for module encapsulation, glass types, cell structures, and associated electronics, according to the company.

Tosoh starts thin-film sputtering target manufacturing in Shanghai

Although Tosoh SMD has supplied the China market for over 20 years, the firm has only now established a thin-film sputtering target manufacturing subsidiary in Shanghai, China. Citing the need to better serve its semiconductor, flat-panel display, solar, and large-area coating customers in China, Tosoh expects the facility will enable it to grow its business in the region.

Suniva adds module capacity to US facility

Monocrystalline silicon solar cell specialist Suniva is adding 25–30MW of module production to its Norcross, Georgia plant, which already has a capacity of 170MW for its 'ARTisun Select' solar cells. The expansion is scheduled to be completed in late August and operational in September 2011, according to the company.

Suniva recently highlighted that its next generation 'Optimus' solar modules were certified and in production with conversion efficiencies of more than 16% at the module level, which equates to producing 260W of power in a 60-cell

Source: Suniva

Suniva's Dr. Rohatgi holds the company's very first solar cell, produced on October 23rd, 2008.

module format. The company believes that this end-to-end R&D, manufacturing and testing capability provided a faster time-to-market and technological advantage.

Yingli Green touts US market share gains, plans to open R&D facility in US

Yingli Green Energy Americas, a division of Yingli Green Energy Holdings, revealed that it has reached a significant milestone for its US module shipments. Yingli America advised that in its shipments to 23 US states, the Caribbean, Mexico and Canada, it had a cumulative shipment total of 250MW, leading the company to deliver more PV modules during the first half of 2011 then it had during the full 2010 year.

Yingli Americas additionally revealed that it had launched its new YGE-Z Series module, which is specially made for use with Enphase Energy's microinverters. Working with Zep Solar under a strategic licensing agreement, Yingli Americas implemented Zep Solar's Zep Groove feature into its 240W product series.

The company also announced at that it is planning to open a new research and development centre in South San Francisco. The facility will serve as a product testing and evaluation centre for the company.

QSolar doubles manufacturing capacity at Shanghai module factory

QSolar has added a second production line to its manufacturing facility in Shanghai, China. The addition of a second line has doubled production capacity at the site from 20MW to 40MW a year. The increased production capacity in Shanghai will help QSolar meet rising demand for its modules, which has recently been boosted by major orders in North America, Europe and Africa.

Source: QSolar

Cell inspection on QSolar's manufacturing line.

Semprius receives over US$7M in incentives to build pilot CPV production plant in North Carolina

Semprius is the recipient of state and county incentive packages totalling US$7.88 million, which will go towards the construction of a pilot HCPV production facility in Henderson, North Carolina. Funding was provided by the State of North Carolina Job Development Investment Grant, grants from the Golden LEAF Foundation, Vance County, the One North Carolina Fund and the North Carolina Community College System. The incentive packages comes just a few weeks after the company closed its Series C venture funding round with US$20 million.

Construction on the plant in North Carolina is anticipated to begin later this month with the first phase of the pilot plant coming in at 50,000 square feet. Semprius is already planning to expand over the next few years so that the facility will encompass a total of 150,000 square feet and employ over 250 people. The pilot plant will have an initial capacity of 5MW with the capability to house 35MW as the company grows.

Anwell scores funding from local government for second thin-film production plant

The Municipal Government of Dongguan has supplied Anwell Technologies' wholly owned subsidiary, Dongguan Anwell Digital Machinery, with US$108.67 million (RMB700 million), which will go towards the company's development of a second thin-film solar panel manufacturing facility in Dongguan.

Since the Dongguan Government invested a significant portion of funds into Anwell, it will become a 19.5% shareholder in Dongguan Anwell, bringing the subsidiary's value to US$680 million (RMB3.6billion). At the end of five years after the initial government financing, the Dongguan Government will have an option to sell its shares in the Anwell subsidiary to Anwell at cost plus interest.

This recent investment comes just one month after Anwell secured over US$100 million from the Municipal Government of An Yang City in Henan Province for the expansion of its thin-film production in China. Combined, the two investments by the municipal governments of both cities total US$186.3 million (RMB1.2 billion). Anwell intends to reach a 1.5GW annual production capacity within five years.

Quick Mount PV plans to move into larger facility and expand its operations

Three years after solar mounting manufacturer Quick Mount PV moved into its present Concord, California facility, the company revealed plans to move all company operations into a larger, 133,000-square-foot home base in Walnut Creek, California. The relocation will take place during the middle of the first quarter in 2012, which, the company states, will allow it to meet the ever-increasing demands for its products.

Source: Quick Mount PV

Installation of a 60kW Quick Mount PV system in Sun Valley, Idaho.

Claudia Wentworth, Quick Mount PV CEO, confirmed that the US$7.5 million purchase was completed with a loan from the Small Business Administration (SBA). Wentworth additionally noted that the company would utilize the larger 90,000-square-foot building for its operations with an intention to sublease a separate 43,000-square-foot office and R&D building located at the front of its new property.

The company plans to hire 20 new employees to help satisfy the manufacturing needs it expects to face in the coming months at its new site.

Dow Chemical to build PV module encapsulant production plants in Thailand and Germany

Dow Chemical is adding production capacity for its Enlight polyolefin encapsulant films for crystalline-silicon and thin-film solar PV modules, with plans to build two new manufacturing plants in Map Ta Phut, Thailand, and Schkopau, Germany in 2012. The company said that the new factory designs will be based on technology used at the initial manufacturing site in Findlay, OH, which began production in December 2010.

Approximately 30–40 new positions will be needed at the site – Dow's largest manufacturing facility in the Asia-Pacific region – once the Enlight films plant is up and running. The expected capital expenditures and ultimate manufacturing capacities of the Thai and German facilities were not disclosed.

Heraeus's PV unit expands presence in Asia with completion of new production facility in Singapore

The photovoltaics division of Heraeus Materials Technology has completed construction on its new Singapore facility, which will produce the company's silver metallization paste for use in crystalline

Heraeus's HeraSol SOL 230H lead-free silver tabbing paste.

Source: Heraeus

solar cells. The site will also house the unit's R&D, sales and technical service operations, all of which began operation in June. The R&D lab was the facility's most recent completion, having been finalized in July. It plans to have qualification samples ready for customers in the coming weeks. The site's official opening ceremony will be held in November.

"This new site was built primarily to expand production capacity into the Asian market, as well as to create our third leg of our global R&D footprint," said Andy London, VP of Heraeus Materials Technology in West Conshohocken. "In the last three years the industry has moved to Asia and we want to remain dynamic and responsive to these industry changes."

Other News

US DOE fronts US$50 million for PVMI Part II, SUNPATH

A US$50 million fund is up for grabs by the US Department of Energy to domestic PV manufacturers wanting to take solar technology from the lab to the fab to help restore the United States' position as being at the forefront of solar manufacturing. The funding program is the second solar Photovoltaic Manufacturing Initiative (PVMI) initiative, dubbed SUNPATH, which stands for Scaling Up Nascent PV At Home.

The SUNPATH initiative is designed to support companies with pilot-level commercial production facilities to scale up their manufacturing capabilities in order to fast-track the ramping process. The key target for the funding is domestic firms that can demonstrate innovative, low-cost solar technologies, which are already being supported in certain areas via the PVMI initiative. The DOE said that its national laboratories were stepping up their validation facilities to ensure that the technologies developed and manufactured in PVMI Parts I and II are tested at scale in multiple locations and climates in the United States.

The DOE is seeking applicants with industrial-scale demonstrations of PV modules, cells, or substrates that offer lower-cost solutions in line with the SunShot goals. Applications for possible funding are due by October 28, 2011. DOE's national laboratories are stepping up their validation facilities to ensure that the technologies developed and manufactured in Parts I and II are tested at scale in multiple locations and climates in the United States.

Fab & Facilities Order Focus

Day4 Energy to help upgrade Austrian solar manufacturer PV Products' module production line

Day4 Energy has signed a deal with Austrian solar module manufacturer PV Products to provide the equipment and technology to upgrade its 30MW production facility for the manufacture of solar panels featuring Day4 DNA crystalline-silicon cells. The upgrade of PVP's automated 30MW production facility to Day4 technology is scheduled to begin immediately, with production anticipated to start in early September, the companies said.

Using proprietary equipment and technology from Day4 Energy, PVP will transition its existing line at the Styria plant to manufacture Day4 solar modules with what is being called "minimum capital investment." Day4 said the panels will feature its DNA PV cells, which do not require soldering, and based on tests conducted by Day4 Energy, virtually eliminate PV cell energy losses after module lamination. They also enable the manufacturing of solar modules based on "work-smart technology," which significantly reduces the effects of shading on module performance, according to Day4.

Petra Solar employs Omnify Software's PLM package to aid in engineering management

Product lifecycle management (PLM) software provider Omnify Software has gained a new customer in the form of Petra Solar, which has purchased the former's Empower PLM solution. The Empower product will be used to automate Petra Solar's processes such as document control, engineering adjustments, compliance and bill of material (BOM) management.

Petra Solar was said to have reported time savings of approximately 74% by applying the software to its engineering change order (ECO) cycles. Design changes implemented during a product's lifespan utilise the Empower PLM system to track those processes that were once manual.

Dyesol ships, installs equipment for DyeTec Solar program at Ohio facility

Dyesol has reported that it has completed the delivery and installation of equipment for DyeTec Solar's dye-sensitized solar cell (DSC)-based BIPV program, which is funded by the Ohio Third Frontier Fund. The equipment was delivered to DyeTec's Toledo, Ohio facility with Dyesol noting that it had relocated staff with a DSC background to the site. Management and technical personnel moved to Ohio in May and completed the first phase of the program, which has allowed Dye Tec to commence building prototype panels.

Solar Frontier's 900MW CIS thin-film plant reaches commercial operational status

Despite reports that Solar Frontier's 900MW, CIS thin-film production plant in Miyazaki, Japan has reached full capacity, the company has not yet reported this fact. Solar Frontier has only revealed that all production lines are now commercially operational having started its production ramp earlier this year.

The Kunitomi Plant was said to be on track to reach its targeted annual capacity of 900MW as average module output continues to increase, without giving a timeline. The Kunitomi Plant is said to be Japan's largest solar module production facility, as well as the largest CIS factory in the world. Solar Frontier recently announced the commercial availability of 150W CIS panels.

BP Solar to close down historic Maryland site

BP Solar's Frederick, Maryland facility is to close by the end of the first quarter 2012, with costs and a change in company focus being cited as the main factors for the plant's closure. In March 2010, the company cut 320 jobs at the Maryland facility after 140 employees had already been let go in 2009.

The announcement that the plant will be permanently closed by next March has left nearly 80 employees displaced from their jobs, although there is speculation that some staff may be able to relocate to the company's Houston, Texas headquarters.

KLNE unveils new manufacturing and R&D centre

KLNE has increased its manufacturing capacity in China by opening a new facility and research and development centre in Changzhou. The 100-acre site was officially unveiled at a ceremony attended by the company's sales director, Wison Qi, and marketing director, Paul Nicholson, as well as dignitaries from the Changzhou local government and staff representing the Wujin Economic Development Zone.

Qi hosted the event, which saw speeches made on behalf of the local government and KLNE before the unveiling of the foundation stone by the Mayor of Changzhou and Paul Nicholson.

"This is a big project, an important project for KLNE," said Qi. "We will have a state of the art manufacturing facility and R&D resources here. The investment is large, not just for the building itself but for the machinery and equipment to go in it. But it's necessary for the future of the company and it's worth it."

KLNE already has manufacturing sites in Shenzhen, Xuchang and Beijing, and furthered its global reach by opening a new office in Melbourne, Australia in June.

Green Energy reports fire in recycling facility

In a brief statement, Green Energy Technology said that smoke was being generated at an independent recycled services company facility, at GET's Southern Taiwan Park manufacturing facilities. The local fire bureau was involved in the incident. However, GET said that the area where the incident took place was separated from its main operating lines and that there was no impact to its manufacturing operations. GET capacity utilization was around 100% with a capacity of 1GW in the second quarter of 2011. The company is testing new equipment in the Southern Taiwan Park to get ready for further capacity expansion.

Location Briefings

Languedoc-Roussillon

Location: Bordering Spain and the Mediterranean coast, the French region of Languedoc-Roussillon provides access to 260 million consumers within one day's reach. Placed in the heart of Southern Europe, the whole Mediterranean Arc is also easily reached.

Introduction: The Languedoc-Roussillon, blessed with some 300 days of sunshine per year reaching an average solar yield of 4.5kWh/m^2 per day, provides exceptional conditions for solar installations and renewable energies. In 1970 the first solar oven was built in Odeillo/Mont-Louis, attracting worldwide attention and research teams to the Pyrenées. This was followed in 1983 by the thermal solar plant Themis in Cerdagne, a spot selected for its exceptional insolation conditions. Both locations were precursors and still provide fundamental results to today's solar industry. This dynamic and innovative environment and steady population and activity growth increase the territory's need for energy regularly. The local government supports solar technologies – which attracts professionals of the solar and energy sector, including: BP Solar, Belelectric, Cap Energie, SunTechnics, Photon Technologies, Tecsol, EDF, ERDF, EDF EN, GDF, Donauer, Tritec, Phaesun, Solaire Direct, Sunnco, Panosol, Urbasolar, Irysolar, Phoenix Solaire, Vol-V and many more.

Infrastructure: DERBI (innovation cluster based in Perpignan), uniting 150 members to accelerate innovation, has so far labelled 75 projects, representing more than €100 million worth of investment and funding.

A local pool of competent suppliers and subcontractors will support expansion projects, providing all services needed (mechanics, robotics, construction, plastics, electronics, logistics – to name but a few).

Cutting edge laboratories and high-level training offer R&D collaboration and qualified personnel. The first French engineering diploma in renewable energies, 'PolyEnr,' can be obtained at the University of Perpignan.

Key features/incentives: In collaboration with the EBI (European Bank of Investment), the region has created a fund endowing €400 million to support local PV projects (conditions apply). A new collaborative R&D institute – Themisol – for thermal and concentrated solar technologies, is also planned.

What they say: Languedoc-Roussillon offers exciting solar business potential and excellent conditions for a set-up in the South of France. Invest-LR will assist you throughout your process.

Key tenants:

Belelectric, ERDF, GDF, Irysolar, Urbasolar & Tecsol.

Sylvia Lamaty, project manager ENR at Invest-LR, the economic development agency of Languedoc-Roussillon
Email: lamaty@invest-lr.com
Mobile: +33(0) 62339 2625
Web: www.invest-lr.com

SOLAR VALLEY Saxony-Anhalt – a sustainable region in the heart of Germany

Location: The SOLAR VALLEY Saxony-Anhalt is located in the centre of Europe – in the German federal state of Saxony-Anhalt in Middle Germany. It is one of the leading solar regions in the world – comprised of a network of 29 international operating firms, nine leading research institutes, and four universities.

Introduction: The density of photovoltaic industrial enterprises in SOLAR VALLEY Saxony-Anhalt is unique throughout the world. Pioneering spirit and entrepreneurial courage, above average qualified and motivated employees, and the support of politicians at the state and federal levels have made Central Germany the most outstanding region for photovoltaics. Making solar power competitive is at the centre of the joint effort. This has resulted in a sophisticated strategic cooperation in which business, science and education are closely intertwined.

In order for solar power to compete against conventionally generated electricity, costs must be reduced at every step in the value chain. The Norwegian Innotech Solar Group (ITS) recently closed a gap in the value chain by locating its new production facility at SOLAR VALLEY Saxony-Anhalt in 2010. In order to make its solar cell production more efficient and environmentally friendly, ITS has developed a technology for reconditioning defective cells deemed unsuitable for manufacturing PV modules. ITS upgrades its non-prime solar cells to full efficiency using a laser-supported process: a Win-Win situation for manufacturers, customers and the environment at the SOLAR VALLEY Saxony-Anhalt.

Key features/incentives:

- Cell Award Winner for "Best Region for Manufacturing Solar Technology" in 2009
- Around 3,500 jobs in the solar industry attest to the area's economic strength
- Generous investment incentives cover a high percentage of capex
- Fast-track project realization, due to the close proximity of the world's leading PV equipment suppliers and superior engineering, excellent labour experience as well as local authority services and support
- Leading glass producers and glass suppliers located in Saxony-Anhalt offer best siting conditions

- Close R&D cooperation with Germany's leading PV research institutes and four universities
- Shorter time to markets, via state-of-the-art infrastructure for lower rate of long-term transport inventories
- Skilled and flexible workforces
- Nearby international schools to join the solar family life
- A modern and environmentally friendly place to live and work

Key tenants:

Q-Cells, Sovello, PV-Crystalox, ITS Innotech Solar and Malibu.

Visit SOLAR VALLEY Saxony-Anhalt at the PVSEC 2011 in Hamburg, Germany Hall B6 Booth A37!

www.invest-in-saxony-anhalt.com

Product Reviews

Edwards

Edwards' hot trap pumping solution enables extended maintenance cycles in depositing TCO films

Product Outline: Edwards has introduced a patented hot trap designed to thermally decompose the liquid diethyl zinc (DEZ) used in depositing some transparent conductive oxide (TCO) films in thin-film solar manufacturing. Edwards' iXH harsh process dry pumps have been optimized for photovoltaic device manufacturing processes, and are designed to handle the high powder loads, high flows of corrosive cleaning gases and large hydrogen flows associated with thin-film silicon deposition processes.

Problem: Zinc oxide-based TCO films deliver a surface topology that improves the light capturing process. However, should un-reacted DEZ enter the vacuum pumps during the deposition process, it decomposes, coating pump surfaces and significantly degrading pump operating lifetimes.

Solution: Gases leaving the process chamber pass through the Edwards hot trap before entering the vacuum pump. The gases flow through the trap's replaceable cartridges, which are heated to a temperature that optimizes DEZ decomposition. The trap incorporates a carefully designed gas path that provides sufficient time for decomposition without restricting flow. Cartridges require a monthly replacement and can be easily cleaned and reused, helping to lower the cost of this solution. The hot trap can extend pump maintenance intervals up to six months, a significant improvement over the weekly intervals required when it is not used.

Applications: Zinc oxide-based TCO films deposition.

Platform: The iXH also offers a range of operating temperatures that can be tuned to specific process requirements.

Availability: Currently available.

Ametek

Ametek offers larger fluoropolymer piping for scaling to larger PV manufacturing facilities

Product Outline: Ametek Fluoropolymer Products has added tubing with diameters ranging from 1.5 to 3 inches to its line of ultra-high purity (UHP) tubing for the semiconductor and photovoltaic industries. Schedule 40 pipe with diameters up to 3 inches also are available to meet the need for larger-scale production sites.

Problem: As the solar energy industry moves to larger cell and module fabrication facilities, traditional tubing and pipe with diameters of up to 1.25 inches cannot handle the higher fluid volumes of acids, etchants and other chemicals used by the state-of-the art equipment.

Solution: Ametek can manufacture tubing and pipe from various grades of fluoropolymer resins to meet specific customer applications and ship them to comply with specific customer JIT delivery requirements. All tubing with a diameter of 2 inches or more is available in straight lengths up to 20 feet; smaller diameters are available in spools or straight lengths. In respect to low-pressure, low-vacuum containment vessels, larger diameter tubing and pipe in longer lengths reduces the number of welds along with process contamination concerns, providing an efficient and cost-effective solution for handling higher volume process fluids. Fluoropolymer containment vessels can replace glass vessels that are more prone to breakage and thinning of the walls due to etching by certain corrosive chemicals such as hydrofluoric acid.

Applications: Bulk chemical distribution processing tanks, storage buffers and heat exchangers.

Platform: Ametek tubing meets all common operating temperatures and pressures, with standard tubing meeting operating pressures up to 70 psi and 73°F.

Availability: Currently available.

Fujitsu

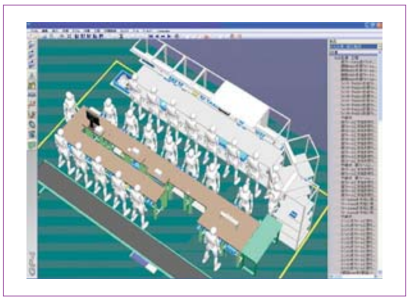

New software from Fujitsu optimizes production line workers' operations

Product Outline: Fujitsu has introduced new software for simulating the movements of production line workers, which is designed for customers in the manufacturing industry, such as automobile parts suppliers and precision electronics manufacturers. GP4 was developed by Lexer Research, and claims a 40% reduction in production line assembly time, achieved in an early-release (beta-release) deployment of the software.

Problem: In the manufacturing industry in recent years, great progress has been made in the area of production innovation prior to actual production, including virtual product design using 3D CAD. However, it is difficult to perform verification in virtual environments, necessitating a resort to a process of trial-and-error on the production line in order to improve efficiency.

Solution: With GP4, users at the production preparation stage can create a virtual production line and run simulations on factors including the most efficient movements or positions of production workers, the optimal alignment of workers in relation to the flow of a production line, and the time required to complete specific production tasks. As a result, in addition to enabling greater efficiency in assembly work on a production line from the standpoint of people, the product enables workers to benchmark their work against the simulation results and share their understanding of problem areas with co-workers, leading to improvements on the front lines of assembly plants.

Applications: Production line optimization through simulations of the movements of production line workers.

Platform: Fujitsu claims the GP4 is user-friendly even for novices. Training is required to effectively use CAD, but GP4 is very user-friendly enabling first-time users who have never used simulation software to employ it.

Availability: Currently available in Japan.

Water management planning for photovoltaic manufacturing facilities

Ralph Williams PE, CH2M HILL, Portland, Oregon, USA

ABSTRACT

Various economic and political influences continue to push high-volume manufacturing of semiconductor and PV devices into relatively arid and water-constrained geographies. As the social, economic and political focus on water resources and sustainability increases daily, the need to address the supply, use and disposal of water at manufacturing facilities is growing increasingly more complex. Historically, PV manufacturing has not been considered a major water consumer so there has been little scrutiny of water management. As the costs of water and wastewater disposal spiral upwards, water resource management becomes a significantly more important factor in the capital and operating costs of PV manufacturing. This paper outlines the preparation of a water management diagram (WMD) with reference to the development of water systems for new PV manufacturing plants, and discusses some cautionary design considerations.

Introduction

Like other modern industries, PV manufacturers are using multiple criteria for selecting new manufacturing sites. Typically, water supply (and discharge) and associated costs of water are not at the top of the list, and sites are often selected with unique water management constraints. An increasing volume of PV manufacturing is being planned for regions where water has become a critical resource. Many oil-rich Middle Eastern nations are looking to establish non-petroleum industries for their future generations; since solar power generation is well suited to these geographies, PV manufacturing facilities are being targeted.

In order to most effectively manage the cost of water operations and the complexities of environmental permitting and social benchmarking, a comprehensive water management plan should be adopted for the facility or site, if not for the corporation as a whole. A primary tool for development of the water management plan for a given site or facility is the water management diagram (WMD). The WMD should be developed as early in the facility design as practical, with the understanding that there may be adjustments during the course of facility design. More frequently nowadays, initial planning permits require estimates of water consumption and wastewater discharge, as well as definitions of measures used to reduce consumption and recycle water internally.

A typical WMD should include:

- all known and projected water users, with supply water criteria and wastewater characterization;
- offsite water sources, flows and quality;
- onsite water treatment systems, with input chemicals, output residuals, output water and quality;
- offsite effluents and residuals from treatment.

This discussion focuses on the general types of information required to prepare the WMD and some caveats to be considered in developing water systems related to designs for new PV manufacturing plants.

Water use requirements

The core water needs for a PV manufacturing plant begin with the specific aqueous processes used in manufacturing, and then propagate into the manufacturing support systems and energy utilities that utilize water. Domestic water needs, e.g. potable water supply and sanitary wastewater, are a function of the site population and related demands, and add to the facility water requirements. The heart of the WMD for the facility will be the process requirements, with support requirements stemming out from this core.

Process water

In the case of silicon wafer PV, the processes requiring water typically include various cooling and cleaning steps associated with bricking, cropping, wafer sawing, wafer removal and cleaning; chemical make-up and rinsing associated with feedstock etching, silicon reclaim, texture etching and isolation / PSG etching; and miscellaneous processes such as glass cleaning. For CIGS on glass the wet processes may only include glass cleaning, cadmium deposition and in situ equipment-cleaning operations. Larger silicon-based plants are more aggressively pursuing cost reduction practices with kerf reclaim and carbide slurry reclaim. Inclusion of these types of system increases the set of process-water requirements. Regardless of PV type, each process should have its water quality and use rates established and in line with the manufacturing process technology.

One of the challenges to water treatment system design is obtaining the specific level of water quality required for each process, especially in emerging PV technologies. The manufacturing process for each step may come from the process equipment supplier, from internal development by the PV manufacturer, or from a third-party process technology supplier. A given project may have a combination of all of these, further complicating the resolution of the number of different water qualities required for the various processes.

Users are accustomed to referring to 'city water,' 'RO water' and 'DI water,' since those are the systems they had in development in previous manufacturing facilities, without realizing that none of these three systems has any industry-accepted quality parameters. Simultaneously, equipment suppliers give resistivity specifications for deionized water that might range from 5 to 15MΩcm, without realizing that this range is not normally available with conventional deionization technology (e.g. mixed-bed ion exchange, which generally delivers more than 17MΩcm when operated effectively).

In the end, from a practical standpoint, the three categories of water quality mentioned do generally work their way into the PV facility design. City water is set as the quality level for incoming supply water, which generally meets USEPA drinking water standards (with some exceptions to be discussed). This water is used to supply relatively dirty processes such as saw coolant, brick rinsing and other front-end rinsing. Deionized water, with nominal resistivity greater than 17MΩcm, is used for all steps requiring a consistent supply of clean water for chemical processing and critical cleaning. RO water is an intermediate quality that is generally hard to define in terms of specific quality parameters. It is often used for a

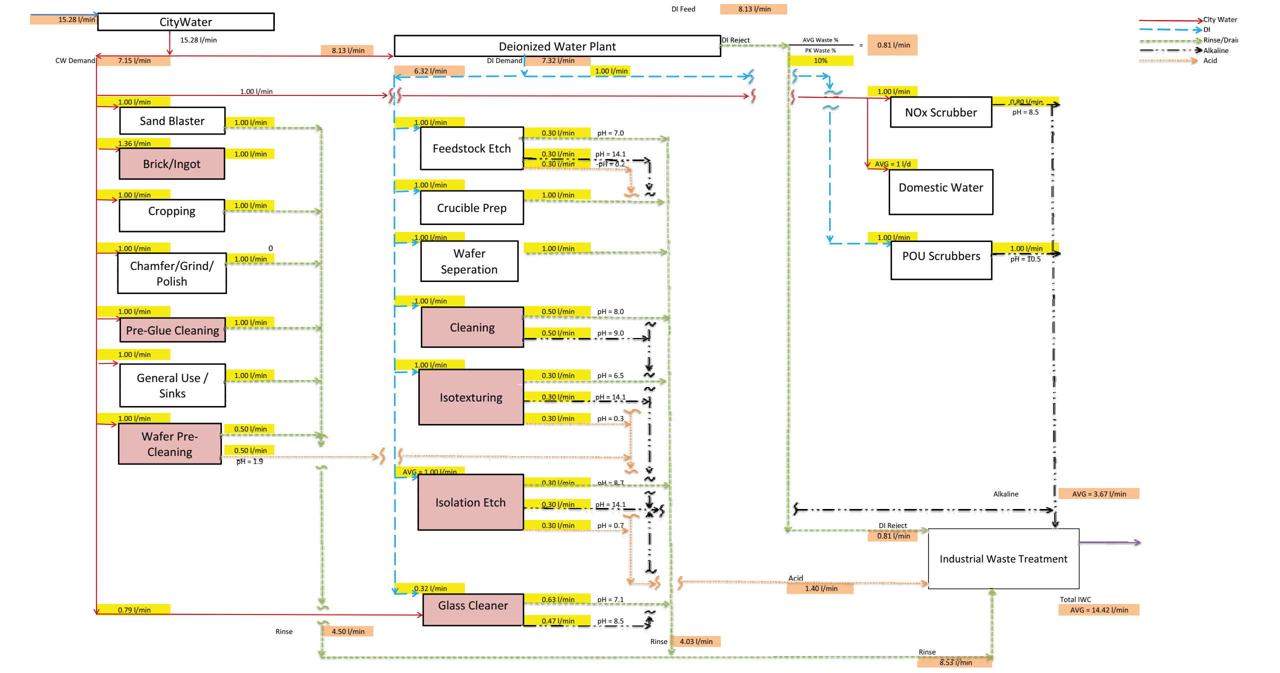

Figure 1. Base WMD for a silicon PV factory.

few manufacturing steps, but is more often specified for facility support systems.

Process-water requirements are a direct function of the processes performed in specific types of equipment and are therefore not at the discretion of facility design. In order to prepare a good WMD, the specific criteria for water supplies should be established early in the project.

Process and facility support systems

One step away from the direct processing of the product are a number of systems designed to support the manufacturing process. These may be supplied along with the process equipment or provided by a centralized system in the facility. It is easy to underestimate the significance of the design of some of these systems for water management.

Scrubbers

Any PV manufacturing facility that utilizes wet etching, plating and vapour deposition processes is likely to require abatement of one or more process exhaust streams. Depending on the facility size and tool set, air abatement may involve a point-of-use (POU) system connected to dedicated tools, or a plant-wide system with a network of collection ducts distributed to multiple tools with similar exhaust contaminants.

The use of packed-bed towers using water for scrubbing of acid and ammonia vapours is reasonably well understood and provides adequate protection for most aqueous cleaning processes. The water requirements are dependent on the scrubber capacity and make-up water quality. The use of chemicals to control pH in these scrubbers is a common practice, but has its pros and cons when weighing water use, chemical consumption and wastewater disposal.

In the fairly common case of silicon etching with acid mixtures, including nitric and hydrofluoric, a significant amount of nitrogen oxides ($NO+NO_2$, or NO_x) is liberated. NO_x is regulated by the USEPA and many other international authorities and requires more aggressive chemical management in the scrubber. If an NO_x scrubber is required, it will have its own make-up water demand, but more importantly a more complex wastewater blow-down. Though not specifically regulated, the silicon etch process may produce silicon tetrafluoride in the exhaust, along with NO_x and hydrofluoric acid fumes. Significant levels of silicon and fluoride in the NO_x scrubber can lead to increased chemical consumption and scaling if not planned for appropriately.

PECVD and similar deposition tools typically require abatement of a mixture of corrosive and flammable/pyrophoric

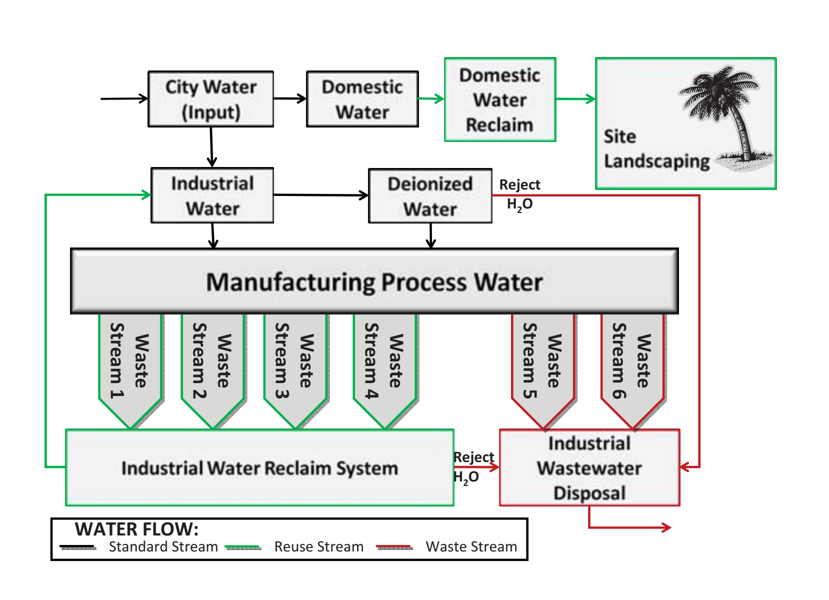

Figure 2. Water reuse scenario for a >120MW PV manufacturing facility.

gases. The most common abatement for these processes is a POU unit with a combustion chamber followed by a wet quench/scrubbing chamber. Due to the high level of fluoride and high temperature of this liquor, hard water will tend to form calcium fluoride and other calcium salts, which deposit in the workings of the scrubber, reducing capacity and eventually clogging it.

Due to scaling concerns in both the NO_x and POU scrubbers, they are often specified to receive RO water. It is likely that, in most cases, simply softened water would be adequate for these. Likewise, scrubbers offer a good opportunity to utilize relatively low-quality reclaimed water, as long as the scaling issues are addressed.

> "Any PV manufacturing facility that utilizes wet etching, plating and vapour deposition processes is likely to require abatement of one or more process exhaust streams."

For purposes of WMD development, it is important to note that wet scrubbers fundamentally evaporate a continuous quantity of pure water into the atmosphere. While the total volume may not be large, this effect contributes to increased concentrations of chemicals in the wastewater.

Cooling water

Most manufacturing facilities have some requirements for cooling of process and facility equipment. In the case of silicon wafering, furnace cooling water becomes a high-use, manufacturing-critical system. Emergency cooling water for furnaces can introduce another level of complexity in water management. Critical cooling of furnaces in the event of power failure can be supported in a number of ways, including expanded water storage capacity.

Typical process cooling water (PCW) systems consist of closed-loop water circuits that provide water at a specified temperature to the tool and reject transferred heat from the PCW to a secondary system. The secondary system may consist of an evaporative cooling system (cooling tower), a CFC-based chilled water system (which in turn rejects its heat to a cooling tower), or some other type of cooling cycle.

Independent of direct-connected PCW cooling, a significant amount of heat from process tools is rejected into the air recirculating in the building. In this case, the tool heat is rejected to the chilled water portion of the building air-conditioning system. In large facilities, this would include chillers and cooling towers, but may simply involve air-cooled direct expansion units that are much less energy efficient.

The industry-standard concept for cooling systems design includes rejection of heat through evaporative cooling in cooling towers. The water quality and related management within cooling towers is a discussion in itself, but the fundamental concept of evaporating pure water to reject heat from a plant significantly complicates the overall water management of the facility. Regardless of water quality considerations, every calorie of heat rejected results in removing unrecoverable pure water from the site, increasing water demand and raising the concentration of all of the constituents in the site wastewater. This impact is exacerbated in hot climates, where a significant cooling load is required just to cool make-up air to the required indoor temperature.

Cooling towers are often considered a good opportunity for reusing lower quality water. While this may be of merit, it is critical to evaluate the impact of the concentration effect of the tower on wastewater discharge. For a recent project in Saudi Arabia, the design included ammonia refrigeration-based cooling, which utilized air-cooled condensers. The capital cost was considerably more than the industry standard, and energy efficiency slightly less, but in the context of water supply limitations, it was a major factor for project success.

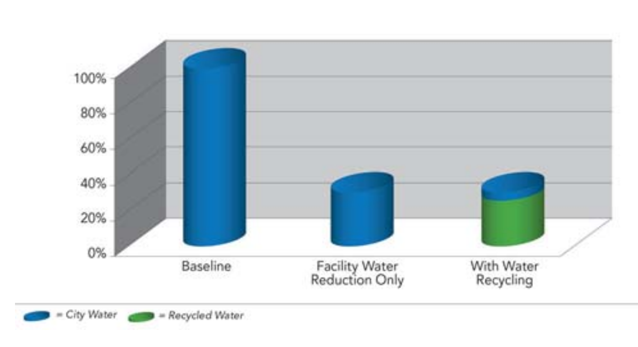

Figure 3. Potential reduction forecast of incoming water – reduction and recycling impacts.

Domestic water

Planning and design of sanitary water systems is a fairly well-defined practice, based on such simple factors as site population requirements for office, food, recreational, healthcare and other personnel facilities. There is little flexibility in the ability to optimize domestic water use, as system designs are heavily dictated by plumbing and sanitation codes.

In remote or developing areas, there may be no sanitary-waste infrastructure for connection. Packaged sanitary-waste treatment systems are readily available, but depend on not being loaded with process wastes. Onsite-treated sanitary effluent may be made suitable for reuse in agriculture. It is not conventional to return sanitary waste to reclaimed process-water systems, as the sanitary use is small compared to process systems usage levels and the potential contamination risk is moderately high. With the increased use of reclaimed tertiary effluent from municipal treatment plants, as with Singapore's NEW water and Fremont's purple pipe systems, consideration of onsite reuse of sanitary waste may become more popular.

Miscellaneous uses

There are always a number of assorted water uses that are not specifically identified or tied directly to processes. Analytical labs, parts cleaning, product conveyance and similar activities use unpredictable amounts of water and can inadvertently contribute unplanned contaminants to a wastewater or reclaim-water treatment system. Some of these minor uses may not be identified in early planning, but it is important to include them in the final water management scheme.

Supply water

Water supply to a manufacturing site is generally limited to the existing resources and infrastructure in the area of the site. Although the specific nature and cost of water are not primary site-selection criteria, the availability of a reliable water supply usually is. Most domestic water supplies are regulated to quality standards, but the actual quality delivered to a site will vary greatly within these standards.

Of course, the availability of adequate supply water volume is most important, but the quality of that water has a major impact on its use in the process, on the cost and complexity of process-water treatment systems and on wastewater disposal. In general, the higher the total dissolved solids or salinity and the higher the hardness, the more costly will be pretreating for process-water uses. Variability of water quality year-round must be reviewed to assure treatment systems are robust enough.

In parallel with the concentrating effect of cooling towers and scrubbers, the dissolved material in the incoming water significantly affects the total dissolved solids (TDS) of the wastewater from manufacturing. This is readily tracked in a WMD where the quality of the incoming water is allowed to be entered into a balancing model.

"One factor to consider is the impact of the wastewater from the new PV plant, in terms of influencing the quality of the reclaimed water derived from the very wastewater system to which the plant discharges."

Increasingly, alternative sources of water are being made available to industry from regional water reclaim activities. Treated municipal wastewater can be clarified and sanitized to a level that is quite suitable for onsite use in manufacturing and cooling systems. A new PV plant in California was required to show in its permitting documents how the future 'purple pipe' reclaimed water would be integrated into the facility upon its arrival in the near future; of course, there is little data available on the long-term water quality from this source. These options can have significant offsite resource management implications and should be considered on a local basis. One factor to consider is the impact of the wastewater from the new PV plant, in terms of influencing the quality of the reclaimed water derived from the very wastewater system to which the plant discharges.

Site effluent constraints

Surprisingly, the main constraints to increasing internal reclaim in manufacturing facilities are the limitations on wastewater discharged from the site. Fundamentally, a PV manufacturing facility brings in water from offsite, adds chemicals to it during processing, then evaporates away pure water in scrubbers, cooling systems and humidification systems. From a site balance perspective, the resulting wastewater will be significantly higher in concentration than the incoming supply water. Add to this efforts to treat and return process and domestic wastewater back to process water, and the effluent rises in concentration of contaminants proportionally to the rate of reclaimed water.

The principal constituents in wastewater can be categorized as dissolved solids (salts and minerals), dissolved organic matter, and suspended solids (both organic and mineral). Treatment processes are available to destroy some and remove all of these contaminants, but with varying degrees of cost and practicality. Organic matter can be degraded biologically and suspended solids removed with clarifiers and filters, resulting in solids for offsite disposal. However, dissolved solids are a different challenge. Specific regulated substances such as cadmium and fluoride can be targeted for treatment, but this usually results in further chemical addition, leading to an increase in TDS. The TDS limits for wastewater vary by site, but are becoming more challenging in the light of increased TDS in supply water, use of softeners in local residential use and the ultimate discharge point of the wastewater (sea, river or other).

In the extreme case, variations of 'zero liquid discharge' (ZLD) can be pursued at significant capital and operating costs. Such systems typically target membrane and thermal separation technologies to increase the salt concentrations up to brine or crystallization states. Use of solar evaporation in brine ponds is a common element in arid climates where land area is available for large ponds.

Conclusion

In the end, the choice of water treatment strategies is developed from a complex set of criteria, many of which are mutually interactive. Development of a water and material balance model estimating water use rates, contaminants and treatment efficiencies is required to evaluate the available alternatives within the constraints defined by incoming and effluent water. Invariably, capital and operating costs become significant decision drivers. The question is, what cost does one put on the future value of water?

About the Author

Ralph Williams PE is a process engineer with CH2M HILL. He holds an M.S. in chemical engineering from San Jose State University and a B.S. from Rensselaer Polytechnic Institute. Mr. Williams has more than 20 years' experience in studies/planning, engineering design, installation and troubleshooting of high-purity water, wastewater treatment, process-water reclaim/reuse, high-purity chemicals and facility support utility systems.

Enquiries

Ralph Williams PE
CH2M HILL
2020 SW 4th Avenue
Third Floor
Portland
Oregon 97201
USA
Tel: +1 503 224 6040
Email: ralph.williams@ch2m.com

Industrial symbiosis in photovoltaic manufacturing

Joshua M. Pearce, Department of Materials Science & Engineering and Department of Electrical & Computer Engineering, Michigan Technological University, Houghton, Michigan, USA

ABSTRACT

As the solar photovoltaic industry has matured from MW-scale pilot plants to large-scale mass manufacturing, costs of solar cells have steadily fallen. To further drive down costs of solar electricity beyond grid parity, a new approach that is being used is to investigate how photovoltaic manufacturing fits into the industrial ecology of a region. Optimizing the utilization of the waste associated with photovoltaic manufacturing itself and its components, while carefully considering geographic proximity, allows for industrial symbiosis. Industrial symbiosis engages traditionally separate industries in a collective approach to competitive advantage, involving physical exchange of materials, energy, water and/or by-products. Preliminary studies and industrial experimentation with co-production/co-location indicate that industrial symbiosis in photovoltaic manufacturing not only improves photovoltaic technology's already stellar life-cycle environmental performance, but also provides for additional revenue streams that can be used to further reduce photovoltaic device costs. For example, simply coupling a glass manufacturing plant making substrates to a GW-scale amorphous silicon thin-film photovoltaic manufacturing plant, and using recycled glass where technically viable, can lead to a reduction of 30,000 tons/year in raw materials and a 12% reduction in embodied energy. Coupling the glass plant to a greenhouse to make use of waste heat means that more than 700 tons of tomatoes can be grown each year. Both these material and energy savings and additional revenue streams contribute to lowering photovoltaic manufacturing costs, which will play a progressively more important role in photovoltaic manufacturing at the large (>GW) scale.

Introduction

Solar photovoltaic (PV) cells offer a technically sustainable solution to enormous projected future energy demands while helping eliminate the negative global destabilizing effects of the use of fossil fuels. With existing technologies, readily available materials and current conversion efficiencies found in manufactured solar modules, an insignificant fraction of terrestrially available sunlight is needed to power the global society [1]. Unfortunately, PV must further drive down costs to be economically competitive, due to both historic and current subsidies of conventional power [2–3] (including direct subsidies, e.g. the ability of oil and gas producers to treat as an expense rather than an asset the exploration and development costs [4]; and indirect subsidies, e.g. the artificial nuclear liability caps that enable the nuclear industry to exist [5]). This article explores the use of industrial symbiosis to help obtain economies of scale and increased manufacturing efficiencies for solar PV cells so that solar electricity can compete economically with heavily subsidized fossil-fuel-fired and nuclear-generated electricity.

Industrial symbiosis

In order to increase both the economic and the environmental performance of the manufacturing sector, large-scale PV manufacturers could be early adopters of industrial symbiosis. In industrial symbiosis, traditionally separate industries are considered collectively to gain competitive advantage by instituting the mutually beneficial physical exchange of materials, energy, water and/or by-products. The key benefits of utilizing industrial symbiosis are collaboration and the synergistic possibilities offered by geographic proximity [6]. Such a system collectively optimizes material and energy use at efficiencies beyond those achievable by any individual process alone. Industrial symbiotic systems such as the now-classic web of materials and energy exchanges among companies in Kalundborg, Denmark have spontaneously evolved from a series of small innovations over a long time-scale [7]. To accelerate the process of creating teams of companies to work together for mutual benefit, it is possible to both 1) engineer the design of the new solar PV manufacturing plants to take advantage of industrial symbiosis and 2) provide appropriate policy incentives. Here, the first approach is considered.

Industrial ecology around photovoltaic manufacturing

Industrial ecology is usually regarded as the study of material and energy flows through industrial systems. It is easy to draw parallels between flows in natural systems (as studied by biologists and ecologists) and the flows in industrial systems. If industrial ecology were applied to PV manufacturing, while looking for potential sources of industrial symbiosis, a large-scale (e.g. GW or multi-GW) PV factory would represent the heart of the ecosystem, which can be referred to as a next-generation eco-industrial park. An eco-industrial park of this type has been proposed [8] and is made up of at least eight symbiotic factories as seen in Fig. 1. The simplified flow of energy and materials between the eight factories is shown in this diagram.

Such a collection of factories would be located close to a major population centre, to provide raw materials, labour and a ready market. The first factory (1) is a conventional recycling facility, which is used to source the glass and aluminium needed to fabricate the solar cell from recycled materials (when viable) and thus have a lower embodied energy (95% lower for aluminium and 20% for glass) [9]. The raw glass from the recycling plant is fed into a sheet glass factory (2) and (at least initially) melted using natural gas. The glass factory outputs cut sheets of 3mm-thick glass with seamed edges and low iron content in order to obtain a high solar transparency. Finally, the glass is tempered for mechanical strength and coated with a transparent conductor, such as tin oxide, zinc oxide or indium tin oxide, to be used as a thin-film photovoltaic substrate [8]. The symbiosis between the glass plant and the PV plant will be detailed in the next section.

The production stages in the glass factory that utilize large amounts of heat have integrated thermal recovery to provide lower grade heat for the other facilities and a multi-acre greenhouse complex (3a). In the greenhouse complex, plants can be grown year-round (northern climates) utilizing the waste heat from the


simply
the best
VISIT US:
PVSEC HAMBURG,
HALL A4, STAND A9
GRINDING
CUTTING
GLUEING
AUTOMATION
ARNOLD
GRUPPE
SINCE 1950
BEST CHOICE FOR BRICK MANUFACTURING.
For more information: www.arnold-gruppe.de

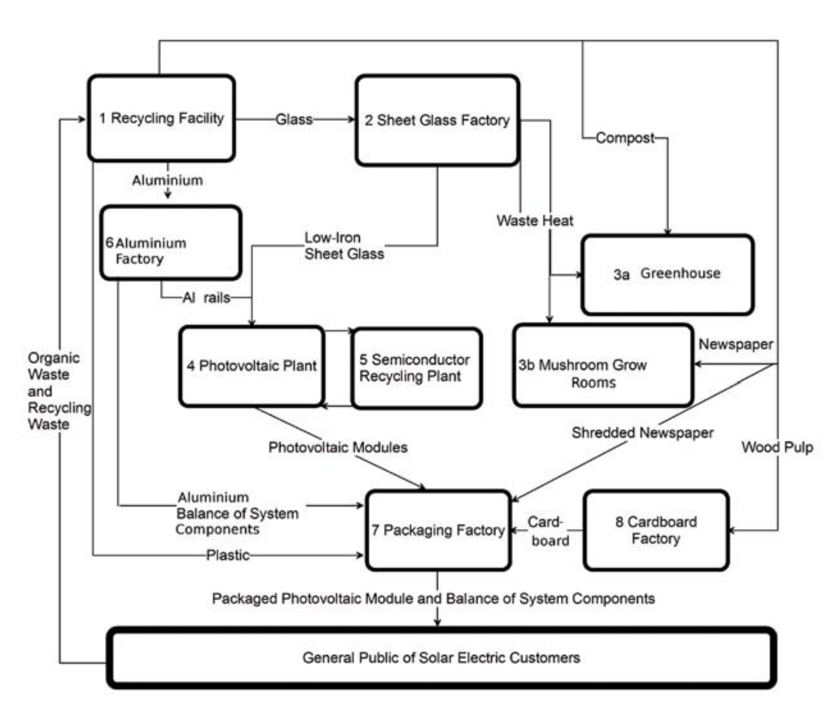

Figure 1. Material and energy flows of an eco-industrial park developed around photovoltaic manufacturing.

manufacturing plants in the eco-industrial park, and this approach will be detailed in a second example below. Similarly, the waste heat could instead (or in addition) be utilized to provide grow rooms for mushrooms (3b). In both agricultural plants, the food or other agricultural produce is sold outside of the park and the growing medium will be provided by the recycling facility (1), namely compost for the greenhouse (3a) and wood pulp or compost for the mushroom grow rooms (3b). In warmer climates, the waste heat could be used to drive absorption chillers to provide cooling (e.g. for an office building).

The substrates are then fed directly into the PV module plant (4), where a group of semiconductor and metal thin-film deposition systems create and pattern the active layers of the PV modules. All waste semiconductors and metals are captured and returned to a semiconductor recycling plant (5) to supplement the incoming and generally expensive high-purity materials going into the deposition systems. The output of the PV deposition and patterning lines will be solar PV modules ready for protective coatings and packaging.

Similarly to how glass from the recycling facility (1) could be used as raw material for the glass factory (2), the aluminium extracted from common drinking cans in the recycling facility (1) is fed into an aluminium fabrication factory (6) that will produce coated aluminium rails to be used for the racking components of the PV modules from the plant (4). The aluminium rails are extruded and used to provide a simple and inexpensive means of attachment to rooftops, ground-mounted systems or building-integrated PV installations. In addition, the extruded aluminium rails could be designed into the ground mounting and flat-roof mounting balance of system components. Again, as with the glass manufacturing plant (2), waste heat will be recovered and used in the symbiotic collective or to heat the greenhouse (3a) or mushroom grow rooms (3b). Next, in the packaging factory (7), the solar panels are interconnected if necessary and sprayed with a protective polymer coating to seal them to the environment. Some of the constituents of the polymer coating could again be acquired from the recycling facility (1), using common polymer chemistry. The panels are then wired with quick connects so they can be easily installed in the field by connecting to each other, or to an inverter or a battery bank. Finally, to prevent damage, the panels are packaged for shipment in cardboard boxes from the factory (8), which would gain its raw materials from the recycling facility (1), and the panels possibly cushioned with shredded newspaper, again from the facility (1).

"By co-locating these factories in the eco-industrial park, both the transportation costs and the transportation energy between them can be minimized, and many of the inputs for the solar PV plant can actually come from waste products generated in the surrounding population centres."

By co-locating these factories in the eco-industrial park, both the transportation costs and the transportation energy between them can be minimized, and many of the inputs for the solar PV plant can actually come from waste products generated in the surrounding population centres. It is important to note that each factory should be scaled appropriately for the symbiotic system and should be individually profitable so that independent businesses can replicate this model by co-locating and benefit from industrial symbiosis in future facilities. To understand how this scaling needs to take place, the

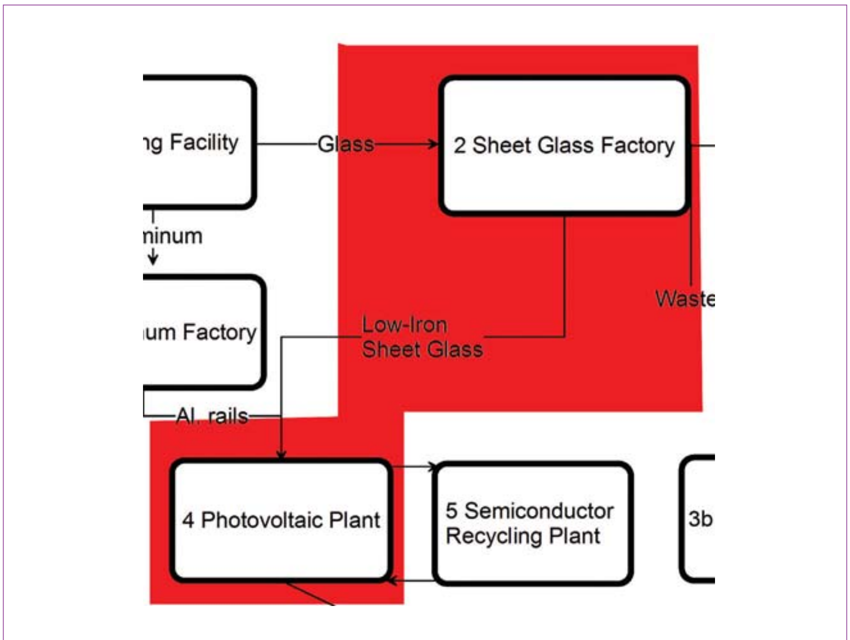

Figure 2. Detail of industrial symbiosis between PV and glass manufacturing.

relationship between PV manufacturing (4) and a glass factory (2) are quantified below.

Industrial symbiosis between PV and glass manufacturing

Building an industrially symbiotic system around the PV manufacturing plant (4) involves optimization of the other plants around it. Here the potential symbiosis of co-locating the glass plant (2) and the PV plant (4) as seen in Fig. 2, and using recycled glass, will be investigated.

The optimization of the glass plant component of the PV eco-industrial park in Fig. 1 is achieved through first quantifying the raw materials and energy requirements required for the production of glass needed by the PV plant, and then allocating the by-products of the glass manufacturing factory to other elements of the PV eco-industrial park. The sheet glass factory provides both substrates and, potentially, back cladding for the PV. Optimization occurs if the demand for the glass materials is large enough to warrant a dedicated line that produces solar-grade glass. This is necessary because glass specifically manufactured with low iron content for PV cells can increase the sunlight entering the cell by about 15% and deliver a corresponding improvement in device performance [8]. In current solar PV manufacturing lines for thin films, altering the glass recipe for small batches is uneconomic, but this is reversed at large scales of manufacturing [10]. Sheet glass is rarely customized for PV cell production (although this is rapidly changing as PV manufacturers couple with glass manufacturers). A recent study quantified the energy savings for a 1GW PV factory constructed due to energy policy in Ontario, assuming a PV output of 100W/m^2, 3mm-thick glass and the use of 40% recycled cullet for the back glass [11].

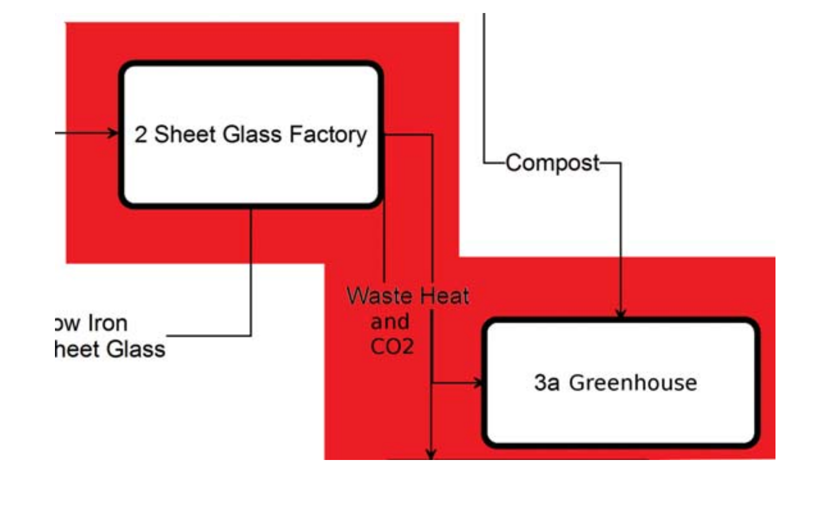

Figure 3. Industrial symbiosis between glass manufacturing and a greenhouse complex.

As can be seen in Table 1, the major benefit of the industrial symbiosis between a PV plant and a glass plant is dramatically reduced transportation energy costs, as well as a reduction in the energy required to produce the back glass, due to the increased allowable cullet content. The transportation numbers assumed a specific energy of 110GJ/mile over a distance of 286 miles (461km). It can be seen that in this case the industrial symbiosis optimum uses 12% less energy, which equates to 5266 tonnes of crude oil. In addition, reductions of 30,000 tons/year in raw materials are achieved if using cullet. These savings in energy and materials can be directly related to reductions in economic costs.

Embodied energy	Status quo (GJ)	Industrial symbiosis (GJ)
Front glass	827,500	827,500
Back glass	827,500	761,300
Transportation	155,000	~0
Total	1,810,000	1,588,800

Table 1. Energy use per GW PV [11].

Industrial symbiosis between glass manufacturing and a greenhouse complex

As was examined in the previous section, coupling two industries together so that one (the glass plant) conventionally feeds the other (PV plant) is not particularly revolutionary and is common in many industries. Where industrial symbiosis really begins to stand apart from conventional industry is when groups of companies can work together as a team and begin to eliminate waste by finding by-product synergies. If the glass plant is examined, it is clear that its two primary 'waste' products are heat and carbon dioxide.

A recent study developed a technical and economic methodology to determine the viability of establishing 'waste heat greenhouses', which use the waste heat from industrial processes in northern climates [12]. A case study was presented of an exchange between a tomato greenhouse and a sheet glass manufacturing plant (ideal for fabricating substrates for the PV industry) as shown in Fig. 3.

The glass plant in the case study produces 500 tons of glass per day, making it a mid-sized float glass operation [13], and utilizes 1.25PJ of natural gas a year [14]. The entire waste heat system is shown in Fig. 4 with the proposed structure and energy flows.

In addition to the heat, the carbon dioxide (CO_2) can, if properly treated, also be useful to the greenhouse complex. Modern greenhouse operations utilize CO_2 enrichment in order to increase crop yields. Particularly in a tightly sealed greenhouse being heated in the wintertime, CO_2 enrichment is required, as a minimum, to maintain the atmospheric concentration of CO_2 at ambient levels (around 380ppm) to account for plant photosynthesis [15]. In Canada, using extremely conservative estimates, it has been found that a sheet glass plant could support a greenhouse complex of about four acres, where 700 tons of tomatoes can be grown each year and can offset between 1000 and 2000 tons of CO_2 annually. Additionally, it has been shown that over a 20-year campaign with a 10% minimum acceptable rate of return (MARR), the waste heat system is significantly less expensive to operate than a purely natural gas system. Finally, the addition of a waste heat greenhouse can reduce the costs of emissions compliance for a company, as the deferred costs of liquid CO_2 can fund millions of dollars for emissions reduction retrofits [12].

The bottom line of this analysis is that, from the greenhouse perspective, the waste heat system is significantly more economic to operate than a purely natural gas system. These economic gains can be transferred to the glass factory since the by-products (heat and CO_2) can be sold for a profit, which can thus lead to a further reduction in glass costs, in turn providing the potential to reduce the costs of PV modules. These savings can provide a significant competitive advantage over those PV manufacturers who do not look beyond their own gates for synergies.

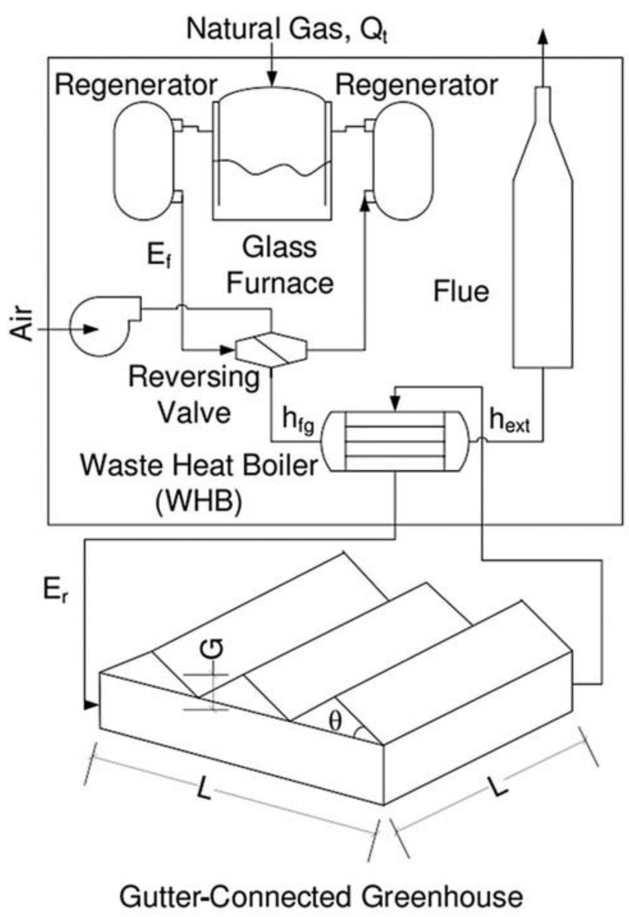

Figure 4. Detail of industrial symbiosis between glass manufacturing and a greenhouse complex showing system structure and energy flows.

Conclusions

This article summarized the technical requirements and some of the preliminary work for a symbiotic industrial system around solar photovoltaic manufacturing, to increase manufacturing efficiency and improve ecological impact while reducing costs. This set of technical concepts, coupled with potential incentive-based policies formulated to encourage them, can be viewed as a medium-term investment by a government interested in speeding up the advance of renewable energy and creating green jobs, which will not only see financial return directly, but also lead to an improved global environment, enhanced national energy security and international favour.

References

[1] Pearce, J.M. 2002, "Photovoltaics – a path to sustainable futures", *Futures*, Vol. 34, No. 7, pp. 663–674.

[2] Roth, I.F. & Ambs, L.L. 2004, "Incorporating externalities into a full cost approach to electric power generation life-cycle costing", *Energy*, Vol. 29, pp. 2125–2144.

[3] Koplow, D. & Dernbach, D. 2001, "Federal fossil fuel subsidies and greenhouse gas emissions: A case

study of increasing transparency for fiscal policy", *Annu. Rev. Energy and Env.*, Vol. 26, pp. 361–389.

[4] Jt. Comm. Taxation 1999, *Estimates of Federal Tax Expenditures for Fiscal Years 2000–2004*, Rep. JCS-13-99, Washington, DC: US GPO.

[5] Zelenika-Zovko, I. & Pearce, J.M. 2011, "Diverting indirect subsidies from the nuclear industry to the photovoltaic industry: Energy and economic returns", *Energy Policy*, Vol. 39, No. 5, pp. 2626–2632.

[6] Chertow, M.R. 2000, "Industrial symbiosis: Literature and taxonomy", *Annu. Rev. Energy and Env.*, Vol. 25, pp. 313–337.

[7] Jacobsen, N.B. 2006, "Industrial symbiosis in Kalundborg, Denmark: A quantitative assessment of economic and environmental aspects", *J. Ind. Ecol.*, Vol. 10, pp. 239–255.

[8] Pearce, J.M. 2008. "Industrial symbiosis for very large scale photovoltaic manufacturing", *Renewable Energy*, Vol. 33, pp. 1101–1108.

[9] Milne, G. & Readon, C. 2005, "Embodied Energy", in *Your Home Technical Manual: Australia's guide to environmentally sustainable homes.* Commonwealth of Australia.

[10] Keshner, M.S. & Arya, R., 2004, "Study of potential cost reductions resulting from super-large-scale manufacturing of PV modules", Final Subcontract Report (SR-520-36846), NREL, USA.

[11] Nosrat, A.H., Jeswiet, J. & Pearce, J.M. 2009, "Cleaner production via industrial symbiosis in glass and large-scale solar photovoltaic manufacturing", *Proc. 2009 IEEE Toronto Int. Conf. Sci. and Tech. for Humanity (TIC-STH)*, Toronto, Canada, pp. 967–970.

[12] Andrews, R. & Pearce, J.M. 2011, "Environmental and economic assessment of a greenhouse waste heat exchange", *J. Cleaner Prod.*, Vol. 19, pp. 1446–1454.

[13] Pellegrino, J., Sousa, L. & Levine, E. 2002, "Energy and environmental profile of the U.S. glass industry", Final Report, Office of Industrial Technologies, U.S. Department of Energy.

[14] U.S. Department of Energy 2007, Industrial Assessment Centers Database [available online at http://www1.eere.energy.gov/industry/bestpractices/iacs.html].

[15] Chalabi, Z.S. et al. 2002, "Structures and environment: Optimal control strategies for carbon dioxide enrichment in greenhouse tomato crops, Part 1: Using pure carbon dioxide", *Biosys. Eng.*, Vol. 81, No. 4, pp. 421–431.

About the Author

Dr. Joshua M. Pearce is currently an Associate Professor cross-appointed in the Department of Materials Science & Engineering and in the Department of Electrical & Computer Engineering at Michigan Technological University. His research concentrates on the use of appropriate open-source technology to find collaborative solutions to problems in sustainability. His research spans areas of electronic device physics and materials engineering of solar photovoltaic cells, and novel photovoltaic systems and resource simulations. He has over 100 publications focused on photovoltaic technology and regularly consults for photovoltaic-related start-ups, manufacturers, developers, VCs and banks.

Enquiries

Dr. Joshua M. Pearce
Department of Materials Science & Engineering
512 M&M Building
Michigan Technological University
1400 Townsend Drive
Houghton, MI 49931-1295
USA
Tel: +1 906 487 1466
Email: pearce@mtu.edu
Website: http://www.mse.mtu.edu/faculty/pearce.html

Materials

MEMC points to 40% decline in PV industry wafer prices in 2Q while hit by weak demand

Excluding the one-time financial benefit of a US$149.4 million influx from a recently announced wafer supply contract cancellation with Suntech, MEMC's solar materials business took a significant hit across key financial metrics in the second quarter of 2011. Solar material revenue was US$323.1 million in 2Q, down 1% sequentially. However, were it not for the Suntech payment, solar material revenue would have been US$173.7 million, a 47% decline from the first quarter.

Solar wafer volumes declined 40% in the second quarter and wafer pricing fell 17% compared with the previous quarter. MEMC management noted that wafer prices in general had fallen 40% from the first quarter.

MEMC posted GAAP revenue in the second of US$746 million, while excluding the Suntech cash benefit, revenue would have been US$596.2 million, a 19% decline sequentially. The decline, excluding Suntech was said to be due to weaker solar wafer pricing and volumes as well as the timing of some SunEdison PV project completions. Management also noted that uncertain solar demand, especially in Europe were to blame.

Source: MEMC

MEMC posted GAAP revenue in the second of US$746 million; excluding the Suntech cash benefit, revenue would have been US$596.2 million, a 19% decline sequentially.

Management noted in a conference call to discuss quarterly results that a further US$29 million of deferred revenue from Suntech was expected to be realized in the second half of the year. MEMC's solar materials business operating profit was US$89.2 million, compared to US$39.4 million in the 2011 first quarter, and US$19.1 million in 2Q10.

The sequential increase was driven by the Suntech contract resolution, partially offset by US$52.4 million in cost of goods sold charges resulting from adverse purchase obligations, US$1.3 million in restructuring charges, and a $14.2 million charge due largely to low initial volumes at Kuching (300mm semiconductor wafers) as the ramp of that facility progresses, according to the company.

Polysilicon News Focus

ReneSola starts producing in-house steel wire, develops higher capacity casting furnace

ReneSola has recently progressed on two manufacturing fronts, with the start of trial production of its in-house steel wire used for slicing solar wafers and the development of a new generation of higher capacity casting furnaces. The company expects to reach a production capacity of 8400MT for its steel wire by the end of 2011. ReneSola believes the in-house wire will cost significantly less than the material provided by the company's current suppliers.

The new G6 casting furnaces will each have a capacity of 650kg and annual output of 8MW, compared to approximately 6MW for ReneSola's current furnaces. The company also plans to upgrade some of its existing casting furnaces through proprietary techniques, which will increase output to approximately 7MW. It will replace all current casting furnaces with the new G6 casting and upgraded tools as early as the end of 2011, the company said.

centrotherm SiTec draws first 450kg ingot for customer; adds diamond wire-based sawing to services range

centrotherm SiTec has claimed a new milstone with 'first ingot out' using its newly designed multicrystalline ingot furnace at Chinese state-owned polysilicon company in Shaanxi Province, China. centrotherm SiTec claimed the ingot exceeded market standards.

Source: centrotherm SiTec

centrotherm SiTec has claimed a new milestone with 'first ingot out' using its newly designed multicrystalline ingot furnace at Chinese state-owned polysilicon company in Shaanxi Province, China.

According to SiTec 'first ingot out' milestone means that the company has demonstrated it can offer technology along the entire solar value chain, and not only in the polysilicon and solar cell areas.

The company is also providing diamond wire-based saw technology for ingot squaring and brick cropping. The company claims that the annual sales potential for the two new equipment systems amounts to double-digit millions of euro.

centrotherm SiTec said that its ingot squaring equipment is set up for an annual capacity of up to 4,400 ingots, corresponding to annual production of around 110,000 bricks. The brick cropping equipment that is said to operate two bricks in parallel is claimed to reach an annual capacity of around 40,000 bricks.

Daqo receives US$150 million loan from Bank of China to expand polysilicon production

China-based polysilicon manufacturer Daqo New Energy has received a US$150 million loan approval from Bank of China, through its Shihezi branch in Xinjiang, China to support its 'Phase II' polysilicon expansion plan in Xinjiang. The loan will take the form of a six-year long-term project finance loan while the company's polysilicon production remains at 100% utilization.

"With this loan, we are confident that we have the funding needed for the completion of the initial phase of our polysilicon expansion plan in Xinjiang," noted Jimmy Lai, CFO of Daqo New Energy.

Jimmy Lai, chief financial officer of Daqo New Energy.

In separate news, the company's second-quarter financial results have shown that polysilicon production is still at 100% utilization and that there was no remaining inventory at the quarter's end.

Daqo guided that 975–990MT of polysilicon will be shipped in the third quarter. The company expects to ship 10MW of wafer as well as 20MW of modules in this timeframe.

Business News Focus

Applied Nanotech signs licensing agreement with YHCC for its solar ink and paste technology

Applied Nanotech Holdings and Chinese company YHCC signed a licensing agreement for Applied Nanotech's solar ink and paste technology. The announcement is the first license agreement between the two companies since they entered into a strategic relationship in February.

The license agreement calls for Applied Nanotech to collect an upfront payment of US$2 million with ongoing royalties of 3% on sales of solar inks and pastes by YHCC. The first US$1.5 million of the initial payment will be due no later than August with the remaining US$500,000 billed in April 2012, assuming that certain technical specifications have been completed.

The license agreement gives YHCC exclusive authorization for Applied Nanotech's solar ink and paste technology in Asia, but excludes Korea and Japan. YHCC has already started construction on a manufacturing facility in China that will produce the solar inks with plans to have Applied Nanotech's aluminium pastes as its first produced products. The manufacturing and selling of the goods is expected to begin in 2012.

The two companies advised that they will continue to discuss other collaboration opportunities as Nanotech's solar inks will be the first products to come out of the strategic partnership.

Saint-Gobain plans to buy Specialty Film unit from Bekaert

Saint-Gobain has disclosed plans to acquire the Solar Gard Specialty Films unit from Bekaert, which will be housed under Saint-Gobain's Performance Plastics division. The agreement, the price of which was not revealed, includes production facilities in San Diego, California, Zulte, Belgium and Suzhou, China, as well as operations under development in China and all global sales and service centres.

Bekaert originally purchased the Specialty Films business in 2001, but found that technological collaborations have been limited over the 10-year period. The purchase is contingent to customary closing conditions, with both companies expecting the deal to be finalized throughout the rest of this year. Conditional on final determination of transaction costs and other expenses, Bekaert anticipates the deal to bring it a capital gain of nearly €10 million and reduce the company's consolidated net debt to around €80 million.

Source: Bekaert Specialty Films LLC

Bekaert's Solar Gard window film range will be taken over by Saint-Gobain.

GT Solar becomes GT Advanced Technologies

Company name changes can often be as part of a rebranding exercise, sometimes due to poor performance or turmoil. But this is not the case with GT Solar, which is outperforming much of its competitor base in the PV equipment market sector. Having secured approximately US$1 billion in order backlogs for its new foray into the LED sapphire wafer manufacturing market and hints by executives of further acquisitions, a new name, GT Advanced Technologies, was seen as better reflection of what the company is now doing and where it intends to play in the future.

Talking to PV-Tech, Tom Gutierrez, GT Advanced Technologies' president and CEO noted that GT had outlived the 'solar' tag and that it was important to have retained the 'GT' aspect as it was the market leader in its fields served.

The 'Advanced Technologies' addition to its name reflects the company's development plans, including the company's 'Monocast' technology, a hybrid technology intended to benefit from lower-cost multicrystalline casting techniques but which produces monocrystalline type purity and higher performing wafers and cells.

However, GT Advanced Technologies is not about to move into the upstream or downstream markets. Gutierrez was adamant that the company remain within its "crystal expert strategy," leveraging core expertise and business models to different industries that have similar profiles to those it has helped influence such as its recent move in the sapphire wafer market for LED production.

GT ADVANCED TECHNOLOGIES

Source: GT Advanced Technologies

GT Advanced Technologies' new logo.

Heraeus's PV unit triples the size of its global technical staff

Having recently announced the completion of its third research and development centre in Singapore, the PV business unit of Heraeus advised that it has tripled the size of its global technical staff so that it can more easily meet the demand for its products and customer timeframes. The Singapore facility joins the company's US and Germany R&D sites, as well as Heraeus's Shanghai and Taoyuan application centres.

Heraeus has tripled its global technical staff base in order to meet customer demand for its products.

"We offer our customers the option to come to one of our research and development sites to personally work with our team," said Andy London, VP of Heraeus Materials Technology in West Conshohocken.

Other News

GCL-Poly starts construction of R&D hub

Billed as the future R&D hub for GCL-Poly's future technological developments spanning polysilicon through to manufacturing equipment, the company has started construction of its 'Industrial Application Research Institute,' located in Suzhou, China. The R&D hub will be operated under GCL-Poly, Suzhou GCL-Poly Industrial

Materials Order Focus

GT Solar wins polysilicon equipment order from new customer in Asia

A new unidentified customer in Asia has placed its first order with GT Solar for polysilicon production equipment totalling US$55.1 million. The order was included in the GT Solar's backlog for the first quarter of FY12, which ended on July 2.

The new order includes a complete range of polysilicon production equipment including hydrochlorination equipment used for the production of TCS, SDR reactors, filament and product processing equipment, and other polysilicon production equipment provided by GT Solar. Delivery lead times were not disclosed.

GCL-Poly to supply 4,200MW of wafers to Realforce Power

China-based PV cell and module manufacturer Realforce Power Co has entered into a long-term wafer supply deal with GCL-Poly. Under the supply contract, GCL-Poly will provide a total of 4,200MW of solar wafer products from July 2011 to December 2016. A price adjustment mechanism is included in the contract, according to the wafer producer. GCL-Poly has been providing wafers to the three-year-old start-up for some time.

Realforce Power claims it will reach a cell capacity of 700MW by the end of the year, up from 300MW earlier in the year. At end-of-year capacity figures, the deal would indicate that the majority of its wafer requirements could be met by the new long-term contract with GCL-Poly. Realforce Power was established in 2008 in Jining, Shandong province, China.

Praxair wins hydrogen supply contract for Hemlock's new polysilicon plant

Hemlock Semiconductor's new polysilicon plant, currently under construction in Clarksville, Tennessee, USA has signed a multi-year contract with Praxair for the latter to supply hydrogen to the facility. Praxair said it would build and operate an on-site hydrogen generating facility and supply liquid hydrogen by truck. The plant start-up is scheduled for 2012, according to Praxair. Praxair also supplies nitrogen and hydrogen to Hemlock's polysilicon facility in Hemlock, Michigan.

Hemlock's new plant is expected to have an initial capacity of greater than 10,000MT and the potential to be expanded to 21,000MT. The project is expected to come on stream next year at an initial cost of US$1.2 billion.

Suntech cancels 4.6GW wafer supply deal with MEMC; incurs US$212 million costs

A 2006 long-term wafer supply deal between Suntech and MEMC has been 'mutually terminated' at a cost to Suntech of approximately US$212 million. Suntech said that the decision to cancel the wafer supply deal was due to 'rapid changes in the market for silicon wafers.' Suntech also announced that it was stopping investment in CSG Solar's research and development operations, which focused on crystalline silicon thin-film technology. MEMC remains a wafer supplier to Suntech under other supply agreements.

GCL places US$193-million order with Meyer Burger

Jiangsu GCL Silicon Material Technology Development has placed an order totalling CHF160 million (US$193 million) for Meyer Burger's wire saws and wafer inspection systems. The equipment, produced by MB Wafertec and Hennecke, will be used to help GCL meet rising demand for its high-grade multicrystalline solar wafers.

Application Research Institute (GCL-Poly Research Institute) and is claimed to be the first industrial application-oriented R&D institution in China.

Shu Hua, Executive President of GCL-Poly, said, "By recruiting top R&D talents and installing sophisticated R&D equipment, GCL-Poly Research Institute will become the leading technological unit and innovative engine of GCL-Poly, enabling GCL-Poly to make a brand-new step in its technological development for its ever-expanding renewable energy business."

The new R&D hub will work closely with GCL-Poly's R&D Centre located in the US in the State of Washington, and is expected to attract top scientists from both within China and overseas.

Source: GCL-Poly

GCL-Poly staff inspect a polysilicon brick.

Ferro offers two new low-cost silver conductor pastes

Two new products that are claimed to reduce cost per watt while maintaining the same adhesion, solderability, and field reliability as current commercial products are being showcased at Intersolar North America by Ferro Electronic Materials. Ferro's new PS 2130 and PS 2131 rear silver pastes have pure silver metallurgy and enable fast printing at speeds of more than 200mm per second, while retaining compatibility with its back surface aluminum pastes, which are said to be co-fired in a wide processing window.

The PS 2130 and PS 2131 silver pastes are designed for target fired thicknesses of 5–7µm and 4–6µm, respectively. Ferro said that the new lead-free pastes offer a typical solar plant savings of up to US$5 million per year. This is based on the current cost of silver and a plant manufacturing 500MW of silicon solar cells annually.

Source: DuPont

DuPont's 'Tedlar' PV2400 polyvinyl fluoride (PVF) film.

Toppan boosting 'Tedlar' PV2400 PV backsheet production via new agreement with DuPont

DuPont has extended the rights of a license agreement with Toppan that will double Toppan's immediate supply capability for the full-scale commercial production of DuPont Tedlar PV2400 polyvinyl fluoride (PVF) film. Toppan's capacity levels were not disclosed.


www.hyundaisolar.com
Imagine
How a single Solar Module
Can save the tree
With a 240Wp solar module
It can reduce the CO_2 as much as 24 big cone pine trees
Solar Energy, that reduces risks of air pollution…
Maintains a younger, healthier lung for the earth
Save my Friends
Hyundai Invites you
to our booth at
EU PVSEC Sep 05th-08th
Booth No. B5/B16
Sales & Marketing, 140-2, Gye-dong, Jongno-gu, Seoul, Korea, 110-793
Tel: +82-2-746-8406, 7589 Fax: +82-2-746-7675 E-mail: hyundaisolar@hhi.co.kr
HYUNDAI
HEAVY INDUSTRIES CO.,LTD.

Product Reviews

Arnold Gruppe

Arnold's squaring saw uses two diamond cutting discs for monocrystalline brick production

Product Outline: Arnold Gruppe has introduced a new squaring saw for monocrystalline brick production that claims to be extremely robust. The type 72/746 squaring saw employs two diamond cutting discs working in parallel that are claimed to reduce kerf loss and increase throughput.

Problem: Monocrystalline wafers offer higher cell efficiencies but have been characterized by higher costs than multicrystalline wafers. Reducing monocrystalline wafer processing costs is a key goal for their competiveness. Replacing conventional saws with diamond cutting discs could eliminate slurry uses and significantly reduce kerf loss.

Solution: The type 72/746 squaring saw employs two diamond cutting discs working in parallel (diameter 700mm) to simultaneously process two sides of a brick in one step. The work piece must be turned only once by 90° in order to process the opposite side, shortening the processing time and improving throughput. The flexible clamping concept offers the possibility of cropping the ingot before the squaring process. For example, one raw ingot with a maximum length of 3000mm or up to five individually cropped ingot pieces with a length between 180mm up to maximum of 1000mm can be processed in one step by making use of the total loading length.

Applications: Monocrystalline brick sawing for volume production.

Platform: The system is controlled by the Arnold Remote Production Analysis Tool (ARPAT), adhering to SEMI E10 standard, and includes the speed, torque of cutting spindle and other information. ARPAT disposes of an open interface to the supervisory MES (Manufacturing Execution System).

Availability: September 2011 onwards.

ECM

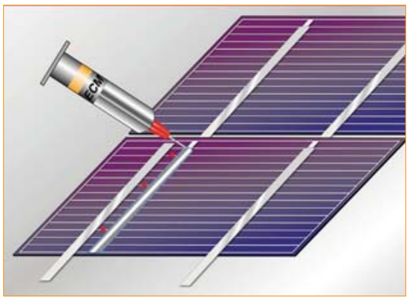

ECM offers two new cost-conscious conductive stringer attach adhesives

Product Outline: Engineered Conductive Materials (ECM) has introduced two new Conductive Stringer Attach Adhesives that are said to reduce costs and can both be used for thin-film, organic and thinned silicon solar modules. The DB-1541-S3 adhesive employs a material formulation that has been optimized for improved conductivity and stability on molybdenum substrates while reducing the silver content to reduce cost. The DB-1538-2 adhesive is available as a one- or two-part adhesive, allowing cost savings on dry ice shipments and -40°C storage.

Problem: Materials make up a considerable part of the cell and module production costs. Efforts are required to offer lower material costs while maintaining quality to provide required end-product lifetime requirements.

Solution: The DB-1541-S3 has more than 12% lower silver loading than the standard DB-1541-S series of conductive stringer attach adhesives, resulting in a significant price reduction while maintaining optimized rheology. The DB-1541-S3 features a rubber-like flexibility that can be used for flexible photovoltaic applications with high peel strength to withstand the stresses induced in reel-to-reel manufacturing processes. The DB-1538-2 Conductive Stringer Attach Adhesive features low bleed on AZO and other transparent conductive oxides while maintaining optimized rheology for dispensing. The DB-1538-2 series absorbs stress to withstand thermal cycling from -40°C to 85°C as required for IEC certification.

Applications: Both the DB-1541-S3 and DB-1538-2 can be used in thin-film, organic and thinned silicon solar modules.

Platform: The DB-1538-2 Conductive Stringer Attach Adhesive is available as a one- or two-part adhesive, while the DB-1541-S3 can be used for flexible photovoltaic applications.

Availability: Currently available.

Zimmermann & Schilp

Zimmermann & Schilp offers ultrasound non-contact handling technology for c-Si wafers

Product Outline: Zimmermann & Schilp's non-contact PV wafer handling systems use an ultrasound air bearing for completely new ways of handling c-Si wafers. The PV technology roadmap dictates that thinner PV wafers will be necessary to aid in material cost reduction, along with equipment performance improvements and higher efficiencies.

Problem: Crystalline solar wafers are extremely fragile and can experience breakages brought about by the various handling technologies in the solar cell manufacturing chain. Material stress can be generated during the handling process, destroying the edges or shattering the wafer, or generating microcracks inside the wafer which are not visible to the human eye.

Solution: Zimmermann & Schilp's non-contact PV wafer handling systems are designed to handle wafers without touching the surface. As a result, wafers can be transported without friction, using pins to touch the wafer edges only with one gram of force. Transportation of wafers from the top side is also possible using this method. Maximum throughput of one track is >7000 wafers/h with a breakage rate of 0.005%. The system has a minimal footprint, consuming only 10% of energy compared with other non-contact handling technologies.

Applications: The technology is suited to loading and unloading of multitrack belts, wet bench cassettes, quartz boats or matrix trays. Systems can also be modified for wafer buffering or other customized applications.

Platform: The systems are extremely flexible, fit several material flow configurations and are ideal for equipment retrofittings.

Availability: Currently available.

Reducing polysilicon materials costs

Jan Maurits, Poly Plant Project, Inc., Burbank, California, USA

Fab & Facilities

Materials

Cell Processing

Thin Film

PV Modules

Power Generation

Market Watch

ABSTRACT

It is well known that the cost of silicon materials is the major cost factor in crystalline silicon PV module production. Polysilicon price accounts for about 30% of total module production costs. While the PV industry has set a polysilicon price target of US$40/kg by 2015, this goal will not be reached if demand continues to exceed supply and if new plants cannot reduce operating costs below US$25/kg. Given a continued 30% annual growth in demand for PV modules, new polysilicon plants and expansions are needed to avoid shortages of high-purity, cost-effective polysilicon. This paper discusses the major factors in polysilicon production costs, the important elements of polysilicon plant design for reducing operating costs, the key cost elements of polysilicon plant operations, and how the design of polysilicon products can reduce crystal growth costs.

Polysilicon demand and supply

Government solar energy associations around the world have detailed their national policies on solar energy at recent conferences. A summary of the national plans charts a continued annual growth rate of over 30% through the next ten years [1,2,3]. Crystalline silicon PV module demand is projected to continue at an average annual growth rate of 30% for the same period, resulting in a demand of over 1 million metric tons of polysilicon per year by 2020. Since worldwide polysilicon production was about 130,000 tons in 2010, production volume will have to increase by 800% to meet demand in 2020. However, polysilicon supply has been increasing at a rate of only 20–22% per year. Even with significant gram/watt conversion rate improvements, polysilicon demand will exceed projected supply, creating shortages that will result in high prices if a number of new plants are not built over the next three years. To avoid a shortage, several new plants and expansions are required, designed for producing high-purity polysilicon at an operating cost < US$25/kg.

"Since worldwide polysilicon production was about 130,000 tons in 2010, production volume will have to increase by 800% to meet demand in 2020."

Cost element	Cost/kg of polysilicon (US$)
Trichlorosilane production	9–12
Electricity	3.5–7
Labour	3.5–5
Materials	2
Maintenance	2
Amortization	0–10
Total	20–38

Table 1. Polysilicon production costs for the Western nation polysilicon suppliers.

Polysilicon production cost elements

The estimated polysilicon production costs for the Western nation polysilicon suppliers are shown in Table 1.

Trichlorosilane production costs

Trichlorosilane (TCS, $SiHCl_3$), used to produce polysilicon, is synthesized either by *direct chlorination*, the exothermic reaction of metallurgical-grade silicon (MG Si) and hydrogen chloride (HCl), or by *hydrochlorination*, the endothermic reaction of MG Si and silicon tetrachloride (STC, $SiCl_4$) in a hydrogen atmosphere. Production costs of TCS range from US$1.50 to $2.00/kg depending on production volume, MG Si cost, HCl or STC cost, TCS yield, electrical power rates, labour and utility costs.

After synthesis, the TCS is purified in a series of distillation columns designed to produce 11-nines (99.999999999 weight %) purity polysilicon with a minimal loss of chlorosilanes. The losses of chlorosilanes in the production and purification process have a major impact on operating costs and can be held to less than 15%. The weight of silicon in the trichlorosilane molecule is 20.6%, so the maximum conversion of TCS to polysilicon is 4.9:1. The 1–2% impurities in MG Si are reduced to sub-part-per-billion (sub-ppb) trace levels by converting to chlorosilane, chloride and hydride compounds, which accounts for the losses in trichlorosilane.

With a purification system based on impurity thermodynamic data, computer simulation and operational plant experience, the ratio of TCS to polysilicon is 6:1. This assumes recovery of the co-product gases, especially the STC. If the STC is not recovered from the synthesis reaction and from the chemical vapour deposition (CVD) reactor vent gas, the ratio of TCS to polysilicon is 20:1. TCS production costs range from about US$1.50 to $2.00/kg, so the conversion ratio determines the cost element of TCS

TCS production costs	@$1.50/kg	@$1.75/kg	@$2.00/kg
	($/kg)	($/kg)	($/kg)
Conversion ratio TCS:poly 6:1	9.00	10.50	12.00
Conversion ratio TCS:poly 8:1	12.00	14.00	16.00
Conversion ratio TCS:poly 10:1	15.00	17.50	20.00
Conversion ratio TCS:poly 20:1	30.00	35.00	40.00

Table 2. Effect of the conversion ratio of TCS to polysilicon on polysilicon production costs.

in the final polysilicon product as shown in Table 2. Poorly designed distillation systems with an excessive number of columns, high chlorosilane losses and/or poor STC recovery systems have a significant impact on operating costs. These systems must be upgraded to realize major cost reductions.

Electricity, utility and labour costs

Electricity rates are region and site specific and subject to unexpected increases. This is a major factor in site selection and it is the primary reason that new plants and expansions are limited in Europe. In addition to low rates, the electrical power must be non-interruptible, meet technical specifications and be available in long-term contracts. Two separate feed lines coming into the plant minimize the risk of power failure, which is a critical safety issue in a polysilicon plant; moreover, unplanned outages can cost tens of millions dollars in lost production. Per kg of polysilicon, total electrical power consumption for an entire plant ranges from about 90 to over 140kWh. Electrical use is reduced by use of steam, recovery of process heat, use of energy-efficient equipment and overall plant design for energy efficiency. Power consumption for TCS production, purification, deposition, and gases recovery is shown in Table 4.

Utilities are also site specific and vary greatly from region to region. The availability of hydrogen and nitrogen gases, fresh water and natural gas must also be considered in site selection. In some remote areas, hydrogen and nitrogen, in addition to HCl, must be synthesized. This adds to the operating costs as well as to capital expenditure (capex). Labour rates are similar from country to country, except for the much lower rates currently available in China.

Item	USA	MENA	Korea	China	Europe
Electricity ($/kWh)	0.03–0.04	0.035	0.055	0.04–0.07	0.11
Labour ($/yr/person)	75,000	70,000	60,000	20,000	75,000
Water ($/ton)	0.26	1.60	0.26	0.26–0.5	2.2
Support	good	good	good	limited	limited

Table 3. Comparison of regional sites for polysilicon plants.

Government support for polysilicon plants varies greatly from country to country and also within a country. Support may include tax incentives, government-backed loans, free or inexpensive land, and building of roads, as well as job training and other support services. While these can reduce capex, the effect on the 10-year amortization portion of polysilicon production costs is small compared to the lower costs of electrical and utilities over an operating life of 30+ years. A comparison of regional sites is charted in Table 3.

Amortization cost

Today's polysilicon plants are often being built at 10,000 MTY (metric tons/year) capacities to achieve economy of scale and reduce labour cost per kg. Capex ranges from US$800 million to $1.1 billion depending on whether the site is 1) an expansion of an existing facility with roads, rail, land, buildings and all utilities available; 2) a brownfield site/industrial park, with roads, utilities and access established; or 3) a greenfield site, where transportation access, land and utilities must be installed. For a 10-year amortization period, US$8–$11/kg is added to operational costs, not including interest on the capital expense. With this large burden on production costs, the remaining cost elements must be reduced below US$25/kg to yield a return on investment and to allow for investment in future expansion. The PV industry polysilicon price target of US$40/kg requires an energy-efficient, high-productivity plant design on a site with favourable power, labour and utilities costs.

> "The PV industry polysilicon price target of US$40/kg requires an energy-efficient, high-productivity plant design on a site with favourable power, labour and utilities costs."

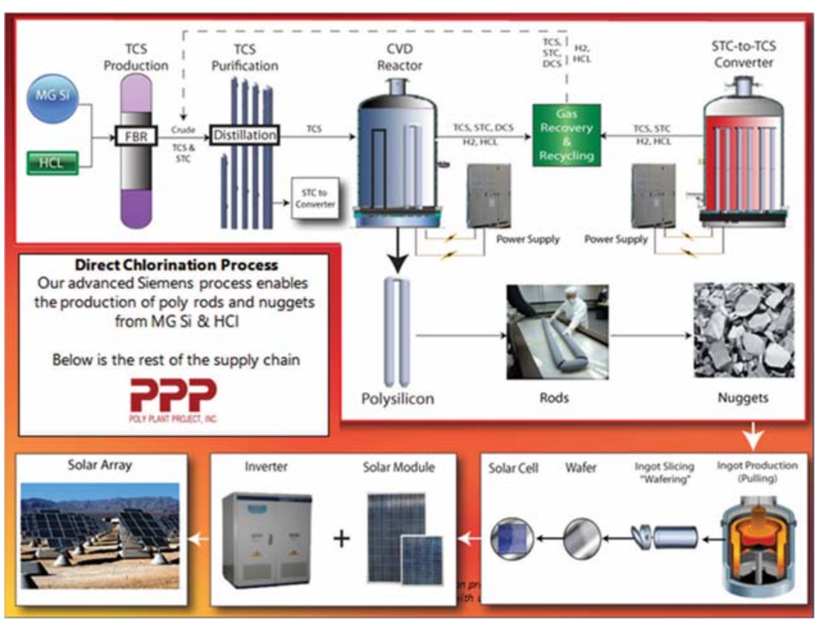

Figure 1. Representation of the direct chlorination process for producing trichlorosilane.

Polysilicon plant design

The key elements of polysilicon plant design are listed below.

Trichlorosilane synthesis technology

TCS is synthesized by hydrochlorination or by direct chlorination. The hydrochlorination reaction, also called *hydrogenation*, is written as: MG Si + $2H_2$ + $3SiCl_4$ = $4HSiCl_3$; original work on this process was described in an early patent [4] and developed in production volumes by Union Carbide in 1984 [5]. Four polysilicon suppliers now use this process to produce TCS-based polysilicon. The direct chlorination reaction, also called the *Siemens process*, is written as: MG Si + 3HCl = $SiHCl_3$ + H_2 and has been in use since the early 1950s. Most polysilicon suppliers use this process for TCS-based polysilicon.

In the hydrochlorination process, co-product gases are recycled in the synthesis fluid bed reactor, using co-product STC as the chlorine source, which eliminates the need for HCl and for STC-to-TCS thermal converters; therefore, the operating cost for the hydrochlorination process is about 10% lower than the operating cost for the direct chlorination process on the same site. A comparison of the two technologies is shown in Table 4.

Item	Hydrochlorination	Direct chlorination
MG Si use (kg/kg poly)	1.05	1.26
HCl use (kg/kg poly)	0	0.74
STC use (kg/kg poly)	0.25	0
Hydrogen use (kg/kg poly)	0.11	0.1
Reaction temperature (°C)	~550	~350
Reaction pressure (bar g)	~30	~5
TCS yield (mol %)	26 to 30	> 90
Electrical energy (kWh/kg poly)	65	75
STC converter (mol % yield)	not required	22%
Capex (normalized)	1.0	1.05

Note: both processes produce STC as a co-product. In the hydrogenation process, the STC is recycled in the TCS synthesis reactor; in the direct chlorination process, the STC is recycled in a separate thermal conversion reactor.

Table 4. Comparison of hydrochlorination and direct chlorination TCS synthesis technologies.

Trichlorosilane purification
An advanced TCS purification system is a combination of distillation and adsorption columns that uses computer simulation with data from operating systems to design the number of trays, reflux ratios, column sizes and number of columns to efficiently purify the TCS with less than 15% losses of chlorosilanes and a 6:1 TCS to polysilicon ratio. An efficient design must take into consideration over 50 different chemical species, with thermodynamic and binary interaction parameters defined for each species.

Energy conservation
To reduce the electrical power costs, energy conservation measures must be implemented throughout the entire plant design. Two major conservation areas are heat recovery from the process equipment and energy-efficient equipment design. The largest energy savings, about 50%, have been realized in the advanced CVD reactor designs with larger capacity, as shown in Table 5.

Co-product gases recovery and recycling
As discussed above, the co-product STC must be recycled to achieve economical use of TCS. Hydrogen and HCl are also recovered and recycled. The materials consumption in Table 4 assumes recovery and recycling of gases.

Plant size
Prior to 1999, 2500 MTY was considered to be a large-capacity plant, since demand was from the semiconductor industry with only a 10% annual growth rate. With the large PV market averaging a 30% growth rate, polysilicon plants are designed for 10,000 MTY to meet growing demand and achieve economy of scale. The larger plants have reduced labour costs and are able to negotiate for lower utility rates and quantity discounts for materials. A limitation on capacity is the ability to contract for sufficient electrical power, water, materials and utilities.

Polysilicon specifications
The plant design must include design of the distillation system for the required polysilicon purity and design of the product handling facility to meet the product specifications. Defining a purity specification for solar-grade polysilicon (SOG) has been problematic, with values ranging from 6 to 11 nines. This is calculated as silicon weight % based on acceptor and donor impurities only. Since a crystalline silicon ingot of 0.1Ωcm *p*-type has a boron dopant level of 2ppmw, the starting polysilicon feedstock must have a purity of at least 7 nines to minimize impurity interferences from the feedstock. SOG polysilicon at 8 or 9 nines, based on acceptor and donor content, is recommended to avoid feedstock resistivity contamination in crystal growth.

The higher purity levels may require additional equipment in the distillation system and/or higher reflux ratios, so capital expense and operating costs may be higher. Electronic-grade (EG) purity is usually specified at sub-ppb levels for donor and acceptor with smooth polysilicon rod surface texture. The smooth surface requires slower growth rates in the CVD reactor, resulting in higher power consumption. An automated rod-breaking system, clean-room processing, surface etching of chunk polysilicon product, and packaging in 5kg clean bags are also required. In addition to increased capital expense, operating costs are higher and can increase by as much as US$8 to $12/kg for EG polysilicon [6].

	rods	kWh/kg	tons/yr
Small	12–24	90–200	80–150
Standard	36	60–70	180–260
Advanced	48–54	< 50	375–500

Table 5. Comparison of energy use for larger capacity CVD reactors.

Redundancy
Redundancy in process design and for key equipment must be included in the polysilicon plant design. It is imperative to avoid long downtimes: a month-long shutdown for a 10,000 MTY plant can result in a US$50 million loss in sales income. A loss this large can justify redundancy in design and operation. Long shutdowns can be avoided by installing two independent electrical feed lines to the plant, installing sufficient TCS storage, building adequate stores of materials and equipment spare parts, preparing for fast maintenance response and adopting safe and reliable operating practices.

> "Redundancy in process design and for key equipment must be included in the polysilicon plant design."

Safe operation
Safety must be an integral part of the plant design since hazardous gases at high temperatures and pressures, high voltage power supplies, crane operations, high structures and heavy loads are some of the risks. A comprehensive, thorough safety system – including facilities and equipment, training and information, policies and procedures, and emergency preparedness – is required to mitigate the risks. The consequences of injury to the workforce or of damage to property or the environment can be far-reaching and lead to long shutdowns, plant closures or liability actions.

Polysilicon plant operations
Even with an efficient plant design and advanced equipment, high productivity is necessary to meet the goal of < US$25/kg production costs. Key elements in achieving high productivity are as follows.

24/7 plant operation
The plant must be fully staffed in order to provide continuous operation


MONOCRYSTAL
Low cost PV materials
Monocrystal's new BSP series tabbing pastes:
• BSP-111, BSP-112 - the silver content is 25% less than in the previous series PPAS
• BSP-122 - the silver content 45% less in comparison with previous PPAS
silver
BPS series
silver
PPAS series
MONOCRYSTAL
BSP-112
30
2000 g
15.05.11
6 months
www.monocrystal.com


SCHMID
Let the Sun shine. Catch the Power.
Fully integrated turnkey solution for wafer fabrication
from crystallization to metrology inspection.
Characterized by unique total cost of ownership.
Now with revolutionary inline Pre-Cleaning process!
WAFER PRODUCTION
Gebr. Schmid GmbH | 72250 Freudenstadt | Germany | phone: +49 7441 538-0 | info@schmid-group.com | www.schmid-group.com

throughout the year. Periodic shutdowns for maintenance or equipment installations must be planned so that CVD reactor operations can continue. This requires adequate TCS storage and redundancy in TCS production.

Operator training

With operational experience, processes become more efficient and bottlenecks are identified and corrected.

Process engineering

The implementation of industrial engineering principles, especially product flow and logistics through the polysilicon processing area, results in a large gain in productivity. For a 10,000 MTY plant using CVD reactors at 400 tons/yr capacity and an 84-hour run cycle, a reactor must be started every 3.5 hours.

Quality control

Quality-control procedures for each process step, from incoming materials to the final product, are required in order to maximize yields and to prevent product loss. A comprehensive laboratory is used to evaluate incoming materials, examine TCS purity and analyze product purity. Daily lab data is used for process control in the TCS, polysilicon deposition and polysilicon product areas.

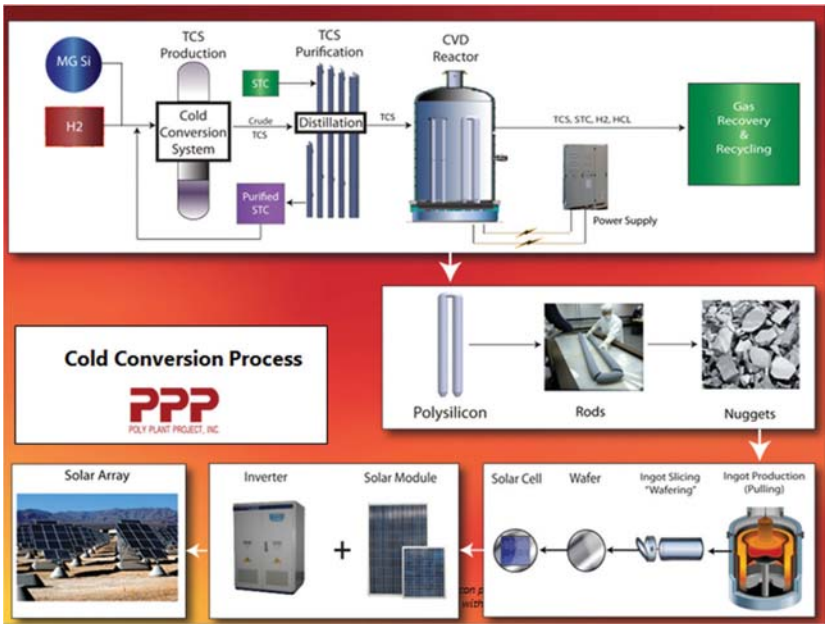

Figure 2. Representation of the hydrochlorination process (cold conversion) for producing trichlorosilane.

Design of polysilicon products

Designing polysilicon specifications for the various crystal growth methods can reduce crystal growth costs. Close cooperation between the polysilicon supplier and the ingot grower can significantly reduce ingot growth costs. Cooperative studies have demonstrated cost reductions in the following areas.

Purity specification

Metals concentration in silicon wafers is known to degrade solar cell minority-carrier lifetime values and resultant cell efficiency. The primary source of metals contamination in TCS-based polysilicon is the contamination of the surface during product processing and packaging. For EG polysilicon, surface metals are specified at less than 10ppbw [7], requiring a surface chemical etch and expensive product handling and packaging. Defining a specification limit for SOG at higher levels, based on ingot and cell lifetime measurements, allows less expensive product processing and bulk packaging.

Bulk packaging

Typical packaging for EG polysilicon is

Figure 3. CVD reactors in the polysilicon plant deposition building.

5kg polyethylene bags in a 30kg carton. Six cartons are required for a Czochralski (Cz) crucible load of 180kg, and 17 cartons for a directional solidification system (DSS) crucible load of 510kg. For SOG poly, 140kg cartons or 1 ton bulk packaging can be used. Package materials and storage costs and packaging and unpacking labour costs result in savings of up to US$1/kg.

Polysilicon form and size

Maximum packing of the crucible, with the optimal mixture of rod sections, chunks and chips, increases crystal ingot weight per run and improves productivity, which reduces ingot growth costs. Granular and chip-form polysilicon have a bulk density of about 1.5g/cc, chunks about 1.7g/cc and rod sections about 2g/cc. The use of an optimal mix can increase ingot weight by 10%.

Load and melt time

Rod sections can be loaded faster than chunks and chips, saving polysilicon load time. In addition, rod sections and large chunks have better bulk thermal conductivity than chips and granules, which reduces the melt time in the crystal growth furnace.

Continuous feed and recharge of crucibles

For Cz growth furnaces, the open crucible allows better packing density and the opportunity to continuously feed or recharge polysilicon. Some vendors provide continuous feed capability for the Cz growth furnace by using granular or chip-form polysilicon to provide a continuous feed into the crucible. A technical concern has been the presence of dislocations and crystal faults caused by introducing cold, solid polysilicon into the hot melt, disturbing melt thermal stability. While these are not acceptable for semiconductor-grade ingots, some level of dislocations is acceptable for solar-grade ingots. Recharge systems are another approach to achieving continuous growth. After the initial ingot growth, the remaining melt is recharged with granules or polysilicon rods, then a second ingot is grown. The major cost benefit of a recharge system is the extension of crucible life to three to five pulls, thereby reducing crucible cost; other cost benefits are an increase in energy efficiency and in hot zone life.

"The major cost benefit of a recharge system is the extension of crucible life to three to five pulls, thereby reducing crucible cost; other cost benefits are an increase in energy efficiency and in hot zone life."

Conclusions

PV module installations are expected to continue at annual growth rates of 30% for the next several years, with crystalline silicon as the dominant technology. Because polysilicon production is increasing at only 20–22% per year, many new plants will need to be built to avoid shortages. These plants must be designed for cost-efficient production of high-purity material, and the polysilicon product must be designed to reduce ingot growth costs and improve electrical characteristics. The major cost factors in polysilicon production have been reviewed, along with key elements of plant design and operations. To effectively reduce total silicon materials costs, the polysilicon supplier must establish cooperative technical programmes with the ingot supplier to define optimal polysilicon specifications, from purity to packaging.

With demand increasing faster than supply, and taking into account the high amortization costs for existing plants, it is unlikely that polysilicon prices will meet the US$40/kg PV industry target over the next ten years, but will remain in the current US$50–$55/kg contract price range. Vertical integration offers several advantages to the PV module supplier, beyond assurance of supply. A cost-effective polysilicon plant would supply production volumes at a US$25 to $30/kg transfer price; provide polysilicon products designed to reduce ingot costs; and design products to meet advanced solar cell requirements.

References

[1] Keynote speeches 2011, five presentations on PV markets in US, Germany, France and Asia, SNEC 5th Int. PV Pow. Gen. Conf., Shanghai, China.

[2] Keynote speeches (European markets) 2011, six presentations on PV markets in Germany, Italy, France, UK, Greece, Turkey. Intersolar Europe Conf., Munich, Germany.

[3] Keynote speeches (global markets) 2011, six presentations on PV markets in US, Canada, Japan, China, India, Australia. Intersolar Europe Conf., Munich, Germany.

[4] Wagner, G.H. & Erikson, C.E. 1952, "Hydrogenation of halogenosilanes", US Patent 2,595,620.

[5] Brenemann, W.C. 1987, "High purity silane and silicon production", US Patent 4,676,967.

[6] Maurits, J.E.A. 2003, "PV feedstock costs – five year outlook", *Proc. 13th Workshop Cryst. Si. Solar Cell Mater.*, Nat. Renew. Energy Conf., Vail, Colorado, USA.

[7] Maurits, J.E.A., Dawson, H.J. & Weaver, C.H. 1991, "The effect of polysilicon impurities on minority carrier lifetime in Cz silicon crystals", *Proc. 22nd IEEE PVSC*, Las Vegas, Nevada, USA.

About the Author

Jan Maurits has over 40 years' experience in the silicon industry, including 16 years' at a major polysilicon supplier, with experience in polysilicon products development, Q.A., analytical methods development, technical marketing and product management. He has published 22 technical papers and made numerous presentations at technical conferences. Jan is co-founder and President of Poly Plant Project, Inc., a specialty engineering company formed in 2005 to provide consulting services, process technology and key equipment for production of high-purity, cost-effective polysilicon.

Enquiries

Email: jmaurits@polyplantproject.com
Website: www.polyplantproject.com

Thermodynamic considerations in wire saw processing

Erik Brown, Argenta Consulting, Coopersburg, PA, USA

ABSTRACT

The last several years have seen a significant number of publications on wire saw data in regard to process optimization theory applied to solar wafering. The methods vary, but fundamentals concern the mechanical dynamics of the wire sawing process, where measurements of the wire forces in the silicon slot using free abrasive are studied; however, these data are not yet fully correlated to a complete thermodynamic analysis of the problem. The objectives of the empirical development of the process theory are also widely varied, but there is industry agreement that it is being faced with the fundamental limits of cutting rates in processes that use free abrasive slurries and a single wire. The limit arises from intrinsic thermodynamic limits of the delivery of work energy to the silicon slot. Similarly, these same principles prevent us from increasing the wafer load to overcome the limitation as work energy transfer rates are countered by higher entropic losses that occur as power and wafer load are increased. The effect results in the problem that the wafer load may not be increased without proportionately reducing table speed. The fundamental nature of these limits suggests that they involve theoretically calculable energy quantities of thermodynamic limiting functions, which restrict the 'useful' work that we can extract from the system, where the work energy of interest is the abrasion of the silicon in forming the wafers. The present work reviews the theoretical issues of determining process efficiency optimums that could be used to achieve throughput gains.

Introduction

High-volume wafer manufacturing in the solar industry is dominated by the use of free abrasive with multi-wire saws, with a large effort now being made to reduce costs of fixed-abrasive processes to be competitive in this market. Although the standard diamond wire fixed-abrasive process is currently very expensive, it has a cutting efficiency advantage that results in higher throughput. This creates a need in the industry to determine if the limit of future cost reductions in diamond wire can result in overall cost effectiveness. This cost effectiveness would need to exceed the ability to achieve those cost reductions and throughput improvements that remain with free abrasive.

> "The approach to solutions concerning the optimization of the wire sawing process is generally best regarded as a thermodynamics problem."

Processing with free abrasive in a PEG (polyethylene glycol) carrier has become increasingly economical over the past decade as high-yield recycling processes have come to the fore. Recovery of the abrasive and the petrochemical carrier is critical to achieving cost effectiveness. Dealing with the chemical control instabilities that result from variation in the wire saw process, as well as the recycling process, is now an industry education effort, since most wafering companies focus on the mechanical aspects of their sawing process and look to the chemical companies to ensure the incoming chemical control. However, the wire-sawing process optimization and stability concern the joint chemical and mechanical processes which need to be analyzed as a single thermodynamic system. Furthermore, the approach to solutions concerning the optimization of the wire sawing process is generally best regarded as a thermodynamics problem.

Process stability

For complex thermodynamic systems, its best to first consider what components constitute the most complete 'system' to be treated. Following this, the different theoretical issues for each component can be isolated and any errors in assumptions can be identified as they arise. In fact, this procedure of dividing the system into components helps identify energies that can be measured or estimated and those that cannot. As thermodynamic problems are often in regard to linear algebraic structures that divide variables between those with values that can be known from those that are unknown, this allows some solutions to be constructed.

Consider that the thermodynamic system for wafering consists of two distinct parts, (1) mechanical: the wire saw structure, the wire and drive motor, and; (2) chemical: a slurry of PEG carrier and SiC abrasive. If we additionally consider the recycling of the slurry, a thermodynamic cycle can be isolated that only considers the state changes of the slurry, as shown in Fig. 1.

The wafering process runs in cycles of accomplishing the 'useful' work of cutting the ingots into wafers and dumping the waste heat and other entropy to the surroundings. The sum of these is the total available work – known as 'free energy' – of the process. The process is repeated by returning all the system components to their original state and beginning again. For the slurry, this means restoring the available work of the chemical which is measured by changes in the Gibbs free energy, ΔG. There is a variability of the total process that is tied up in the precision with which we repeat the detailed steps of returning to the original state. These include returning the saw table to its original position, and replacing the wire and inserting new ingots; however, none of these pose much of an issue in terms of repeating the original thermodynamic state.

> "The wafering process runs in cycles of accomplishing the 'useful' work of cutting the ingots into wafers and dumping the waste heat and other entropy to the surroundings."

Nevertheless, returning the slurry to its original state in a recycling process has a significant impact on the total process. As it is not possible to measure all of the free energy changes of the slurry during the cutting process, it is difficult to determine whether or not it has a negative impact on

EUPVSEC_Info_210x297

e:	Close:
	7/25/11
t	8/10/11
/Sept	8/11/11
t	8/16/11

Medium,
nd Black

lurphy

68169_10-AMA-043v1_Infinity__EUPVSEC_Info_210x297.indd 1

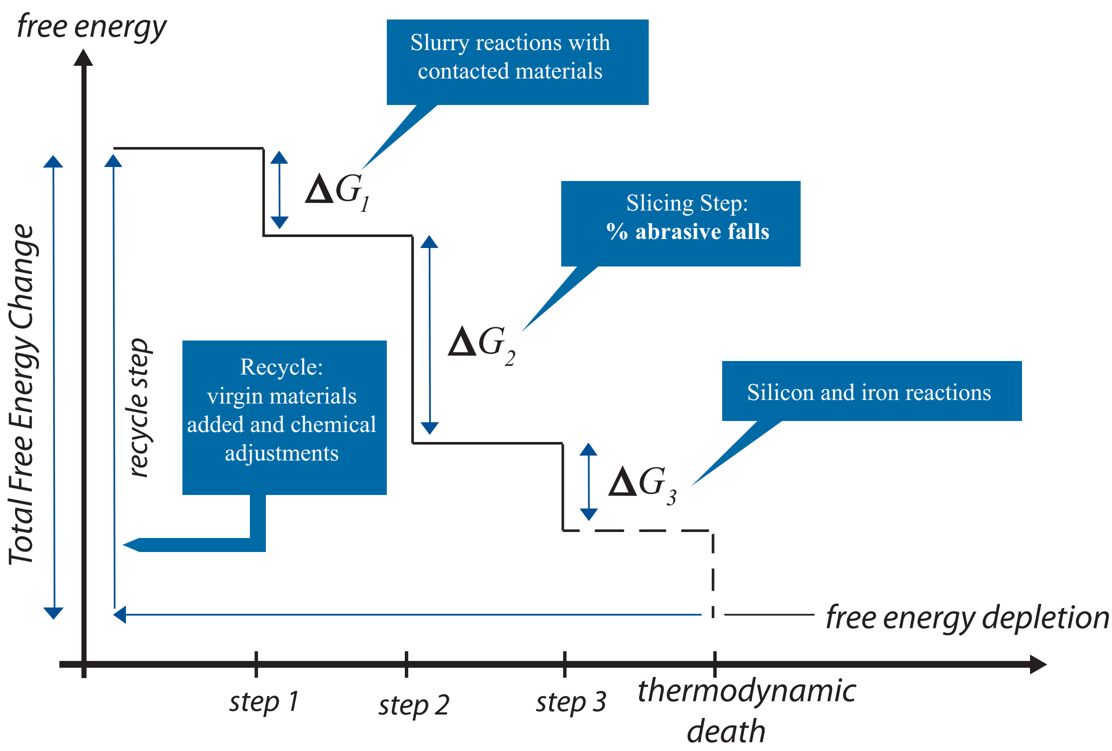

Figure 1. Repeatability of the slurry 'state' changes affects process control run to run. Some free energy declines are chemical state changes that provide no useful work.

the work energy of abrasion in the silicon slot (e.g. certain chemical reactions). However, repeatability of the change in ΔG impacts the overall process control. The largest decline in the free energy of the slurry that impacts the ability of the system to achieve the work of abrasion directly is the kerf rise in the slurry during the slicing operation. The percentage of kerf in the slurry reaches a limit such that the rate of work that can be delivered to the slot must be declining during the slicing operation. This loss of ability on the part of the slurry to accomplish work in the slot can be associated with the rising entropy of dilution of the pure SiC.

This presents a potential problem in terms of assigning the free energies. As the work that the slurry does in conjunction with the wire is mechanical work, the measure of the system's potential to do work is called 'availability' and belongs to a calculation of Helmholtz's free energy, A, for mechanical work. Yet all the entropic losses of the slurry in the diagram are shown to be Gibb's free energy which, it has been suggested, denotes the chemical changes of the slurry. There is actually nothing wrong here. The largest entropy decline of dilution of the abrasive can be reversed by mechanical processes of separating the kerf from the SiC, so we are not prevented from assuming that the ΔG of dilution and the decline in ΔA closely correspond for this particular change. However, the remaining slurry changes are purely chemical, and so do not have a direct correspondence to change in work energy of abrasion. The problem can be solved by devising a test that measures their impact on ΔA. Crucially, we have identified what can be measured or estimated with respect to the chemical changes.

Fig. 2 gives a list of control factors for chemical changes in slurry as it is used in wire saw processing. One measure of chemical process control can thus be defined by the repeatability of the associated free energy changes of all the possible chemical reactions that might occur. The point here is that the total process variation is the sum of the individual variations, so one must either eliminate the source of the variability or repeat it precisely each run.

Defining the thermodynamics for the slicing operation

Our interest lies in determining the maximum work that can be delivered to the silicon slot for a given process arrangement (e.g. length of ingot, length of wire, etc.). There are other criteria for optimization that concern the details of how this work is delivered, so we need to determine precisely what should be optimized. The work function A is the 'availability' of work for a given system arrangement and the intention is to isolate just the process of abrasion for its analysis. The limit of delivering work to the silicon slot as useful work of abrasion is again determined by loss of the available work energy to entropy.

> "The limit of delivering work to the silicon slot as useful work of abrasion is again determined by loss of the available work energy to entropy."

Unfortunately, determining the maximum of this limit in thermodynamic theory concerns reversible processes alone, which are those conducted at infinitesimally low rates. We may, however, use real rate processes (those that are practical) and make measurements to empirically determine new functions of the limits of the work which can be accomplished for those real processes. The outcome of this type of methodology is that for real processes, the rate of losses to entropy (per unit volume of silicon) rise with power input to the system [1]. So the requirement is to experimentally determine the rate of work against the rate of entropic energy loss for several process conditions. At this point, our objective is to assess a function of these two rates with increasing wafer load. In order to assess this, it is necessary to define the system and properly identify the known and unknown quantities in our estimating procedure.

Possible Control Factors	Parameters Affected
- Chemical adjustments at recycle	- pH, chemical activity
- Si and Fe kerf level in reservoir	- chemical reactions
- Kerf level in recycled slurry	- chemical potential
- Interactions with distribution system	- shear forces
	- sluffing of contaminants
	- liquid-solid phase separation
- Viscosity control	- slot width control
	- cutting efficiency
- Slurry lot blending	- lot to lot consistency
- Ingot temperature	- temperature variation and entropic effects
- % water control	- saw marks, chemical activity
- minimize contacted materials	- chemical reactions
- Slurry heat capacity & heat ex settings	- high temp in saw
- Abrasive loading	- saw performance
- reservoir replenish control	- kerf level consistency, pH consistency
- kerf level in reservoir	- chemical reactions, saw marks

Figure 2. Factors Which Vary Total ΔG

To this end, the silicon abrasion process is analyzed, where there is work being done on the ingots plus heat lost to friction in the silicon slot, and the sum of these must amount to the energy change of the system occurring at only the point where this type of work is being done. This leads us to the following, according to the energy conservation principle which is the first law of thermodynamics:

$$\Delta E_{\text{system}} = q_{\text{out (friction)}} + w_{\text{in (abrasion)}} \qquad (1)$$

This is simple enough, but the heat lost to friction is for the silicon abrasion process alone and we must avoid confusing it with other heat losses that need to be identified within the remainder of the system, and those that do not belong to the ΔE of this defined system alone. Here, E only concerns the energy spent in the silicon slot, directly associated to the work at the silicon interface. If we consider the wire motor that supplies the energy as having its own loss of heat to the surroundings in its operation, it is only the portion of the motor's energy not lost to heat that can be said to result in the work energy. The contribution of the motor to the work energy is reduced further by the energy spent on moving the wire web,

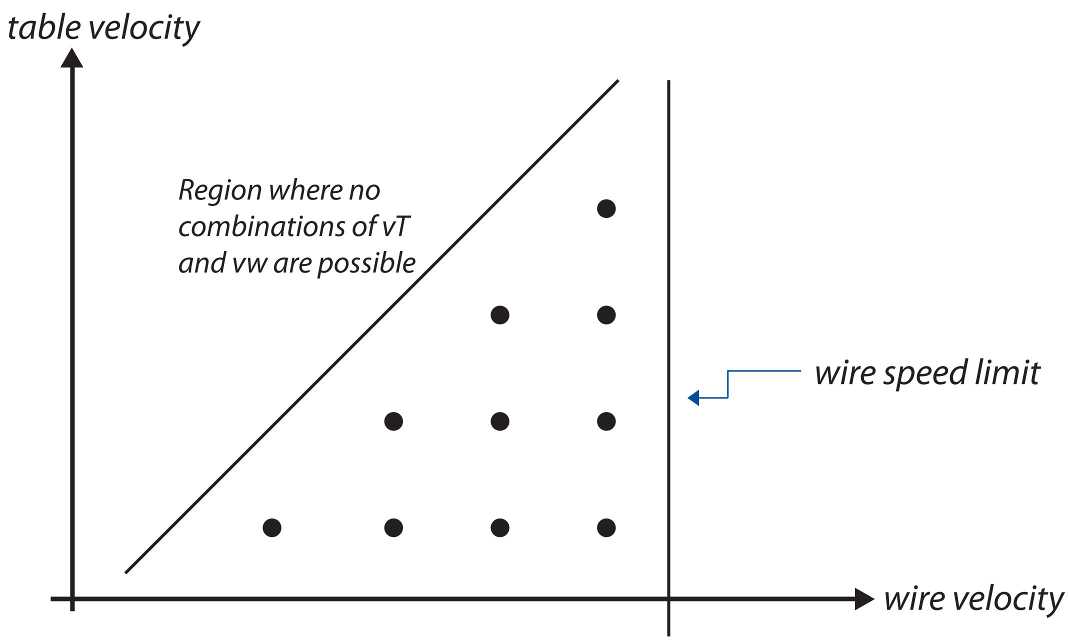

Figure 3. Free abrasive slurries are restricted by limits of rates at which the wire can deliver work energy to the slot. As silicon load and system power increases, table speeds must be lowered due to rising entropic losses which further reduces the work energy delivery rate.

or the energy associated with the web's motion when it is not cutting. This energy needs to be excluded from the energy of the abrasion. It is important to remember that energy ΔE is internal energy and it is independent of any physical part of the system or surroundings; hence, it denotes the energy transformation alone, and occurring precisely within the defined system and not outside of it.

By now, one can see that there are several divisions of the total mechanical and chemical system which all have separate energy considerations associated with them. At this point we have no ability to form an optimization function from the first law energies alone, and only thermal efficiencies can be calculated from this data. Instead, we require a function that accounts for the sum all the entropic energy losses that occur across the boundary of the system.

The work function and process throughput

Now consider the problem of what limits the ability to increase the throughput of slicing. Given a sufficiently small ingot, cuts can be run at extremely high table speeds of 800µm/min or more. So what change in dynamics is occurring at large production loads that limits our processing below, say, 400µm/min? Fig. 3 shows that there is a range of working ratios of the velocity of the table and the horizontal wire velocity, (vT/vw). The limit of achieving high vertical table speed indicates there is a limit to the rate at which work is delivered to the slot by the wire.

But as the table speed must be reduced when the silicon load is increased, regardless of the wire speed, we must look at what mechanisms are degrading the ability to deliver the available work energy to the slot. It is obvious that the wire itself is being abraded and loses a large percentage of its mass by the time it reaches the last wafers on the table, so there is momentum reduction occurring. However, the problem with the end wafers (wire marks, etc.) is only an indicator of the approaching load limit which is being caused by falling work energy across all the silicon slots. Degradation of the rate at which work is done is occurring from all sources of entropic loss and the wire abrasion is only one of these sources.

The second law of thermodynamics allows us to assess all the sources of entropic loss in one term and gives a unifying principle that the resultant work energy of abrasion will be equal to the change in work availability ΔA, minus all of the entropic losses. Further, as power of the system increases (ingot load), the system moves further away from an ideal reversible process; however, all entropy loss as a proportion of ΔA will rise by a function that can be determined empirically. At this point, regardless of whether or not all of the sources of the entropy can be known or measured, the total and its rate of change can be determined because of the second law requirement of the balance of these energies.

Optimization principles

Regardless of the particular experimental approach, some method is required to provide values for only the abrasion process in determining the work energy of abrasion. We further wish to eliminate the vast potential for errors in energy accounting when doing this. The value is obtained either through direct measurement, or from calculation where knowing the internal energy change and heat loss determines the work energy. Any optimization function will have to additionally account for all the entropic loss mechanisms and not just the sensible heat lost to the friction, since we suspect the optimization problem requires the minimization of the rising entropic losses as the size of the silicon load increases.

Now, if we consider ΔE as the energy intensity in the slot, part of it is producing the work of abrasion while another part is producing heat of friction (solid-to-solid and friction of viscosity). If we search for conditions that maximize the intensity in the slot and simultaneously produce the largest slot, we might expect that this optimum would be general and produce the most work in the slot despite variation in other parameters. The function that produces this is thermodynamic effectiveness:

$$\varepsilon = \frac{\text{work of silicon abrasion}}{\Delta \text{A}} \tag{2}$$

where the second law of thermodynamics for mechanical work defines $\Delta A = \Delta E - T\Delta S$.

For this function, whether the work of abrasion rises or the entropic losses ($T\Delta S$) declines, the effectiveness of the process improves. Further, we would expect that whether high loads are cut or one slot is cut with the determined optimal conditions, the maximum work possible is being produced in every slot, even if the work per slot was declining with position on the saw table as the wire wears down.

Now assume the rate of increase in entropy must rise with the rising power (load), so that the average work energy per slot is dropping due to the increasing rate of entropy loss – this is our existing condition for high production throughput. All that can be done in this case is to maximize the average work production rate by setting conditions that minimize the entropic losses, and this counters the effect of wire momentum transfer rates dropping along the series of silicon slots on the table.

In publications by Anspach et al. [2,3], a novel approach involving single-wire slot cuts was conducted to make determinations of process efficiency. These approaches took direct measurements on the horizontal wire force to isolate the work energy required per unit volume of silicon abraded. In this way, the authors avoided explicitly measuring heat losses of either the motor or the friction in the slot and obtained efficiency values for the optimization procedure. In effect, their efficiency measure produces the following:

$$efficiency = \frac{\text{silicon mass abraded}}{\Delta E} \tag{3}$$

The heat loss is known implicitly since the silicon mass abraded completely determines the work of abrasion. This is a modification of the 'effectiveness' calculation shown in Equation 2, but the net result is similar. The important point to be made is that the method directly determines the direction of maximum work produced in the slot. Since the force directly determined the energy in the slot, none of the entropic loss needs to be estimated because it is not contained in ΔE. Then one can simply assume that entropic losses are reasonably minimized when work is maximized. With suitable modifications, the method could be used for cutting multiple slots, and this data used to determine if efficiency optimums for cutting one slot will result in process optimums that are valid when many slots are cut.

Conclusion

The optimization analysis presented speculates that free-abrasive slurries could be used at higher efficiency conditions to increase the throughput. The increasing rates of energy losses with rising silicon loads are due to intrinsic limits imposed by entropy in the thermodynamic theory. It is not possible for these effects to be analyzed by dynamics alone. It has been shown that it is then necessary, at some point in the analysis of process optimums, to measure the useful work produced by system if any meaningful calculations are to be made from empirical studies.

"The increasing rates of energy losses with rising silicon loads are due to intrinsic limits imposed by entropy in the thermodynamic theory."

Materials

Efficiency results published by Anspach, which have been mentioned, show that water-based slurries have higher efficiency, necessarily from the reduced friction of viscosity. Yet other testing shows that we cannot simply implement lower viscosity carriers to achieve throughput gains, since the distribution of abrasive size carried into the slot is reduced, which in turn reduces the work energy in the slot.

A cooperative of companies that includes Avantor Performance Materials, PPT Research and Hoffman Materials in the US are testing additives which modify the liquid's abrasive 'carry' performance in the slot using water-based formulae, thereby maintaining higher average work energy intensity across the slot length. It is probably not lost on the reader that a schema to raise the work energy in the slot will abrade both the wire and the silicon at a higher rate. Thus, a universal objective is the increase of the value of wafers produced per hour at a faster rate than the cost increase (entropy loss) which occurs for achieving that gain. This is simply another way of stating the optimization of the process effectiveness criteria.

References

[1] Andresen, B. et al. 1984, "Thermodynamics for Processes in Finite Time", Acc. Chem. Res., Vol. 17.

[2] Anspach, O. & Schulze, F.W. 2007, "Glycol to Water-based Slurry, Investigation on the Wire Sawing Process", *Proc. 22nd EU PVSEC*, Milan, Italy.

[3] Anspach, O. et al. 2008, "Investigations of Single Wire Cuts in Silicon", *Proc. 23rd EU PVSEC*, Valencia, Spain.

[4] Behm, T. et al. 2011, "Challenges of the Wire Saw Wafering Process", *Photovoltaics International*, Edn. 11.

About the Author

Erik Brown is an independent consultant for marketing and technology in solar and semiconductor materials. He has a B.A. degree in chemistry from the University of Rhode Island where he also did graduate study in theoretical thermodynamics. Working in the semiconductor industry for the past 30 years, he spent the last six years managing marketing and applications engineering in solar wafering for PPT Research. He is currently consulting for Avantor Performance Materials.

Enquiries

7001 N. Rte. 309, Suite 169
Coopersburg,
PA 18036
USA
Tel: +1 484 221 1590

Turbo mode for solar modules: Second- and third-generation front glasses

Daniel Pohl, EuPD Research, Bonn, Germany

ABSTRACT

Competition in the premium sector is becoming more and more fierce. This is forcing PV module manufacturers to differentiate themselves through product benefits and better performance in terms of efficiency. While attention has previously been focused on cell technology, it is likely that, in the future, all module components will become part of this competition – a competition in which premium front glasses present an especially promising element. Anti-reflective coating (ARC) is only the beginning of this evolution. Not only do deeply textured front glasses promise significant increases in output – up to 7% – but their specific product characteristics also make them suitable for niche applications, such as airplane entry lanes and airport buildings. EuPD Research has issued a white paper devoted to solar glass, of which a synopsis is presented here.

Introduction

The worldwide PV market is currently experiencing an upheaval. Previously strong sales markets – such as Germany, with an installation volume of 7.4 gigawatts (GW) in 2010 – are experiencing a decline in demand. The promising markets in the USA, Italy, France and the UK are lagging behind in their expectations. In view of the decreased demand in the first half of the year and the simultaneous increases in production capacity on the part of the manufacturers, the industry is currently steering towards an overproduction scenario, in which unsold products will have to be left in storage. Although cyclic demand is a normal occurrence in other branches, it poses a significant problem for the PV industry because of the dramatic decreases in price that solar modules and components experience. Differentiation via product features and services, especially increased efficiency at competitive prices, affords the best conditions for a strong position in the market. Module price is still the most important aspect of differentiation.

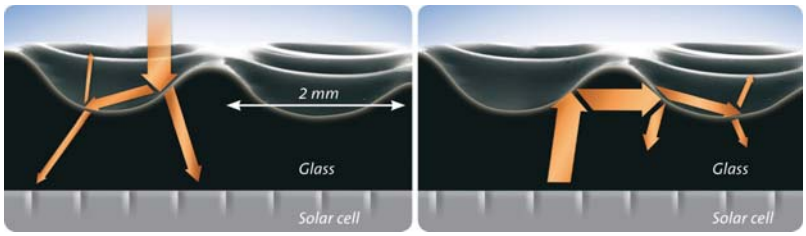

Figure 1. Deeply textured glass uses the geometric 'light-trapping' effect that boosts energy output.

Differentiation is not just a question of cell types

So far, most manufacturers have focused on their cell technologies as the driver for higher efficiency and increased output, but it is also worth taking a closer look at other module components. While contacts, EVA encapsulation foils, junction boxes and frame mouldings all offer marginal potential for lowering costs and increasing output, another crucial component is gaining in importance: front glass. This is particularly interesting, since various refinement and texturing processes have been developed in the last few years, which have prompted a dramatic improvement. With their white paper, EuPD Research, the leading service provider in the analysis of the solar energy and CleanTech markets, have taken account of this development. For the first time, experts have carried out a detailed analysis of the subject of front glasses.

In an increasingly competitive market environment, PV manufacturers are well advised to differentiate their products from those of their competitors by marketing their specific features. So far, mainly the price and origin of the modules have provided this differentiation, but in today's market, manufacturers are focusing ever more on the design and visual aspects, as well as on the suitability of the modules for use in niche sectors. Comprehensive studies conducted by EuPD Research have concluded that the main arguments which convince end customers are still price, efficiency and yield; this analysis takes into account the previous value-added steps of the installer or wholesaler. The use of anti-reflective glass or deeply textured front glasses has been proved to achieve increases in output of up to 7% (in kWh/kWp), depending on a system's alignment. Deeply textured glass has so far shown the best results, through the use of geometric 'light-trapping' effects and because of the increased temperature reduction due to its larger surface area, giving owners of east- and west-oriented roofs, for the first time, a product that boosts energy output to a convenient level for such installations.

Deeply textured glass proved to increase efficiency

The main disadvantage of textured glass technology is the higher cost of producing the specialized front glasses. Although there is currently a surplus of extra-white solar glass, and a high level of price-based competition among glass manufacturers, it is still necessary to carry out a critical examination of the situation. The independent Institut für Solarenergieforschung (ISFH) in Hameln, Germany, has conducted a study of the effects of deeply textured front glasses on module output, and established an average increase in output of 5.4% when the modules were ideally aligned at a 30-degree angle and faced directly towards the south. The researchers found that the increases in output through the use of deeply textured glass were more significant when it was used in installations with less ideal alignments and in more northerly sales markets, due to the optimum exploitation of indirect light provided by the specialized glass. Increases in output of more than 7.5% have been shown both in laboratory tests and in practical use. In the latter, temperature effects on the modules led to a further 0.5% increase in efficiency, due to the larger surface area of the deeply textured glass in comparison to normal front glasses. This was first verified by the scientists at

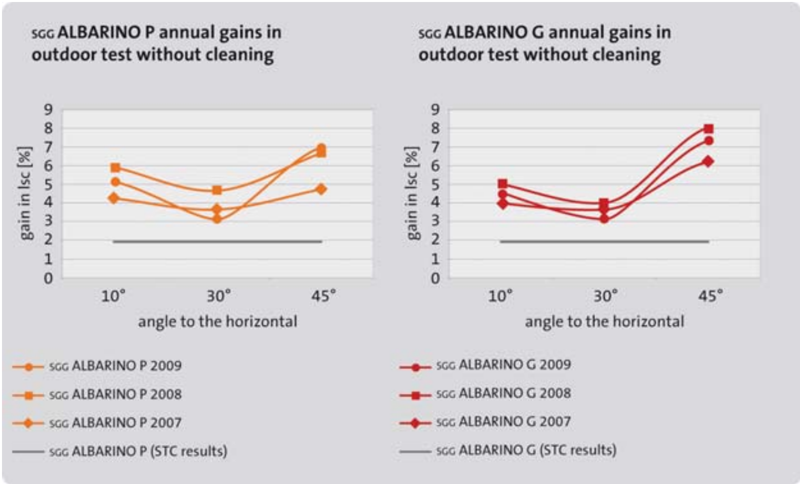

Figure 2. Outdoor field tests show that the annual energy gains depend on the angle between the panel and the horizontal. Cleaning has only a marginal effect.

Boston Fraunhofer Center for Sustainable Energy Systems. However, this effect can barely be measured in a laboratory, as such tests cannot simulate either the temperature increases of the modules in use or the cooling effects of the wind.

Unlimited product lifespan and better suitability for niche markets

The proven effects on temperature and the usage of indirect light provide two clear efficiency benefits for PV panels with deeply textured glass, as opposed to those with anti-reflective glass. Comparative calculations show that the extra costs involved in the use of specialized glass for solar modules are offset during the product's lifespan. These benefits can even be realized in the mid-term in the form of significant increases in efficiency (see model calculation in below), which over-compensate for the initial extra costs. Another fortunate side effect of textured glass is the reduction of the 'dazzle effect' caused by the shiny glass of normal PV modules. This is of particular benefit for use in densely populated areas, areas near to traffic hubs, and airports. While the use of solar panels in airports – for example on the roofs of parking lots, airport buildings, entry lanes or hangars – is currently banned in many countries because of the possible danger caused by the dazzle effect, this could open a new market niche for specialized modules using deeply textured glass. These modules would also prevent arguments among neighbours who are troubled by dazzle effects caused by solar panels.

Running field tests has also shown that cleaning modules incorporating textured glass is unproblematic and no more or less inconvenient than cleaning smooth test models. A significant benefit of this kind of surface, which is given to the glass by textured metal rollers, is that it is especially long lived. An anti-reflective coating (ARC) is either sprayed or rolled onto the glass, positioned via a vacuum process or, occasionally, etched on. Scientists are already researching ways to combine deeply textured glass and ARCs. The future of solar glass lies in deeply textured glass surfaces with added ARC. The first laboratory tests have been successful, and it is expected that the technology will be ready for mass production within the next few years.

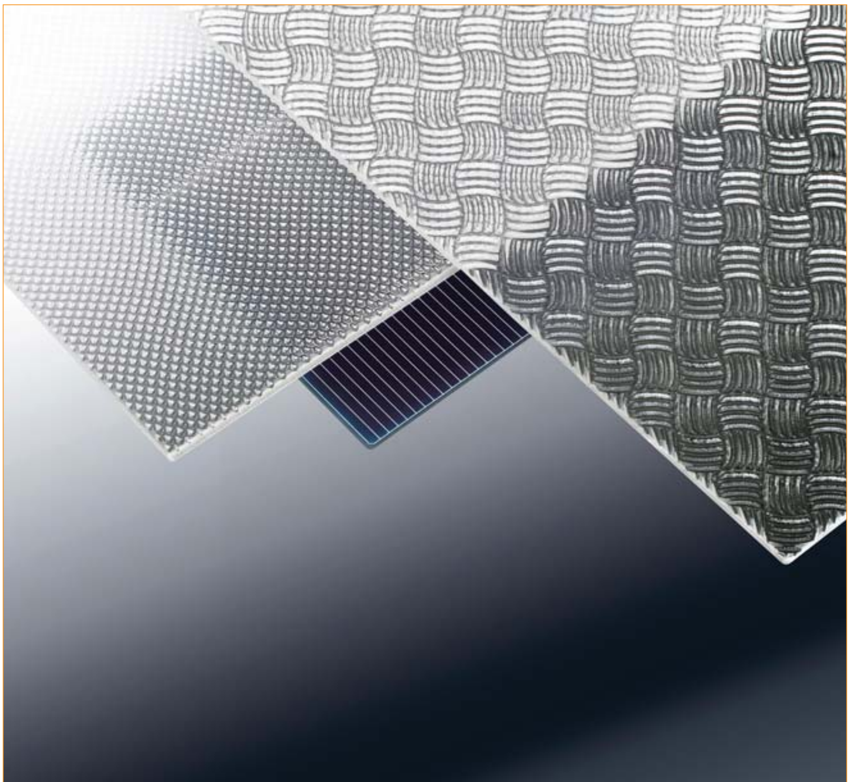

Figure 3. The French manufacturer Saint Gobain Solar is the current leader in the production of deeply textured solar glass. The unique front glasses have textured shapes of either pyramids or waves.

Model calculation

Base: 150W/m^2

Assumption: 7% relative surplus production at 750kWh/kWp because of non-ideal installation conditions = +7.9kWh (annually)

Result: +€2.15/m^2 per year; over a 20-year lifespan = +€43.00/m^2

Textured front glasses: functional and aesthetic benefits

The benefits of third-generation solar glass can be classified into two groups. On the one hand, there are the functional benefits, which lead to increased efficiency and therefore to higher output for the system operators; on the other hand, there are the visual benefits, although these are of secondary importance. Alongside increases in efficiency of more than 7%, and even more in unfavourable alignments, temperature effects and a longer lifespan also lead to increased functionality of textured front glass. Initial market research surveys have shown that specialists and customers notice other, incidental benefits in the improved surface structure, which allow these modules to be used in niche markets. The aspects of decreased dazzle effects and recognition value of the modules were barely even touched upon.

These examples show that there are still neglected niche markets and room for product optimization that manufacturers

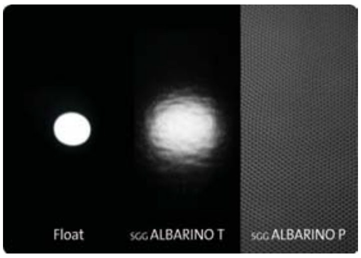

Figure 4. The non-reflective effect is evident when making a direct comparison of regular float glass (left), structured glass (centre) and deeply textured glass (right).

could take advantage of. In view of the decreasing cost-reduction potentials of solar modules in general, manufacturers can secure new market shares through a differentiation in individual product components while simultaneously optimizing output levels. The use of functional front glasses is particularly appealing in the premium sector, which is starting to show the first signs of saturation. The efficiency-heightening benefits of third-generation solar glass provide a special marketing feature for this sector. Alongside Germany, the French sales markets, which are specialized in building integrated PV, as well as the less sunny regions in the UK and Scandinavia, where its optimal usage of indirect light would come into effect, could also benefit greatly from the use of textured solar glass. Nevertheless, Spanish and Italian installations can also benefit from improved performance by using textured glass fronts.

Readers and subscribers can download the entire solar glass white paper in the 'Technical Papers' section of the PVTech.org website, or directly via EuPD Research.

Technological terminology

First-generation solar glass: this category includes high-purity, non-reflective front glasses with a strongly reduced iron content. A reduction of light-absorbing iron-oxide compounds results in an extra-white glass that reflects 4% of the light reaching it.

Second-generation solar glass: this includes bright-white non-reflective front glasses, with an ARC. The light flow-rate is increased, and the light reflection is decreased, although 2.5% of the light is still reflected.

Third-generation solar glass: this glass not only has a low iron content and an improved light flow-rate, but also creates a 'light-trapping' effect because of a textured surface which is either pyramid or wave shaped – the geometric refraction of the light means that more of it is trapped inside the module.

Rolled glass: the most important types of flat glass are rolled and float glass. Rolled glass, also known as cast glass, is rolled while it is still molten, and is generally slightly 'purer', contains less iron and is therefore whiter. This flat glass is more suitable for photovoltaic applications.

Float glass: instead of being rolled like rolled glass, float glass is pulled while it is still slightly liquid and then 'floated' in a bath of tin. Because of the low material embedding, float glass is a little clearer, but slightly more reflective. However, it is still suitable for photovoltaic applications.

Light-trapping effect: this effect is based on the reduction of reflection and the geometric enclosure of the light through repeated refraction. More light is directed into the glass through the surface treatment, while the refraction of the light directs it into the module. This way, up to 10% more light can be trapped inside the module, depending on the alignment and installation site.

About the Author

Daniel Pohl graduated with an M.A. in North American studies, literature and political science from the University of Bonn and Paris-Sorbonne University. He has been working as an editor and media consultant in the field of economics and renewable energies, and is currently head of the corporate communications department at EuPD Research and 360Consult in Bonn. Throughout his career he has published numerous articles on diverse energy topics in national and international special interest magazines. Aside from that he has worked for national newspapers as well as broadcasting stations and a TV production company.

Enquiries

EuPD Research
Adenauerallee 134
Bonn D 53113
Germany
Email: d.pohl@eupd-research.com
Website: www.eupd-research.com

Cell Processing

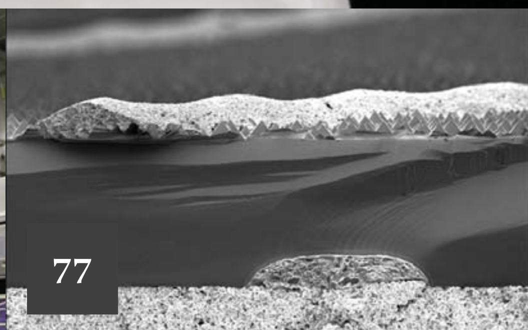


bundle of energy loves regeneration
Innovative solutions from BASF ensure that solar panels remain full of energy even if the sun doesn't shine for brief periods. Our solutions and expertise cover the entire solar cell production process from wafer cutting to module framing. Sunlight can be efficiently turned into energy. At BASF, we create chemistry.
solar-cells@basf.com
BASF
The Chemical Company

News

Industrial manufacturer acquires Despatch Industries for undisclosed sum

Thermal processing equipment specialist Despatch Industries has been acquired by Illinois Tool Works (ITW), which does not have any direct previous involvement in the PV industry, for an undisclosed sum. Despatch had posted record revenue in 2010 of US$200 million and is expected to produce revenue above US$200 million this year. ITW's revenues exceeded US$15 billion in 2010.

"We are excited about this acquisition as the company's core thermal technology aligns well with certain of our other existing electronics equipment businesses," commented Steve Martindale, executive vice president, ITW. "As a leader in thermal processing, Despatch provides us with immediate access to attractive and high growth industries such as solar and carbon fiber as well as the opportunity to extend sales of certain of our existing products into these new markets."

Source: Despatch Industries

Despatch Industries' CF Series furnace.

According to a PV-Tech guest blog by Finlay Colville, senior analyst at Solarbuzz, earlier this year, Despatch had benefited from the significant c-Si cell capacity expansions seen primarily in Asia. This year's SNEC event in China saw Despatch garner orders and letters of intent for more than 50 of its latest c-Si furnace models.

ITW's key business are said to include welding, automotive OEM, industrial packaging, food equipment, construction, polymers and fluids, test and measurement, electronics and automotive aftermarket segments. The company employs more than 60,000 people worldwide.

Cell Production News Focus

Natcore Technology takes delivery of its first LPD tool for AR coatings on solar PV cells

Natcore Technology revealed that it had received its first intelligent processing station, the AR-Box, which will be used for the liquid phase deposition (LPD) process to grow antireflective (AR) coatings on silicon wafers. Housed at the company's R&D centre in the Kodak Eastman Business Park in New York, installation and testing were anticipated to have been completed by September 9.

Chuck Provini, president and CEO of Natcore, Mike Alt, Kodak park's director and David Tennity, Kodak project manager met with local contractors last week to discuss bids for electrical, plumbing and ductwork, which will be needed to render the AR-Box functional. The LPD tool is a completely enclosed system that houses a pre-clean subsystem. Described to be the size of an SUV, the tool has an LPD process subsystem that uses Natcore's latest sizing and process control input and a drying module.

Natcore advised that the AR-Box can identify and eliminate undesired invisible particles to ensure uniformity, consistency and a lack of contamination form suspended matter. The tool has a cooling and heating option, which keeps the chemical bath in the rage of +/-0.5° C. The AR-Box is said to additionally include a module that passivates the surface of 'black silicon' solar cells, which is said to diminish the cell's average reflectivity to less than 1.5% and can potentially increase power output.

Source: PRNewsFoto/Natcore Technology/Stephen Kelly

Chuck Provini, president and CEO of Natcore Technology, explains operation of the AR-Box to Mike Alt, director of Eastman Business Park.

The company maintains that the tool is able to monitor the coating process and measure the thickness of the AR coating on a wafer while it is immersed in a chemical bath. It can then change the composition and duration of the bath so that the solar cells can be produced with ease and better precision.

MEMC to fabricate solar cells in JV

MEMC is filling-in a missing link in its polysilicon to solar projects manufacturing portfolio with the establishment of monocrystalline cell production through a joint venture with equipment supplier Jusung Engineering. At a cost of US$32 million, shared equally between the new partners, an initial 100MW of capacity is expected to begin production in the first half of 2012. The deal was signed by MEMC Singapore, though it was unclear whether the location of the cell plant would be in Singpaore or Korea, where Junsung is headquartered. The cells will used in modules for MEMC's project arm, SunEdison.

The new partnership said it would combine MEMC's proprietary Solaicx CCZ (Continuous Czockhralski) monocrystalline wafers with Jusung's high efficiency cell manufacturing equipment to provide high-efficiency solar cells at a low cost to support overall cost reductions for PV power projects. The collaboration will also support Junsung's business efforts as the deal struck will mean it can offer the same equipments set used in the JV to potential customers.

OAI features advanced 350nm to 1800nm Class AAA solar simulator

OAI's Solar Test Division now features the capabilities of a recently introduced 350nm to 1800nm Class AAA solar simulator, which is said to be ideal for multijunction solar cell testing, high current I-V testing, and for use as a solar power meter.

OAI expanded its manufacturing facility at the beginning of 2011 to meet the increased demand for its products. It offers as standard, 50mm, 156mm, 210mm and 300mm simulators, low and high current I-V testers, test fixtures, and power meters with reference cells.

ReneSola cites continued 100% wafer utilization rate but is impacted by price declines

ReneSola has revised downwards second quarter 2011 shipment and revenue guidance due to steeper than expected price declines for c-Si wafers and modules. Total solar wafer and module shipments are now expected to be in the range of 290MW-300MW, compared to its previously guided range of 330MW-350MW.

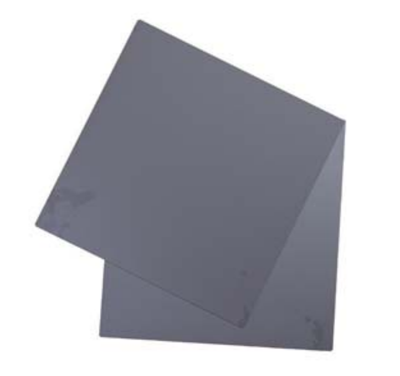

Source: Renesola Ltd

ReneSola's Virto wafers.

As a result, revenues previously guided in the range of US$280 million-US$300 million have been lowered to between US$235 million-US$245 million. ReneSola follows a growing number of PV suppliers making downward revisions to second-quarter financial guidance due to weak demand in the first-half of the year. ReneSola also said that it expected gross profit margin to be in the range 17% to 19%, compared to its previously guided range of 25% to 27%.

JinkoSolar opens new R&D centre, sees cell efficiencies reaching 18.6% by end of 2011

Chinese manufacturer JinkoSolar is opening a new R&D center to focus on improving conversion efficiencies of solar cells and next-generation photovoltaic technology. The company aims to boost the efficiencies of its monocrystalline-silicon cells from 18.1% to >18.6% and its multicrystalline cells from 16.8% to >17.5% by year's end. The firm is also planning to launch the first generation of its Blue Cell modules in Q3, featuring the high-efficiency monocrystalline cell technology.

Chaolin Zha, JinkoSolar's R&D technology director of JinkoSolar, has been tapped to head the center. He holds a PhD in semiconductor physics from Fudan University and has completed postdoctoral work involving c-Si cells and micro/nanoelectronics at University of Notre Dame, Indiana, Norwegian University of Science and Technology in Norway, and Royal Institute of Technology in Sweden. Zha worked for Shanghai Tomi Solar Technologies and has over four years of working experience in the PV industry and over 10 years of scientific research in crystalline silicon solar cells. The company also announced the resignation of CTO Guoxiao Yao, for personal reasons.

Rasirc Steamer promotes 20.2% efficiency in back-contact c-Si solar cells, says Fraunhofer ISE

Fraunhofer ISE has reported that use of the Rasirc Steamer in the production of back-contact silicon solar cells led to cells reaching efficiencies of 20.2%. Fraunhofer used the steamer system to provide ultrapure water vapour for its metal wrap through (MWT) and passivated emitter and rear cell (PERC) solar cell manufacturing processes.

Source: Rasirc

The Rasirc Steamer '02 Series.

Rasirc's Steamer is said to eradicate volatiles, ionic pollutants and other impurities from steam generated from DI water so that the steam can be applied in critical solar cell manufacturing processes. Additionally, the company states that yield becomes higher because metals, hydrocarbons and particles are excluded from the non-porous membrane in order to provide steam with purity in the parts per trillion.

Other News

4JET wins Deutscher Gründerpreis Award

German laser system supplier 4JET has won the Deutscher Gründerpreis Award 2011. The award, sponsored by Porsche, German magazine Stern, ZDF Television and the Sparkasse Banking Group, was presented to 4JET not just for its exceptional financial growth over the past 12 months, but also for creating a business model that promises further growth in the years ahead.

Source: 4Jet

4Jet's robot system for edge deletion of thin-film solar cells.

The award was presented to 4JET at an awards ceremony in Berlin. Runners-up included thin-film module supplier Inventux Technologies.

Amtech makes management moves, promotes Brad Anderson to EVP, names Albert Hasper as Tempress GM

Amtech Systems has made changes to its executive management with Dr. Albert Hasper being named general manager of Tempress Systems and Brad Anderson being promoted to executive vice president. Serving most recently as VP of global operations at ASM International, Hasper began his full-time appointment with Tempress at the start of July. He brings over 20 years of semiconductor industry experience including his positions as product manager for ASM's vertical furnace capital equipment product line and general manager of ASM Europe.

Blue Chip Energy files for insolvency

Solar cell manufacturer Blue Chip Energy has filed for insolvency. The company informed a court in Eisenstadt about its financial state on Thursday and production was abandoned with immediate effect.

Blue Chip has attributed the current economic climate and the accompanying dip in module demand as the reason behind the company's financial plight. Despite 11th hour bailout talks with a number of banks, the Güssling-based manufacturer was unable to find a solution.

PV giant Solon holds an 18.28% stake in the company, which it acquired in 2006 to help equip its project pipeline. However, with Blue Chip's demise now all but secured, Solon is faced with a valuation allowance totalling €18 million.

NREL receives three awards for its solar advancements from R&D Magazine

The US Department of Energy's (DOE) National Renewable Energy Laboratory (NREL) was selected by R&D Magazine as one of the top 100 contributors of innovations for its liquid silicon, FlashQE

News

Cell Processing Order Focus

SoLayTec ships first four ALD tools to customers

TNO spin-off company SoLayTec has sold the first four of its Al_2O_3 ultrafast ALD (atomic layer deposition) Process Development Tools (PDT) to separate customers that include imec, Fraunhofer ISE and two unidentified Asia-based solar cell manufacturers. SoLayTec said that the tools would be installed in the third and fourth quarter of 2011.

All the tools are being supplied for research applications such as surface passivation, and SoLayTec sees this important milestone as preceding volume production implementation of the technology with cells capable of 20%-plus conversion efficiencies.

AccuStrata secures largest Asian sale to date

AccuStrata has signed a contract to sell its monitoring and automation systems to one of India's largest crystalline silicon solar cell manufacturers. The platform will help to increase the yields of the unnamed firm and represents AccuStrata's largest deal to date in Asia.

By increasing the efficiency of solar cells and panels at fixed cost, AccuStrata's platform technology reduces per-Watt manufacturing costs and also increases energy production, subsequently driving more revenue to manufacturers.

BTU 2Q results impacted by major equipment order put on hold

Thermal processing equipment specialist BTU International has reported that a major order for its in-line diffusion tools for a PV manufacturing customer, originally announced in January, 2011 had been put on hold. Deliveries of the first half of the order have started but will extend into 2012, according to the company. The equipment supplier noted a broad weakening of demand from PV manufacturers that it expected to continue through 2011.

BTU reported second quarter net sales of US$19.0 million, down from US$25.4 million in the preceding quarter. Net income for was at breakeven, compared to a net income of US$1.8 million in the preceding quarter.

Management noted changes in customer engagements in regard to migration from batch furnace technology to inline diffusion systems as cost issues continue to dominate PV manufacturers' purchasing requirements.

Order increase of 70.6% could bring Singulus back to profitability in 2011

Singulus Technologies has seen a new order intake increase of 70.6% to €115.0 million in the first half of 2011, and as a result is expecting to return to profitability for the first time in three years. The equipment supply reiterated previous guidance that sales would reach €160 million this year. Though management were quick to highlight a slowdown in PV equipment purchases due to overcapacity and inventory build, sales to the PV sector actually made-up 33.1% of first-half sales, which reached €64.6 million, substantially higher than the prior-year level of €49.3 million, an increase of around 31.0 %.

Singulus noted that it is still in negotiations regarding major projects in terms of its silicon and thin-film solar technology, but actual deals have not been concluded to date.

Akrion receives US$5 million equipment order from European cell manufacturer

A Europe-based cell manufacturer has purchased GAMA-Solar production equipment from Akrion Systems, worth US$5 million. The systems are used for texturization, advanced cleaning and surface conditioning of c-Si wafers. According to Akrion, the equipment will be installed later this year in the customer's new manufacturing facility.

Akrion's GAMA-Solar tool uses a patented 'ICE-1' concentration monitoring and control system, enabling the optimization of the chemical bath performance as well as an advanced drying technology.

PV tool supplier Roth & Rau cuts Q2 expectations, rescinds 2011 forecast, as customers cancel orders

Citing the "deterioration in the overall industry climate as well as delays in the recognition of sales and earnings for projects currently under way," Roth & Rau has cut expectations for the second half of 2011 and withdrawn its forecast guidance for the year. The firm noted a downward trend in its order book, saying it received new bookings of around €29 million in the second quarter, but saw these orders offset by cancellations of €17 million.

As a result, Roth & Rau said it will "have generated a lower level of consolidated sales and significantly negative EBIT in the first half of 2011."

---

and optical cavity furnace. The three awards bring NREL's total R&D 100 awards, since 1982, to 50.

NREL's first award was for its silicon ink, a liquid form of silicon, which was developed under a partnership with Innovalight. NREL points out that this is the first time silicon has been sold as a liquid and states that the Innovalight Silicon Ink process can increase a solar production plant's end product by 20% while making solar cells 6% more efficient. The silicon ink process was achieved by adding a screen printer to the manufacturing line, which NREL states increased the solar cell's efficiency by allowing lighter doping and improving the response to the blue portion of the spectrum.

The NREL won its second R&D Magazine 100 award for Flash Quantum Efficiency System for Solar Cells, a process that was developed with Tau Science and is said to evaluate a solar cell's quality at a speed that is 1,000 times faster than traditional methods. The FlashQE uses light-emitting diodes, high-speed electronics and mathematical processes to measure the quantum efficiency of solar cells. David Young, a senior scientist at NREL, maintains that this process allowed for a random sample of cells to have their efficiency monitored in one second, compared to 20 minutes.

NREL's final award came for its new furnace innovation, the Optical Cavity Furnace, which employs photons to evenly-heat crystalline solar cells and semiconductor materials. Bhushan Sopori, NREL principal scientist, advised that the furnace improved solar cells' efficiency by 3% to 4% with a cost that is 75% below an industrial thermal or infrared furnace. The furnace is licensed to AOS Solar and branded as the Optical Processing Furnace.

Representatives from NREL will join other R&D 100 winners for an awards ceremony in Orlando, Florida on October 13.

Product Reviews

Ferro

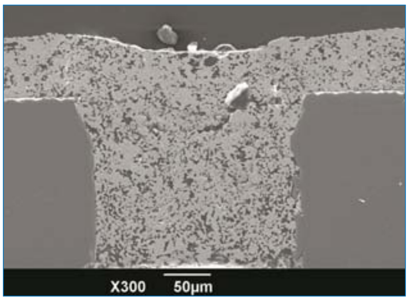

Ferro develops optimized paste system for p-MWT solar cells

Product Outline: Ferro Electronic Materials is introducing a new optimized paste system to enhance performance of p-type metal wrap-through (MWT) cells. The materials include a next-generation rear silver plug hole paste, high efficiency front silver contact pastes, and a back-contact aluminium paste.

Problem: MWT cell technology holds promise of boosting electrical efficiency of polycrystalline silicon-based solar cells to more than 18%. New materials that have been optimized to work with the new cell designs are required to achieve this goal.

Solution: Several areas offer the potential to increase the efficiency of MWT cells, and Ferro's new materials have been developed to address all of these features. The pastes are said to improve contact resistance to high-performance shallow emitter passivated with SiN_x or SiN_x/oxide antireflective coatings; conductivity in holes; shunt resistance in the holes; adhesion and strong back-surface field formation of aluminium; structural reliability of various interfaces. It is claimed that the paste provides excellent conductivity and contact with the front silver paste. It then forms a solid plug upon firing. The plug hole paste is also suitable for use as the p-contact paste, with strong adhesion to the silicon wafer and robust soldering behaviour. Significant efficiency gains are also provided by the system's front silver contact pastes and the MWT back contact aluminium paste.

Applications: Silver plug hole paste that also can be used as the p-contact paste, the back-contact aluminium paste or as the high-efficiency front silver contact pastes for p-type MWT cells.

Platform: Novel glass chemistry has been developed that is claimed to provide excellent shunt resistance.

Availability: Currently available (product being launched at the 26th EU PVSEC in Hamburg, September 2011).

KLA-Tencor

KLA-Tencor's FabVision Solar provides real-time defect analysis for PV cell makers

Product Outline: KLA-Tencor has introduced FabVision Solar, a new integrated solution designed to help crystalline-silicon photovoltaic cell manufacturers improve production yield and profitability by enabling them to react more quickly to metrology and defectivity excursions. The software package takes the company's ICOS PVI-6 optical inspection system data through a wide range of analysis and monitoring features to provide better control and improve visibility in the manufacturing process.

Problem: Until now, PV manufacturers have had to rely on time-consuming, inconsistent manual defect analysis methods. The ability to review in-line data at any point, not just for excursions, can dramatically improve production quality.

Solution: FabVision helps manufacturers identify the root causes of defectivity issues by applying production-proven defectivity and metrology methodologies from the IC and bare-wafer markets. Excursion/process monitoring (statistical process control) provides process control through in-line monitoring of all PVI-6 measurement parameters and provides alarms or email notifications on excursions. Features include: automated report generation, increasing visibility into manufacturing process with time-based automated reporting analysis of optical inspection measurement results from multiple inspection modules; detection of repeating defects and warning capabilities, with configurable rules set by proximity, defect type, and frequency of occurrence.

Applications: c-Si solar cell production.

Platform: The PVI-6 software includes improved ease of use and analytical tools to increase the overall yield of the solar wafer and cell manufacturing process.

Availability: Currently available.

Merck

Merck's isishape etching concepts boost crystalline solar cell efficiencies

Product Outline: Merck has developed an alternative structuring technology with its etching pastes and as a result is now offering patterning concepts under the isishape product portfolio. isishape SolarEtch was used in the production of the industry's first selective emitter and became a proven structuring method in various production lines of leading solar cell manufacturers.

Problem: Improved efficiency and additional process optimizations with smallest investments are essential for solar cell manufacturers. New cell designs for improved performance are always under development and can lead to new process solutions.

Solution: Merck's isishape SolarEtch product program offers a broad range of structuring materials that are claimed to enable simplified, environmentally friendly processes and improved efficiency for applications such as selective emitter, metal wrap-through, local back-surface field or other modern cell designs. isishape allows precise structuring of SiO_2, SiN_x and/or Si. All of Merck's concepts are said to lead to efficiency increases from 0.2 to 0.5% absolute (minimum). The isishape process consists of three steps: firstly, the application by screen printing or by another printing technique; secondly, activation of the etching process through temperature settings and thirdly, a rinsing step to remove the etched materials and paste residues.

Applications: Selective emitter, metal wrap-through, local back-surface field and other modern cell designs and edge isolation.

Platform: isishape products are well-balanced paste formulations that do not require any organic detergents for cleaning in DI water. Both features result in extremely low COD (chemical oxygen demand) and BOD (biological oxygen demand) values, allowing for a green factory concept.

Availability: Currently available.

Product Reviews

MKS Instruments

MKS Instruments' GLM-2000 measures photoconductance in c-Si wafers

Product Outline: MKS Instruments has introduced the GLM-2000 PV and Silicon Wafer Monitor for quality control in photovoltaic and c-Si wafer processing for solar applications. The multi-function GLM-2000 uses high-speed, non-contact RF detection technology to measure photoconductance in PV and silicon feedstocks and partially processed cells, either in-process or post-process.

Problem: The quality of silicon used for crystal silicon PV cells has a direct influence on the conversion efficiency of the final product. The objective is to transfer as much of the incoming energy, or carriers, to the output of the circuit or cell, which is achieved, in part, by minimizing any recombination of the carriers.

Solution: Measuring minority carrier lifetime is a way to quantitatively assess the quality of the base silicon, since lower minority carrier lifetime is an indication of impurities and defects in the silicon. Additionally, measuring sheet resistance and Photoconductance Decay (PCD) give further information on surface recombination effects from as-cut inspection through ARC deposition. The GLM-2000 metrology tool employs a novel implementation of the current RFPCD measurement technique to instantaneously measure sheet resistance, minority carrier lifetime (G_T), PCD and photoconductance rise (PCR).

Applications: Quality control of photovoltaic and c-Si wafer processing for solar applications.

Platform: The flexibility of the sensor design permits easy integration into the production line as either a standalone benchtop unit or integrated within OEM or custom system components. Information is displayed via easy-to-use software that works with 32 or 64 bit 'Windows' XP and higher operating systems.

Availability: Currently available.

OM Group Solar Chemicals

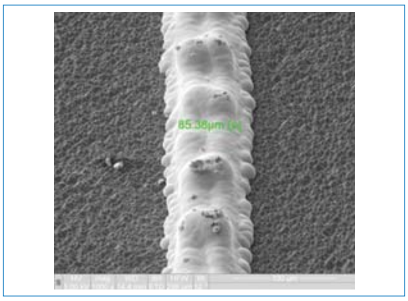

OM Group Solar Chemicals' complete process for plated metal stack on fine-line printed Ag paste for c-Si cells

Product Outline: OM Group's Solar Chemicals division has developed a revolutionary Ni/Cu/Ag plating process for plating on top of fine line silver screened pastes. This economical and efficient process brings cost savings while generating cells with higher efficiencies, as well as improved cell-to-cell consistencies.

Problem: While standard silver pastes have proven to be adequate for producing silicon PV cells, the process has several major drawbacks. Most notably, the continued instability in silver market pricing has led to Ag paste becoming very costly. Additionally, there are limitations to reducing line widths with Ag paste screening. The wider lines create added shading and less surface area on the cell surface, leading to less sunlight being absorbed for energy generation. Finally, because Ag pastes are not pure metal, but metal combined with fillers, there will be variability in the conductivity of the Ag paste lines.

Solution: OM Group Solar Chemicals' Solar Plate Ni PV80, Cu PV73 and Ag200 baths were developed for maximum compatibility with the top silver pastes in the market. PV cells manufactured with these chemistries are said to have higher efficiencies, higher fill factor and lower series resistance. Furthermore, there is no attack of the front-side silver paste, the aluminum BSF, the ARC or the silver back-side contacts. Most importantly, the adhesion of the metal stack layer is said to be excellent after soldering.

Applications: OM Group's chemistries can be used either in LIP, standard electrolytic or combined LIP/electrolytic mode.

Platform: OM Group's chemistry have been designed to be used with the top wet process equipment systems available on the market.

Availability: Currently available.

Targray

New rear aluminium paste from Targray increases V_{oc} and reduces cell breakage

Product Outline: Targray Technology International is presenting a new paste from manufacturer Giga Solar Materials Corp. This new aluminium paste is said to provide excellent back surface field (BSF) for mono- and multicrystalline silicon solar cell wafers. The paste is designed for excellent efficiency, high material compatibility, adhesion strength and a wide process window.

Problem: New low bowing aluminium pastes are necessary to enable cell manufacturers to save costs and move to thinner silicon wafers while maintaining low cell breakage rates. In addition, cell manufacturers are under constant pressure to deliver efficiency gains to drive down the cost per watt.

Solution: A good rear aluminium paste must provide an excellent BSF to enable high cell efficiency. In addition, it must be highly compatible with a variety of silicon wafers and have excellent adhesion qualities to overcome environmental stress testing at the module level. Another important property is its printability; a paste must transfer in a reliable and consistent manner for tight manufacturing controls and performance. This new paste is compatible with a variety of front- and back-side silver pastes and is said to perform well under a wide process window for co-firing of all three pastes.

Applications: Mono- and multicrystalline solar cells.

Platform: Giga Solar's back-side aluminium paste includes the following capabilities: low bowing (<1.5mm for 180µm thickness wafer); compatible with mono- and multicrystalline wafers and back-side silver paste; adhesion quality >3N/cm; co-fireable with back- and front-side Ag pastes; wide process window with silver front-side paste; RoHS compliant and Pb free.

Availability: Currently available.

The influence of etch depth on electrical properties of solar cells

Rui Tong, **Jiayi Liu** & **Stone Shih**, Motech Renewable Energy Co. Ltd., Kunshan City, China

ABSTRACT

In a multicrystalline silicon (mc-Si) cell production process, acid texturing is the most popular way of carrying out surface texturing. In general, the surface reflectivity and etch depth are the criteria used for quantifying the texture quality. In this study, four groups of cells were created with different etch depths of 2.82µm, 3.83µm, 4.41µm and 5.92µm. It was found that the etch depth had a notable effect on the efficiency of a cell. Also, the best texture was obtained with an etch depth of 4.41µm, at which there was a balance between a low reflectance and the removal of the saw-damage layer. As the etch depth increased, the film deposition thickness and the front bus-bar tensile strength were seen to increase. However, no linear relationship was found to exist between the diffusion sheet resistance and the etch depth.

Introduction

In order to obtain high-efficiency solar cells, a light-trapping process is necessary [1]. The most common texturing technique is wet etching in a hot alkaline solution [2], which results in the formation of pyramids protruding from the silicon wafer surface. This surface structure has a very low reflectivity, but the wet-etching method is available only for <100>-orientation single-crystal Si wafers [2]. For multicrystalline silicon wafers (mc-Si) [1], alkaline texture solutions are unsatisfactory due to the existence of different crystal face grains. However, acid texture solutions have been successfully applied to mc-Si wafers and, because this method is low cost and suitable for mass production, it has been adopted for mass production of mc-Si wafers. In general, the mixture solutions (including nitride acid, hydrofluoric acid and deionized water) are used to etch an mc-Si wafer to obtain a surface that is covered in shallow pits, which improves the absorption of light and enhances the short-circuit current density of solar cells. Hauser [3] considers that a good texture needs a balance of low reflectance and the amount of damaged layer removed; the cause of dark lines on the mc-Si wafer surface and their influence on the efficiency of solar cells have been studied by Cao [4].

Texture conditions have a significant effect on the backend process and the efficiency of solar cells. In this paper, the variations of surface morphology with different etch depths are analyzed. The influences of morphology variations on diffusion, antireflective film deposition and bus-bar adhesion are also studied. Finally, the best etching depth is determined in relation to the efficiency of the solar cells.

1	Pre-cleaning (4 groups)
2	Texture (measure etch depth and reflectance)
3	Diffusion (measure sheet resistance)
4	Edge isolation
5	PECVD (measure thickness of antireflective film)
6	Printing and firing (measure bus-bar tensile strength)
7	Cell test (measure electrical properties of cells)

Figure 1. Test process sequence.

Experimental procedure

In this work, a selection of 156mm × 156mm boron-doped mc-Si wafers are used, having resistivities ranging from 0.8 to 3.0Ωcm and thicknesses of (200±10) µm. The wafers are first immersed in an ultrasonic bath with a cleaning agent at 60°C to remove any greasiness. In the second part of the procedure, the different etch-depth wafers are obtained by adjusting the process temperature and operating time of the texture machine. Making the solar cells in the next stage involves the following processes: diffusion, isolation, antireflective film coating, electrode printing and co-firing. Finally, the cells' IV characteristic curves and electrical properties are determined using pulsed solar simulators and a measuring system.

The wafers are divided into four groups of different etch depths as shown in Table 1. The characteristic parameters of the different groups are analyzed in each process, according to the test sequence given in Fig. 1.

Group	A	B	C	D
Etch depth [µm]	2.82	3.83	4.41	5.92

Table 1. Etch depths of test groups.

Results and discussion

Influence of etch depth on surface reflectance and texture profile

Measuring the saw-damage layer thickness is always a difficult task [5], but we were able to determine this value in our experiments. The etch depth is calculated from the etching quality and the area; for example, if the quality = 0.55g and the area = 156 × 156 = 243.36cm^2, then the depth = [(0.55/2.33)/243.36]/2 = 4.85µm (where the density of Si = 2.33g/cm^3). The surface profiles, observed by a scanning electron

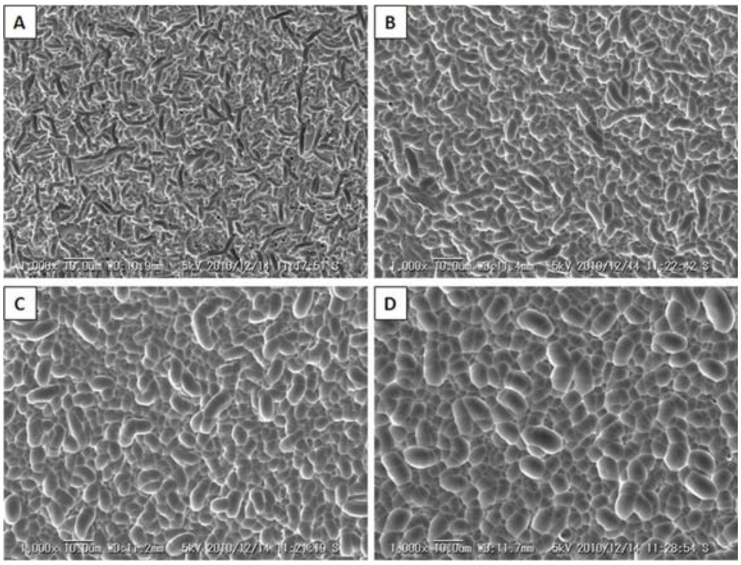

Figure 2. SEM images for samples of different etch depths: a) 2.82μm, b) 3.83μm, c) 4.41μm and d) 5.92μm.

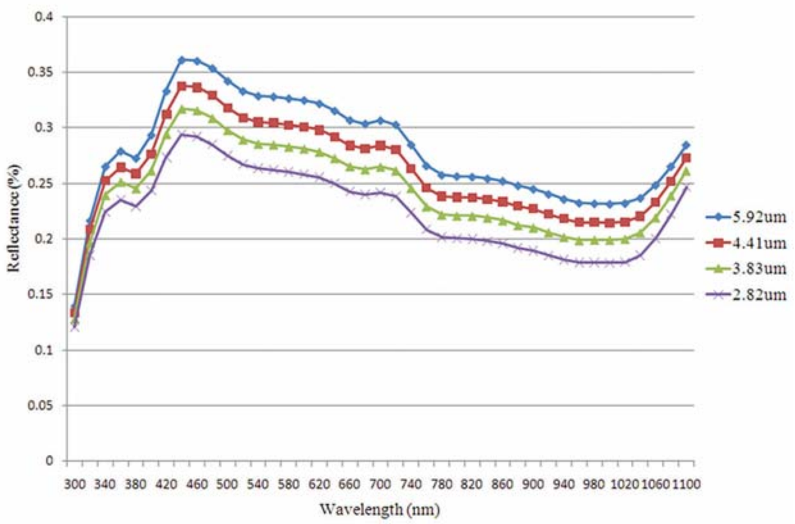

Figure 3. Surface reflectance at different wavelengths for etch depths of 2.82μm, 3.83μm, 4.41μm and 5.92μm.

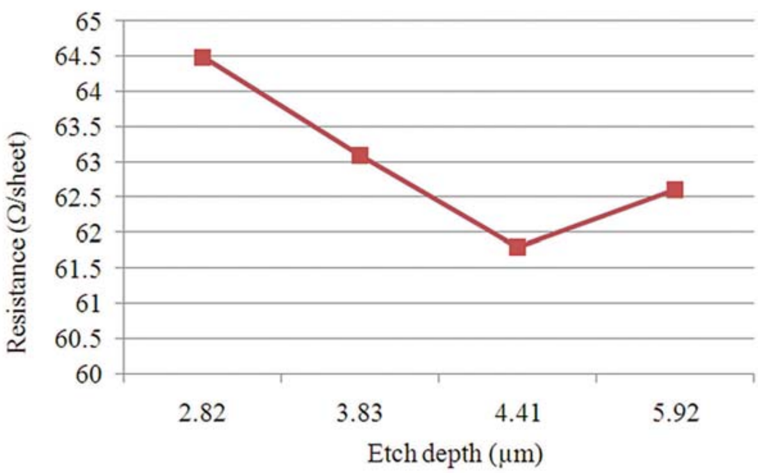

Figure 4. Sheet resistance for etch depths of 2.82μm, 3.83μm, 4.41μm and 5.92μm.

microscope (SEM), are shown in Fig. 2, and the surface reflectances, measured by the reflectance tool (ZOLIX Instruments SCS1011) at different wavelengths, are shown in Fig. 3.

Based on the SEM images, it is evident that the etch pits become larger as the etch depth increases. At the beginning of the reaction, the saw damage is the starting point of the reaction in the HF and HNO_3 mixture texture solution. The etch rate of the position of crystal dislocation is higher than the etch rate of other areas. So, as the etch progresses, the wafer surface forms long, narrow bow-like pits that have no specific orientation. These etch pits are similar in shape to crystal dislocation, but are much denser. As the etch depth increases further, the damage layer is completely removed, the etch rate becomes equal in all directions and the adjacent holes begin to merge. These factors finally cause the pits to become larger and circular, resulting in shiny wafers that can be observed by the naked eye. With increasing etch depth, the reflectance of the surface increases, causing greater loss of light.

Influence of etch depth on the diffusion sheet resistance

The test uses a tube diffusion machine to perform the phosphorus diffusion and a four-point probe (4pp) resistance measurement [6] to determine the sheet resistance (R_{sq}). The results are shown in Fig. 4. It is seen that initially R_{sq} decreases as etch depth increases, but at an etch depth of 5.92μm, R_{sq} is increasing.

It was also found in our subsequent verification experiments that there is no clear relationship between R_{sq} and etch depth. According to Fick's first law:

$$J = -D\frac{\partial c(x,t)}{\partial x} \tag{1}$$

the impurity diffusion current density J is proportional to the surface concentration gradient of the impurity. The diffusion coefficient D depends on the diffusion temperature, the type of diffusion impurities and the concentration of impurities, as well as other factors [7].

Liquid $POCl_3$ is used as the diffusion source and reacts with the oxygen in the tube at 800°C, according to the equation:

$$4POCl_3 + 5O_2 \rightarrow 2P_2O_5 + 6Cl_2 \tag{2}$$

At the correct temperature, the reaction product P_2O_5 reacts with the silicon and generates SiO_2 and phosphorus. This reaction equation is:

$$2P_2O_5 + 5Si \rightarrow 5SiO_2 + 4P \tag{3}$$

It can therefore be concluded that when $POCl_3$ and O_2 concentrations are saturated, R_{sq} depends on diffusion

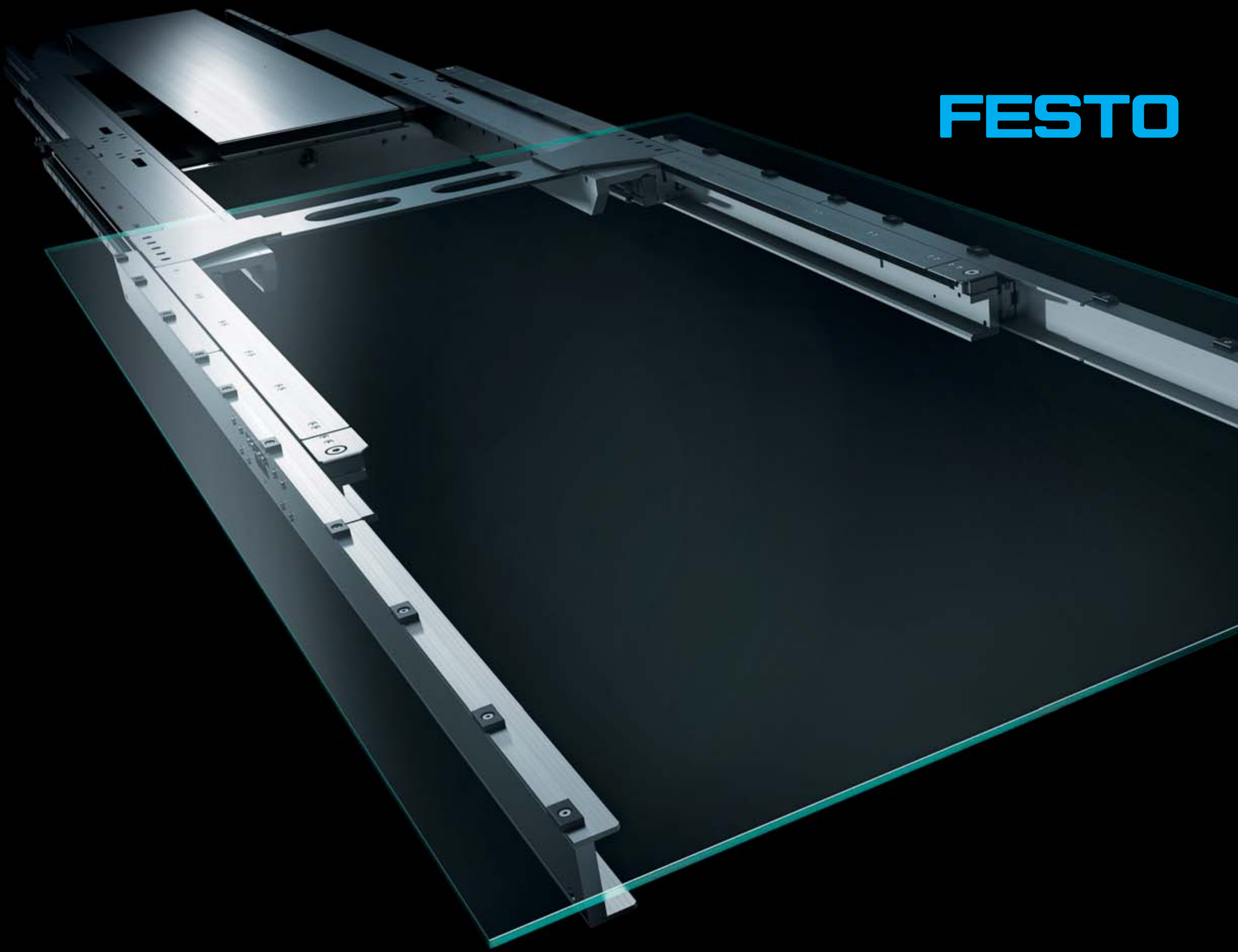

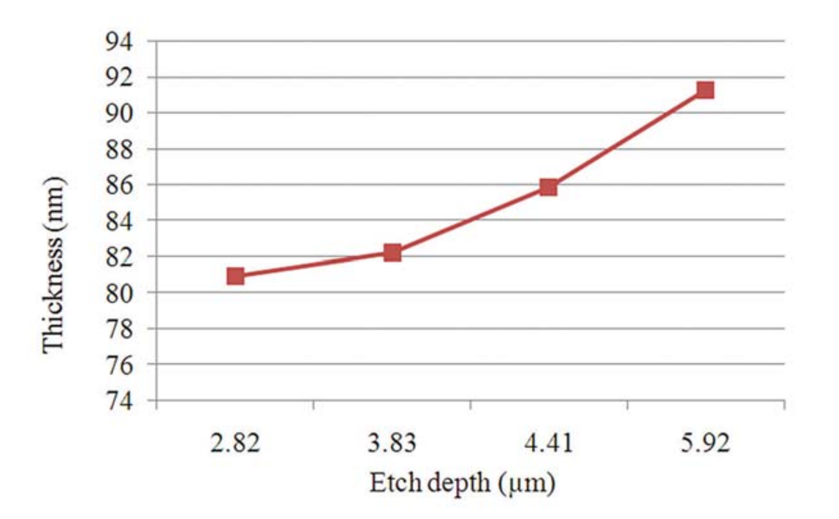

Figure 5. Antireflective film thicknesses for etch depths of 2.82µm, 3.83µm, 4.41µm and 5.92µm.

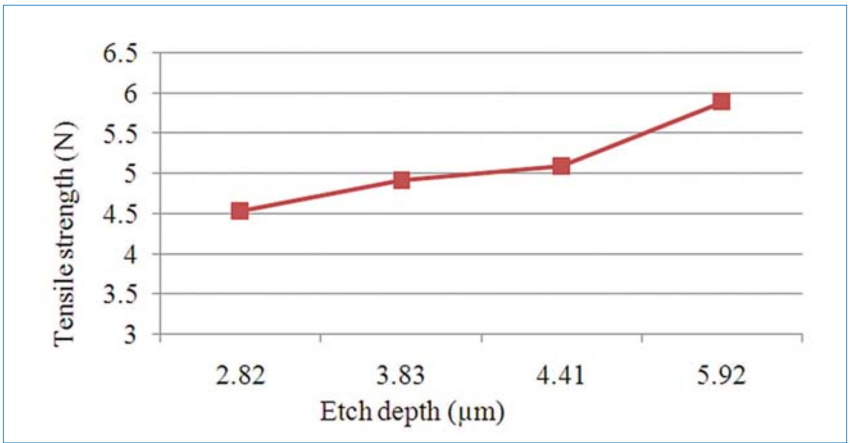

Figure 6. Bus-bar tensile strength for etch depths of 2.82µm, 3.83µm, 4.41µm and 5.92µm.

temperature, but there is little relation to surface conditions.

Influence of etch depth on thickness of the PECVD film

A tube-type plasma-enhanced chemical vapour deposition (PECVD) machine is used to deposit the SiN_x layer, and the reaction gases are SiH_4 and NH_3. The film thickness is measured by ellipsometry, and the values obtained for the thickness are shown in Fig. 5. The results indicate that the thickness of the film is greater as the etch depth increases.

> "The results indicate that the thickness of the film is greater as the etch depth increases."

The PECVD coating mechanism is described as follows [8]. High-frequency RF electric fields ionize the reaction gases to generate electrons. After several collisions, the reaction gases generate a large number of photons, electrons, ions and chemically reactive groups. Finally, high-density plasma is formed in a closed chamber. Active groups are deposited on the wafer surface and react to form an SiN_x film layer on it, which will reduce light reflection. The reaction equation is:

$$SiH_4 + NH_3 \rightarrow SiN_x + H_2 \qquad (4)$$

Because plasma deposition technology is used, wafer surface morphology has an important effect on SiN_x film thickness. When the etch depth is greater, the surface etch pits are larger and circular. This surface morphology has a smaller area and causes the film thickness to increase.

Influence of etch depth on bus-bar tensile strength

The most popular crystalline silicon solar cells produced today have two or three bus bars on both the front and rear sides, with electrodes for transferring the electricity. Screen printing is used, followed by co-firing, to form the bus-bar contact with the silicon. In the process of making modules, a welding rod needs to be attached to the bus bar to concatenate the cells one by one, and it is important to ensure adequate contact between the bus bar and the silicon. The tensile strength of the bus bar was measured in order to find out the relationship between etch depth and tensile strength. The bus-bar tensile strength was found to be greater as the etch depth increased, as shown in Fig. 6.

> "... the bus-bar tensile strength was greater as the etch depth increased."

SEM images were taken to analyze the contact of the silver paste of the bus bar with the wafer surface. Fig. 7 shows the sectional views of this contact for groups A and D. Group A, which had an average etch depth of 2.82µm, is seen to have much narrower etch pits, which may be caused by the inability of the silver paste to pass through the pits to form a better contact with the silicon, resulting in a lower tensile strength. On the other hand, Group D, with an average etch depth of 5.92µm, shown in the right image of Fig. 7, has a higher tensile strength. This is due to the larger etch pits and therefore better contact.

Influence of etch depth on solar cell efficiency

Energy transfer efficiency is the most important electrical property for solar cells, so it is important for industrial mass production to determine the

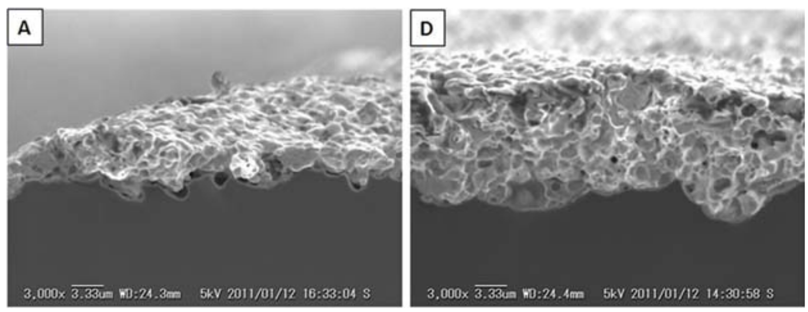

Figure 7. SEM images of bus-bar contact sections for different etch depths. Left: group A with etch depth 2.82µm. Right: group D with etch depth 5.92µm.

Test group	A	B	C	D
V_{oc} [V]	0.617	0.617	0.620	0.619
I_{sc} [A]	8.406	8.460	8.474	8.417
R_s [mΩ]	3.192	3.039	3.072	3.062
R_{sh} [Ω]	87.16	106.82	108.16	117.62
I_{rev} [A]	0.322	0.386	0.338	0.349
FF [%]	77.95	77.98	78.14	78.08
Eff [%]	16.61	16.73	16.87	16.72

Table 2. Electrical properties of the cells for the different etch-depth groups.

connection between etch depth and cell efficiency. Table 2 shows the efficiency results for different etch depths, and it is clear that the etch depth does have an effect on efficiency. The open-circuit voltage (V_{oc}) initially rises with increasing etch depth, but at some point between 4.41µm and 5.92µm, V_{oc} starts to drop. At the beginning, the saw-damage layer is considered to be the main influence on V_{oc} and is a minority carrier recombination centre. As the etch depth increases (groups A–C), the saw-damage layer decreases and V_{oc} and the short-circuit current (I_{sc}) increase remarkably. So, according to the V_{oc} values, it is known that the saw-damage layer is totally removed at an etch depth of ~4.41µm. For groups C and D, when the etch depth continues to increase, I_{sc} decreases. This is because the etch pits become larger and the surface reflection becomes greater. The best V_{oc} and I_{sc} are achieved when the etch depth is ~4.41µm. As mentioned above, this is due to the surface having a lower reflectance around this etch depth and the saw-damage layer being totally removed as well. Furthermore, the best efficiency is obtained when the etch depth is ~4.41µm.

Conclusions

For mc-Si solar cells, in a certain etch-depth range, the surface reflectance decreases as the etch depth decreases, and vice versa. At the same time as the etch depth increases, the etch pits become larger and circular. Moreover, as the etch depth increases, the anti-reflecting film thickness shows an increasing trend and the bus-bar tensile strength is improved. Experiments also show that the diffusion sheet resistances are not linearly dependent on surface morphology. The relationship between solar cell efficiency and etch depth was determined, resulting in a best etch depth of ~4.41µm for our mc-Si wafer samples. Around this etch depth, the saw-damage layer has been completely removed, while the surface still has a low reflectance. In parallel, it should be noted that the wafer surface morphology will change continually with the development of silicon crystalline growth and silicon ingot cutting technologies. Therefore the best etch depth should be regularly checked and revised accordingly.

References

[1] Stensrud, E. et al. 2005, "Acidic texturing of multicrystalline silicon wafers", *Proc. 31st IEEE PVSC*, Lake Buena Vista, Florida, USA, pp. 1309–1312.

[2] Seidel, H. et al. 1990, "Anisotropic Etching of Crystalline Silicon in Alkaline Solutions", *J. Electrochem. Soc.*, Vol. 137, pp. 3626–3632.

[3] Hauser, A. et al. 2005, "A simplified process for isotropic texturing of mc-Si", *Proc. 3rd World Conf. on PV Energy Conv.*, Osaka, Japan, pp. 1447–1450.

[4] Cao, Y. et al. 2011, "Study of dark lines on the polycrystalline silicon solar cell and their influence on cell electrical properties", *Photovoltaics International*, 11th Edn, pp. 64–69.

[5] Schneider, D. et al. 2002, "Quality control of ultra-thin and super-hard coatings by laser-acoustics", *Surf. Coat. Tech.*, Vol. 153, pp. 252–260.

[6] Liu, X. et al. 2004, "The principle and application of testing sheet resistance using four-point probe techniques", *Semiconductor Technology*, July, pp. 1094–1097.

[7] Guan, X. 2003, *Fundamentals of Silicon Integrated Circuit Technology*, Peking University Press, Beijing, p. 65.

[8] Wang, X. et al. 2002, "Research progress in SiN for multicrystalline silicon solar cells", *Materials Review*, March, pp. 23–25.

About the Authors

Rui Tong obtained a master's degree in material physics and chemistry from the Nanjing University of Science and Technology. He has been with Motech for two years and is currently working in the R&D division. His main research area is c-Si solar cells.

Jiayi Liu studied at Zhejiang University and was awarded a master's degree in physics in 2007. He joined Motech in June 2010 as a senior engineer in the R&D division. In his current work he focuses mainly on wafer surface texturing.

Stone Shih has been the director of the R&D division of Motech (Suzhou) since June 2010. Prior to joining the company, he gained 11 years' experience as manager of the Material Analysis Department at UMC Co., worked for one year as manager of the Reliability Department at FOXCONN, and spent two years at the NCU Instrument Centre. He holds both a Ph.D. in material engineering from TUST and a master's degree in chemical engineering from NCU. His research interests include cell design and characterization, particularly of high-efficiency solar cells.

Enquiries

Rui Tong
Motech Renewable Energy Co. Ltd.
No. 1, Mao-di Rd
Kunshan City
Jiangsu Province
P. R. China 215316
Email: tongruihuainan@163.com

High-efficiency rear-passivated screen-printed silicon solar cells

Fab & Facilities
Materials
Cell Processing
Thin Film
PV Modules
Power Generation
Market Watch

Thorsten Dullweber[1], **Sebastian Gatz**[1], **Tom Falcon**[2] & **Helge Hannebauer**[1]
[1] Institute for Solar Energy Research Hamelin (ISFH), Emmerthal, Germany; [2] DEK Printing Machines Ltd, Weymouth, UK

ABSTRACT
Approximately 80% of today's silicon solar cells industrially manufactured worldwide apply screen printing for the metallization of the silver front and aluminium rear contacts. In production, conversion efficiencies of ~18–18.5% are achieved using monocrystalline silicon wafers. A baseline process has been implemented at ISFH that is very similar to the industry-standard process, displaying conversion efficiencies of up to 18.5%. An analysis of the solar cells reveals that the conversion efficiency is limited in particular by the shadowing loss due to the silver front-side metallization, as well as infrared light being absorbed in the aluminium rear-side metallization. This paper summarizes recent developments at ISFH that resulted in a 19.4% efficient large-area screen-printed solar cell, when applying a print-on-print silver front-side metallization and an SiO_2/SiN_x rear-surface passivation.

Introduction

Today, about 80% of silicon solar cells industrially manufactured worldwide apply screen printing for the deposition of the silver front and the full-area aluminium rear metal contacts, as shown in the schematic drawing in Fig. 1a. In production, conversion efficiencies of ~18–18.5% are demonstrated on monocrystalline silicon wafers [1]. Among other factors, two loss mechanisms limit the conversion efficiency of these cells: 1) the silver front-side metallization with finger widths of ~90–100µm reflects about 7% of the incident solar radiation; and 2) the screen-printed full-area aluminium back-surface field (Al-BSF) exhibits only a moderate passivation quality, with typical rear-surface recombination velocities ($S_{eff,rear}$) ranging from 200 to 600cm/s [2,3]. In addition, only about 65% of the infrared light reaching the aluminium rear contact is reflected back into the silicon wafer [4].

To reduce the front-side shading loss, one promising approach is the print-on-print (PoP) technique, in which the silver front contact is deposited in two consecutive screen-printing steps, resulting in a smaller finger width with a higher aspect ratio and hence increased conversion efficiencies [5–7]. The electrical and optical losses of the full-area Al-BSF on the rear side can be reduced by PERC (passivated emitter and rear cell) solar cell design, which is shown in the

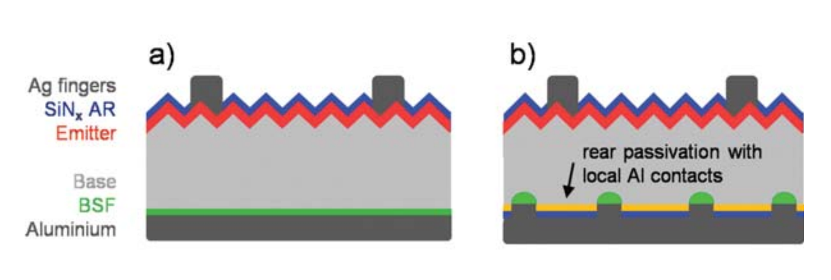

Figure 1. Schematic drawings of a) typical industrial screen-printed silicon solar cell with full-area Al-BSF, and b) PERC solar cell with dielectric rear passivation and screen-printed local aluminium contacts to the silicon base. The rear passivation layer typically consists of a passivation layer (yellow) and an SiN_x capping layer (blue).

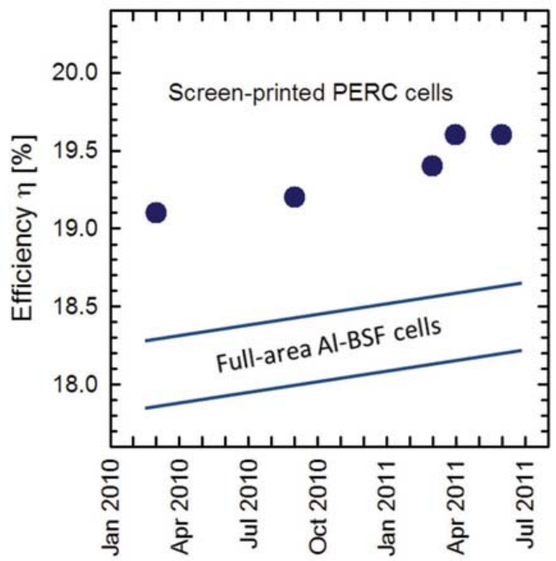

Figure 2. Recent record conversion efficiencies [14–19] of screen-printed rear-passivated PERC solar cells, applying large-area monocrystalline p-type silicon wafers. As a reference, typical conversion efficiencies [1] of industrially manufactured monocrystalline silicon solar cells, with a screen-printed full-area Al-BSF are also indicated.

schematic drawing in Fig. 1b. The PERC cell design has already been applied to laboratory-type silicon solar cells in 1989 [8]. At the rear of the cell, a significantly improved surface passivation and optical reflectance is achieved by dielectric layers, such as SiO_2 [9,10], SiN_x [9], SiC_x [11] and Al_2O_3 [12,13], compared to the full-area Al-BSF. Fig. 2 shows recent record conversion efficiencies for industrial-type (large-area wafers, screen-printed metallization) PERC *p*-type silicon solar cells, which improved from 19.1% in March 2010 to 19.6% in April 2011 [14–19].

This paper presents a summary of recent results demonstrated at ISFH for screen-printed rear-passivated PERC cells, with conversion efficiencies of up to 19.4% [16]. We describe our baseline process for screen-printed solar cells, provide details of the PoP silver front-side metallization and compare two different rear passivation layer stacks: SiO_2/SiN_x and Al_2O_3/SiN_x.

ISFH baseline process for screen-printed full-area Al-BSF silicon solar cells

At ISFH we have established a reference process for screen-printed silicon solar cells and consider it to be very similar to today's standard industrial processing sequence. Pseudo-square 125 × 125mm^2 2–3Ωcm *p*-type boron-doped Cz-silicon wafers with a starting thickness of 200µm are used in this process. After applying a KOH/IPA-based wet chemical surface texture, the n^+-emitter is formed by $POCl_3$ diffusion with a sheet resistance R_{sheet} of 60 to 70Ω/sq. The phosphorus silicate glass is removed by an HF etch. The front side is coated with an SiN_x antireflective layer with a refractive index of 2.05 and a thickness of 70nm. Afterwards, the Ag front contacts are screen printed using a DEK PVP1200 printer, resulting in a finger width ~110µm (see Fig. 3b). The Al rear contact is full-area screen printed, and after each printing step, the pastes are dried in a belt furnace. The processing is completed by a co-firing step in a conveyor belt furnace, followed by the laser edge isolation.

The resulting standard screen-printed solar cells show conversion efficiencies η of up to 18.5%, as displayed in Table 1, cell A. On a larger number of identically processed standard screen-printed solar cells, the standard deviation of the conversion efficiency was determined to be ±0.1%. The small spread of the conversion efficiency allows statistically relevant experiments with a small number of solar cells, e.g. 5 or 10 cells, per split group.

PoP silver front-side metallization

We significantly reduce the silver finger width by applying and optimizing the PoP process. In this case, the Ag front contact is deposited in two consecutive screen-printing steps using a DEK PVP1200

Cell	Type	Rear side	Pitch [mm]	Finger width [µm]	η[%]	V_{oc} [mV]	J_{sc} [mA/cm^2]	FF [%]	Rs [Ωcm^2]
A	Ref.	Al-BSF	-	110	18.5	633	37.0	79.2	0.6
B_1	PoP	Al-BSF	-	70	18.9	634	37.4	79.7	0.6
B_2	PoP	Al-BSF	-	70	18.7*	632	37.1	79.8	0.6
C	PERC	Al_2O_3/SiN_x	1	90	19.0*	652	38.9	75.1	1.3
D	PERC	SiO_2/SiN_x	2	90	19.4*	664	38.5	75.8	1.6

* independently confirmed by FhG-ISE CalLab

Table 1. Solar cell parameters measured under standard testing conditions. Cell A refers to a standard screen-printed solar cell with a full-area Al-BSF and single-printed Ag front contacts. Cells B_1 and B_2 received a PoP Ag front-side metallization with reduced finger width. Cells C and D apply a rear-side passivation of Al_2O_3/SiN_x and SiO_2/SiN_x, respectively, in addition to the PoP Ag metallization.


Continuing 25 years of innovation and reliability
• Leading supplier of all major PV pastes
• First-to-market with:
- Screen printable Ag & Al pastes
- Pb-free Ag pastes
- Low Bow Al pastes
- Seminal research in front contact formation
- Patented Hot Melt ink technology
• Next Generation Solar Materials
FERRO
ELECTRONIC MATERIALS
Delivering material advantages
• Reduced Ag consumption for front & rear surface conductors
• Advanced cell architectures
• Next Generation aluminum technology
• Back surface cell configurations
• Thin film & module applications
Visit Us at the 26th European Photovoltaic Solar Energy Conference and Exhibition, Stand B1U/A12
Tel: 760-305-1000 Fax: 760-305-1100 In Europe, Tel: +44 1440 711 980 Facsimile: +44 1440 711 981
In Asia, Tel: +81-3-5323-7322 Facsimile: +81-3-5323-7396 Internet: www.ferro.com Email: solarsolutions@ferro.com

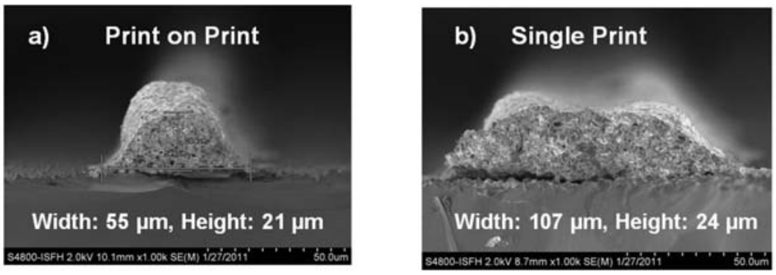

Figure 3. SEM cross-section images of silver front-contact fingers after firing on fully processed solar cells, applying a) PoP screen printing, with finger width 55µm and height 21µm, and b) standard single printing, with finger width 107µm and height 24µm.

printer. Both screens used in the two printing steps are mesh-type screens. In the first screen-printing step, an Ag paste Ag1 is applied, which is designed to establish a good contact resistance to the emitter. After drying, the second Ag screen-printing step follows, using an Ag paste Ag2 with low specific resistivity, in order to reduce the finger line resistance. The second print is completed again by a drying step. Both printing steps are highly accurately aligned towards the four edges of the silicon wafer by a vision camera system in the PVP1200 printer, which ensures ±12.5µm alignment accuracy at 6 sigma and hence an excellent alignment of the second print on the first print.

> "The PoP solar cells achieve conversion efficiencies of up to 18.9%."

The resulting PoP Ag finger profile after firing is shown in the scanning electron microscope (SEM) cross section in Fig. 3a. For comparison, a standard single-printed Ag finger is given in Fig. 3b. The PoP process reduces the finger width to 55µm while maintaining a similar finger height of 21µm. Optical-light microscope measurements reveal average finger widths of (70±5)µm (see cells B_1 and B_2 in Table 1). The smaller finger width reduces the shadowing loss from 6.7% for single print, to 5.4% for PoP with 70µm finger width.

The PoP solar cells achieve conversion efficiencies of up to 18.9% (see cells B_1 and B_2 in Table 1). The value of J_{sc} increases by 0.4mA/cm^2 to 37.4mA/cm^2, due to the reduced shadowing loss. In addition, the PoP cells show an excellent fill factor (FF) of up to 79.8% and a series resistance (R_s) of 0.6Ωcm^2, which indicates that there is no issue regarding contact resistance or line resistance. Besides increasing the conversion efficiency, PoP also reduces the amount of Ag paste deposited on a solar cell by approximately 20–25%, which is important due to the high costs of Ag pastes.

Numerical simulation of screen-printed PERC solar cells

In order to estimate the efficiency potential of industrial-type solar cells with dielectric rear passivation, PC1D simulations are carried out assuming typical input parameters derived from the analysis of our screen-printed solar cells, e.g. a front-side metallization shadowing loss of 6.7%, a 60Ω/sq emitter with a saturation current density of 230fA/cm^2 and a bulk minority carrier lifetime of 400µs. The rear-surface recombination velocity $S_{eff,rear}$ and the internal reflectance R_{rear} at the rear of the cell are varied; both of these strongly influence the efficiency as shown in Fig. 4. Whereas the full-area Al-BSF with $S_{eff,rear}$ = 400cm/s and R_{rear} = 65% limits the efficiency of typical industrial cells to ~18.5%, PERC cells with dielectric rear passivation have the potential to achieve efficiencies $\eta > 19.5\%$ if $S_{eff,rear} < 100$cm/s and $R_{rear} > 90\%$.

Process sequence of screen-printed PERC solar cells

Based on the process flow of the full-area Al-BSF solar cells described above, we have developed a process sequence that includes a passivation of the rear side of the cell by applying dielectric layer stacks. Full processing details are described in [16], but here only the most important process steps will be highlighted. Before texturing and phosphorus diffusion, a dielectric protection layer is deposited on the rear side of the solar cell, leaving the rear side planar and boron doped. Two different rear passivation layers are investigated: a 10nm plasma-assisted ALD-Al_2O_3 layer [20] and a 10nm thermal SiO_2 layer. The double-sided oxidation step for the PERC cells with SiO_2 passivation affects the n^+-emitter profile, leading to reduced emitter saturation currents [16,21]. A PECVD-SiN_x layer is deposited on top of the passivation layer at the rear to improve both the optical reflectance and the surface passivation quality. The dielectric layer stacks at the rear are locally ablated by laser contact opening (LCO) in order to form local line openings. The approximately 80µm-wide line openings are equidistantly spaced with a pitch of either 1mm or 2mm for cells C and D, respectively (see Table 1). Line openings are chosen instead of point

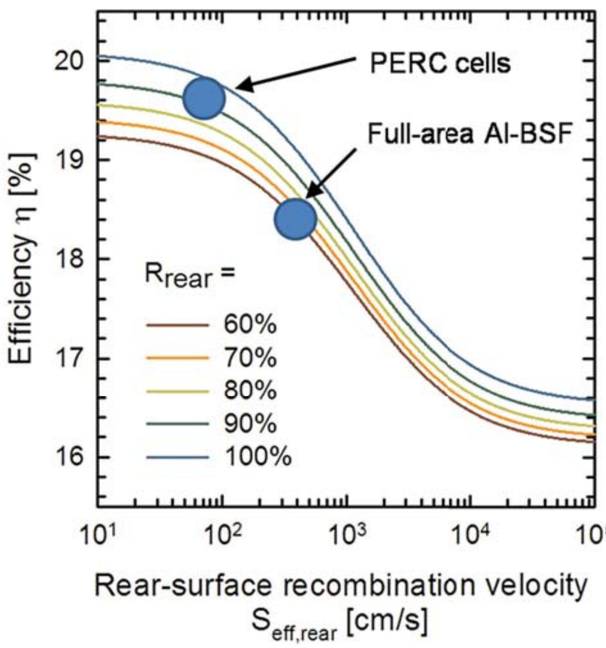

Figure 4. PC1D simulation of the conversion efficiency η vs. the rear-surface recombination velocity $S_{eff,rear}$ for different internal rear reflectance values R_{rear}. Whereas the full-area Al-BSF of typical industrial-type silicon solar cells with $S_{eff,rear}$ = 400cm/s and R_{rear} = 65% limits the conversion efficiency to ~18.5%, screen-printed PERC cells with dielectric rear passivation have the potential to achieve 20% conversion efficiency.

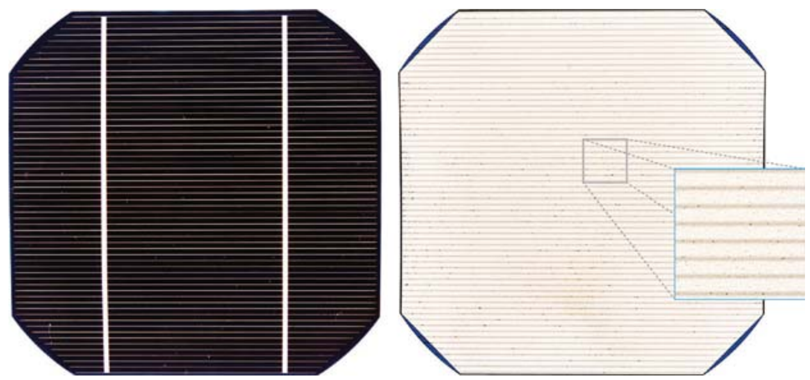

Figure 5. Photographs of the front and rear sides of a PERC solar cell with 19.4% conversion efficiency. Whereas the front side is very similar to a standard screen-printed solar cell, the rear side shows the dielectric passivation layer and the local line contacts.

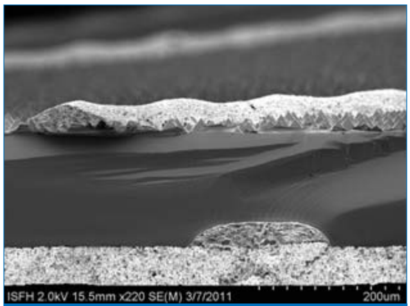

Figure 6. SEM cross-section image of a screen-printed, rear-side-passivated PERC solar cell with local line contacts on the rear side. Horizontal dimensions of the finger width and the line contact width deduced from this image have to be divided by √2, due to the 45-degree cross-section angle.

contacts, since line openings facilitate the formation of a deep and uniform local Al-BSF [22].

The Ag front contacts are deposited by the same PoP screen-printing process as described in the previous section. However, for the rear-passivated cells, the Ag finger width is ~90µm instead of 70µm, which might be partly caused by the increased reflectance of the rear side of the wafer, reducing the wafer edge alignment accuracy of the PVP1200 printer. However, this is still subject to further analysis and optimization. The first PoP evaluations on PERC cells applying a DEK Eclipse printer show very promising results. The Al rear contact is formed by standard full-area Al screen printing. We apply an Al paste Al2, designed for local contacts for the PERC cells C and D, as compared to the standard paste Al1, used for the cells A and B in Table 1. In [23], we show that the paste Al2 achieves a deeper and more uniform local Al-BSF, resulting in significantly lower surface recombination velocities. The laser edge isolation is not required for PERC cells C and D, since only the front side is phosphorus doped. Fig. 5 shows photographs of the front and rear sides of the final cell. The contact lines on the rear side of the cell as well as the passivation layer are clearly visible.

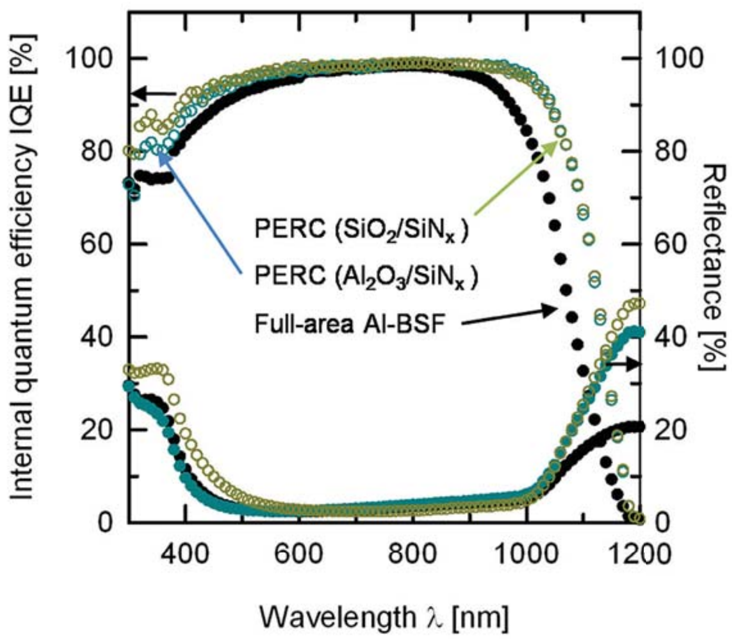

Figure 7. Comparison of IQE and reflectance between PERC solar cells with Al_2O_3/SiN_x (cell C in Table 1) and SiO_2/SiN_x (cell D) passivation stacks at the rear and a full-area Al-BSF reference cell (B_2).

> "Screen-printed PERC cells with dielectric rear passivation have the potential to achieve 20% conversion efficiency."

The SEM cross section of the PERC solar cell in Fig. 6 shows the local Al contact at the rear, with a uniform Al-BSF above the Al-Si eutectic layer. The Ag finger is approximately 90µm wide, and the local Al contact has a width of approximately 140µm. (The cross section has been taken along the <110> crystallographic orientation at an angle of 45 degrees with respect to the Ag fingers and local line contacts at the rear. Accordingly, the horizontal dimensions of the finger width and the line contact width deduced from this image have to be divided by √2.)

IV and IQE analysis of screen-printed PERC cells

Table 1 shows the measured cell parameters of the PERC solar cells C and D with Al_2O_3/SiN_x and with SiO_2/SiN_x rear passivation stacks. The PERC cells are measured after deactivation of boron-oxygen-related recombination by simultaneously annealing for 6 hours at 140°C and illuminating with white light [24,25]. PERC solar cells C and D achieve independently confirmed conversion efficiencies of 19.0% and 19.4%, respectively. Both PERC solar cells show a noticeable improvement in J_{sc} of up to 38.9mA/cm^2. Moreover, the SiO_2/SiN_x-passivated PERC cell D shows a significantly improved open-circuit voltage V_{oc} of 664mV, which is attributable to the changed emitter profile as described above. However, the FF of ~75% for the PERC solar cells is much lower compared to the FF of 79.8% for the reference cell B_2. The decreased FF is caused by a considerably increased series resistance from 0.6Ωcm² for the full Al-BSF reference cells, to 1.3Ωcm² and 1.6Ωcm² for the PERC cells C and D, respectively. The analysis and investigation [26] reveals that, in particular, a relatively high specific contact resistance of 55mΩcm² of the local screen-printed Al contacts is the cause of the marked increase in series resistance and hence the reduced FF. This is subject to further analysis and optimization.

The reflectance and internal quantum efficiency (IQE) of PERC and Al-BSF solar cells are shown in Fig. 7. In the long-wavelength region $\lambda > 900$nm, the dielectric rear-surface passivation significantly improves the reflectance and the IQE. With analytical modelling, we obtain $S_{eff,rear} = (70\pm30)$cm/s for PERC cell C and $S_{eff,rear} = (80\pm30)$ cm/s for PERC cell D, compared to the full-area Al-BSF solar cell B_2 with $S_{eff,rear}$ of (350±100)cm/s. In the short-wavelength region $\lambda < 500$nm, the SiO_2/SiN_x-passivated PERC cell D shows the highest IQE, due to the changed emitter doping profile ($R_{sheet} = 80\Omega$/sq), as compared to the Al_2O_3/SiN_x-passivated PERC cell ($R_{sheet} = 70\Omega$/sq) and the full-area Al-BSF reference cell ($R_{sheet} = 55\Omega$/sq).

The reduced surface recombination velocities at the rear contribute to the improvement in V_{oc} shown in Table 1 for the PERC cells. The increase in J_{sc} of up to 1.5mA/cm² is due to the excellent rear-surface passivation, combined with an improvement of the internal rear reflectance from 61% to 89% and 91%, respectively.

Conclusions and outlook

Based on a solar cell process that is very similar to today's industrially manufactured full-area Al-BSF screen-printed solar cells, we have shown that the PoP silver front-side metallization reduces the finger width to 70µm and minimizes the shadowing loss to 5.4%, which increases the conversion efficiency to 18.9%. The implementation of a dielectric rear passivation greatly reduces the rear-surface recombination velocity $S_{eff,rear}$ to 70cm/s for Al_2O_3/SiN_x and 80cm/s for SiO_2/SiN_x. Additionally, the dielectric layers significantly increase the internal reflectance to 91%, which results in independently confirmed increased conversion efficiencies to 19.4% for large-area silicon solar cells metallized by screen printing. The conversion efficiency is mainly limited by a relatively low fill factor of 75.8% due to a high specific contact resistance of ~55mΩcm² of the local Al contacts. Future improvements of the screen-printed local Al contact formation should enable conversion efficiencies close to 20%. The implementation of a selective emitter into the PERC cell, as well as a reduction of the Ag finger width to 70µm, represent additional opportunities to further increase the conversion efficiency. Accordingly, the results presented in this paper show the potential of large-area screen-printed PERC solar cells to achieve conversion efficiencies exceeding 20%.

Acknowledgements
We would like to thank our colleagues at ISFH for fruitful discussions and support in solar cell processing, as well as Heraeus and Ferro for providing the screen-printing pastes. Parts of this work were funded by the German Federal Ministry for the Environment, Nature Conservation and Nuclear Safety under Contract No. 0327529A.

References
[1] International Technology Roadmap for Photovoltaics (ITRPV.net), Results 2010 [available online at http://www.itrpv.net/doc/roadmap_itrpv_2011_brochure_web.pdf], March 2011, p. 15.
[2] Narasimha, S. & Rohatgi, A. 1997, "Optimized aluminum back surface field techniques for silicon solar cells", *Proc. 26th IEEE PVSC*, Anaheim, USA, pp. 63–66.
[3] Peters, S. 2004, "Rapid thermal processing of crystalline silicon materials and solar cells", Ph.D. thesis, University of Konstanz,

Germany, p. 62.

[4] Lorenz, A. et al. 2010, "Influence of surface conditioning and passivation schemes on the internal rear reflectance of bulk silicon solar cells", *Proc. 25th EU PVSEC*, Valencia, Spain, pp. 2059–2061.

[5] Galiazzo, M. et al. 2010, "Double printing of front contact Ag in c-Si solar cells", *Proc. 25th EU PVSEC*, Valencia, Spain, pp. 2338–2340.

[6] Pham, T. et al. 2010, "Improving electrical performance by double print method and non-contact busbars", *Proc. 25th EU PVSEC*, Valencia, Spain, pp. 2378–2380.

[7] Falcon, T. 2010, "High accuracy, high aspect ratio metallization on silicon solar cells using a print on print process", *Proc. 25th EU PVSEC*, Valencia, Spain, pp. 1651–1655.

[8] Blakers, A.W. et al. 1989, "22.8% efficient silicon solar cell", *Appl. Phys. Lett.*, Vol. 55, pp. 1363–1365.

[9] Schmidt, J., Kerr, M. & Cuevas, A. 2001, "Surface passivation of silicon solar cells using plasma-enhanced chemical-vapor-deposited SiN films and thin thermal SiO_2/plasma SiN stacks", *Semicond. Sci. Technol.*, Vol. 16, p. 164.

[10] Hoffmann, M. et al. 2007, "Firing stable surface passivation using all-PECVD stacks of SiO_x:H and SiN_x:H", *Proc. 22nd EU PVSEC*, Milano, Italy, pp. 1030–1033.

[11] Martín, I. et al. 2001, "Surface passivation of p-type crystalline Si by plasma enhanced chemical vapor deposited amorphous SiC_x:H films", *Appl. Phys. Lett.*, Vol. 79, pp. 2199–2201.

[12] Schmidt, J. et al. 2008, "Surface passivation of high-efficiency silicon solar cells by atomic-layer-deposited Al_2O_3", *Prog. in Photovolt.*, Vol. 16, pp. 461–466.

[13] Sperlich, H.-P. et al. 2010, "High productive solar cell passivation on Roth&Rau MAiA® MW-PECVD inline machine – a comparison of Al_2O_3, SiO_2 and SiN_x-H process conditions and performance", *Proc. 25th EU PVSEC*, Valencia, Spain, pp. 1352–1357.

[14] Sunways AG press release, March 2010 [available online at http://www.sunways.eu/en/company/press].

[15] Münzer, K.A. et al. 2010, "Advanced rear side technology for industrial high efficiency solar cells", *Proc. 25th EU PVSEC*, Valencia, Spain, pp. 2314–2318.

[16] Gatz, S. et al. 2011, "19.4%-efficient large-area fully screen-printed silicon solar cells", *Phys. Status Solidi RRL*, Vol. 5, pp. 147–149.

[17] Bosch Solar Energy AG press release, April 2011 [available online at http://www.bosch-solarenergy.com/media-service/press-releases/].

[18] Böscke, T. et al. 2011, "Fully screen-printed PERC cells with laser-fired contacts – an industrial cell concept with 19.5% efficiency", *Proc. 37th IEEE PVSC*, Seattle, USA [in press].

[19] Lai, J.-H. et al. 2011, "Large area 19.6% efficient rear passivated silicon solar cells with local Al BSF and screen-printed contacts", *Proc. 37th IEEE PVSC*, Seattle, USA [in press].

[20] Schmidt, J., Veith, B. & Brendel, R. 2009, "Effective surface passivation of crystalline silicon using ultrathin Al_2O_3 films and Al_2O_3/SiN_x stacks", *Phys. Status Solidi RRL*, Vol. 3, pp. 287–289.

[21] Kerr, M.J. et al. 2001, "Surface recombination velocity of phosphorus-diffused silicon solar cell emitters passivated with plasma enhanced chemical vapor deposited silicon nitride and thermal silicon oxide", *J. Appl. Phys.*, Vol. 89, pp. 3821–3826.

[22] Müller, J. et al. 2011, "Recombination at local aluminum-alloyed silicon solar cell base contacts by dynamic infrared lifetime mapping", *Proc. 1st SiliconPV Conf.*, Freiburg, Germany [in press].

[23] Gatz, S. et al. 2011, "Analysis of local Al-doped back surface fields for high efficiency screen-printed solar cells", *Proc. 1st SiliconPV Conf.*, Freiburg, Germany [in press].

[24] Herguth, A. et al. 2006, "Avoiding boron-oxygen related degradation in highly boron doped Cz silicon", *Proc. 21st EU PVSEC*, Dresden, Germany, pp. 530–537.

[25] Lim, B., Bothe, K. & Schmidt, J. 2008, "Deactivation of the boron–oxygen recombination center in silicon by illumination at elevated temperature", *Phys. Status Solidi RRL*, Vol. 2, pp. 93–95.

[26] Gatz, S., Dullweber, T. & Brendel, R. 2011, "Contact resistance of local rear side contacts of screen-printed silicon PERC solar cells with efficiencies up to 19.4%", *Proc. 37th IEEE PVSC*, Seattle, USA [in press].

About the Authors

Thorsten Dullweber received his Ph.D. from the University of Stuttgart, Germany, in 2002. From 2001 to 2009 he worked as a project leader at Siemens, Infineon and Qimonda. Since 2009 he has led the Solar Cell Production Processes Group in R&D at ISFH, which focuses on process and efficiency improvements of industrial-type silicon solar cells.

Sebastian Gatz has studied in Regensburg, Dublin and Munich. He received his physics diploma from the Technical University of Munich, where he specialized in aluminium-induced crystallization of silicon-germanium for photovoltaic applications. Since 2007 he has been a Ph.D. candidate at ISFH, carrying out research on front- and rear-side-passivated screen-printed solar cells.

Helge Hannebauer studied technical physics at the Leibniz University of Hanover from 2005 to 2009. For his diploma thesis at ISFH he investigated the optimization of screen-printed solar cells. In 2010 he started a Ph.D. program at ISFH, focusing on advanced screen printing and selective emitters.

Tom Falcon has been with DEK since 2001, initially specializing in process development for DEK's Semiconductor Packaging Technologies Team, before moving to DEK Solar in 2008. He is currently responsible for developing metallization processes for silicon solar cells. Prior to joining DEK he held senior engineering positions with IBM, Nortel and Cookson Electronics.

Enquiries

Thorsten Dullweber
Tel: +49 5151 999 638
Fax: +49 5151 999 400
Email: t.dullweber@isfh.de

Enhancing industrial c-Si cell efficiency by chemical treatment of the SiN layer

Yang Song, Chinalight Solar Co. Ltd., Beijing, China

ABSTRACT

The need for higher efficiency solar cells is becoming more and more urgent nowadays in the photovoltaic industry. In this paper, a new method of increasing efficiency is described whereby SiN is coated by a special commercial chemical after the final step of manufacturing, which is screen printing. No mask is required for this method, but a drying temperature of 200–400°C is mandatory to activate the SiN layer. It is shown that the efficiency of a crystalline solar cell can be increased by at least 0.16% (absolute value) on average. At the same time, modules made from these solar cells do not degrade after sun exposure, and have the potential to pass the stringent standards of a potential-induced degradation (PID) test. The total cost for all the equipment and the chemical is around US$300,000 for retrofitting two (30MW each) production lines.

Introduction

The traditional processes for manufacturing crystalline silicon solar cells are: texturing, diffusion, edge and back-side isolation, surface passivation and screen-printing metallization. The average conversion efficiency achieved is 16.4–16.8% for industrial multicrystalline solar cells. Various technologies have been used to optimize each step, but the manufacturing process is still not perfect. For industrial solar cells, there are a number of ways to reduce the optical losses [1]:

- Minimize the top contact coverage of the cell surface (although this may result in increased series resistance).
- Apply anti-reflection coatings (ARC) to the top surface of the cell.
- Use surface texturing to reduce reflection.
- Make the solar cell thicker to increase absorption (although any light which is absorbed more than a diffusion length away from the junction will not typically contribute to short-circuit current, since the carriers recombine).
- Increase the optical path length in the solar cell by a combination of surface texturing and light trapping.

In this paper, the ARC layer is the main focus and the other factors mentioned above will not be considered. The ARC method developed at Chinalight Solar involves coating the cell with a special chemical and activating the SiN layer. By doing this, all the optical and electrical properties of the cell are enhanced. This technique can be easily

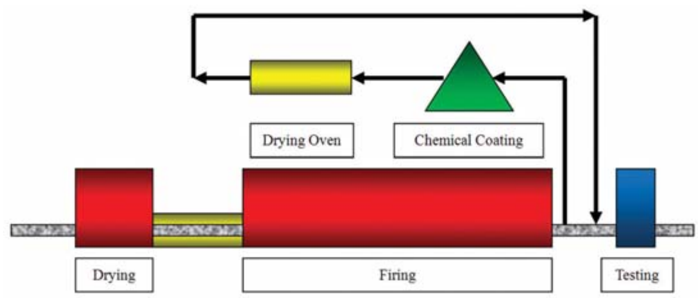

Figure 1. Formation of the coating in the ARC-layer manufacturing process.

incorporated into existing metallization process lines, as well as being beneficial for already manufactured cells.

State of the art of ARC

The most common method of forming the ARC layer in the solar industry is plasma-enhanced chemical vapour deposition (PECVD). Roth & Rau and Centrotherm are the two main manufacturers of PECVD machines, which are remote and direct in terms of plasma generation. At the same time, other competitors, for example Applied Materials, use sputtering to deposit the ARC layer. Although this method yields a high SiN density, the equipment costs are too high.

The thickness of the ARC is chosen so that the wavelength in the dielectric material is one quarter of the wavelength of the incoming wave. For a quarter-wavelength ARC of a transparent material with a refractive index n, and light incident on the coating having a free-space wavelength λ, the thickness d that causes minimum reflection is calculated by: $d = \lambda/4n$. Reflection is further minimized if the refractive index of the ARC (n_1) is the geometric mean of that of the materials on either side; that is, glass or air (n_0) and the semiconductor (n_2). This is expressed by: $n_1 = (n_0 n_2)^{1/2}$.

The thickness and refractive index of the ARC layer are dependent on the wavelength, so zero reflection occurs only at a single wavelength. For photovoltaic applications, the refractive index and thickness are chosen in order to minimize reflection for a wavelength of 600nm. This wavelength is chosen since it is close to the peak power of the solar spectrum [1]. However, for the real application of a solar cell, the significant reflectance below 600nm is still too high (as evidenced by the graph of reflectance vs. wavelength discussed in the next section). Dielectric stack layers – such as SiO_2/SiN/Si, SiN/SiO_2/Si and SiN(N rich)/SiN(Si rich)/Si – have been used to further reduce the surface reflectance, but this process is still complicated and expensive, and sometimes has no effect at all.

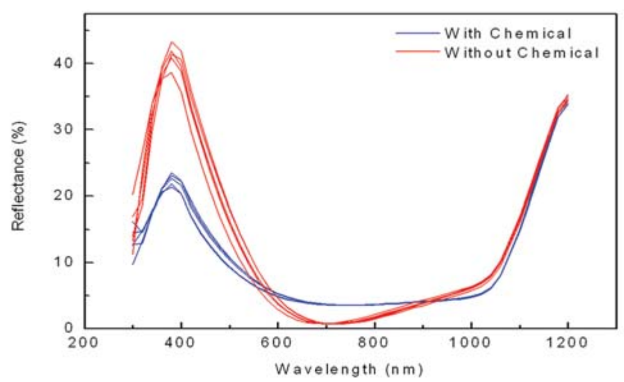

Figure 2. Reflectance of incident light with chemical treatment (blue lines) and without (red lines).

An additional ARC-layer manufacturing step – chemical coating

Formation of the coating

Only two machines and one chemical are required in this process. Commercial spin-coating, dip-coating or spray equipment can be used to disperse the chemical; a spray machine is chosen here, for speed considerations. After the chemical spraying, a drying oven at a temperature of 200–400°C is used to activate the SiN layer, requiring no special environment apart from air. These two processes are illustrated in Fig. 1, between the firing furnace and the tester. At Chinalight Solar, we use a Despatch firing furnace and a Berger efficiency tester.

Function of the coating

The chemical applied in this technique can activate the SiN layer surface and change its refractive index and thickness, thereby causing a solar cell to absorb more light. Fig. 2 shows the surface reflectance of five industrial solar cells (without back-side metal), with chemical treatment (blue lines) and without (red lines). It can be clearly seen that light reflectance for wavelengths below 600nm is dramatically reduced (by half) after chemical coating and activation. For a band gap of silicon of 1.1eV, the maximum

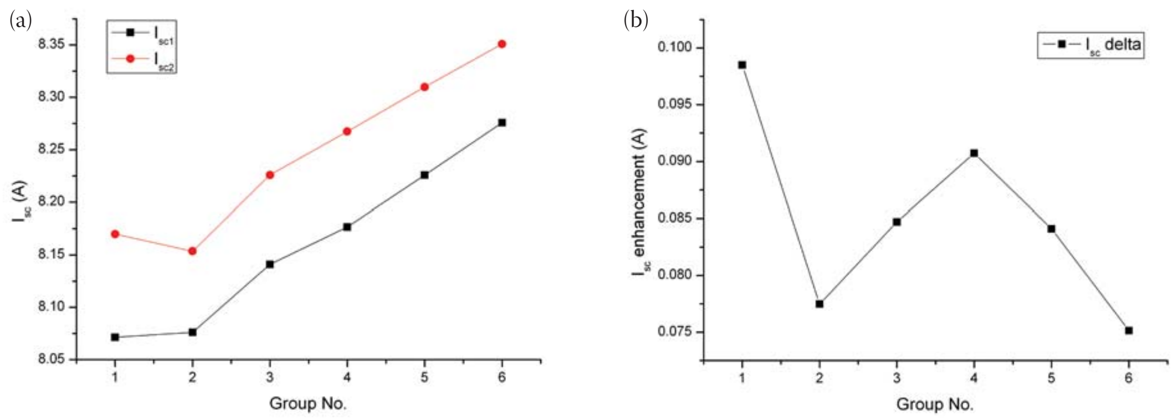

Figure 3. (a) I_{sc} before and after chemical treatment; (b) I_{sc} enhancement after treatment.

SONY

make.believe

Low temperature and low stress bonding provides the reliable interconnection.

Solar Cell Conductive Film "SP100 series"

What's Solar Cell Conductive Film?

The SP100 series is a film type conductive bonding material that interconnects the solar cell with the metal ribbon and is capable of low - temperature bonding at 180℃, enabling significant reductions of residual stress on the cell. Thereby contributing to improved yield during module production. In addition, the SP100 series is capable of bonding thinner cells (approximately 150 μm) that are weaker against thermal stress during soldering than standard thick cells. Free of materials that may impact on the environment such as flux and lead, the SP100 series has been designed with the aim of alleviating the environmental impact after disposal.

Solar Cell Conductive Film makes the stringer beautiful and reliable.

Sony Chemical & Information Device's SP100 series is a bonding material that uses Anisotropic Conductive Film (ACF) technology utilized for applications such as the mounting of driver IC on LCD panels. The SP100 series enable stable interconnection between the solar cell and the metal ribbon by heat-curing and pressuring the epoxy-type resin with the conductive particles distributed in it. In addition, because this material is a film type, there is no dispersal of material to the light receiving area, resulting in a module with beautifully finished and less power loss. Moreover, the material is suitable for narrow width (approximately min. 1.0mm), making it possible to ensure a wide light-receiving area by reducing the width of ribbon and busbar and SP100 series may realize the bonding without busbar on the cell, resulting in reduction of Ag paste.

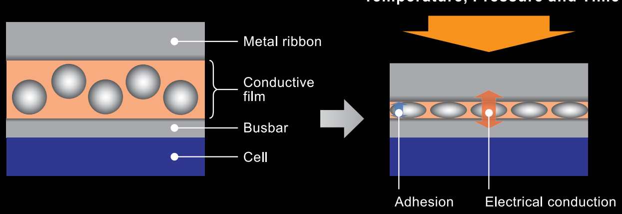

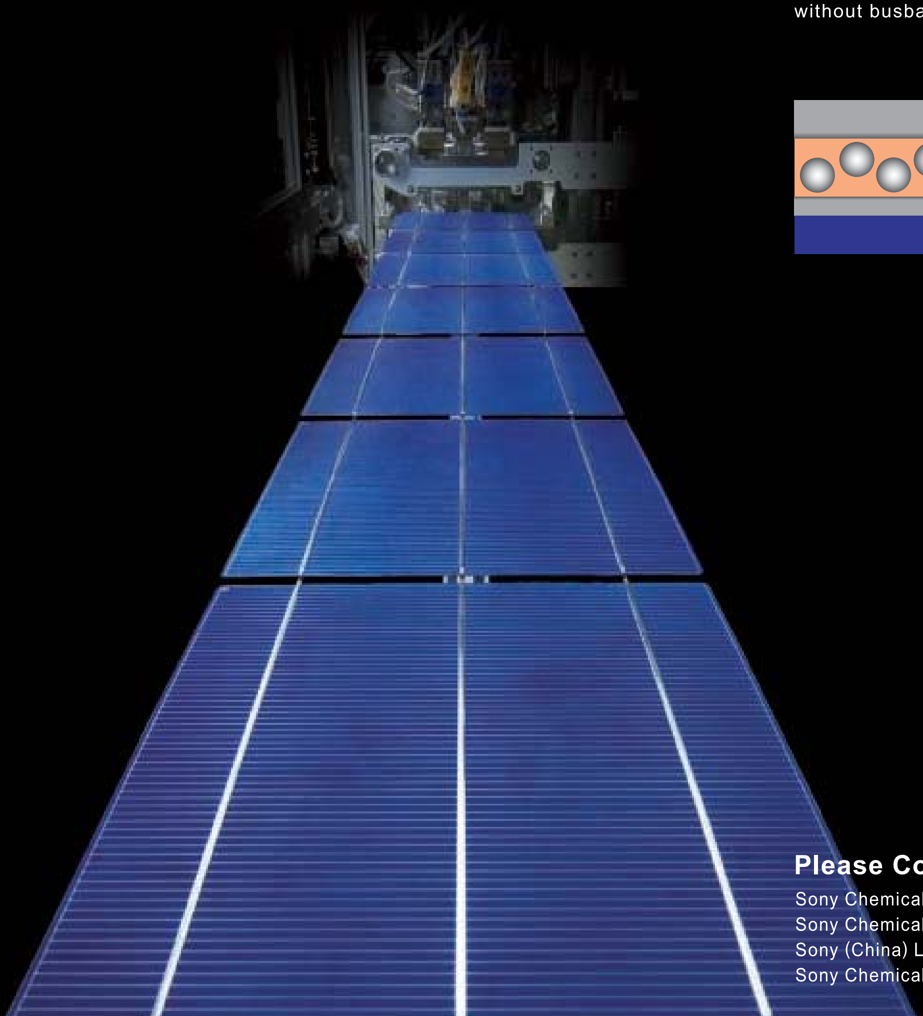

Please Contact Us

Sony Chemicals Europe B.V.	TEL:+31-20-4499-700
Sony Chemicals Corporation of America	TEL:+1-858-942-1282
Sony (China) Ltd.	TEL:+86-21-6162-7750
Sony Chemical & Information Device Corp.	TEL:+81-3-5435-3946

Sony Chemical & Information Device Corporation

http://www.sonycid.jp

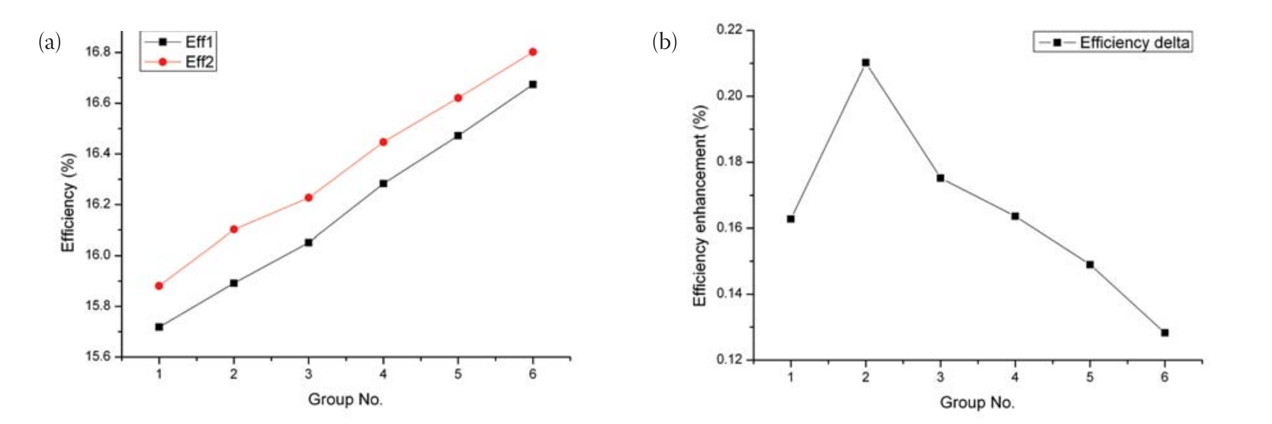

Figure 4. (a) Efficiency before and after chemical treatment; (b) efficiency enhancement after treatment.

wavelength is 1128nm, where photons can be used to generate electron-hole pairs. Short-wavelength photons are very useful; they will contribute to the whole cell performance. This phenomenon is indicated by short-circuit current (I_{sc}) enhancement.

Cell experimental results

Six groups of cells (each group containing 50 screen-printed cells from Chinalight Solar's multicrystalline silicon production line) were measured before and after the chemical treatment. Fig. 3 shows that the value of I_{sc} after treatment (I_{sc2}) is up to ~0.1A higher, no matter what the previous cell efficiency. Fig. 4 shows that the efficiency is at least 0.12% (absolute value) higher than before, with a maximum value of 0.21% for group 2. The efficiency of all the cells is boosted by 0.16% on average by the chemical treatment, but the best results are obtained when the cells' efficiency is close to 16%. Another factor to note is that this treatment can be used throughout the whole cell efficiency range, from below 16% to ~17%. This is especially important for solar cell manufacturing.

There is almost no change in the open-circuit voltage (V_{oc}), series resistance (R_s) and shunt resistance (R_{sh}). The only problem is that there is a small fill factor (FF) loss during the chemical coating and further heating. The reason for fill factor deterioration is still unknown, but the trend is that the stronger the chemical treatment is, the lower the fill factor will be. The relationship between fill factor loss (ΔFF) and efficiency change (ΔEff) is illustrated in Fig. 5. ΔEff and ΔFF exhibit a near-linear relationship. When fill factor loss can be controlled to less than 1 (absolute value), the efficiency of all the cells will increase. When there is no fill factor loss, the efficiency will increase by ~0.2% (absolute value).

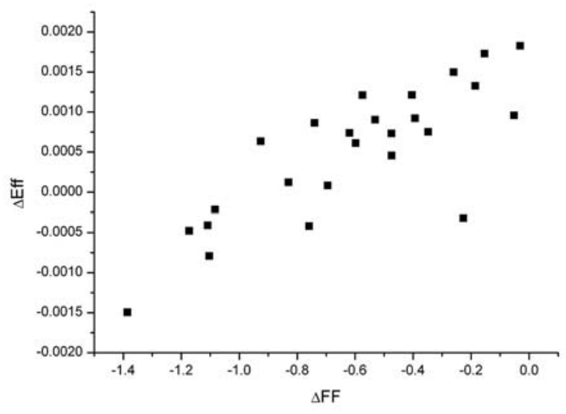

Figure 5. Relationship between fill factor loss (ΔFF) and efficiency change (ΔEff).

Module experimental results

Sixty cells constructed with a chemical coating (with an average cell efficiency increase from 16.16% to 16.30%) were integrated into a module. Soldering on the busbar was not a problem and therefore no mask during coating was needed. The module colour was identical to the one made by traditional screen-printed cells.

The module was tested at an ambient temperature of 25–26°C. Detailed information about the module is shown in Table 1. The maximum power output is 231W and the theoretical power is 238W, giving an assembling power loss of 2.94%.

The module was put outdoors and exposed to the sun for two weeks prior to the experiments. Compared to traditional modules, where a 1–2% degradation is quite normal, there was no degradation for this special module. As shown in Table 1, I_{sc} and R_s became worse, but V_{oc}, R_{sh}, P_{max}, FF and Eff were better after exposure. We can assume there was no hot spot on the infrared image, where the EVA would turn yellow and deteriorate very fast, leading to early damage of the module. The deterioration of I_{sc} and R_s may be due to partially broken soldering on the busbars (after two weeks' exposure); in any case, the silver front contacts are coated by some of the chemical, leading to non-perfect soldering. Therefore, as little as possible of the chemical must be used, so that there is no significant loss of efficiency.

Normally the light-induced degradation of monocrystalline solar cells and modules is stronger than in the case of multicrystalline cells. Because Chinalight Solar only has multicrystalline production lines, the mono tests will need to be carried out in the future as well, to prove the quality

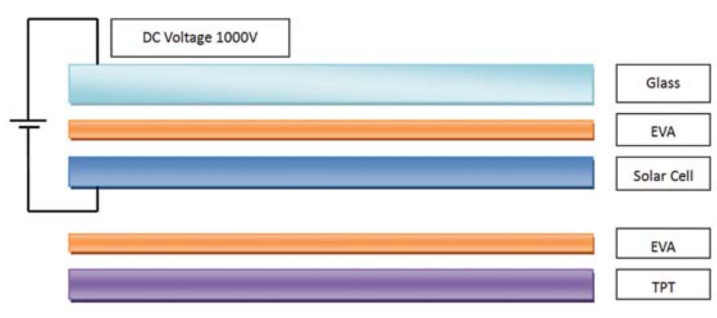

Figure 6. PID test setup showing the structure of the module [3].

OM Group
Solar Chemicals

Plated metal stack on Ag paste

BENEFITS

- ✔ **Plating shows good adhesion on frontside Ag pastes**
- ✔ **No attack of aluminum BSF**
- ✔ **No attack of the backside silver bus bar**
- ✔ **No drop in backside silver paste pull strengths after plating**
- ✔ **Efficiencies increased with plating**
- ✔ **Rs lowered by plating**
- ✔ **FF increased with plating**
- ✔ **CoO significantly reduced**
- ✔ **Better cell to cell consistency**

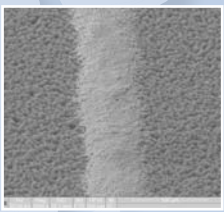
Ag Paste

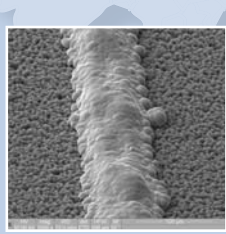
Metal plated stack on Ag Paste


Metal stack plate on Ag Paste

Customer feedback of OMG plating

Paste	Plated Metals	Efficiency Gain	FF Gain
A	Ni / Cu / Ag	13.13%	14.21%
A	Cu / Ag	6.53%	7.61%
B	Ni / Cu / Ag	2.52%	3.63%
B	Cu / Ag	4.17%	5.0%
C	Ni / Cu / Ag	3.93%	4.93%
C	Cu / Ag	0.82%	1.86%

Product	Current Density (ASD)	Temperature (C)	Time (sec)	Thickness (um)
Solar Plate Ni PV80	18	60	17	1
Water Rinse		Ambient	10	
Solar Plate Cu PV73M	10	25	163	6
Water Rinse		Ambient	10	
Solar Plate Ag 200	4	25	12	0.5
Water Rinse		Ambient	10	
Dry				

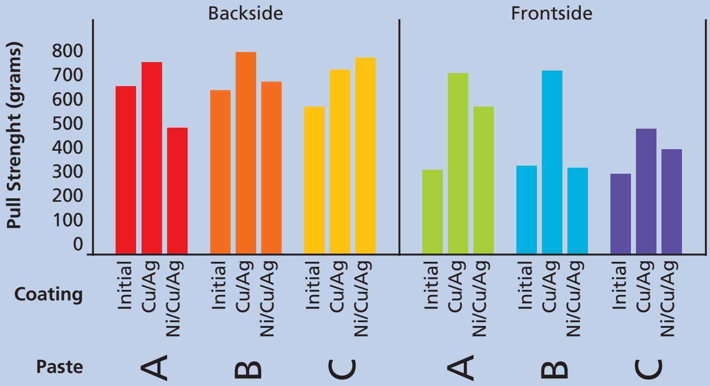

A Greener Future

solar@omgi.com | www.omgi.com

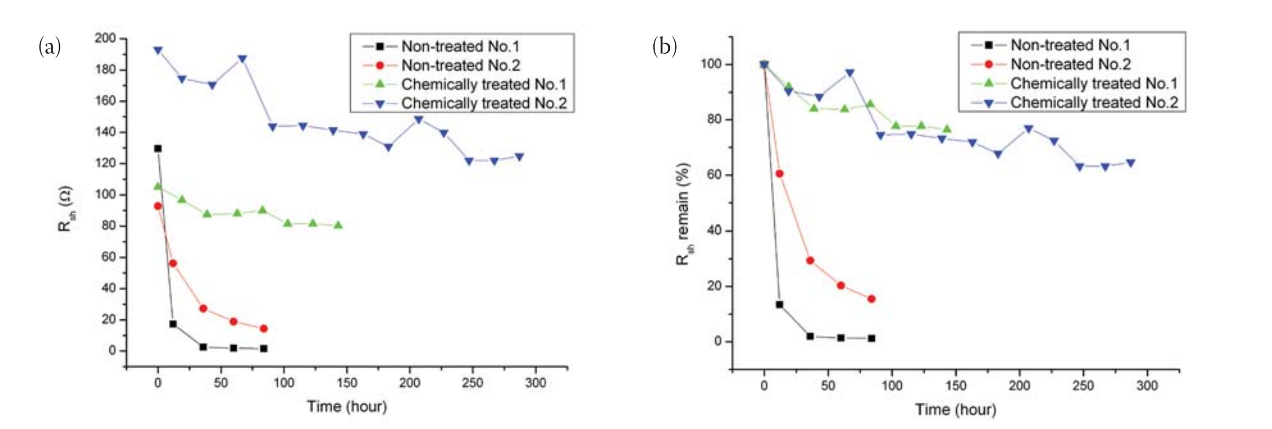

Figure 7. PID test results for normal and chemically treated modules: (a) change in R_{sh}, and (b) percentage R_{sh} remaining.

of the chemical treatment. Light-induced degradation is usually caused by boron–oxygen recombination pairs, which leads to a decrease in minority carrier lifetime. The reason for the non-degradation of this module is still under investigation.

Potential-induced degradation (PID) test results

Recently, module degradation and power loss have started to become more and more common in solar plants. When solar cells are interconnected in series, high system voltages can lead to unwanted leakage currents between the solar cells, bedding materials, glass and grounded module frame. This allows a positive charge to build up on the ARC at the surface of the cells [2]. There are two main ways to solve the PID problem. First, at the cell level, a better ARC layer having better dielectric ability can be applied. Second, at the module level, a better encapsulation foil can be used.

To perform the PID test [3], at Chinalight Solar we encapsulate each cell in a 156mm-square glass frame to make a one-cell module. The detailed structure of the module is shown in Fig. 6.

In Fig. 7 it is seen that the R_{sh} of normal modules degrades dramatically over the first 50 hours, but chemical-treated modules retain most of the R_{sh}, even after 300 hours. A possible explanation is that an insulation layer is formed on top of the solar cell during the chemical treatment, making up for the drawbacks of low density of SiN and pin holes inside the ARC layer. This phenomenon is still under investigation.

Alternative coating techniques

Other coating methods, such as coating before drying and coating between drying and firing, were also used to test the chemical. At one stage the cells' efficiency soared from 16.29% (mass production average) to 16.64% (continuous average of ten cells) – an increase of ~0.35%. A possible explanation for this big jump is that the chemical not only changes the optical property of SiN, but also functions as a cap layer during the firing process. Hydrogen is used to passivate the dangling bonds on the wafer surface and inside the bulk material, for example the grain boundaries. When cells that have not undergone the chemical treatment go through the firing furnace (maximum temperature of 920°C), hydrogen diffuses from the bulk material and the SiN layer to the ambient air, and the passivation quality deteriorates to a greater or lesser degree. When a capping layer is formed, the hydrogen is prevented from leaving the solar cell, and the passivation quality is maintained. This phenomenon is indicated by an increase in the open-circuit voltage (V_{oc}), from 620mV to 621mV. When there is no protection on the SiN surface, any high-temperature process will reduce the value of V_{oc}.

Because the cells are taken out for the chemical treatment before entering the drying furnace, the silver busbars and fingers are still wet and no efficiency data is available at this stage. The possibility of existing high-quality wafers inside the 10 cells cannot be excluded. The earlier example of an increase in efficiency to 16.64% could therefore be just a coincidence. Repeat experiments have been conducted, but all the cells show a poor sheet resistance (R_{sh}) below 20Ω/sq, which indicates that the p-n junction has been contaminated during the high-temperature firing. Further tests in this area are ongoing.

Potential for mass production

A specially designed accurate coating machine can accommodate six rows of 125mm wafers or five rows of 156mm wafers. The normal transport speed is 120 inch/min. A Despatch drying and firing machine can operate at 240 inch/min, yielding a production capacity of solar cells of ~700–900 pcs/hour in one screen-printing line, which equates to 30MW. The capacity of the coating machine is 2.5 times that of a screen-printing line. Therefore, based on this figure, one coating machine has a production capacity of 75MW. Taking into account the machine downtime, the coating machine can support at least two production lines, which would be 60MW.

A drying oven can produce 1500 pcs/hour, equivalent to two screen-printing lines, which are 60MW. To avoid the manual insertion of cells into the boat, a continuous conveyer-driven oven (like a Despatch) is the best option. To put this innovation into practice, manual handling or a Robert arm is

	I_{sc} [A]	V_{oc} [V]	R_s [Ω]	R_{sh} [Ω]	P_{max} [W]	V_{pm} [V]	I_{pm} [A]	FF	Eff [%]
Original									
With junction box	8.4643	36.8557	0.5299	102.0390	231.3204	29.2055	7.9204	0.7415	14.1610
Without junction box	8.4665	36.8368	0.5176	98.2200	232.6565	29.3572	7.9250	0.7460	14.2428
After exposure									
With junction box	8.4531	36.9104	0.5603	113.4711	231.6265	29.2404	7.9214	0.7424	14.1798
Without junction box	8.4562	36.8714	0.5308	106.1162	233.0796	29.3744	7.9348	0.7476	14.2687

Table 1. Module CLS-SP110611RD001 made from chemically treated cells.

required between the stages 1) firing and chemical coating, 2) chemical coating and drying oven, and 3) drying oven and Berger tester.

Cost of ownership (COO) evaluation

As mentioned previously, a specially designed accurate coating machine costs in the region of US$300,000 for an industrial application. The total annual cost for the chemical is only US$1500 and the price of the drying oven is only US$1000. Including machine maintenance, workforce salaries and power usage (electricity, water, vacuum and compressed air), this technology innovation is a relatively cheap option for the solar industry, but detailed calculations would need to be performed to estimate the cost of a fully automated process.

Summary

Solar cells with an efficiency below 16.4% are becoming increasingly unacceptable to industrial manufacturers, so ways of improving their efficiency are currently being sought. At Chinalight Solar, a method involving chemical treatment of the SiN layer has been developed, resulting in the efficiency of all the cells being boosted by 0.16% on average. This technology can meet the requirements for mass production in terms of practicality and cost. The installation cost for this method is acceptable and the annual running costs are relatively low. Moreover, experiments have shown that the integrated module does not degrade after two weeks' exposure to the sun and also withstands high voltage for longer in the PID test. This innovation has a potential for becoming an additional stage of the current manufacturing line of crystalline silicon solar cells. However, the scope for adaptability still needs to be proven.

Acknowledgements

The author would like to express his appreciation to his R&D team colleagues at Chinalight Solar for their excellent collaboration and fruitful discussions during this work. The company's financial support for this project is also gratefully acknowledged.

References

[1] Honsberg, C. & Bowden, S. 1998, Photovoltaics CDROM, UNSW, Sydney, Australia.

[2] "Performance degradation in solar plants" [available online at http://ecogeneration.com.au/news/performance_degradation_in_solar_plants/055947/]

[3] Berghold, J. et al. 2010, "Potential induced degradation of solar cells and panels", *Proc. 25th EU PVSEC*, Valencia, Spain, pp. 3753–3759.

About the Author

Yang Song is a senior engineer at Chinalight Solar Co., Ltd. He joined the company in 2009 and works in the R&D centre for industrial solar cell improvement and new types of innovation. He received his M.E. in 2009 from the School of Photovoltaic and Renewable Energy Engineering at the University of New South Wales, Sydney, Australia. He also holds a B.S.E. degree (2001) and a Ph.D. degree (2006) in materials science and engineering from Tsinghua University, Beijing, China.

Enquiries

Dr. Yang Song
Senior Engineer
Chinalight Solar Co. Ltd.
No. 3, Xingguangsan Street
Opto-Mechatronics Industrial Park
Tong Zhou District
Beijing, China
Tel: +86 10 81506158
Email: songyang@chinalightsolar.com
Website: http://www.chinalightsolar.com/

Atomic layer deposition of Al_2O_3 for industrial local Al back-surface field (BSF) solar cells

Aude Rothschild, **Bart Vermang** & **Hans Goverde**, imec, Leuven, Belgium

ABSTRACT

Al_2O_3 deposition has received a lot of attention in the last few years for its attractive passivation properties of c-Si surfaces. Within the local Al back-surface field (BSF) cell concept, we considered several avenues of study: surface preparation, thermal stability, charge investigation and the 'blistering' phenomenon. The investigations converged on a passivation stack that includes a thin interfacial SiO_2-like layer and a thin Al_2O_3 layer (~10nm), which undergoes a high-temperature anneal (> 600°C). In order for a surface passivation with Al_2O_3 to be a cost-effective step for the PV industry, a high Al_2O_3 deposition rate is required. Compared to the different high-throughput tools that have recently emerged on the PV market, such as atomic layer deposition (ALD) and plasma-enhanced chemical vapour deposition (PECVD), our tool screening revealed quite similar results. The differences therefore seem to have an origin primarily in the tool specifications rather than in the achievable Al_2O_3 material properties.

Introduction

The atomic layer deposition (ALD) technique has its roots in the 1960s, but it was only in the mid 1990s that the semiconductor industry started to pay attention to this technique, to satisfy the demands of the ever-shrinking dimensions of CMOS devices. The reason for such interest comes from the fact that ALD offers excellent thickness and uniformity control at the nanometre level, on top of the fact that ALD layers can be deposited in a conformal way in structures of high aspect ratio, making ALD suitable for 3D structures as well.

For some years, ALD for photovoltaic applications, in particular ALD-Al_2O_3, has been gaining interest for new c-Si solar cell generations too [1–5]. As a major difference from most other dielectrics, such as Si_xN_y or SiO_2, where fixed positive charges are stored at the interface region, Al_2O_3 can lead to the presence of negative charges at the silicon surface. These negative charges induce a field effect, which repels the minority carriers at the interface and thereby enhances the passivation level reached on *p*-type surfaces. However, in order to be applicable to industrial solar cell manufacturing and cost effective in solar applications, conventional ALD has to find a way to be compatible with high-throughput and high-yield requirements.

Given a fairly low deposition rate of about 1–5nm/min and the throughput requirement of solar cell manufacturers (currently about one 156 × 156mm^2 wafer/s), equipment vendors have tackled the challenge from two different directions: either by tweaking 'temporal' ALD into 'spatial' ALD or by adjusting the batch size ('batch' ALD). Two companies, Solaytec and Levitech, have built their tools (PDT and Levitrack) based on the first approach, which offers ALD deposition rate in the nm/s range. On the other hand, the companies ASM and Beneq have chosen the second approach, producing the batch ALD tools A412 and TFSNX300, respectively. A plasma ALD approach appears to be another possible option, but is not currently available for high-throughput applications.

Al_2O_3 deposition, however, is not restricted to the ALD approach: there are also other techniques available on the PV market, for example plasma-enhanced chemical vapour deposition (PECVD) (such as the SiNA system from Roth&Rau) and reactive sputtering.

Some potential applications of ALD-Al_2O_3 layers in future solar cells are the rear-side passivation of *p*-type c-Si substrates in PERL-type (passivated emitter, rear locally diffused) solar cells, and the front-side passivation of *p*-type emitters on *n*-type c-Si substrates, such as i^2-BC (industrial interdigitated back contact) solar cells [6]. ALD-Al_2O_3 could also serve as a tunnelling barrier layer for metal-insulator-semiconductor (MIS) contacts [7]. Each of these applications might eventually require a different passivation stack (different cleaning, annealing, additional layer, etc.) to satisfy the electrical and optical requirements.

This paper concentrates on the concept of a PERL-type local Al back-surface field (BSF) solar cell and the steps towards improving its rear-side passivation stack with Al_2O_3. Among the different process parameters that can improve the passivation level, two important aspects will be discussed in more detail: the surface preparation before the Al_2O_3 deposition [8] and the thermal stability of the layer, as in the 'contact firing' treatment in typical local Al BSF process flow [9]. In the next part of the paper, the focus will be on the charge characterization of the c-Si/SiO_2/Al_2O_3 passivation stack. This will be followed by addressing another important aspect that appears to be relevant when integrating Al_2O_3 into a local Al BSF process flow: the outgassing from Al_2O_3 layers that can cause blistered regions on the surface of rear-side passivation stacks (Al_2O_3/Si_xN_y) [10]. To conclude, we discuss the advances recently made in high-throughput Al_2O_3 tools and imec's position in that respect.

Surface preparation

The ALD process is very surface sensitive and therefore surface preparation prior to deposition of any passivation layer is a key parameter of the technique. This parameter will determine the physical properties (such as layer closure, density and roughness) and the electrical properties of the c-Si/dielectric interface (such as interface trap density D_{it} and fixed charges Q_f). As a consequence, the surface preparation before Al_2O_3 deposition will have an impact on the passivation level.

"The ALD process is very surface sensitive and therefore surface preparation prior to deposition of any passivation layer is a key parameter of the technique."

The ALD reaction mechanism and its various growth per cycle (GPC) modes have been extensively studied within the semiconductor industry for

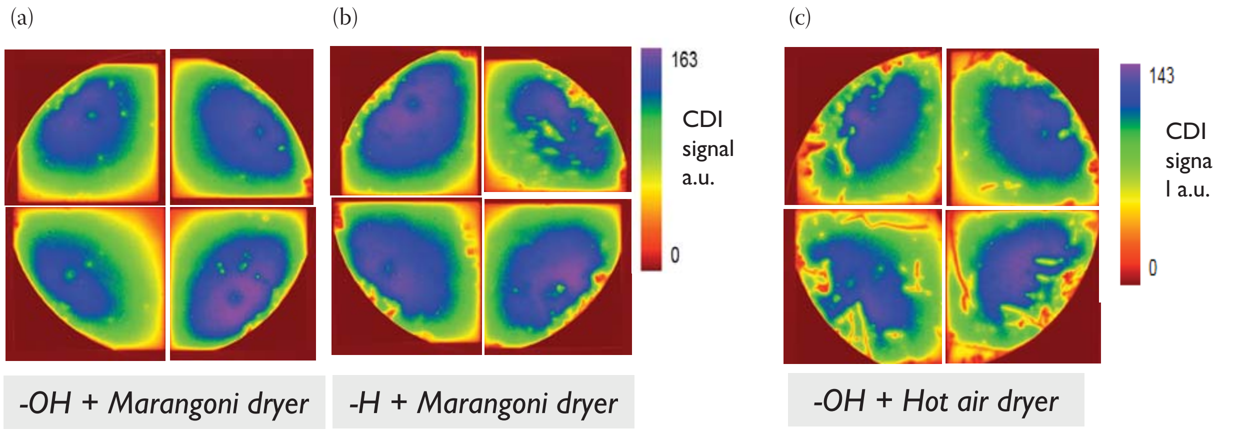

Figure 1. Comparison of passivation levels reached after annealing for different surface preparations before ALD-Al_2O_3 deposition: a) -OH terminated + Marangoni; b) -H terminated + Marangoni; c) -OH terminated + hot air dryer. Lifetime measurements were performed by carrier density imaging (CDI).

different high k layers (Al_2O_3, HfO_2, etc.) [11,12]. Besides many other parameters influencing the ALD growth of Al_2O_3 layers, such as precursor gas selection and deposition conditions, the surface preparation itself can strongly affect the initial interface growth mode type. It has often been reported that the *two-dimensional* growth mode (associated with a surface that is -OH terminated) is the preferred choice for its better transistor performance over the *island* growth mode (-H terminated) [13].

Drying of the surfaces after cleaning is just one of many influencing factors in the surface preparation prior to ALD deposition. In the semiconductor industry, a so-called Marangoni drying technique has become the standard drying process, resulting in wafers that are spotless and free of water marks, whereas the PV industry mostly uses a hot-air dryer approach.

Different surface treatments (-OH vs -H), in combination with two drying techniques (Marangoni vs hot air), have been studied for solar cell applications, taking into account the following criteria: a minimum level of defects, assessed by light scatterometry measurements; a wide within-wafer uniformity, evaluated by carrier density imaging (CDI); and a high minority-carrier lifetime level, measured by quasi-steady-state photoconductance (QSSPC).

As can be seen from Fig. 1, a hydrophilic clean (-OH) that is dried using the Marangoni technique leads to an improved surface passivation level and uniformity, as compared to the one dried by the hot air method. The surface preparation was performed using the following cleaning sequences: sulphuric peroxide mixture (SPM = H_2SO_4/H_2O_2) + HF/HCl + ammonium peroxide mixture (APM = $NH_4OH/H_2O_2/H_2O$), for the -OH terminated surface; and SPM + HF/HCl, for the -H terminated surface [8]. The 8" wafers were cut into four pieces for measurement

Figure 2. Interfacial SiO_2 regrowth is observed on a hydrophobic surface after annealing c-Si/3nm Al_2O_3 by FGA@350°C.

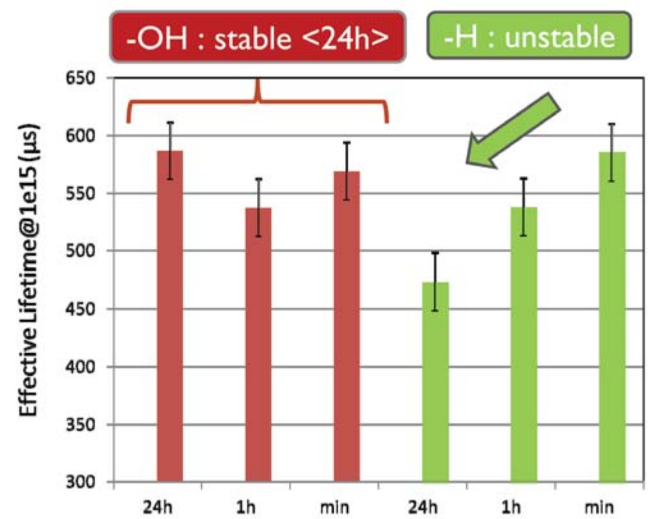

Figure 3. Stability of the passivation level over time for two types of clean: hydrophilic (-OH) vs hydrophobic (-H).

purposes, each piece receiving the same treatment. Surprisingly, the hydrophobic starting surface (-H) with Marangoni drying leads to a passivation level and uniformity similar to the hydrophilic clean. A physical analysis of the c-Si/Al_2O_3 interface indicates the growth of an SiO_2-like layer during the forming gas annealing (FGA) at 350°C (a low-temperature anneal in forming gas atmosphere). This growth reflects the H_2O release from the Al_2O_3 film during the annealing process, leading to an oxidation of the interface (Fig. 2). This is most likely the reason that similar passivation levels are reached after annealing for both hydrophilic and hydrophobic cleans, since both types will include an SiO_2-like interface.

However, a hydrophobic surface is more sensitive to moisture and hydrocarbons and its hydrophobicity is therefore time critical. Consequently, a hydrophilic clean is preferred for its stability over time: a hydrophilic state can be guaranteed for 24 hours, whereas a hydrophobic state will degrade within a few hours, affecting its passivation level (Fig. 3). This stability is of practical interest since it avoids the need to perform the clean/Al_2O_3 deposition steps in a short timeframe.

Thermal stability

There are reports in the literature regarding surface passivation studies (based on lifetime measurements) that are typically carried out on high-quality *p*- or *n*-type float-zone (FZ) material [14] with a high bulk lifetime in order to be sensitive to the contribution from the surface rather than from the bulk. However, one needs to make sure that the trends observed for FZ material remain valid for solar-grade Czochralski (CZ) material as well, especially regarding the thermal stability of Al_2O_3 above 800°C, which corresponds to the thermal budget of the firing step once integrated into a local Al BSF cell concept.

In that context, a study of CZ material has been undertaken, in which different Al_2O_3 thicknesses and thermal budgets were considered. Solar-grade *p*-type CZ material (2Ωcm) received saw damage removal (SDR) and polishing steps (160µm-thick final thickness) prior to passivation with ALD-Al_2O_3. The Al_2O_3 thickness deposited was in the range 5–30nm. The thermal budgets applied were either a low-temperature anneal (FGA@350°C) or a high-temperature anneal around 800°C (firing temperature) in order to determine the thermal budget limitations in low- and high-temperature regimes.

As can be seen in Fig. 4, for all Al_2O_3 thicknesses in a 5–30nm range, the passivation level is increased after FGA@350°C and is maintained for a firing thermal budget [9]. In terms of thermal stability, this CZ behaviour is therefore different from the one that is usually observed for FZ material. This difference illustrates the strong impact of the starting substrate in assessing the passivation level reached with Al_2O_3 and underlines the need for studying both substrates in parallel.

"Besides thermal stability, the stability of Al_2O_3 over time is another important aspect to consider: the high passivation level reached with Al_2O_3 once annealing is performed has to be maintained."

The results shown in Fig. 4 also emphasize that the Al_2O_3 thickness required to achieve a high enough passivation level does not need to be excessive: approximately 10nm of Al_2O_3 is sufficient to reach a high passivation level, even after a high thermal budget. The minimum Al_2O_3 thickness is an important element for the high-throughput requirement that will be discussed later. Besides thermal stability, the stability of Al_2O_3 over time is another important aspect to consider: the high passivation level reached with Al_2O_3 once annealing is performed has to be maintained. This point is currently under investigation [15].

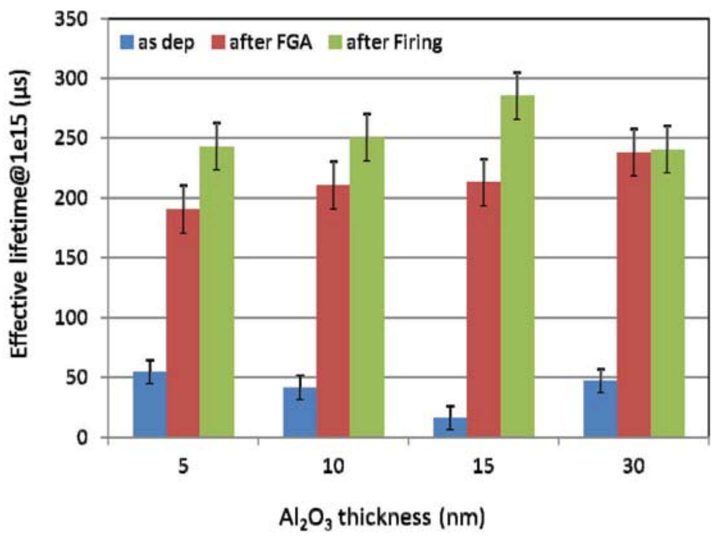

Figure 4. Thermal stability of different Al_2O_3 thicknesses on *p*-type CZ (2Ωcm), with SDR and polishing prior to passivation.

Charge characterization

Whereas other dielectrics such as SiO_2 and Si_xN_y introduce fixed positive charge Q_f, Al_2O_3 induces a build-up of negative fixed charge within the dielectric passivation stack [2]. This negative fixed charge, which induces a *field-effect* passivation, is considered to be one component that controls the low surface recombination velocity reached with Al_2O_3.

The second component is the *chemical* passivation, which is related to the interface trap density D_{it}. Benick et al. [16] reported that the weight of these two components is not the same, however, and that a low D_{it} is a prerequisite in order to benefit from the strong field-effect component.

Two approaches have been developed to investigate the electrical parameters and process parameters that control the passivation quality. The first (so-called *double-thickness series*) approach offers, through a statistical capacitance–voltage (CV) analysis, information related to charge polarity and charge quantity, as well as a decoupling of the location of the charge within the passivation stack c-Si/SiO_2/Al_2O_3 [17]. Fig. 5 shows a schematic of the model used for charge extraction at the different interfaces. The principle of the technique relies on the evolution of the flat-band voltage V_{fb} as a function of the equivalent oxide thickness EOT, according to Equation 1, where φ_{ms} is the work function difference between the metal and the semiconductor material, and T_{Al2O3} corresponds to the EOT contribution of the Al_2O_3 layer to the total EOT. To be able to determine the different charge densities, independent variation of the SiO_2 thickness and Al_2O_3 thickness is required. From a straight-line fit of the V_{fb}–EOT plot of the SiO_2 thickness series, the slope allows extraction of the charge density at the interface Si/SiO_2 (Q_{Si/SiO_2}). Charge densities at the SiO_2/Al_2O_3 interface ($Q_{SiO2/Al2O3}$) and in the bulk of the Al_2O_3 (ρ_{Al2O3}) can be estimated from the fit of the V_{fb}–EOT plot of the Al_2O_3 thickness series.

The experiment was performed using 8" 700µm-thick *p*-type CZ wafers. A slant-etched SiO_2 approach was followed, which has the advantage of increasing accuracy, avoiding wafer-to-wafer non-uniformity and enabling a large number of data points to be generated from each wafer. The SiO_2 slant-etch, performed by a controlled immersion speed at HF, was in the range 1–6nm and the Al_2O_3 thickness was in the range 2–30nm. FGA@350°C was then performed as the last processing step, to

$$V_{fb} = \mathrm{EOT}\left[-\frac{Q_{Si/SiO_2}}{\varepsilon\,\varepsilon_{ox}}\right] + \left\{\varphi_{ms} - \frac{\rho_{Al_2O_3}\cdot T_{Al_2O_3}{}^{2}}{2\,\varepsilon\,\varepsilon_{ox}} - \frac{Q_{SiO_2/Al_2O_3}\cdot T_{Al_2O_3}}{\varepsilon\,\varepsilon_{ox}}\right\}$$

Equation 1.

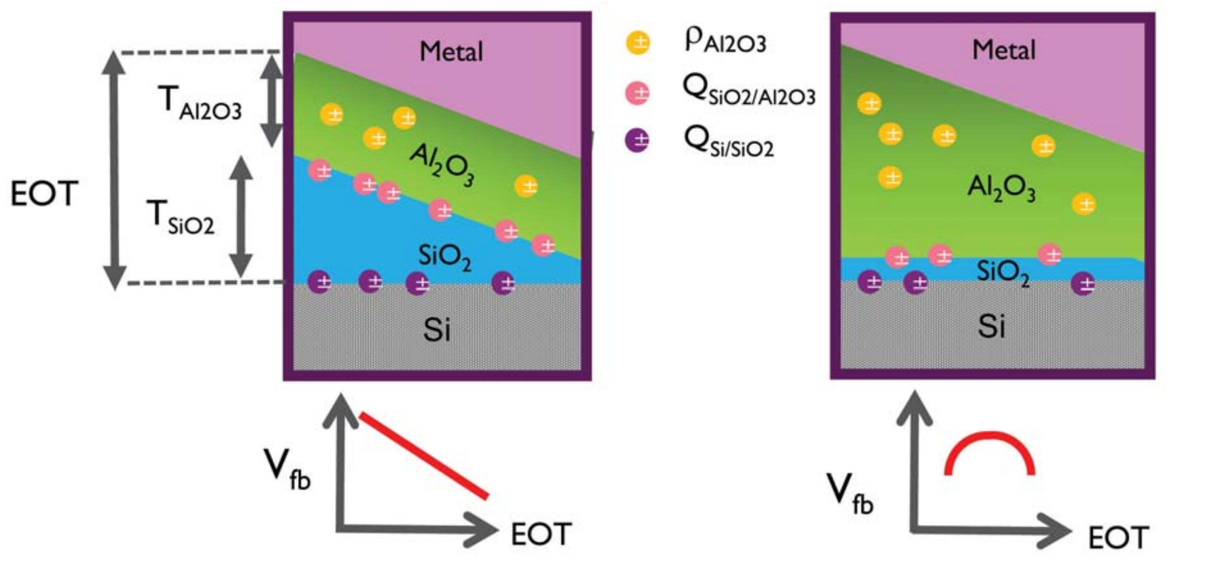

Figure 5. Charge extraction model – double-thickness series approach for determination of fixed charge within the passivation stack (Si/SiO_2/Al_2O_3): (a) varying only SiO_2 thickness enables Q_{Si/SiO_2} extraction; (b) varying only high-k thickness enables $Q_{SiO2/Al2O3}$ and ρ_{Al2O3} extraction.

Q_{Si/SiO_2}(cm^{-2})	Q_{SiO_2/Al_2O_3}(cm^{-2})	$\rho_{Al_2O_3}$(cm^{-3})
2E+11	−4E+11	−1E+19

Table 1. Estimation of charge density and distribution within the c-Si/SiO_2/Al_2O_3 stack.

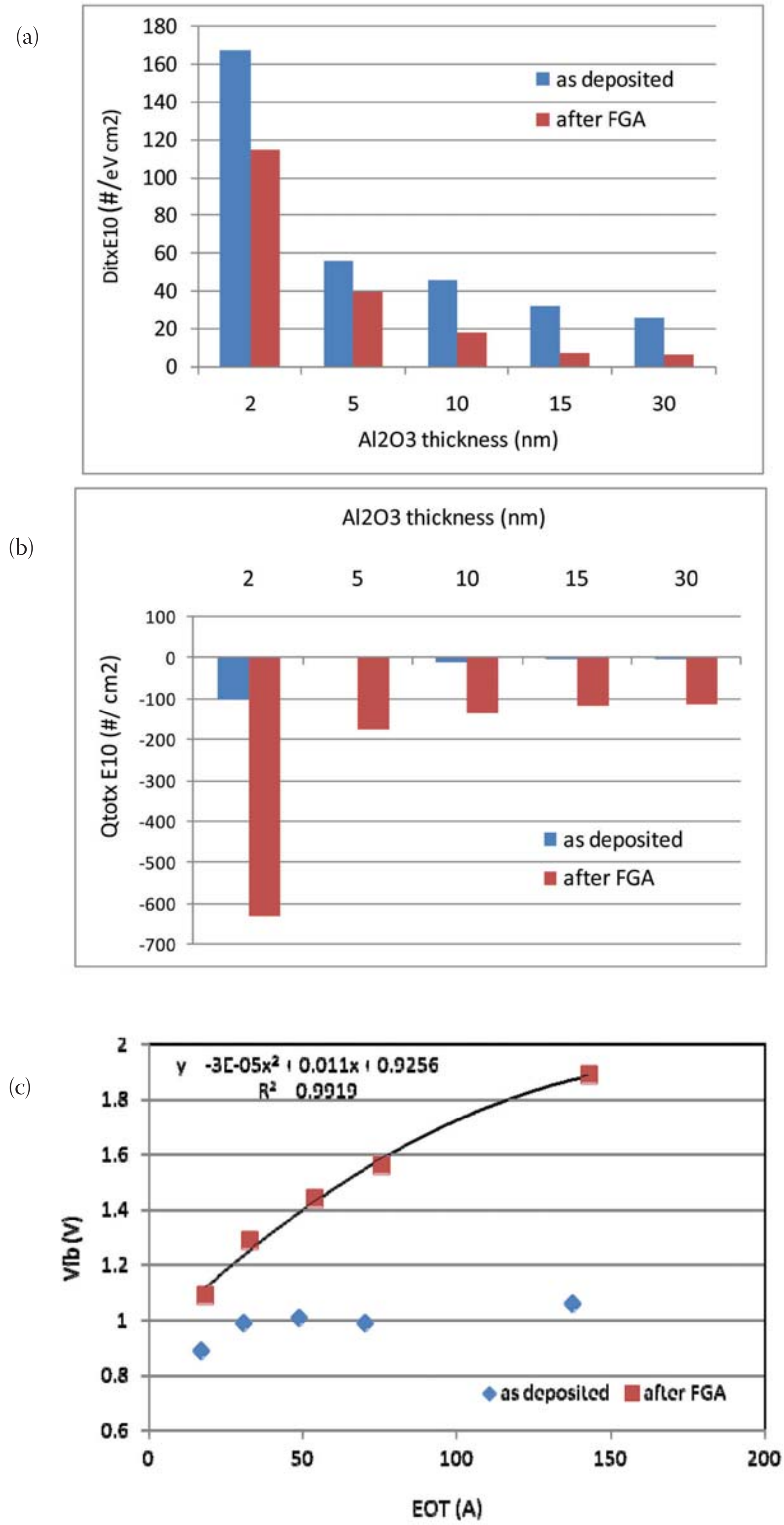

Figure 6. (a) Interfacial trap density D_{it} and (b) total amount of charge Q_{tot} extracted from V–Q measurements for Al_2O_3 as deposited and after FGA@350°C; (c) flat-band voltage versus equivalent oxide thickness EOT for Al_2O_3 as deposited and after FGA@350°C. The annealed samples exhibit a positive slope, indicating the presence of a global negative charge build-up within the c-Si/SiO_2/Al_2O_3 stack.

mimic the annealing performed within the thermal stability evaluation that was discussed earlier.

The results indicate positive fixed charge at the interface Si/SiO_2 (Q_{Si/SiO_2}>0), negative fixed charge at the interface SiO_2/Al_2O_3 (Q_{SiO_2/Al_2O_3}<0) and a non-negligible charge density in the Al_2O_3 bulk. Charge density at the Si/SiO_2 interface (Q_{Si/SiO_2}) is of the order of +7×10^{10}cm^{-2}, but once the Al_2O_3 layer is deposited the amount of charge at this interface increases. The orders of magnitude of the different resulting charge densities are given in Table 1.

The negative fixed charge build-up by the deposition of Al_2O_3 is therefore rather complex. At the interface, the charge polarity and quantity reflect the signature of an SiO_2-like interface. The low D_{it}, as can be measured by CV or deep-level transient spectroscopy (DLTS) [18], is an electrical confirmation of the physical presence of an SiO_2-like layer.

The second methodology that was investigated was the *corona-charging technique*, which allows the consolidation of spatially resolved information on charge and carrier lifetime, in a fast learning cycle [19]. As can be observed from Figs. 6(a) and 6(b), D_{it} and the total amount of charge Q_{tot} depend on the Al_2O_3 thickness. Increasing the Al_2O_3 layer from 2 to 30nm leads to a reduction in D_{it}. This reduction is larger than the effect of the FGA itself, which is mostly visible for the very thin 2nm layer. Q_{tot}, which is a sum of different charge contributions, indicates a rather low amount of charge for the Al_2O_3 as-deposited samples. Once an FGA@350°C has been performed, the charge polarity becomes strongly negative, whatever the thickness of Al_2O_3 deposited.

This is clearly reflected by the flat-band voltage evolution vs EOT, which shows a positive slope, indicating a global negative-charge build-up in the c-Si/SiO_2/Al_2O_3 stack (Fig. 6(c)). The Al_2O_3 layer does not need to be excessively thin to minimize D_{it}, and at the same time the quasi-linear V_{fb}–EOT relationship when varying Al_2O_3 thickness indicates that fixed charges are located mostly at the interface. Increasing the Al_2O_3 thickness does not seem to play a major role.

The two approaches reveal the following information. First, the low D_{it} has the same signature as an SiO_2-like interface, indicating the key role of this interfacial layer in the passivation mechanism. Second, the global negative-charge density is in fact decoupled into two components: positive at the interface Si/SiO_2 and negative at the interface SiO_2/Al_2O_3. Third, a thin Al_2O_3 (5–10nm) provides the low D_{it} and amount of negative fixed charge required to passivate the surface, and there is no need to deposit a thicker Al_2O_3 layer.

‘Blistering’

The integration of Al_2O_3 into solar cells has recently uncovered potential issues with the appearance of ‘blisters’ [20]. This phenomenon is a concern, since a local delamination of the Al_2O_3 layer, and therefore a reduction of the overall passivated area, decreases the cell performance. Investigation of outgassing behaviour and formation of blisters has consequently been conducted in more detail, and strategies to minimize their negative impact have been developed [10].

Annealing a sufficiently thick ALD Al_2O_3 layer and capping it with PECVD-Si_xN_y can lead to blister formation. A top-view scanning electron microscopy (SEM) picture of typical blistered Al_2O_3 layers can be seen in Fig. 7(a). The blisters can fully open when a high thermal budget is applied (during the firing step), thereby creating random local metal-semiconductor contacts. In order to investigate at which process step the blisters originate, thermal treatments were applied in the range 350–900°C. Atmospheric pressure ionization mass spectrometry (APIMS) was performed to detect any gas desorption within this temperature range. The thermal desorption spectroscopy (TDS) profiles indicate mainly the release of H_2O (m/e = 18 (H_2O^+)) and H_2 (m/e = 29 (N_2H^+)) around 400°C. The blistering phenomenon starts exactly when this gas desorption is first observed. One important parameter, which plays a role in whether or not blisters are present, is the Al_2O_3 thickness. As can be seen in Fig. 7(b), for a thin Al_2O_3 layer (≤ 10nm) there are no blisters, while for a thick layer (30nm) the blisters can be as large as a few microns. This illustrates the fact that the Al_2O_3 layer acts as a gas barrier and that the thicker the Al_2O_3 layer, the more pronounced the blister formation.

The blistering phenomenon is also intensified if the Al_2O_3 is capped with Si_xN_y, because the stack creates an even more effective gas barrier. In order to avoid blistering, a sufficiently thin Al_2O_3 layer is necessary and an outgassing step prior to the Si_xN_y capping and co-firing should be performed. The outgassing temperature should be chosen as a function of the Al_2O_3 thickness and of the firing temperature to be applied in the processing sequence. As shown in Fig. 8, an outgassing temperature above 600°C is adequate to avoid blistering for 5nm-thin Al_2O_3 layers in the passivation stack, whereas a temperature of 400°C is not. PERL-type solar cells with local Al BSF rear contacts having an Al_2O_3/Si_xN_y rear-side passivation stack were made using an outgassing step with temperatures up to 700°C. For these cells, the reduction in blistering, and hence improvement in rear surface passivation, is clearly reflected in the open-circuit voltage gain (V_{oc}) as a function of outgassing temperature (Fig. 9). Furthermore, after outgassing at 600 or 700°C, the Al_2O_3-passivated local Al BSF cells are clearly better passivated at the rear, compared to the SiO_2/Si_xN_y-passivated reference cells.

High throughput

So far, research on Al_2O_3 for passivation of solar cells has been carried out mostly on lab-scale reactors (Savannah from Cambridge Nanotech Inc. or FlexAL from Oxford Instruments). Although there is no doubt that the passivation results obtained with Al_2O_3 have potential for PV application, its implementation on an industrial scale is solely dependent on the throughput of the deposition technique and the costs associated with it. To reach such objectives, a technological breakthrough in the ALD deposition technique has been necessary. Equipment vendors have tackled the challenge from two different perspectives: either by extending the batch size concept further (e.g. ASM and Beneq with batch ALD) or by completely redesigning the concept itself (e.g. Levitech and Solaytec with their respective spatial ALD concepts). The approaches currently taken are:

1. **Spatial ALD:** the different precursor gases trimethylaluminium (TMA) and H_2O are spatially separated, and the wafers pass sequentially through the different deposition zones, which are appropriately surrounded by inert gas bearings to prevent the precursor gas flows from mixing.

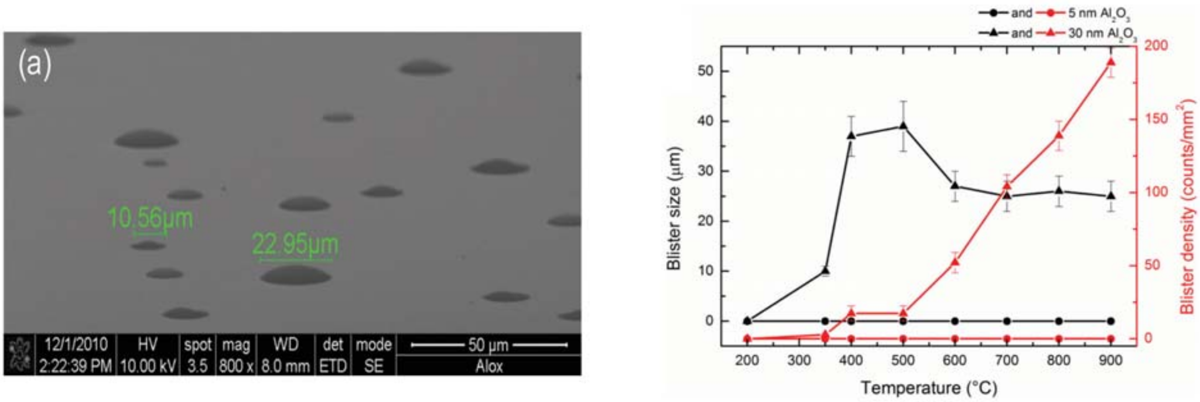

Figure 7. (a) Top-view SEM of a thick Al_2O_3 layer showing blister formation; (b) blister density and size as a function of annealing temperature (350–900°C) for both a thin and a thick Al_2O_3 layer.

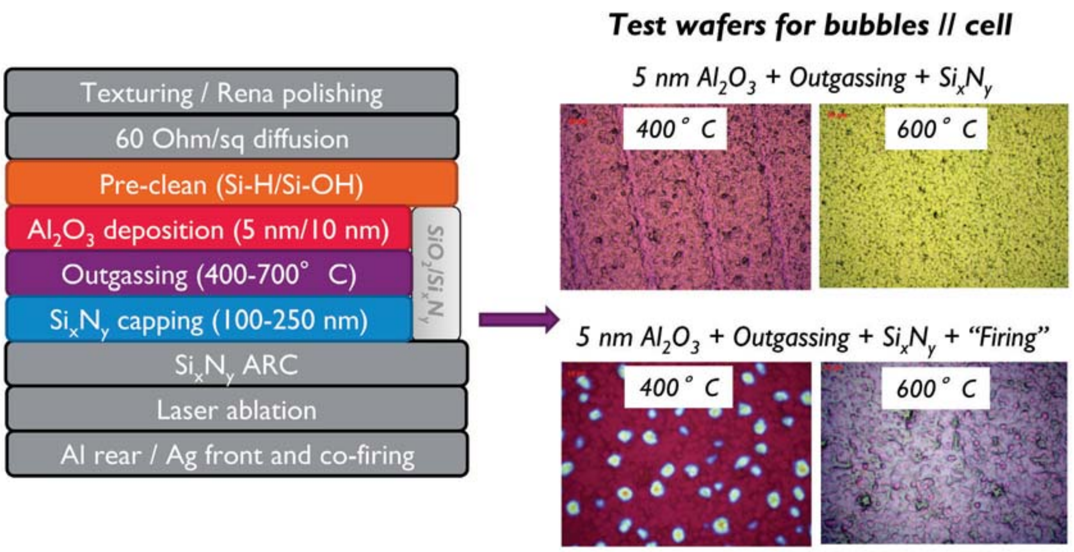

Figure 8. Blistering reduction with outgassing prior to Si_xN_y capping.

2. **Batch ALD:** this concept is based on conventional temporal ALD, where the deposition reaction is divided into two time-sequenced reactions – alternating TMA pulse and H_2O pulse, each one being separated by purge steps.

Imec has carried out a screening of the different high-throughput options, which include spatial ALD, batch ALD and PECVD. When comparing the deposition techniques side by side, the study did not uncover any major differences in terms of lifetime results, which tends to confirm previous data reported by Schmidt et al. [21]. In our opinion, the difference mostly comes from the process and hardware specifications (wafer size, wafer thickness, parasitic deposition, etc.) that the tools are able to achieve, rather than differences in Al_2O_3 material properties. Every tool on the market offering fast throughput Al_2O_3 claims to achieve the required throughput (> 3000 wafers/hour), under assumptions made for a 10nm Al_2O_3 deposition production process. What makes a difference is therefore linked to the tool design itself. The tool design and its impact on the process window, consumption of consumables (cost of TMA precursor gas is essential), yield and maintenance costs [22] appear to be the final criteria to consider.

Conclusions

Al_2O_3 appears to be a suitable candidate for passivation of *p*-type surfaces in a number of advanced solar cell concepts. In the case of PERL-type solar cells with local Al BSF rear contacts and a passivation stack on the rear side, a hydrophilic surface followed by the deposition of a thin Al_2O_3 layer and an outgassing step prior to completing the passivation stack seems to be the most suitable approach for achieving advantageous solar cell results, compared to a reference process with an SiO_x/Si_xN_y passivation stack that has been developed by imec in recent years [1]. High lifetime, no blistering and improved V_{oc} have been achieved using this approach, whereby Al_2O_3 is integrated into the passivation stack and processing sequence. Based on lifetime studies, no major differences were found when screening different high-throughput Al_2O_3 deposition tools. The tool selection seems to be more driven, therefore, by the process and hardware specifications than the Al_2O_3 material properties.

With respect to the future of ALD in PV manufacturing, Al_2O_3 can very likely be considered as a case study. If adequate efficiency improvement and cost of ownership numbers can be demonstrated, this could be the start of many other ALD applications within solar cell manufacturing, such as new materials (dielectrics, metals, etc.) and new applications for current and advanced technologies (antireflection coating, isolation, diffusion barrier, contacting layer, etc.). What makes ALD so special is only partially used today: *thickness control* is the major requirement in current cell technologies but the *conformality* aspect has not yet been explored very much (e.g. deposition on plasmonic structures

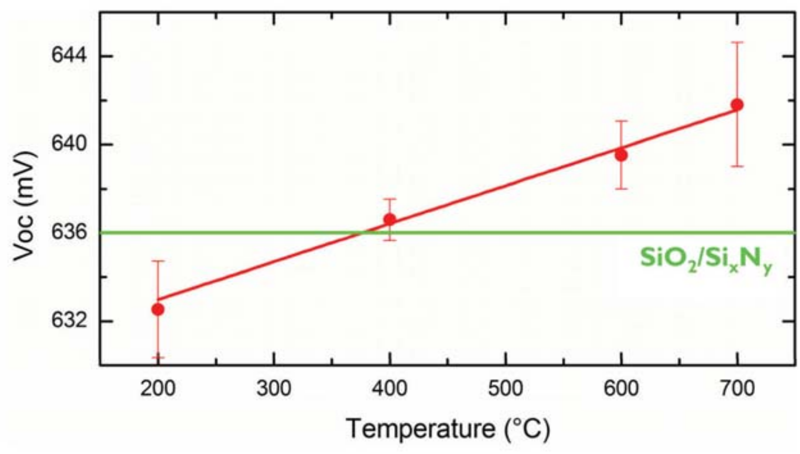

Figure 9. Increase in open-circuit voltage (V_{oc}) as a function of outgassing temperature. Higher values than the reference SiO_2/Si_xN_y passivation stack are reached.

and deposition on Si nanowires for Si multijunction solar cells). For advanced cell concepts, where high aspect ratio structures enter the equation, there is a good chance that ALD will make a difference compared to other deposition techniques. ALD has potentially a bright future, therefore, within solar cell manufacturing.

References

[1] Agostinelli, G. et al. 2006, "Very low surface recombination velocities on *p*-type silicon wafers passivated with a dielectric with fixed negative charge", *Solar Energy Mat. & Solar Cells*, Vol. 90, p. 3438.

[2] Hoex, B. et al. 2007, "Excellent passivation of highly doped p-type Si surfaces by the negative-charge-dielectric Al_2O_3", *Appl. Phys. Lett., Vol.* 91, p. 112107.

[3] Hoex, B. et al. 2008, "On the c-Si surface passivation mechanism by the negative chargedielectric Al_2O_3", *J. Appl. Phys.*, Vol. 104, p. 113703.

[4] Saint-Cast, P. et al. 2009, "Very low surface recombination velocity on *p*-type c-Si by high-rate plasma-deposited aluminum oxide", *Appl. Phys. Lett.*, Vol. 95, p. 151502.

[5] Dingemans, G. et al. 2010, "Silicon surface passivation by ultrathin Al_2O_3 films synthesized by thermal and plasma atomic layer deposition", *Phys. Stat. Sol. RRL*, Vol. 4, No. 1, p. 10.

[6] Reichel, C. et al. 2010, "Decoupling charge carrier collection and metallization geometry of back-contacted back-junction silicon solar cells by using insulating thin films", *Proc. 35th IEEE PVSC*, Honolulu, Hawaii, USA, p. 1034.

[7] Hezel, R. et al. 1997, "Recent progress in MIS solar cells", *Prog. Photovolt.*, Vol. 5, p. 109.

[8] Vermang, B. et al. 2010, "Surface passivation for Si solar cells: a combination of advanced surface cleaning and thermal atomic layer deposition of Al_2O_3", *Proc. 25th EU PVSEC*, Valencia, Spain, p. 1118.

[9] Rothschild, A. et al. 2011, "ALD-Al_2O_3 passivation for solar cells: firing stability", *Proc. 26th EU PVSEC*, Hamburg, Germany [in press].

[10] Vermang, B. et al. 2011, "On the blistering of atomic layer deposited Al_2O_3 as Si surface passivation", *Proc. 37th IEEE PVSC*, Seattle, Washington, USA [in press].

[11] Puurunen, R.L. 2005, "Surface chemistry of atomic layer deposition: A case study for the trimethylaluminum/water process", *J. Appl. Phys.*, Vol. 97, p. 121301.

[12] Puurunen, R.L. 2003, "Growth per cycle in atomic layer deposition: a theoretical model", *Chem. Vap. Deposition*, Vol. 9, p. 249.

[13] Green, M.L. et al. 2006, "Nucleation of atomic-layer-deposited HfO_2 films, and evolution of their microstructure, studied by grazing incidence small angle x-ray scattering using sychrotron radiation", *Appl. Phys. Lett.*, Vol. 88, p. 032907.

[14] Dingemans, G. et al. 2010, "Firing stability of atomic layer deposited Al_2O_3 for c-Si surface passivation", *Proc. 35th IEEE PVSC*, Honolulu, Hawaii, USA, p. 705.

[15] Penaud, J. et al. 2011, "Impact of ageing on AlO_x layer passivation properties for advanced cell architectures", *Proc. 37th IEEE PVSC*, Seattle, Washington, USA [in press].

[16] Benick, J. et al. 2010, "Effect of a post-deposition anneal on Al_2O_3/Si interface properties", Proc. 35th IEEE PVSC, Honolulu, Hawaii, USA, p. 891.

[17] Rothschild, A. et al. 2010, "ALD-Al_2O_3 passivation for solar cells: charge investigation", *Proc. 25th EU PVSEC*, Valencia, Spain, p. 1382.

[18] Simoen, E. et al. 2011, "Impact of Forming Gas Annealing and Firing on the Al_2O_3/p-Si Interface State Spectrum", *Electrochem. Solid-State Lett.*, Vol. 14, No. 9, pp. H362–H364.

[19] Rothschild, A. et al. 2011, "Al_2O_3 surface passivation: electrical characterization using the Quantox tool", *Proc. 37th IEEE PVSC*, Seattle, Washington, USA [in press].

[20] Richter, A. et al. 2010, "Firing stable Al_2O_3/SiN_x layer stack passivation for the front side boron emitter of n-type silicon solar cells", *Proc. 25th EU PVSEC*, Valencia, Spain, p. 1453.

[21] Schmidt, J. et al. 2010, "Surface passivation of silicon solar cells using industrially relevant Al_2O_3 deposition techniques", *PVI*, 10th edn, p. 52.

[22] Chunduri, S.K. 2011, "Looking back to go forth", *Photon Inter.*, March, p. 146.

About the Authors

Aude Rothschild received her Ph.D. degree in inorganic chemistry of materials from the University of Versailles St Quentin, France, in 1997. From 1998 to 1999, she carried out work on inorganic nanotubes at the Weizmann Institute of Science in Israel. Aude has been with imec since 2000 and has worked on medium-k and high-k dielectrics for CMOS and NVM applications. Her current research area is dielectric passivation of solar cells with Al_2O_3.

Bart Vermang is a Ph.D. student at the University of Leuven, Belgium, while performing his research within imec. In 2005 he graduated in physics from the University of Ghent, Belgium, having carried out research for his master's thesis in surface science studies of model metallic catalyst systems at the Norwegian University of Science and Technology. Bart's present research focuses on the integration of Al_2O_3 in surface passivation of industrial Si solar cells.

Hans Goverde is a master's student at the Eindhoven University of Technology. Hans is currently doing research at imec on the integration of Al_2O_3 in surface passivation of industrial Si solar cells.

Enquiries

Aude Rothschild
imec
Kapeldreef 75
3001 Leuven
Belgium
Tel: +32 16 28 83 47
Fax: +32 16 28 10 97
Email : Aude.Rothschild@imec.be
Web: www.imec.be

Exploiting the microelectronics toolbox to boost Si PV manufacturing

Jef Poortmans, **Philip Pieters** & **Kris Baert**, imec, Leuven, Belgium

ABSTRACT

To make solar energy cost effective, the photovoltaic (PV) industry has to reduce its manufacturing costs well below 1€/Wp. To reach this cost target, roadmaps for c-Si technology foresee a drastic reduction in the amount of high-purity Si used and an increase in solar cell efficiencies beyond 20%. But this requires advanced cell concepts that put more stringent requirements on process steps such as doping, cleaning and surface passivation. Several processes in the technology and analysis toolbox of microelectronics offer opportunities to meet these stringent requirements. In this paper, we give examples of recent progress in solar cell development that has been achieved by implementing CMOS-like process steps, and we discuss how these processes can be attuned to the needs and benefits of the solar industry.

Introduction

For several years, the photovoltaic (PV) market has been dominated by crystalline Si (c-Si) solar cells, with a market share of about 85% of the total worldwide solar cell production in 2010. Today, the majority are manufactured from Si wafers which are about 180µm thick and have an Ag metal grid at the front side and an Al contact fully covering the back side. The cells are then assembled into modules and the resulting PV system costs about 2–3€/Wp, which in north-western Europe is equivalent to an electricity cost of 0.25–0.35€/kWh. This is still too high if economic competitiveness of PV electricity with conventional power plants is to be ensured. Consequently, the PV industry is systematically lowering the production costs of this process. It is doing this by increasing the cell's efficiency, in combination with improved manufacturing practices, increase of areal throughput of equipment, upscaling of fabs and vertical integration within the value chain. With the implementation of these measures, the '1€/Wp' system cost is now coming in sight [1].

Yet this will not be sufficient to reach a cost target of 0.5€/Wp, prompting the need for innovative solar concepts that use new materials and production techniques. For example, solar cells using less of the precious Si per Wp (at present 8–9g/W) are needed, and other expensive and non-sustainable materials like Ag must be replaced. We foresee that the industry will gradually move to back-contact cells, which may eventually become as thin as 80 or even 40µm, if novel techniques to realize and handle such thin foils become available. Such thin cells can be handled only by module-level processing in which the processing of cell and module eventually merges. Simultaneously, the high cost of PV module assembly can most readily be reduced by assembling even more efficient PV cells, with efficiencies that go beyond 21%, in a cost-effective way [2,3].

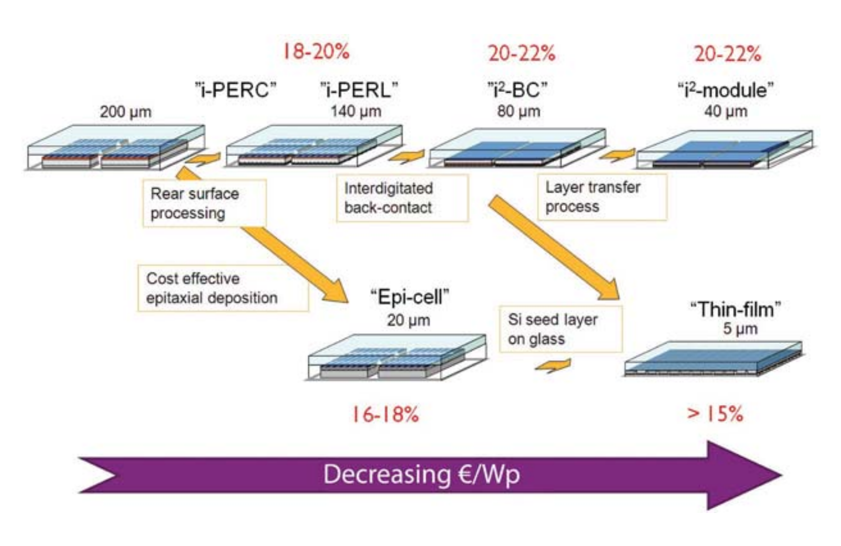

Figure 1. Schematic representation of the imec vision for c-Si solar cell technologies, indicating target thickness and efficiencies for large-area industrial-type c-Si solar cells.

"We foresee that the industry will gradually move to back-contact cells, which may eventually become as thin as 80 or even 40µm, if novel techniques to realize and handle such thin foils become available."

In order to realize such high efficiencies in very thin cells, engineers are facing challenges that have never been an issue before now. For example, doping profiles have to be controlled more precisely than is currently possible by diffusion, the prevailing approach in cell production today. Also, the lifetime of the minority carriers needs to be increased, calling for very efficient cleaning and handling methods to reduce metal contamination. Solar cell performance can be enhanced by replacing Ag by Cu, but this requires diffusion barriers that prevent the metal from diffusing into Si. Several processes in the technology toolbox of CMOS manufacturing are attractive ways to meet these stringent requirements. Obviously, this only makes sense when the technologies are compatible with the required low cost of ownership for photovoltaic applications. Below, we will give some more detailed examples of how the photovoltaic industry can benefit from the microelectronics experience and what is needed to further 'solarize' the CMOS toolbox – that is, adapt it to the needs of the PV community [4].

Ion implantation – road to better-controlled doping profiles

Si solar cells need a junction in order to operate and to collect electron-hole

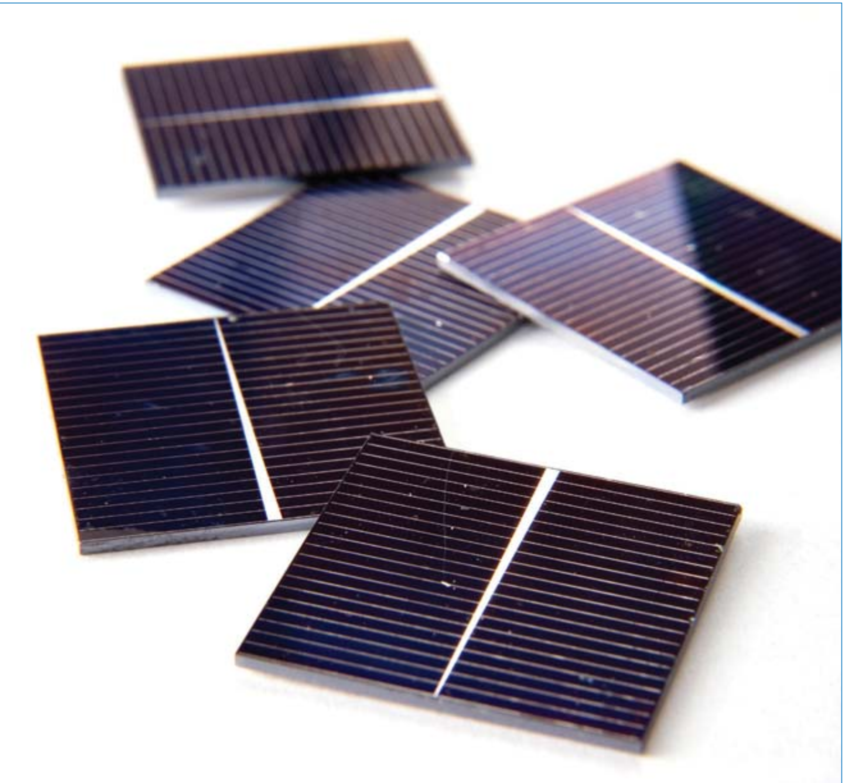

Figure 2. Imec's thin-film epitaxial Si solar cells – one of the pathways to working with very thin Si layers.

pairs. The resulting dopant profiles are tailored to enhance the cell performance. If the ultimate in cell performance is to be reached, the dimensions of these doping profiles need to be optimally controlled. For example, by better engineering the emitter profile, the UV response of the cell and its open-circuit voltage V_{oc} can be increased. Currently, dopants are introduced by diffusion, but this does not offer the required degree of precision. Ion implantation provides a possible alternative, as it yields an excellent areal uniformity and run-to-run producibility. Moreover, the design and integration of advanced profiles (e.g. very shallow emitters) is facilitated by the tool flexibility, and the design of back-contact solar cells can be significantly simplified. However, the tools developed for the IC industry have proved to be ill suited to reaching the required throughput of PV manufacturing lines (> 1500 wafers/hour). Therefore, the industry is now moving on to making new types of equipment that allow a higher throughput, but at the same time maintaining a sufficiently wide process window attuned to the specific profiles required by PV cells.

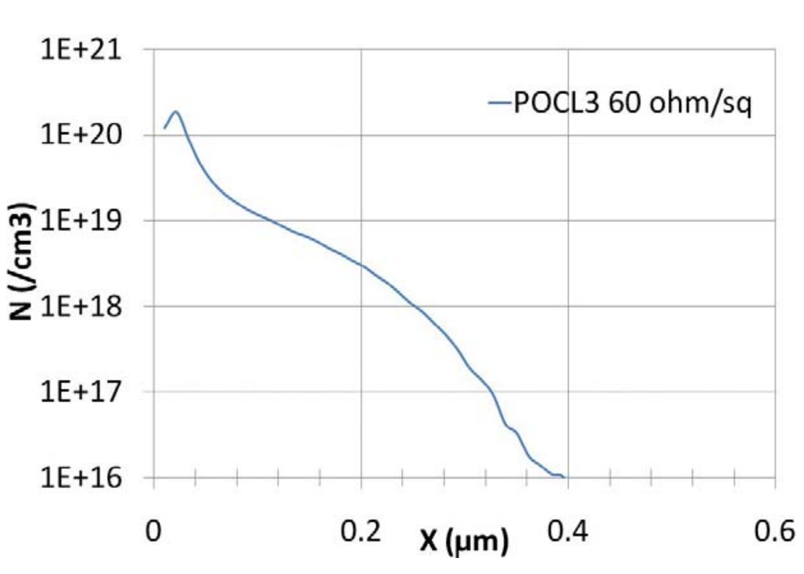

Figure 3. SIMS of a typical diffusion profile of a $POCL_3$ 60Ω/sq emitter.

It is in this context that imec has very recently developed an innovative process flow that consists of replacing the double-sided, high-temperature diffusion step taking around one hour, by a one-sided, low-temperature implantation step taking just a few seconds. This process flow was used to implant 160µm-thick *p*-type c-Si wafers with phosphorus. Next, the front side was passivated using a plasma-enhanced chemical vapour deposition (PECVD) SiN_yH_x layer. The dopants were electrically activated by a rapid thermal anneal step in a firing furnace. Wafers were then locally ablated on the rear side, metallized and fired to create the local back-surface field (BSF). The cells were metallized using a Cu-plating technique. The complete process resulted in an efficient solar cell with 18.8% efficiency, a V_{oc} of 638mV, a J_{sc} of 38.5mA/cm^2 and a fill factor of 76.6%. The implanted phosphor emitter had a sheet resistance of around 60Ω/sq. The innovativeness of the technique is the low-energy (10keV) implantation and short anneal step, creating shallow emitter profiles, but a major advantage, compared with traditional diffusion, is the reduction of the cycle time and the amounts of material and energy that are consumed. Techniques such as these will bring the industrialization of implantation for the solar industry one step closer [5].

Atomic layer deposition (ALD) of Al_2O_3 – a new option for surface passivation

For cells much thinner than 180µm, the influence of the non-illuminated side of the cell becomes increasingly important. Indeed, on this side, carriers can easily recombine due to the high number of surface defects. Traditional passivation schemes of Si solar cells are based on 'regular' dielectrics such as silicon-nitride (SiN_x), but these cell types do not have the potential to achieve efficiencies above 20%. For example, on *p*-type surfaces, SiN_x contains positive charges that attract minority carriers instead of repelling them. A next generation material for surface passivation of c-Si is ALD Al_2O_3, a dielectric with negative fixed charges [6]. At imec, know-how gained from semiconductor processing has been used in order to study the amount of charge in the dielectric layers and to understand the passivation mechanism. In addition to electrostatic-field-assisted passivation, ALD Al_2O_3 has the remarkable property of introducing very little interface carrier traps with Si. This chemical interface passivation was improved by the screening of several cleaning and drying methods derived from semiconductor processing. The cleaning cycle turned out to be one of the critical parameters

in achieving low surface recombination velocity values on large-area wafers. As a result, excellent recombination velocities (< 10cm/s) have already been demonstrated by ALD Al_2O_3 on the lab scale and are now being implemented in industrial-type solar cells.

"At imec, know-how gained from semiconductor processing has been used in order to study the amount of charge in the dielectric layers and to understand the passivation mechanism."

However, conventional time-resolved ALD is limited by its low deposition rate. The deposition reaction of this type of ALD is divided into two time-sequenced, self-limiting half reactions, each one being separated by a purge step to preserve a clean reaction chamber. It is clear that a faster and cost-effective ALD concept is needed in order to cope with the required low cost of ownership for PV. Therefore, several higher throughput pathways are under investigation and are now competing for market introduction. One of them is spatially separated ALD of Al_2O_3: instead of temporal separation of the half reactions, this ultra-fast ALD concept is based on a spatial separation. It makes purge steps obsolete and brings half-reaction timescales down to a few milliseconds. In this way, very high deposition rates are achieved, while maintaining the required high film quality. By using an experimental high-deposition-rate prototype ALD reactor based on the spatially separated ALD principle, imec was able to demonstrate that, on *p*-type CZ Si, 10 and 30nm spatial ALD Al_2O_3 layers can achieve the same level of surface passivation as equivalent temporal ALD Al_2O_3 layers [7].

Cu metallization – key to sustainable and efficient solar cells

At the moment, the most widely used industrial method for making the top contacts of c-Si solar cells is screen printing of Ag pastes. But this technique is one of the limiting factors in moving towards lower costs and higher efficiencies. Being a contact metal, Ag is among the most material-intensive parts of a Si solar cell and today accounts for a large part of the cell's manufacturing cost. And this will only get worse: factoring in the increasing size of the PV market, experts predict a shortage of the scarce Ag within the next

Figure 4. Traditional surface passivation technique: in-line vacuum system for etching, and subsequent passivation by very high frequency PECVD of SiN.

10 years. A safe solution is to replace Ag by a conducting material that is not on the list of rare materials. The most likely candidate for this replacement is copper (Cu), a metal with a conductivity comparable to Ag. The preferred metallization scheme is the creation of laser-ablated via holes to open the passivation layer, and the subsequent deposition of Cu using electroplating, a technique that is well known in the metal industry.

Besides an obvious material-cost advantage, an electroplated Cu metallization scheme can lead to more efficient solar cells. Not only does the process reduce the shadowing losses (since narrower fingers – down to 40µm – with higher aspect ratios are possible) but it also improves J_{sc} and V_{oc}. Recently, imec was able to demonstrate large-area Cu-contact cells (170µm thick, 125 × 125mm^2) with efficiencies up to 19.8% and shadowing losses under 4% [8].

"Besides an obvious material-cost advantage, an electroplated Cu metallization scheme can lead to more efficient solar cells."

But the introduction of Cu equally brings along some challenges for the solar cell manufacturing engineer. First of all, Cu has a severe impact on the lifetime of Si, and therefore adequate barriers are necessary to prevent Cu from reaching the active Si region. Once again, we can rely on experience in microelectronics: several years ago, Cu was introduced as a replacement for Al in advanced interconnect integration schemes, mainly due to its lower resistivity. Several materials such as titanium nitride and tantalum nitride were investigated for

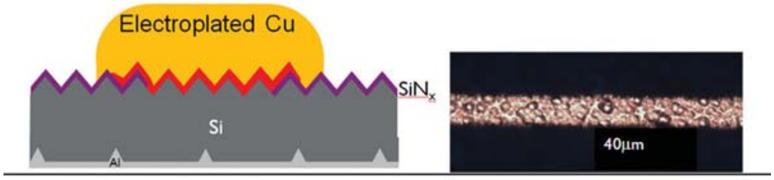

Contact Layer	Emitter (Ω/sq)	J_{sc} (mA/cm²)	V_{oc} (mV)	FF (%)	η (%)	R_s (Ωcm²)
Ti	60	38.5	638	80.6	19.8	0.20
Ti	120	38.7	652	77.6	19.6	0.29

125mmx125mm - Cz

Best cell results

Figure 5. Cells with 40μm Cu front grid metal reach efficiencies approaching 20%.

use as an effective barrier layer against Cu diffusion, and the experience gained provided an interesting starting point for the integration of such barriers in a c-Si solar cell process flow. Another key question is the long-term reliability of Cu-based metallization. For example, unlike Ag, Cu oxidizes into a porous oxide when exposed to air. To address this issue, we can rely on the progress made with Cu in IC packaging and interconnection technologies such as, for example, Cu through Si vias (TSV) in 3D stacked integrated circuits.

... and many more

The knowledge and experience gained within the context of microelectronics are helping us to improve on doping profiles, surface passivation and contact metallization to make c-Si solar cells more efficient, cost effective and sustainable. However, this list from the processing technology toolbox is far from complete. In order to enhance the carrier lifetime, very efficient cleaning and handling methods are necessary in view of metal contamination. More precise patterning methods are required to cope with the ever more complex cell patterns. In the longer term, small optical features in the cell will probably be needed to enable more efficient light trapping. In addition, the toolbox contains a myriad of analytical tools and techniques that facilitate, for example, the study of the types of charges at the Al_2O_3 passivated surface, the characterization of the quality of the Si substrate, and an understanding of the degradation phenomena taking place in the solar cell.

'Solarizing' the microelectronics toolbox

All these examples illustrate that the microelectronics toolbox can be exploited to make highly efficient, thin, large-area solar cells. But the examples also highlight the fact that processes from CMOS manufacturing cannot simply be copied over to our PV lines. The throughput of techniques such as ion implantation and ALD is much too low, and the cost of most of these techniques is far too high, for use in the PV industry. So, if these tools are to be successfully introduced in the PV industry, adapted equipment and new processes must be developed that allow for an increased throughput and reduced tool costs. As discussed, we are witnessing the first steps in this direction. Moreover, the emergence in the PV field of many semiconductor equipment companies, also involving the above-mentioned non-conventional approaches, represents clear proof that the required low cost of ownership is achievable.

Imec and its partners are developing the c-Si solar cell technologies in an industrial affiliation programme. This programme aims to bring together established PV manufacturers, microelectronic companies wanting to exploit their semiconductor expertise in PV manufacturing, and newcomers from the energy sector. The technical content of the affiliation programme is oriented towards the development of process technologies for advanced crystalline Si solar cells and modules. The programme's goal is to deliver to imec's partners short learning cycles for the development of new processes so as to help the partners to be well placed in the race towards lower costs. Besides increasing the efficiency of industrial crystalline Si solar cells to greater than 20%, the programme also aims to improve the reliability of crystalline Si solar cell modules in order to guarantee lifetimes exceeding 20 years.

Conclusion

We have given clear examples of how materials and process methods derived from IC manufacturing are improving the cost per Wp of c-Si solar cells. Ion implantation can be used instead of thermal diffusion to better engineer dopant profiles and lower the energy and material budget of the doping step. Al_2O_3 deposited by ALD is a likely candidate for passivating the surface of high-efficiency c-Si solar cells, and Cu as a top metal can boost the cells' efficiency and, at the same time, replace the rare and costly Ag. The first cells to be made using these new process steps look promising.

But, just as importantly, the IC-manufacturing processes cannot simply be copied over to our PV lines. Instead, they must be adapted to the benefit of the PV community by increasing their throughputs and lowering their costs. In this context, equipment manufacturers are supplying the first tools to the PV industry. We are convinced that this close association with microelectronics will play a significant role in achieving the cost and performance goals of solar cell manufacturing, in crossing the 1€/Wp barrier.

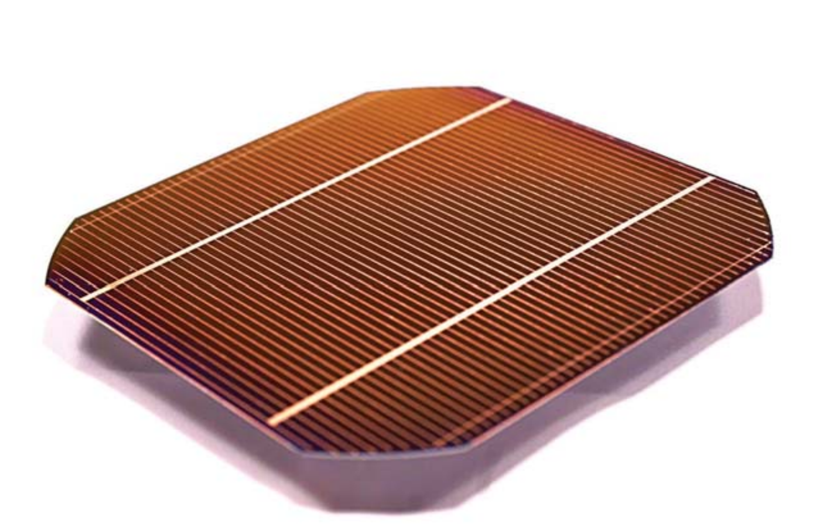

Figure 6. Imec's Cu-plated large-area Si solar cell.

Acknowledgements

The authors would like to acknowledge all their co-workers in the imec Photovoltaics group for contributions to the experiments and discussions related to the cross-fertilization of Si PV and microelectronics.

References

[1] tobuildsolarpanel.net 2011, "REC announce competitive cost position" [available online at http://tobuildsolarpanel.net/rec-announce-competitive-cost-position].

[2] Baert, K. et al. 2009, "Crystalline Si solar cells and the microelectronics experience", *Photovoltaics World* [available online at http://www.electroiq.com/articles/sst/2009/08/crystalline-si-solar-cells-and-the-microelectronics-experience.html].

[3] Baert K. & Poortmans, J. 2010, "Improving cell efficiency and reducing costs: Applying experiences in microelectronics", *PVI*.

[4] Baert, K. et al. 2011, "Crystalline Si solar cells: Where microelectronics meets photovoltaics", *Proc. 26th EU PVSEC*, Hamburg, Germany [in press].

[5] Prajapati V. et al. 2011, "Diffusion-free high efficiency silicon solar cells", *Proc. 26th EU PVSEC*, Hamburg, Germany [in press].

[6] Hoex, B. et al. 2007, "Excellent passivation of highly doped p-type Si surfaces by the negative-charge-dielectric Al_2O_3", *Appl. Phys. Lett.*, Vol. 91, No. 11, p. 112107.

[7] Vermang, B. et al. 2011, "Spatially separated atomic layer deposition of Al_2O_3, a new option for high-throughput Si solar cell passivation", *Prog. Photovolt: Res. Appl.* [available online at http://onlinelibrary.wiley.com/doi/10.1002/pip.1092/full].

[8] imec 2010, press release [available online at http://www2.imec.be/be_en/press/imec-news/archive-2010/siliconsolarcellvalencia.html].

About the Authors

Jef Poortmans received his degree in electronic engineering from the Katholieke Universiteit Leuven in Leuven, Belgium, in 1985 and his Ph.D. degree in June 1993. Jef is the Director of the Department of Solar and Organic Technologies at imec.

Kris Baert obtained his Ph.D. on PECVD of thin-film c-Si from the Katholieke Universiteit Leuven in Leuven, Belgium, in 1990. In 1992 he joined imec, where he managed research and development in various areas of MEMS and integrated microsystems. Since 2008 Kris has been Programme Manager of solar cells in the SOLO department.

Philip Pieters received a master's degree and Ph.D. in electrical engineering from the Katholieke Universiteit Leuven in Leuven, Belgium. He joined imec in 1994 doing pioneering R&D work for innovative heterogeneous integration and RF-SIP technologies. Today, Philip is the Business Development Director of Energy, creating the bridge between imec's high-tech research on PV technologies and market needs.

Enquiries

imec
Kapeldreef 75
3001 Leuven
Belgium
Email: Jef.Poortmans@imec.be

Thin Film


118

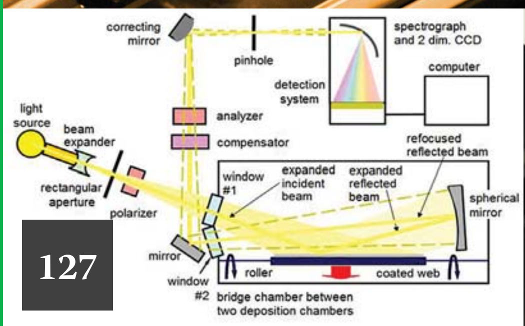
127
correcting mirror
pinhole
spectrograph and 2 dim. CCD
detection system
computer
light source
beam expander
analyzer
compensator
refocused reflected beam
rectangular aperture
polarizer
window #1
expanded incident beam
expanded reflected beam
spherical mirror
mirror
window #2
roller
coated web
bridge chamber between two deposition chambers

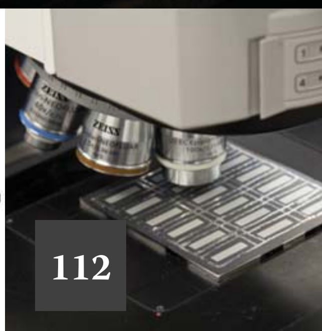
112

Veeco exits CIGS thin-film PV systems business, sees commercial timeframe, cost as unacceptable

In another sign of trouble in the PV capital equipment sector, Veeco has decided to exit the CIGS solar systems business. Announced as part of the company's second-quarter financials, the move results in a combined negative impact and backlog removal of approximately US$71 million on its Q2 GAAP results.

CEO John Peeler cited "various reasons," for the decision, "including" the improved performance of mainstream solar technologies and the lower-than-expected end-market acceptance for CIGS technology to date. While CIGS remains an important thin-film solar technology, we have determined that the timeframe and cost to successful commercialization are not acceptable to Veeco."

The company had been active in the sector, making several acquisitions and product launches over the past four years, including the purchases of toolmaker Mill Lane and CIGS developer DayStar Technologies assets in New York state and the rollout of its FastFlex and FastLine equipment systems. Veeco had also landed Global Solar, Daiyang Metal, GroupSat and others as customers.

Effective Q3 2011, the company said it will treat its CIGS solar systems business, which operated at a loss, as a discontinued operation.

CIGS systems like Veeco's FastFlex will be discontinued as a result of the company's exit from the space.

R & D News Focus

NREL, German researchers sign MOU for advancement of solar cells, fuels

American researchers from the US Department of Energy's (DOE) National Renewable Energy Laboratory (NREL) signed a memorandum of understanding (MOU) with German researchers aiming to make new developments in solar cells and solar fuel production. The MOU will also see the two teams working to improve the performance of concentrating solar thermal power systems.

Signed in Berlin by NREL Director Dan Arvizu and leaders from the Research Center Jülich (FZ Jülich), the Helmholtz Center Berlin (HZB), and the German Aerospace Center (DLR), the MOU will have the researchers investigating several key areas for new materials that can potentially lead to the development of more efficient solar cells and fuels. The scientists plan to create and use fast imaging techniques that will enable the characterization of thin-film materials on the micrometer to nanometer scale while also characterizing the in-situ growth process.

The research teams are also seeking a better understanding of grain boundary/interface passivation in thin-film silicon and plan to explore the potential and limits of wide band-gap thin-film solar cells. Furthermore, the MOU will see the NREL and German researchers measure the performance and reliability of solar cells and modules by using electroluminescence, photoluminescence and thermography.

Solar cells' stability will be tested by exposing them to high temperature and light exposure while new device structures and lower-cost catalysts will be explored for the development of hydrogen in photocatalytic solar fuel generation.

The MOU's directive to work on CSP systems builds on an MOU NREL signed two years ago with DLR. The original MOU aimed to progress standard test methods for the assessment of the reflectance and durability of solar mirrors in CSP systems and required round-robin testing of commercial reflector samples and parabolic trough receivers. In this updated MOU between with the NREL, the two organizations will work towards acquiring a more in-depth awareness of the essential mechanisms for soiling rates on CSP mirrors.

TÜV Rheinland certifies Solar Frontier CIS thin-film PV modules as RoHS compliant

Copper-indium-selenide thin-film PV manufacturer Solar Frontier said that its CIS modules have been certified by TÜV Rheinland as RoHS compliant. Solar panels are exempt from RoHS (which stands for 'reduction' or 'restriction' of hazardous substances) compliance, and Solar Frontier claims to be one of the few manufacturers able to meet the requirements, having completed voluntary testing with TÜV to make it official.

RoHS, which was adopted by the European Union in 2003, sets a 0.01% concentration limit on cadmium, and a 0.1% limit on lead, mercury and three other hazardous substances, for any component of a certified device.

Pyron Solar's ground-breaking CPV system outperforms rivals during prototype testing

Pyron Solar has made a major breakthrough in the field of concentrated photovoltaics (CPV), after a prototype for its floating power system posted output figures nearly 20% higher than those of its commercial rivals.

Generating high concentration levels while also maintaining low cell temperatures is one of the major dilemmas facing CPV project developers. Pyron's proprietary system is suspended in and cooled by water, enabling cells to produce up to 20W per cell while being maintained at a relatively low operating temperature. Testing was carried out over a five-month period and under contract to San Diego Gas & Electric.


Solar Frontier's SF140–155 CIS module series.

Source: NexPower

NexPower said it has successfully produced 160W μc-Si tandem modules with a conversion efficiency reaching over 10.4%.

NexPower to produce μc-Si tandem modules with 10.4% efficiency

Six months ahead of schedule, Taiwan-based NexPower said it has successfully produced 160W μc-Si tandem modules with a conversion efficiency reaching over 10.4%. NexPower noted that having converted all production lines to tandem technology earlier in the year, the 160W modules would go through testing and certifications before mass production would commence. In March this year, NexPower entered volume production of μc-Si tandem modules with 9.7% efficiencies.

Manz receives German state funding for CIGS and c-Si R&D

Under the German federal government commitment to the 'Photovoltaics Innovation Alliance,' launched in August 2010, Manz has received partial R&D funding for two projects, covering CIGS thin-film technology and crystalline silicon technology.

Manz noted that it had entered into the first cooperative research project in relation to CIGS thin-film technology since licensing the technology from Würth Solar. The project is also in collaboration with Würth Solar's former technology partner, the Center for Solar Energy and Hydrogen Research (ZSW) in Stuttgart.

The project has a total budget of €12.5 million, which will be delivered in subsidies over the next four years from Germany's Federal Ministry for the Environment. The project will focus on how to rapidly increase CIGS module efficiency levels in manufacturing, since ZSW's laboratory holds the 20.3% world record for efficiency of the technology, but manufacturing efficiency levels have yet to reach 13%.

The project will simultaneously cover ways to reduce the capital investment requirements for CIGS production lines and focus on reducing overall manufacturing costs.

The second program involves Manz and solar module manufacturer Schott Solar in a project to develop key, novel technologies that are affordable in the real-world production environment, while boosting solar cell conversion efficiencies.

The silicon solar cell project will be carried out in collaboration with the Fraunhofer Institute for Solar Energy Systems (ISE) and has been allocated €7.7 million, with €1.85 million coming from government subsidies. The contributions being made by Manz and Schott Solar were not disclosed.

Testing and Certification News Focus

DuPont Apollo claims first LEED Gold rating for thin-film PV manufacturer

DuPont Apollo's Shenzhen, China PV module manufacturing facility has laid claim to being the first Leadership in Energy and Environmental Design (LEED) Gold certified for Existing Buildings, Operations and Maintenance (EB, O&M) thin-film PV site in the world. The LEED certification was granted by the US Green Building Council (USGBC), which pointed to several of the company's environmentally friendly designs as a basis for their certification.

The Shenzhen facility's top claim to the LEED certification lies on its rooftop with its 1.3MW amorphous silicon PV module installation. The modules, manufactured by the plant itself, produce around 1.5 million kilowatt hours of electricity per year to offset the facility's daily operational energy needs.

Other environmentally sound practices the plant has introduced include an upgraded HVAC system, water saving features, a sustainable buying plan that sources materials and supplies locally and an EnergyStar solid waste management system. DuPont Apollo additionally offers its employees an arranged transportation system for their daily commuting requirements and promotes facility wide recycling.

NREL confirms 16.3% efficiency reached in XsunX CIGS technology

The National Renewable Energy Laboratory (NREL) confirmed that XsunX's CIGS PV devices had reached a peak efficiency conversion of 16.36%. The samples tested had efficiency ratings that ranged between 15.3% and 16.36%, which led to an average efficiency of 15.91%. XsunX supplied the NREL with a 125mm substrate sample, which after deposition was sub-divided into quadrants in order for NREL to generate device test structures and analytical equipment test structures. The organizations advised that this method was used in order to produce a substantial amount of data for XsunX to use as the basis of its future improvement efforts.

First Solar's Series 3 thin-film PV modules granted new IEC certification for coastal installations

First Solar's Series 3 CdTe thin-film solar modules have received the International Electrotechnical Commission's (IEC) 61701 certification for salt mist corrosion, confirming the use of the Series 3 modules in coastal environments. The certification involves testing and studying the module's performance in coastal environments, which are prone to corrosive salt mist.

TÜV Saarland certifies Avancis CIS thin-film modules for ammonia resistance

Avancis's PowerMax CIS PV modules have passed the ammonia test conducted by German certification body TÜV Saarland. With this demonstration of their long-term resistance to the corrosive gas, the glass-glass panels are certified as particularly suitable for use in agricultural applications.

Avancis thin-film PV modules have already passed the salt mist corrosion test conducted by TÜV Saarland in compliance with IEC 61701, which means that the panels are suitable for use in salt-heavy coastal areas.

NREL confirms new CdTe cell efficiency record from First Solar

First Solar has reported that its test cadmium-telluride cells have reached 17.3% conversion efficiencies. The figure – confirmed by NREL – trumps the previous record of 16.7%, which was achieved back in 2001.

Although test cells, First Solar noted that they were constructed using commercial-scale manufacturing equipment and materials. First Solar has recorded full-module efficiencies over 13.5%, with a 13.4% module confirmed by NREL in the

Source: First Solar

First Solar has reported that cadmium-telluride cells have reached 17.3% conversion efficiencies, confirmed by NREL.

Thin-Film Order Focus

IMA Automation Berlin ships first modu-contec systems to unnamed vendor

MA Automation Berlin has shipped the first of its first modu-contec systems to a major vendor of production tools for thin-film modules. The modu-contec is based on IMA's proven modular production tools, and fully automates the backside contacting process of thin-film modules up to the junction box connection.

The system combines all the production steps and tools needed for thin-film photovoltaics in one system, while also ensuring high processing speed. At a throughput rate of up to 130 modules per hour, modu-contec will produce modules at a total capacity of 160MW per year.

Solar Frontier supplies Nissan with thin-film modules for rooftop system

Solar Frontier has supplied Nissan Motor with around 40kW of CIS thin-film modules for the recently-completed rooftop solar system at its global headquarters in Yokohama, Japan. The system, built in partnership with Showa Shell Sekiyu, will primarily be used to power rapid charging systems for electric vehicles on site.

The project, built by Nissan Motors and Showa Shell Sekiyu and sponsored by the Ministry of Economy, Trade and Industry, combines CIS thin-film solar cells and lithium-ion batteries and follows on from a successful trial of the charging system. Any excess electricity left over from daytime consumption can be efficiently stored using lithium-ion batteries.

Abound Solar enters supply agreement with ABEL ReTec

German-based PV project developer, ABEL ReTec is to use Abound Solar's CdTe thin-film modules in large-scale free-field projects, with an initial order of 1.2MW, which was shipped during the second quarter of 2011. The long-term purchase agreement was based on testing Abound's AB1-series modules for rooftop installations.

Abound Solar is still in the early phase of ramping capacity at its 65MW panel production line in Longmont, Colorado.

past. In the first quarter of 2011, First Solar reported manufacturing average module efficiencies of 11.7%.

Uni-Solar gains initial thin-film silicon cell efficiency of 16.3%

United Solar (Uni-Solar) has announced that it has achieved a new cell efficiency world record of 16.3% for thin-film silicon solar technology, beating the company's previous record of 15.4%. This initial efficiency figure was achieved on a small-area (0.25cm^2) cell using a triple-junction structure, and used the company's new Nano-Crystalline silicon technology. Independent testing of the cell will be carried out by the NREL.

NREL has confirmed Uni-Solar's claimed initial conversion efficiency of 12% for a large-area encapsulated cell (400cm^2) using the company's Nano-Crystalline technology.

Business News Focus

Avancis, Singulus, Heraeus and IfG Institute partner on CIS cluster tool project

Four German companies, Avancis, Singulus Technologies, Heraeus Noblelight and the IfG Institute for Scientific Instruments, have come together to work on the Photovoltaics Innovations Alliance CIS Cluster Tool project. The project aims to develop new manufacturing procedures for CIS semiconductor panels in order to produce high-efficiency thin-film solar modules. With a three-year investment financed by €2.9 million from the Photovoltaics Innovations Alliance and contributions from participating companies, the companies plan to develop an industrial manufacturing process based off findings from a planned demonstration plant.

New plant concepts and processes, full process chains and in-situ analytics will be the main focus of the companies during the tool cluster project. Under the new plant concepts and processes objective, research of innovative rapid thermal processing (RTP) plant concepts and processes will be investigated. The new full process chain goal will see selenide coating combined with the RTP of CIS semiconductors so that the process control can be increased. Additionally, the new in-situ analytics focus will see research of new measurement processes that will improve process control and the understanding of physicochemical processes in semiconductor production.

Solar Frontier ramping 150W CIS modules as customer engagements go global

CIS thin-film module manufacturer Solar Frontier has started shipping 150W modules with 12.2% conversion efficiencies after accelerating its production roadmap and achieving production targets ahead of schedule at its Kunitomi plant in Japan.

Source: Solar Frontier

Solar Frontier has started shipping 150 Watt modules with 12.2% conversion efficiencies after accelerating its production roadmap and achieving production targets ahead of schedule at its Kunitomi plant in Japan.

Based on 'keen' interest in its low-cost, high-yield technology, which benefits from the 'light soaking effect,' unique to CIS technology, Solar Frontier said shipments were going to customers on a global basis, though quantity figures were not released.

Solar Frontier also noted that it expects both TÜV and UL certification in the near future for a 155W module. The performance improvements are said to come from continuous manufacturing improvements as the state-of-the-art Kunitomi plant ramps successfully.

Solar Frontier officially opened the Kunitomi plant in Miyazaki, Japan in April 2011, which was extensively covered by PV-Tech after a factory visit. This is the third but most advanced facility owned and operated by Solar Frontier, which claims to have an annual capacity of approximately 1GW.

TFG Radiant, Ascent Solar sign long-term partnership, including deal to establish CIGS fab in China

Flexible CIGS thin-film PV developer/manufacturer Ascent Solar and TFG Radiant have signed a long-term strategic partnership that encompasses more than US$275 million plus royalties. The deal includes investments by TFG Radiant in Ascent and a joint development agreement between the two companies to establish manufacturing facilities in East Asia. Under the terms of the agreement, TFG Radiant has also committed US$165 million for the initial East Asia fab, bringing the total deal value to about US$450 million plus royalties.

TFG Radiant is a joint venture of Radiant Group, a Chinese conglomerate in construction and real estate, and Tertius Financial Group, a private investment firm based in Singapore.

Product Reviews

dr. schwab IT

dr. schwab IT's FPI solar metrology system enables fast full surface thickness evaluation of thin-film layers

Product Outline: dr. schwab IT's FPI series is a metrology system that is said to cover all aspects of the production process for thin-film panel manufacturing. The new system meets volume production speed requirements with full surface measurement for quality assurance as well as continuous monitoring of all process parameters, thus helping to increase productivity and yield of production lines.

Problem: Due to the chain-like structures of PV modules, total efficiency is usually less than the average of the individual panels. High productivity and efficiency require process stability from uncoated substrates to final panels. The highest possible uniformity of the coating layer and the optimum surface haze are necessary for maximum light trapping and energy conversion.

Solution: dr. schwab IT's FPI solar series offers inline inspection for the manufacturing of large-scale a-Si or µ-Si and CIS/CIGS-based thin-film panels. Equipped with in-house developed spectrometers, the system provides fast full-surface thickness evaluation of multiple layers at nanoscale resolution and simultaneously analyzes the spectral haze of the TCO layer. Both tasks are performed for the complete surface in one pass within the cycle time of production. The modular design of the FPI solar suits virtually any sample size, e.g. a panel width of 2.2m.

Applications: a-Si or µ-Si and CIS/CIGS-based thin-film panels.

Platform: Due to the modularity of the FPI solar series, it can handle almost any sample size and can easily be integrated into modern production lines. Depending on the application purpose, the system can also be equipped with InGaAs cameras or with CCD line scan cameras.

Availability: Currently available.

Gerold

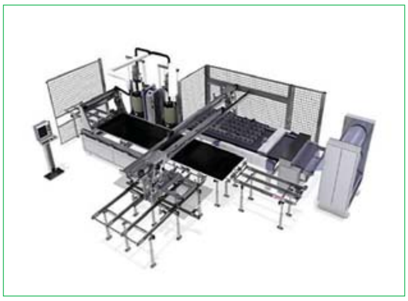

Gerold's HMA-system offers automatic hot melt edge-sealing of thin-film modules

Product Outline: Gerold's HMA-system automatically applies liquid butyl (hot-melt) for edge-sealing of thin-film modules, replacing the need for butyl tape, which has limiting use factors in high-volume production applications. Gerold claims the HMA-system offers more economical packing drums, less waste, and improved product quality.

Problem: The overall objective is better encapsulation properties of the module. This brings about improved cell protection and prevention of corrosion thanks to prevention of moisture vapour ingress.

Solution: The advantages of liquid butyl application, as carried out by the HMA-system, include less waste, improved product quality and use of more economical packing drums. Furthermore, butyl bead acuity and repeat accuracy are said to be more favourable. Adding encapsulant sheeting and lay-up to bulk butyl dispense are both processes that are incorporated in the HMA+-system. This is sequentially performed when upgrading the HMA-system: the encapsulant is fed from a roll and automatically placed onto a cutting table where it is sheeted with perpendicular and longitudinal cuts. A repeat-accurate pick-and-place device transfers the sheeted encapsulant onto a centred substrate and places it into the butyl frame. A third process step, dubbed the HMA++-system, can handle glass-glass-modules.

Applications: Liquid butyl (hot-melt) edge-sealing of thin-film modules.

Platform: Gerold's HMA-system features a drum unloader with drum redundancy. One or two dispensers can be used, depending on the system configuration. The dispensers bridge is a gantry mechanism with servo-controlled X- and Y-movement.

Availability: Currently available.

LayTec

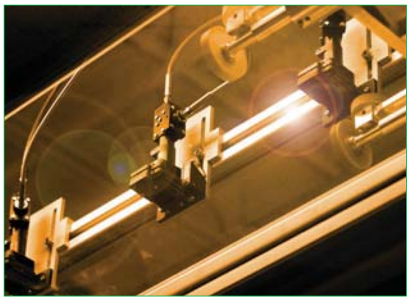

LayTec's PearL system measures photoluminescence spectra of CIGS thin films

Product Outline: LayTec has launched PearL, a new optical in-line monitoring system, measuring photoluminescence spectra of CIGS thin-film modules in production lines. Photoluminescence spectra allow a fast detection of the effective Ga content of the absorber during the production process; a product option for CdTe absorbers is also available.

Problem: Measurements in thin-film PV processes are mainly performed off-line and not on each batch in today's manufacturing processes.

Solution: PearL is LayTec's advanced laser stimulated spectral photoluminescence (sPL) technology for PV absorber layer characterization and process control. Spectra are taken after each layer deposition (n and k of all materials have been determined off-line prior to this process). On-line fitting of an optical multi-layer model to the measured data gives the layer thickness of each layer. The results for the last n^{-1} layers are used to obtain the thickness of the n layer. Operating in a different manner than integral imaging solutions (iPL), PearL delivers fast quantitative material parameters based on the spectroscopic response. In a production environment, the continuous recording of the photoluminescence spectra is a highly valuable measurement for quality control.

Applications: Controlling the optical band-gap of PV absorber layers in thin-film CIGS and CdTe in industrial mass production lines.

Platform: PearL is part of the LayTec product line for solar applications and can be combined with the industry-proven LayTec SolR.

Availability: Currently available.

Manz AG

Manz offers XRF-Inline Quality System for thin-film metrology requirements

Product Outline: Manz AG has launched an XRF-Inline Quality System (IQ-XRF) as an extension of its Manz IQ Series. The fully-automated x-ray fluorescence system has been designed to qualify various deposition process steps in photovoltaic production lines. The systems have demonstrated ability to perform in 24/7 operations.

Problem: The efficiency of a thin-film solar module is mainly driven by the properties of the absorber material. Thus, one of the most critical processes in the production of thin-film solar modules is the deposition of the absorber stack. It is therefore necessary to control this process step perfectly to optimize the total yield. Measurement tools that act as quality gates in a mass production environment must guarantee a high throughput and consequently has to be fully automated.

Solution: According to these requirements, Manz's fully automated XRF-System is claimed to provide outstanding accuracy and flexibility. The measurement performance is provided by IFG's ELBRUS.compact.duo measurement head. Its high accuracy is mainly due to its sophisticated SD-detector, monitoring the intensity variations with a marker technology and by measurement and correction of the distance between the measurement head and substrate. The IQ-XRF is equipped with Manz's automation and control systems, which is a proven measurement solution for qualifying thin films in various applications.

Applications: Inline thin-film quality control applications such as determination of composition, measurement of thicknesses and measurement of homogeneity.

Platform: Manz Inline Quality Series: Manz IQ-XRF.

Availability: Currently available.

NSG Group

TCO thin-film coatings from NSG offer wide application optimization

Product Outline: The NSG Group's TEC product range includes a comprehensive range of TCO coated glass, optimized to suit a variety of thin-film photovoltaic technologies. With different haze and conductivity levels, the NSG TEC product range is designed to offer complete flexibility in TCO coatings to thin-film module producers' individual requirements.

Problem: Thin-film module manufacturers need to maximize module efficiency while maintaining performance guarantees that meet an expected 25+-year lifetime. However, cost reduction requirements support the need for more economical coating solutions in high-volume applications.

Solution: TEC products offer a range of conductivity, morphology and haze requirements to help maximize module efficiency. The durable on-line pyrolitic coating gives the products virtually unlimited shelf life, making them easy to transport, store, handle and process, and therefore reducing costs and lead times. The coated products are also resistant to high processing temperature and can be fully tempered and toughened or heat strengthened without any damage to the coating, and without any drop in performance. In addition, the multi-layer TCO coating stack claims excellent sodium blocking properties, ensuring the module's performance is unaffected by sodium migration from the glass superstrate.

Applications: All thin-film photovoltaic technologies, including a-Si, a-Si/µ-Si, CdTe, DSSC and CIGS/CIS.

Platform: Available in a range of properties and cut sizes to suit all of the leading thin-film photovoltaic platforms, the NSG TEC products can also be tailored to suit individual customer requirements.

Availability: Currently available.

Singulus Technologies

Vitrum Gen 2 from Singulus simultaneously cleans back-sides and edges of thin-film solar cells

Product Outline: Singulus Technologies has launched an enhanced wet-chemical processing system for thin-film solar module manufacturing dubbed the Vitrum Gen 2. The upgraded system is said to offer substantial cost-saving potential.

Problem: In comparison to dipping processes, the second-generation Vitrum enables homogeneous, reliable and reproducible etching. It features further advantages compared to a dipping bath such as a higher etch length and concentration.

Solution: The Vitrum Gen 2 simultaneously cleans back-sides and edges of thin-film solar cells in a single working step. In addition to the automated process control, the new single-side etching tool protects the active layer by process hoods and performs pencil and rear-side etching with brushes and chemicals. Vitrum Gen 2 is claimed to be the only tool on the market that cleans the rear side and the edges in one single step without any harm to the active layers. It is used for cleaning after oven processes as well as for etching of undesirable coatings on rear side and edges, for example CdTe or CdS. The Vitrum Gen 2 provides the platform for several different process steps; for example, in the CdTe manufacturing process it performs six steps, starting with glass washing, back-side cleaning CdTe, $CdCl_2$ deposition using roller and salt removal, to glass washing and developer.

Applications: Wet chemical processing system for thin-film solar modules.

Platform: The new design improves accessibility for optimized maintenance work in a large installation cabinet. Piping is similar for all liquid circuits. It offers a high cycle rate and is also easy to integrate into existing production lines.

Availability: Currently available.

Reactive magnetron sputtering of ZnO:Al

Volker Sittinger, **Wilma Dewald** & **Bernd Szyszka**, Fraunhofer Institute for Surface Engineering and Thin Films (IST), Braunschweig, & **Florian Ruske**, Helmholtz-Zentrum Berlin für Materialien und Energie GmbH, Berlin, Germany

ABSTRACT

Transparent conductive oxides (TCOs), such as aluminium-doped zinc oxide (ZnO:Al), play an important role in thin-film photovoltaics. As a material for front contacts, ZnO:Al is standard in industrial-scale production, especially in the field of Cu(In,Ga)Se_2 solar cells. Over the last few years, there has been a strong push to use ZnO:Al films on glass as substrates for amorphous or amorphous/microcrystalline silicon solar cells, and these films have now been introduced as an alternative to the typically used fluorine-doped tin oxide (SnO_2:F) films in production. Sputtering coaters for large area deposition of ZnO:Al are widely available, and ZnO:Al films are produced in these coaters by sputtering of ceramic targets. This technology offers high process stability and is therefore favoured over reactive sputtering of metallic targets. With respect to cost and quality, however, the reactive process is an interesting alternative. In this paper we will give an overview of the process of reactive sputtering of ZnO:Al and discuss the most important insights.

Introduction

Despite the advantages of reactive sputtering, the process of sputtering of ceramic targets has taken the lead in industrialization, due to the simplicity of process operation. Once suitable deposition conditions have been established, the process is easy to control and promises high yields. In contrast, the reactive sputtering process has to be thoroughly controlled. Nevertheless, reactive deposition via magnetron sputtering is a well-known technique for the deposition of oxides and nitrides. During this process a metallic target is sputtered, with oxygen or nitrogen acting as a reactive gas. Stoichiometric films are typically reached under excess of the reactive gas.

In general the operation can be conducted in two stable modes. If oxygen is fed into the discharge zone in abundance, the metallic target will form an oxidized surface and the process is characterized by low deposition rates and films with high transmission. This mode is referred to as 'oxide mode.' On the other hand, in 'metallic mode,' oxygen partial pressures are low and the target will essentially be sputtered as clean metal. The resulting films are deposited at high rates but usually suffer from sub-stoichiometry and hence high optical absorption. Fig. 1 shows the typical hysteresis behaviour that often occurs during the process of reactive sputtering of ZnO:Al. Such curves are predicted from the Larson model [1]. An accurate description of the reactive process can be found in Berg & Nyberg [2] and Depla & Stijn [3]. In order to obtain both highly transparent and highly conductive films that are necessary for transparent conductive oxides (TCOs), the reactive process has to be controlled in the normally unstable transition mode. Different control mechanisms are possible to stabilize such a process. Mass spectrometry or a lambda sensor would be a direct method for the measurement of the partial pressure. An indirect method would be the use of the target voltage (impedance) [4] or the optical emission spectroscopy (OES) of the sputtered atoms of the reactive gas [5] to determine the partial pressure. To stabilize the partial pressure with this signal, it is necessary to adjust, for example, the power as shown in Fig. 1 or adjust the gas flow. Nevertheless, in either case a high-speed control is necessary. Dependent on the material and reactive flow rates, sometimes a very fast control of a few milliseconds is essential, especially for TCOs.

"In order to obtain both highly transparent and highly conductive films that are necessary for transparent conductive oxides (TCOs), the reactive process has to be controlled in the normally unstable transition mode."

At Fraunhofer IST, a stable oxygen partial pressure is maintained by a closed-loop process control system that constantly adjusts the discharge power of the targets [6]. Films can be deposited at different oxygen partial pressures and film properties will differ significantly. For example, the resistivity of ZnO:Al films will usually reach a minimum at an intermediate oxygen partial pressure, with a steep increase to higher values towards the oxide mode.

Transmission of deposited films is normally constant for higher values and will steeply decrease for low oxygen partial pressures. In order to fully exploit the potential of the reactive sputtering process, the optimum operating point has to be stabilized during deposition and adjusted throughout the lifetime of the targets: therefore closed-loop feedback control systems are necessary. In addition, stabilization along the target is required, as well as the detection of process drifts to adjust operating-point settings in long-term operation.

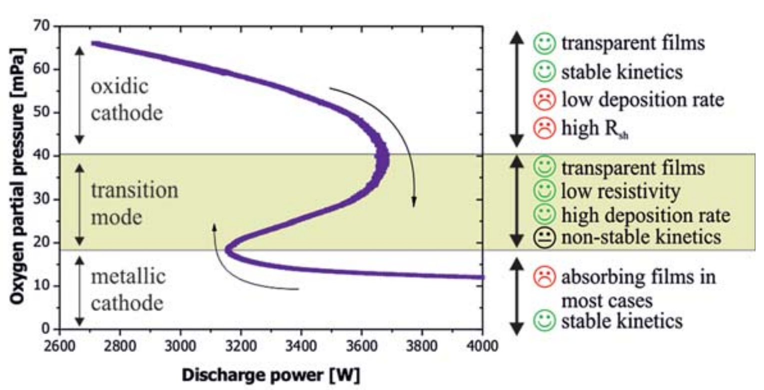

Figure 1. Process curve of a reactive magnetron sputtering process. In this example, the discharge power was varied in order to stabilize oxygen partial pressure at a constant oxygen flow rate.

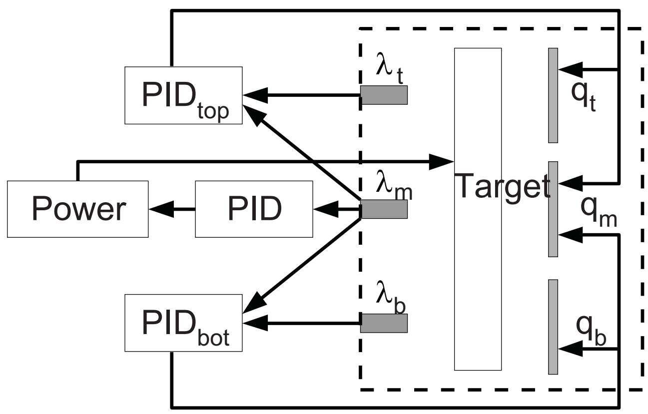

Figure 2. Principal setup of the symmetry control system used at Fraunhofer IST. Three λ-sensors are used to monitor oxygen partial pressure at different positions along the target. The measured values are used as input to a control loop for adjusting the flow of the threefold oxygen inlet.

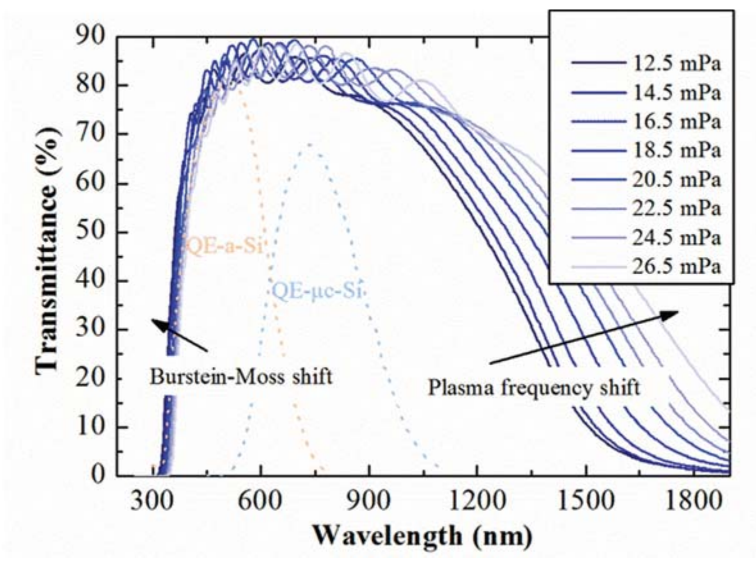

Figure 3. Transmittance of reactively sputtered ZnO:Al films at different operating points. The Burstein-Moss shift and also the shift in plasma frequency can be observed.

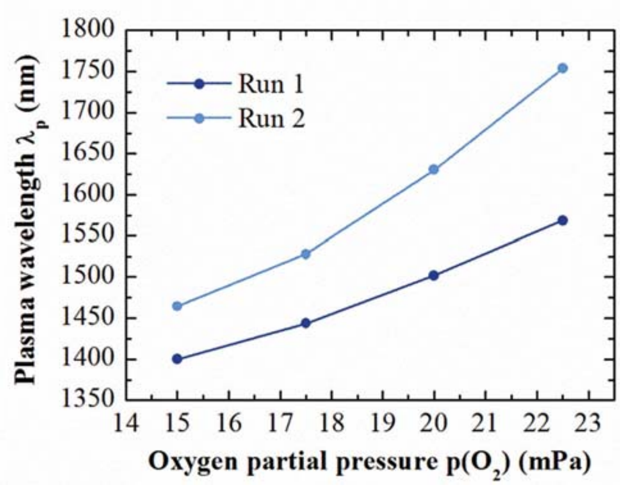

Figure 4. Drift of plasma wavelength of films deposited at the same operating points but in different runs. The film properties are highly dependent on the history of the target.

In the last few years reactive sputtering has been tested for different solar cell applications [7-11]. Every application has its own needs. Besides the requirements of optimal conductivity and lowest possible absorption for CIGS and HIT solar cells, the deposition temperature has to be less than or equal to 200°C due to the sensitive heterojunction. For a-Si/μSi solar cells, because of the superstrate structure and the need for an optimized light-trapping texture, a higher deposition temperature can be used.

Long-term stabilization

A. Target symmetry control

At Fraunhofer IST, ZnO:Al films are deposited in the in-line coater Leybold A700V using two PK750 cathodes run as a dual magnetron and fed by MF power generators. A constant oxygen flow is introduced into the chamber in a separate, threefold gas-inlet system and a lambda sensor monitors oxygen partial pressure in the centre of the discharge. MF power is then controlled by a proportional-integral-derivative (PID) control so that the oxygen partial pressure is kept constant at a desired operating point. With this control, it is possible to operate the discharge in the transition mode between oxide and metallic modes.

We coat the glass substrates of 100 × 60cm^2 with Al-doped zinc oxide. These films are meant to act as front contacts in solar cells [12]. So far, deposition at higher pressures on large-scale substrates has led to strong inhomogeneity of film thickness, sheet resistance and optical transmittance. It has been observed repeatedly that, in the vertical direction, one side of the film is insulating while the other side shows strong absorption. Moreover reproducibility of results obtained using the same deposition parameters was poor.

This behaviour is also known to occur with industrial-size cathodes for architectural glazing, where cathode lengths can exceed 3.75m. As the operating point is only stabilized at the target centre, the outer parts can operate in different discharge states, and fall into either the metallic or the oxide state. The effect has been explained by the decrease of the mean free path of the electrons running along the racetrack at higher pressures [13]. If this mean free path becomes too small with respect to cathode length, the coupling of different target regions is impaired and the process becomes unstable. In order to overcome these difficulties, symmetry control systems are used.

For the additional symmetry control, two more λ-sensors have been added to the setup, at the upper and lower sides of the target. These sensors can be used to monitor the distribution of oxygen partial pressure along the cathode. If symmetry

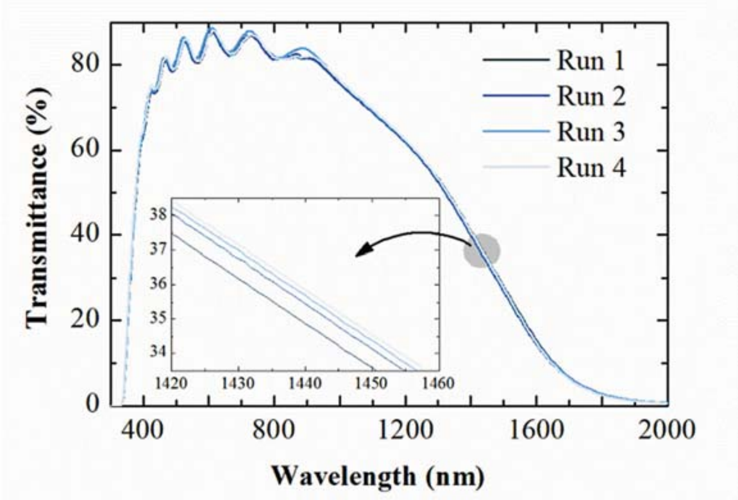

Figure 5. Transmittance of reactively sputtered ZnO:Al films at the same operating points in four different runs. A slight shift of the spectra can be seen in the inset.

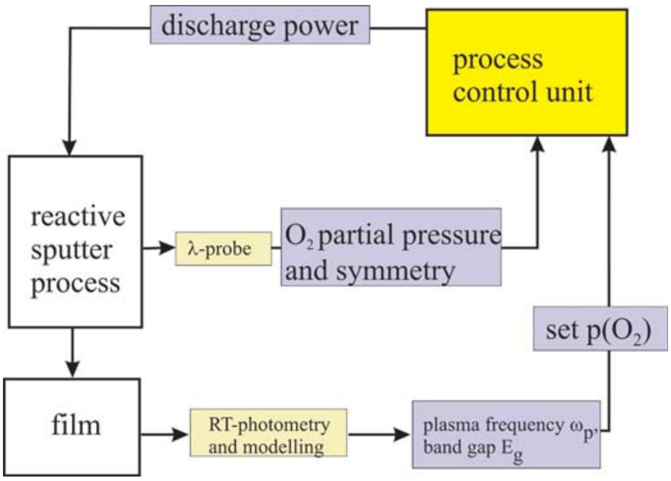

Figure 6. Schematic of the closed loop of the online control. The first cycle (top loop) controls oxygen partial pressure during deposition by adjusting power, and the symmetry by adjusting the flow. The second cycle (bottom loop) controls the deposited film properties by adjusting the set point for $p(O_2)$ via taking optical measurements and curve fitting.

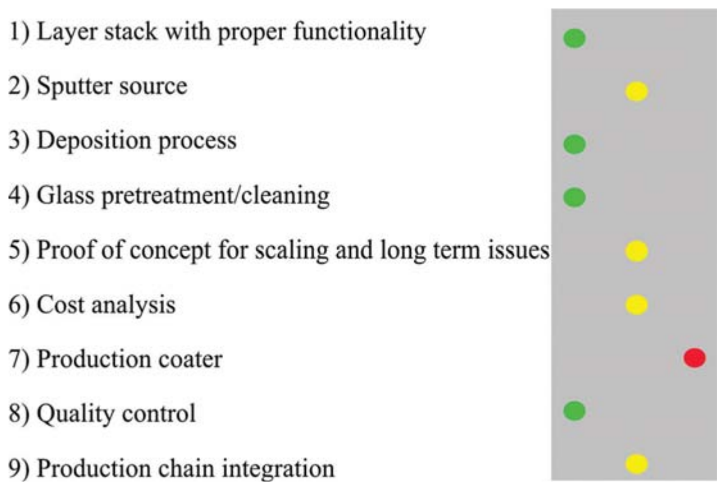

Figure 7. Estimation of the readiness for production of the reactive large area ZnO:Al process.

control is activated, an additional closed-loop control system continuously adjusts the oxygen flow distribution of the threefold gas inlet in order to maintain a suitable oxygen partial pressure distribution (Fig. 2). This type of symmetry control has described in detail elsewhere [14].

All three λ-sensors are calibrated by measuring the pressure increase in the vacuum chamber on increasing the oxygen flow, and recording the sensor signals. Set points for the oxygen partial pressures $p(O_2)_t$, $p(O_2)_m$ and $p(O_2)_b$, monitored by the sensors λ_t, λ_m and λ_b, respectively, were obtained by experiment. First the optimum value of $p(O_2)_m$ is determined by deposition onto small substrates until a highly transparent film with high conductivity is obtained in the middle of the discharge. An oxygen flow distribution known to lead to good homogeneity at lower total pressures is chosen, and partial pressures λ_t and λ_b are monitored throughout the coating process. These values are taken as the starting point for a series of coatings deposited with activated symmetry control. The pressures $p(O_2)_t$ and $p(O_2)_b$ are then tuned to achieve optimal homogeneity.

Generally a fast response and high repetition rate of the PID cycle controlling the gas flow distribution is important to keep the discharge balanced. The control has been shown to be capable of stabilizing homogeneous partial-pressure distributions, even at high total pressures. A more detailed description can be found in [15]. Another example of a partial-pressure distribution control with plasma-emission monitoring is given in [16].

B. Long-term drift control

An online control method that is able to detect process drifts and offers the possibility of adjusting operating-point settings in long-term operation is necessary. This type of control system is based on the evaluation of spectroscopic photometry measurements in the visible and near-infrared wavelength regime. The measured spectra are analyzed with respect to their band-gap and free-carrier absorption.

Fig. 3 shows that the band gap and plasma frequency shift as a function of the oxygen partial pressure. One explanation for this is the mechanism of zinc desorption that occurs at the substrate at low oxygen partial pressures [17,18].

By this mechanism, the relative aluminium content and accordingly the free-carrier density are increased compared to films deposited at high oxygen partial pressure. In contrast, a high oxygen flow causes a better infrared (IR) transmittance and a lower band gap, while a low oxygen flow decreases the IR transmittance and increases the band gap, due to the Burstein-Moss shift. (A more detailed description can be found in [19].) Nevertheless, all fabricated

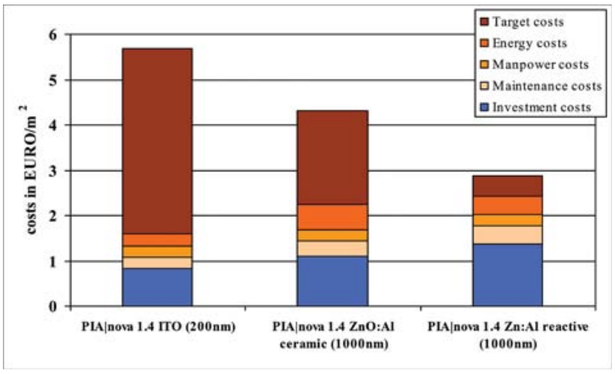

Figure 8. Comparison of typical cost-of-ownership calculations for ITO, ZnO:Al (ceramic process), and ZnO:Al (reactive process)[21].

films show a sufficient transmittance for applications in a-Si/μc-Si tandem solar cells, which is demonstrated by the quantum efficiencies (QE) plotted in Fig. 3. In experimental practice, however, samples prepared under the same process parameters can show very different properties. As an example, Fig. 4 gives the plasma wavelength of such films for two runs in succession.

Besides the long-term target change due to target erosion, the recent target operation history also seems to be important. There are significant differences when starting from a poisoned target or from the metallic mode. In this regard, it might even be necessary to control the oxygen flow in situ during deposition instead of film-by-film control. Fig. 5 shows four consecutive runs carried out at the same operating points. There is only a slight change in the optical transmission spectra.

At least for normal production processes with constant parameters, an online control (substrate by substrate) is sufficient. The closed-loop diagram of the online control is shown in Fig. 6.

There are three loops necessary:

1. Closed-loop control of the oxygen partial pressure during deposition, by adjusting the power with a cycle time smaller than 20ms for high oxygen consumption.

2. Symmetry control, by adjusting the flow with a cycle time of a few seconds.

3. Closed-loop control for adjusting a new set point for oxygen partial pressure, regarding the optical analysis and shifting of the optical spectra (plasma frequency) as shown in Fig. 5 on a large timescale (substrate by substrate).

Besides these, a further important control will be the interconnection of the different cathodes in a typical in-line coater, which has not been addressed so far. However, taking into account our successful experiments for homogeneous large area deposition and the modelling and simulation capabilities available today, we feel that process control is a delicate issue, but a resolvable one.

We have estimated the readiness for production as shown in Fig. 7 [20]. Our next step is the transfer to rotatable cathodes using an environment for closed-loop control that is fully programmable logic controller (PLC) integrated.

Cost aspects

For a discussion of costs, it is instructive to proceed with the analysis shown in Fig. 8 for large area ceramic rotatable target sputtering of either 200nm ITO or 1000nm ZnO:Al at T_S = 200°C, using Gen 5-size coaters, compared with a reactively sputtered 1000nm ZnO:Al. This is done for a CIGS-based front contact, and therefore

Thin Film

a linear depreciation is foreseen for seven years, as noted by Linss et al. at VON ARDENNE Anlagentechnik (VAAT) [21]. The main cost is driven by the target material. Changing from ceramic target sputtering to reactive magnetron sputtering allows the target costs to be reduced by a factor of three, since casting of Zn:Al alloy is a very robust and cost-effective technique compared to more complex sintering or plasma-spraying processes necessary for $ZnO:Al_2O_3$ tube targets. Furthermore, a reduction in energy costs by roughly a factor of two can be expected by taking into account the difference in sputter yield for ceramic and metal targets. As a consequence of this preliminary analysis, a potential cost reduction of the order of 65% for a Gen 5 can be envisaged.

References

[1] Larsson, T. 1989, "A model for reactive sputtering with magnetrons", *Vacuum*, Vol. 39, p. 949.

[2] Berg, S. & Nyberg, T. 2005, "Fundamental understanding and modeling of reactive sputtering processes", *Thin Solid Films*, Vol. 476, p. 215.

[3] Depla, D. & Stijn, M. (Eds) 2008, *Reactive Sputter Deposition*, Springer, Berlin.

[4] Affinito, J. & Parsons, R. 1984, "Mechanisms of voltage controlled reactive planar magnetron sputtering of Al in Ar/N2 and Ar/O_2 atmosphere", *J. Vac. Sci. and Tech.*, Vol. A, No. 2, p. 1275.

[5] Schiller, S. et al. 1982, "On the investigations of DC plasmatron discharges by optical emission spectroscopy", *Thin Solid Films*, Vol. 96, p. 241.

[6] Bringmann, U. et al. 2001, "Method for controlling reactive sputtering processes", European Patent EP1268872.

[7] Sittinger, V. et al. 2006, "ZnO:Al films deposited by in-line reactive AC magnetron sputtering for a-Si:H thin film solar cells", *Thin Solid Films*, Vol. 496, pp. 16–25.

[8] Sittinger, V. et al. 2006, "Stability of CIGS mini modules with ZnO:Al films prepared by reactive mid-frequency magnetron sputtering", *Proc. 21st EU PVSEC*, Dresden, Germany, pp. 1814-1818.

[9] Koble, C. et al. 2009, "DC reactive sputtering of aluminium doped zinc oxide films for solar modules controlled by target voltage", *Thin Solid Films*, Vol. 518, No. 4, p. 1204.

[10] May, C. & Strümpfel, J. 1999, "ITO coating by reactive magnetron sputtering – comparison of properties from DC and MF processing", *Thin Solid Films*, Vol. 351, p. 48.

[11] Menner, R. et al. 2011, "Low-cost ZnO:Al transparent contact by reactive rotatable magnetron sputtering for Cu(In,Ga)Se_2 solar modules, *Thin Solid Films* [in press] [available online at http://www.sciencedirect.com/science/article/pii/S0040609011004603].

[12] Szyszka, B. et al. 2003, "Transparent and conductive ZnO:Al films deposited by large area reactive magnetron sputtering", *Thin Solid Films*, Vol. 442, pp. 179–183.

[13] Pflug, A. et al. 2003, "Process simulation for advanced large area optical coatings", *Proc. 46th SVC*, San Francisco, California, USA, pp. 241–247.

[14] Bruch, J. 2001, "Stabilization and regulation of oxide sputter processes", *Precisions*, November.

[15] Ruske, F. et al. 2006, "Process stabilization for large area reactive MF-sputtering of Al-doped ZnO", *Thin Solid Films*, Vol. 502, pp. 44–49.

[16] Bellido-Gonzales, V. et al. 2009, "Uniformity control in reactive magnetron sputtering", *Proc. 52nd SVC*, Santa Clara, California, USA, pp. 350–353.

[17] Szyszka, B. & Jäger, S. 1997, "Optical and electrical properties of doped zinc oxide films prepared by AC reactive magnetron sputtering", *J. Non-Cryst. Sol.*, Vol. 218, pp. 74–80.

[18] Szyszka, B. et al. 2003, "Transparent and conductive ZnO:Al films deposited by large area reactive magnetron sputtering", *Thin Solid Films*, Vol. 442, pp. 179–183.

[19] Sittinger, V. et al. 2010, "Optical on-line monitoring for the long-term stabilization of a reactive mid-frequency sputtering process of Al-doped zinc oxide films", *Thin Solid Films*, Vol. 518, pp. 3115–3118.

[20] Szyszka, B. et al. 2009, "Reactive magnetron sputtering of ZnO:Al – a status report", *Proc. 52nd SVC*, Santa Clara, California, USA, pp. 42–48.

[21] Linss, V. et al. 2011, "ZnO:Al for CIGS solar modules deposited by reactive sputtering from rotatable magnetron", *Proc. 54th SVC*, Chicago, Illinois, USA [in press].

About the Authors

Volker Sittinger is a senior scientist at the Fraunhofer IST in the Large Area Coating Department and is currently working on magnetron sputtering for photovoltaic applications. He previously held the role of scientific assistant at the Institute of Solar Energy Research GmbH (ISFH). Volker received his doctoral degree in optical and electrical characterization of electrodeposited $CuInSe_2$ solar cells from the University of Oldenburg in 2003 and studied physics at the University of Karlsruhe.

Wilma Dewald has been a junior scientist in the Magnetron Sputtering Group at the Fraunhofer IST since 2008. She is currently working on her doctoral thesis on the subject of electrical and optical properties of TCOs and light management in thin-film solar cells. She studied physics at the University of Göttingen and received a diploma degree in 2007.

Bernd Szyszka is head of the Large Area Coating Department at the Fraunhofer IST, which he founded in 2003. After studying physics at the TU Brunswick, he started his scientific work at the Fraunhofer IST in 1995, and received his doctorate degree Dr. rer. nat. in 1999 on the topic of reactive magnetron sputtering of transparent conductive oxides.

Florian Ruske is a senior scientist at the Institute for Silicon Photovoltaics at Helmholtz-Zentrum Berlin (HZB). He works on transparent conducting oxides and functional layers for silicon-based photovoltaic devices. Florian studied physics at the University of Bonn and afterwards worked at the Fraunhofer IST in the Large Area Coating Department as a Ph.D. student. He received his doctoral degree from the University of Gießen in 2008 for a thesis on reactive sputtering of Al-doped ZnO for photovoltaic applications.

Enquiries

V. Sittinger
Fraunhofer Institute for Surface Engineering and Thin Films (IST)
Bienroder Weg 54E
38108 Braunschweig
Germany

Helmholtz-Zentrum Berlin für Materialien und Energie GmbH
12489 Berlin
Germany

Polarized light metrology for thin-film photovoltaics: Manufacturing-scale processes

Robert W. Collins, **Lila R. Dahal** & **Nikolas J. Podraza**, Center for Photovoltaics Innovation & Commercialization and Department of Physics & Astronomy, University of Toledo, Toledo, Ohio, **Kenneth R. Kormanyos**, Calyxo USA, Perrysburg, Ohio, & **Sylvain Marsillac**, Department of Electrical & Computer Engineering, Old Dominion University, Norfolk, Virginia, USA

ABSTRACT

In situ, real-time and off-line polarization spectroscopies have been applied in studies of large-area spatial uniformity of the components of multilayer stacks in hydrogenated silicon (Si:H) and cadmium telluride (CdTe) thin-film photovoltaic (PV) technologies. Such reflection spectroscopies involve first the measurement of spectra in the reflected-to-incident polarization state ratio of the light wave (or the ellipsometry angles of the reflecting multilayer stack), and then the analysis of these spectra to determine the thicknesses and properties of component layers of the stack. In addition, expanded capabilities result from measurement/analysis of the irradiance ratio and the degree of polarization of the reflected beam, simultaneously with the polarization state ratio, particularly for rough surfaces with in-plane roughness scales of the order of the optical wavelength or greater that scatter and depolarize the light beam. This paper provides examples of 1) real-time monitoring of texture etching of the transparent conducting oxide ZnO:Al; 2) real-time monitoring and off-line mapping of roll-to-roll deposited hydrogenated amorphous silicon (a-Si:H); and 3) large-area mapping of coated glass panels used in low-cost CdTe PV technology. For a-Si:H and CdTe thin-film PV technologies, the focus is on the characterization of the window layers, which are *p*-type protocrystalline Si:H and *n*-type cadmium sulphide (CdS), respectively. Analysis of the thickness, phase and structure of the window layer material over the area of the PV panel is critical in order to design processes for uniformity of high performance. Descriptions are given of future directions in novel instrumentation development that will enable mapping for uniformity evaluation at the high speeds required for on-line analysis.

Introduction

Non-invasive monitoring and control tools are needed on production lines for thin-film photovoltaic module manufacturing [1]. Polarized light spectroscopy is valuable in this application due to its capacity for rapid measurement of film thicknesses in multilayer stacks – even at the sub-nanometre level of sensitivity – by exploiting the experimental techniques of multichannel spectroscopic ellipsometry (SE) at a single sample spot [2]. Additional film properties, such as the composition or crystalline grain size, influence the wavelength dependence of the index of refraction and extinction coefficient (n, k) (alternatively expressed as the complex dielectric function ($\varepsilon = \varepsilon_1 + i\varepsilon_2$)) of the films, and, as a result, can be extracted in the same optical analysis that provides thicknesses [3]. It is advantageous to use *ellipsometry* over *reflectometry* because the former involves measurement of two parameters related to a ratio of the polarization properties of a light wave after and before oblique reflection. In contrast, reflectometry involves measurement of one parameter – the ratio of the irradiance property.

The information content in the polarization state of a light wave at a given wavelength is derived from the AC characteristics of an oscillatory irradiance waveform at the associated pixel of the ellipsometer's multichannel detection system [2]. These characteristics include the AC component phases and their amplitudes relative to the DC component. In contrast, the irradiance is derived from the DC component alone. As a result, small fluctuations in the position of the detected light beam due to photovoltaic (PV) substrate/film motion during continuous on-line measurement affect optical alignment and thus calibration of the irradiance measurement. In contrast, the polarization state measurement is self-calibrating with respect to irradiance, through continuous normalization of the AC component by the DC component. Furthermore, because of the determination of a phase difference shift upon reflection, the polarization measurement is much more sensitive to the very thin layers of the PV stack than the irradiance measurement. In spite of the challenges of maintaining irradiance calibration, it is valuable to perform irradiance, polarization state, and degree of polarization measurement and analysis simultaneously, as in *polarimetry*. This approach is particularly well suited for measurements of rough surfaces, in which case the predicted reflected irradiance from a polarization analysis can be compared with the measured reflected irradiance to extract information about haze – light loss from the specular beam due to scattering by the substrate/film [4].

With the integration of a multichannel detection system for high-speed ellipsometric spectroscopy and with the expansion of the spectral range, SE has gained significant analytical power for on-line monitoring of thin-film fabrication [2,4–7]. As a consequence, minimum acquisition times for full spectra of the order of tens of milliseconds are possible. These spectra yield thickness and optical property information about a wide variety of materials from metallic and transparent conducting oxide contacts to dielectric antireflecting and semiconducting materials, the latter with bandgaps over the solar photon energy range of 0.8 to 2.5eV [3]. The analysis of data collected in on-line and off-line applications poses a significant challenge, and the development of multilayer optical models along with (n, k) databases in the research laboratory reduces the analysis of a complex multilayer stack to the determination of a set of wavelength-independent parameters. These parameters include not only thickness but also basic material properties of composition, crystalline grain size, stress and temperature – properties that define (n, k) [3,8].

Examples to be presented in this paper of metrology applications based on multichannel ellipsometry as a polarization spectroscopy include previous and ongoing activities in texture etching of aluminium-doped zinc oxide (ZnO:Al), an application that demonstrates the full potential of a polarimetric analysis [4]; on-line, single-spot analysis of thin-film

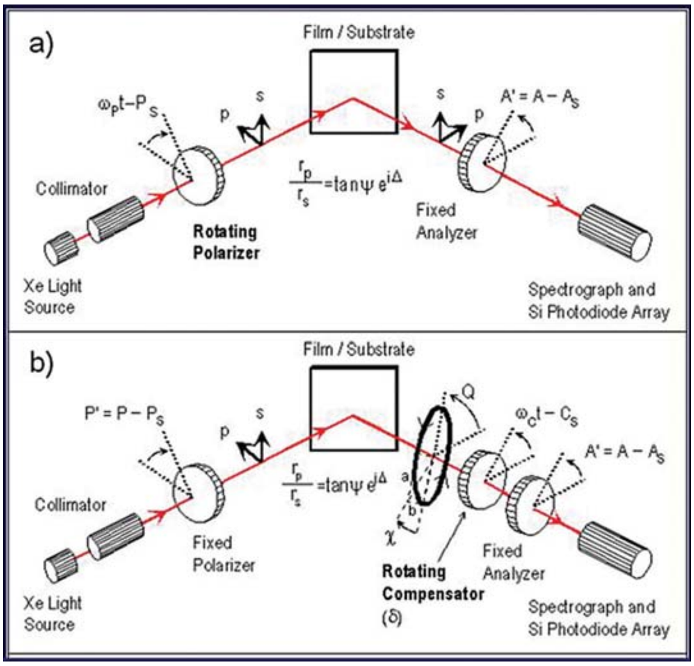

Figure 1. Two multichannel designs for high-speed measurements: (a) rotating polarizer configuration for ellipsometry, and (b) rotating compensator configuration for polarimetry. Both instruments enable measurement of spectra in the ellipsometry angles (ψ, Δ); for an isotropic sample, these angles are related to the *p*-to-*s* ratio of complex amplitude reflection coefficients according to $\tan\psi \exp(i\Delta) = r_p/r_s$. The rotating compensator instrument shown in (b) also has polarimetric capability through measurement of the reflected beam Stokes vector, which incorporates the irradiance I_r, the tilt angle Q_r and ellipticity angle χ_r of the ellipse of polarization, and the degree of polarization p_r.

hydrogenated silicon (Si:H) solar cells in roll-to-roll fabrication [9]; off-line, large-area, multispot mapping of multilayer stacks used in cadmium telluride (CdTe) technology [10]; and future directions in expanded-beam imaging analysis for mapping of rigid and flexible roll-to-roll substrates undergoing linear motion on the production line [11]. Given existing bright sources and high-speed two-dimensional array detectors, the last application of imaging/mapping spectroscopy shows promise for monitoring large-area coated substrates at the linear substrate/film speeds used in production.

Multichannel spectroscopic ellipsometry and polarimetry

Instrumentation

Fig. 1 shows schematics of ellipsometric and polarimetric instruments that have been developed to probe substrate/film structures with a single beam spot, ranging in size from ~0.1 to 10mm [2]. As depicted in Figs. 1(a) and (b), respectively, these instruments use a continuously rotating polarizer or retarder (also called a 'compensator') to measure the effect of the sample on the incident beam polarization state. The light source – such as Xe, D_2 and tungsten halogen lamps, individually or in tandem – is designed for broadband emission. The detection system consists of a spectrograph and one or more linear detector arrays, also designed for broadband detection, with the widest spectral range spanning from 0.19 to 1.7μm [5–7]. Because typical mechanical rotation frequencies $\omega/2\pi$ of the polarizer or compensator range from 5 to 50Hz, a single ellipsometry or polarimetry measurement can be performed in a time of π/ω (half mechanical cycle), ranging from 10 to 100ms. In this time, the array detector(s) must be scanned a minimum of three times for the rotating polarizer instrument in Fig. 1(a) to extract ellipsometric spectra, and five times for the rotating compensator instrument in Fig. 1(b) to extract polarimetric spectra. In many applications, a 10–100ms acquisition time is not needed, and so the spectra are collected as averages over ~100 measurement cycles to improve signal-to-noise ratio, leading to an acquisition time of 1 to 10 seconds.

For both instruments, the typical data output consists of (ψ, Δ) spectra, which can be extracted in a single cycle in a time as short as ~10ms, or from an average of cycles in ~1 second [2]. The (ψ, Δ) values can be understood by an analogy with the reflectance as follows. For a polarized optical plane wave obliquely incident on a surface, one can identify both an irradiance I_i (describing the energy crossing a unit area per unit time) and a polarization state $\xi_i = (E_{xi}/E_{yi}) \exp[i(\delta_{xi} - \delta_{yi})]$ (describing the relative amplitudes E_{xi}/E_{yi} and the phase difference $\delta_{xi} - \delta_{yi}$ for two orthogonal *x*-*y* field components). The reflectance of a surface is defined as the ratio of the irradiance in the reflected beam to that in the incident beam: $R = I_r/I_i$. Reflectometry involves measuring *R* as a function of wavelength. Similarly, the ellipsometry angles are defined by the ratio of the reflected beam polarization state to the incident beam polarization state: $\tan\psi\exp(i\Delta) = \xi_r/\xi_i$. Thus, tanψ is a ratio (reflected-to-incident) of relative amplitudes and Δ is a shift (upon reflection) in the phase difference. In this case, the *x* and *y* orthogonal axes are the *p* and *s* directions of the reflecting surface, parallel (*p*) and perpendicular (*s*) to the plane of incidence, which is defined as the plane that contains the incident and reflected propagation vectors of the plane waves. Combining the expressions for (ψ, Δ) and ξ, one can show that, for an isotropic sample, $\tan\psi \exp(i\Delta) = r_p/r_s$, where r_p and r_s are the complex amplitude reflection (or Fresnel) coefficients for linearly polarized light with electric fields vibrating along the *p* and *s* directions.

Although the rotating polarizer ellipsometer in Fig. 1(a) is the simplest such design, its simplicity leads to limitations [2]. If the substrate is non-absorbing and incorporates a very thin film on its surface, e.g. the first layer of a transparent conducting oxide stack on glass, then incident linearly polarized light is reflected as nearly linearly polarized light. Under these conditions, accuracy in the determination of the film properties is reduced. In addition, if the thin film is rough on the scale of geometric optics or is spatially non-uniform, depolarization of the incident beam will occur. This means that, over the cross-section of the light beam, a distribution of polarization states will be generated due to the distribution of local thicknesses or film properties. If unrecognized, this depolarization effect can be misinterpreted as an increase in ellipticity angle of the polarization state when the rotating polarizer ellipsometer is used; in fact, this ellipsometer configuration cannot distinguish randomly polarized or unpolarized light reflected by the sample from circularly polarized light. For these reasons, the more advanced version of the ellipsometer with a rotating compensator as shown in Fig. 1(b) is necessary to provide polarimetric data – independent measurements that can separate the polarization ellipse and the degree of polarization – and is preferable in studies of the very rough surfaces and interfaces that may be encountered in thin-film PV (even if the separate information about the degree of polarization is not exploited).

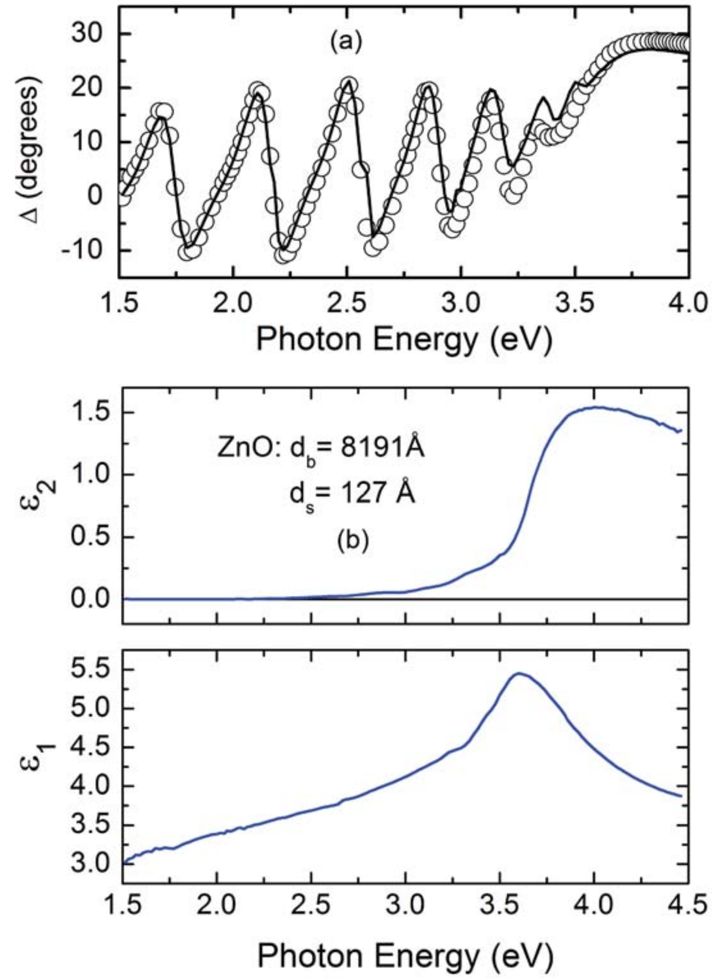

Figure 2. (a) Best fit (solid line) to the measured spectrum in the ellipsometry angle Δ (points) for a ZnO:Al film on glass, prior to etching with 22ppm (by vol.) HCl in H_2O for macroscopic roughness enhancement; (b) dielectric function of the ZnO:Al film along with its microscopic surface roughness and bulk layer thicknesses (d_s, d_b) deduced in the fit. The real and imaginary parts, ε_1 and ε_2, of the dielectric function ε are related to the index of refraction *n* and the extinction coefficient *k* via the expressions $\varepsilon_1 = n^2 - k^2$ and $\varepsilon_2 = 2nk$.

Operationally, the compensator acts on the polarization state in a similar way to a reflecting sample, but with three differences [12]: 1) it operates in transmission at normal incidence (rather than in reflection at oblique incidence); 2) the orthogonal coordinate system consists of fast (*F*) and slow (*S*) axes which are defined, not by the incident beam, but rather by the orientation of the compensator component crystal(s); and 3) the ratio of relative amplitudes (transmitted-to-incident) is unity for an ideal device, meaning that the polarization state ratio is given by $\exp(i\delta) = \xi_t/\xi_i$, where δ is the shift upon transmission in the *S*-*F* phase difference. Because of this phase-shifting ability of the compensator, it serves, in conjunction with the second fixed polarizer (or analyzer) in Fig. 1(b), as a polarimeter, meaning that when rotated it can extract all four components of the Stokes vector of the reflected light beam. The Stokes vector incorporates not only polarization information – the tilt angle Q_r and ellipticity angle χ_r of the reflected beam polarization state – but also the reflected irradiance I_r and the degree of polarization p_r. From this set of spectra, one can extract not only the standard ellipsometry angles of the sample (ψ, Δ), but also direct information on thin-film non-idealities associated with non-uniformities and geometric optics scale roughness, as will be described in the next part of this section.

Advanced data analysis for rough surfaces

In this illustrative example, a rotating compensator instrument has been used in a full polarimetric analysis of rough surfaces that are often encountered in thin-film PV manufacturing [4]. A glass substrate coated with ZnO:Al, which acts as a transparent conductor, has been 'texture etched' in a solution of ~22ppm HCl by volume in H_2O while monitoring with real-time SE. Texture etching involves enhancing the macroscopic roughness, which leads to greater light scattering by the film. This in turn promotes light trapping within the photoactive intrinsic (or *i*) layer when a thin-film Si:H solar cell in either the *p-i-n* or the *n-i-p* sequence is deposited on the surface of the substrate/ZnO:Al. Fig. 2(a) shows the starting Δ spectrum for the glass/ZnO:Al before etching and a best fit, which (along with corresponding results for ψ) provides the optical properties, bulk layer thickness d_b and microscopic roughness layer thickness d_s given in Fig. 2(b). The initial values at t = 0 of (d_b, d_s) before etching are (8191Å, 127Å); the final values after 30 minutes of etching are (7969Å, 232Å). The *microscopic roughness* deduced in this analysis is defined as roughness with an in-plane scale on the atomic level and above (1–500Å), but remaining much less than the central wavelength of the probe beam (~5000Å). This roughness is simulated using standard ellipsometry analysis, replacing the rough surface region with a discrete surface layer having well-defined interfaces to the ambient and underlying 'bulk' layer. The thickness of this surface layer describes the amplitude of the surface modulations, and the optical properties of the layer are described by the Bruggeman effective medium theory [13].

Two results can be expected from the polarimetric data in the absence of roughness on scales larger than the above-described microscopic scale. In the absence of *macroscopic* roughness (having an in-plane scale 500Å to 5µm – within an order of magnitude of the central wavelength of the probe beam), the measured reflectance is predictable from the ZnO:Al bulk layer thickness, its microscopic surface roughness layer thickness, and the glass substrate and ZnO:Al thin-film optical properties (*n*, *k*). In the absence of geometric optics scale roughness (having an in-plane scale 5µm to 5mm – much greater than the central probe wavelength, greater than the lateral coherence of the light beam, but smaller than the beam spot on the substrate/film) and in the absence of other non-uniformities (e.g. large-scale thickness gradients), the fraction of the irradiance that is not purely polarized ($1 - p_r$) is expected to be zero.

Even for the starting ZnO:Al-coated substrate, however, the reflectance measured experimentally deviates from that predicted by the ellipsometry model, as shown in the top panel of Fig. 3 (open circles). The difference – characterized by a lower measured reflectance spectrum than the prediction – can be understood in terms of light scattering by macroscopic roughness and can be modelled using a simple scalar light-scattering theory [14]. This theory yields reflection and transmission coefficients c_j ($c = r, t$; $j = p, s$) of the form

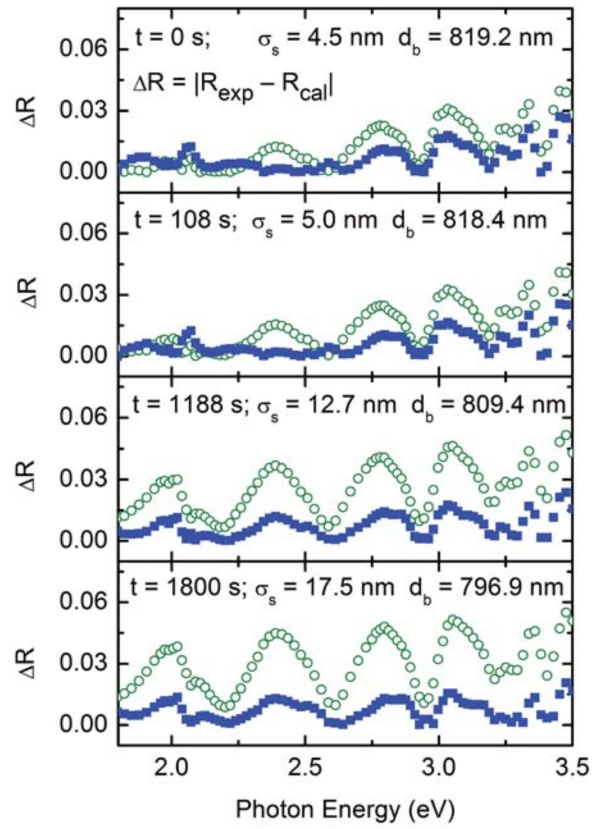

Figure 3. Difference between the experimental and predicted unpolarized specular reflectance spectra for the ZnO:Al sample at four different times during etching. The open points are the results of a prediction assuming an ideal specularly reflecting surface without macroscopic roughness (σ_s = 0); the filled squares are the results of a prediction on the basis of scalar diffraction theory, leading to best-fit macroscopic roughness thickness values σ_s as follows: 1) t = 0s, σ_s = 45Å; 2) t = 108s, σ_s = 50Å; 3) t = 1188s, σ_s = 127Å; and 4) t = 1800s, σ_s = 175Å.

$c_j = c_j(0)\ \exp(-\sigma_s \Delta k_z)$, where Δk_z is the change in z-component of the propagation vector upon reflection or transmission and σs is the width of the surface height distribution, which is assumed to be Lorentzian, $h(z) = (2\sigma_s/\pi)(4z^2 + \sigma_s^2)^{-1}$. The top panel of Fig. 3 shows a smaller difference between the experimental reflectance and the prediction when this theory is applied (filled squares). A best-fit value of σ_s = 45Å is found for the width of the Lorentzian distribution, which yields better fits in this study than the more commonly used Gaussian distribution [14]. In the scalar light-scattering theory, *p* and *s* polarizations are reduced by the same amplitude, and, although the reflectance is reduced, the polarization of the specularly reflected beam is unaffected. As etching proceeds, the deviation of the measured reflectance from the ellipsometric prediction increases, and this deviation enables the determination of the time evolution of σ_s, a measure of the macroscopic roughness thickness, as shown in the lower panels of Fig. 3. Using this simple scattering theory, residual deviations between the measured and predicted reflectance are of the order of the irradiance calibration uncertainties.

For the glass/ZnO:Al before etching, very weak features near 2.2, 2.6 and 2.9eV can be observed in the depolarization spectra of the reflected beam (see the topmost panel of Fig. 4; open circles). This in turn implies that the unetched film exhibits non-uniformity on in-plane scales larger than the lateral coherence length of the light wave (> 5μm); the non-uniformity is associated with geometric optics scale roughness, but near the instrument detection limits. As etching proceeds, these weak features in the depolarization spectra are enhanced, as shown by the results in the lower two panels of Fig. 4. These spectra have been modelled assuming an incoherent superposition of irradiance waveforms from the probed area of the film and a Lorentzian film thickness distribution with an average thickness value deduced from the (ψ, Δ) spectra. The only free parameter in the analysis is the width of the distribution, which controls the height of the depolarization features. The width is determined to be 21Å at the onset of etching (which represents a 0.25% thickness variation over the beam area), and this value increases by more than a factor of three as etching proceeds (see bottom panel in Fig. 4).

Fig. 5 summarizes the results for the evolution of the microscopic, macroscopic and geometric optics scale roughness thicknesses during the etching process. The results are in reasonable agreement with ex situ atomic force microscopy (AFM) and profilometry on companion samples etched under the same conditions but for intermediate etching times. To evaluate microscopic and macroscopic roughness, the AFM rms roughness was measured from 0.2 × 0.2μm^2 and 10 × 10μm^2 images, respectively; and to evaluate geometric optics scale roughness, 5mm-long profilometry scans were analyzed. The lower value of roughness from profilometry is a consequence of its inability to detect roughness on the 5–50μm in-plane scale.

Thin-film Si:H photovoltaics

Optical properties

The optical properties of amorphous semiconductor alloy thin films, including hydrogenated amorphous silicon (a Si:H), amorphous silicon-germanium (a-Si$_{1-x}$Ge$_x$:H), and amorphous silicon-carbon (a-Si$_{1-x}$C$_x$:H), incorporated as the *i*-layers in solar cells, have been determined in situ in the research laboratory using real-time SE. These optical properties can be expressed in terms of a relatively small number of wavelength-independent parameters [3]. In fact, for a set of alloys of highest PV quality at any given temperature of measurement, the optical properties can be determined through specification of a single parameter – the optical bandgap value. This is possible via a Kramers-Kronig consistent mathematical expression in which each parameter is linked to the bandgap. Fig. 6 shows these sets of optical properties, generated mathematically for three different bandgap values E_g. The optical properties of each set are given in the forms (ε_1, ε_2) and (n, α), where $\varepsilon_1 = n^2 - k^2$ and $\varepsilon_2 = 2nk = n\lambda\alpha/2\pi$. In modelling other amorphous PV materials such as doped layers, or *i*-layers prepared

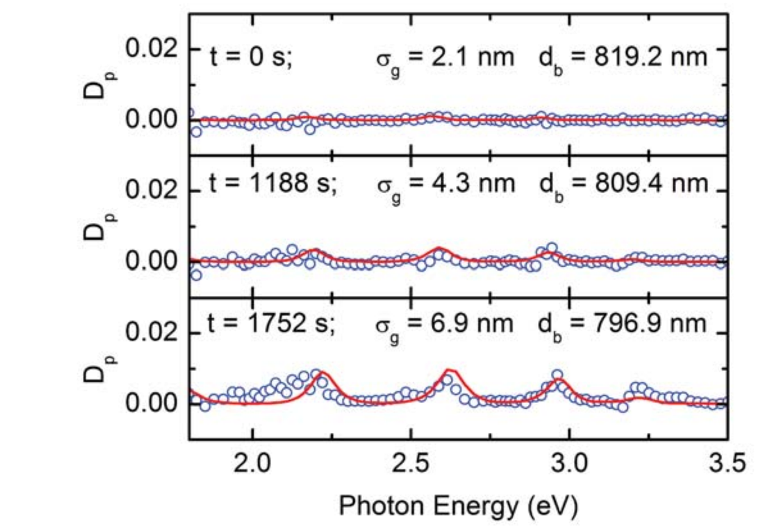

Figure 4. Experimental depolarization spectra for the ZnO:Al sample at three different times during etching (open points); also shown are modelled spectra based on incoherent superposition of irradiance waveforms from regions of different bulk layer thickness (solid lines), yielding geometric optics scale roughness thickness values σ_g as follows: 1) t = 0s, σ_g = 21Å; 2) t = 1188s, σ_g = 43Å; and 3) t = 1752s, σ_g = 69Å.

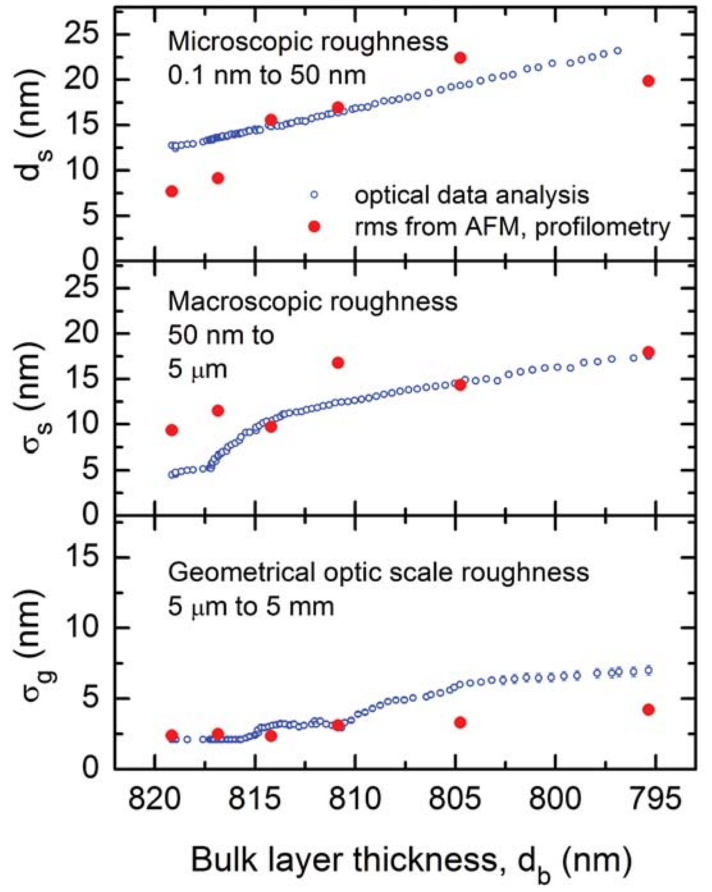

Figure 5. Evolution of surface roughness thicknesses on three different in-plane scales relative to the central wavelength λ ≈ 5000Å, obtained from a polarimetric analysis of spectra collected during ZnO:Al etching. These scales include microscopic (top, in-plane scale L << λ), macroscopic (centre, L ≈ λ) and geometric optic (bottom, L >> λ). The solid points are rms values of surface roughness from atomic force microscopy (AFM) (top: from 0.2 × 0.2μm^2 images, and centre: from 10 × 10μm^2 images) and profilometry (bottom: from 5mm-long traces).

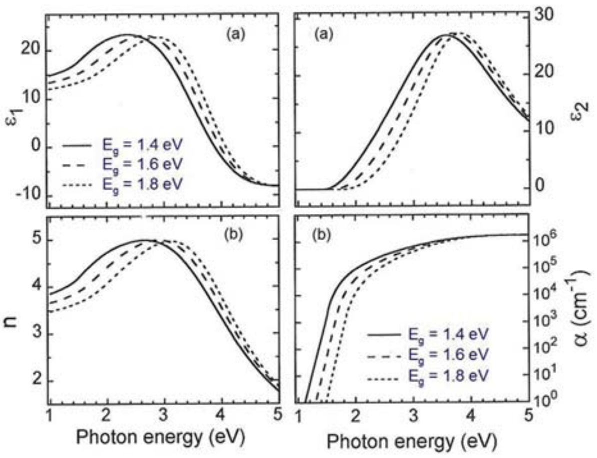

Figure 6. Room temperature optical properties (a) (ε_1, ε_2) and (b) (n, α) for hypothetical hydrogenated amorphous silicon (a-Si:H) alloys of optimum PV quality, computed on the basis of a single specification of the optical bandgap E_g. These results were deduced from an analytical expression that includes 1) Lorentz oscillator behaviour at high energies, 2) a bandgap onset consistent with parabolic densities of states and a constant dipole matrix element, and 3) an exponential Urbach tail connecting to the absorption onset at low energies.

differently from the standard optimized radio-frequency (RF) plasma-enhanced chemical vapour deposition (PECVD) method, then additional parameters must be incorporated in order to decouple the energy, width and amplitude of the oscillator feature in Fig. 6 from the bandgap. These additional parameters may include the void volume fraction and the Lorentzian oscillator width.

On-line roll-to-roll monitoring

Fabrication of thin-film a-Si:H *n i-p* solar cell stacks has been investigated using PECVD within a cluster tool having roll-to-roll cassette capability [9]. The substrate for the solar cell stack is flexible plastic in the roll-to-roll configuration, coated with a back reflector (BR). Real-time monitoring of the thin-film deposition processes has been performed by SE at an incidence angle of 65 degrees, using a rotating compensator multichannel instrument with a spectral range of 0.75–5.8eV (M2000-XI, J.A. Woollam Co.) [5–7]. Monitoring occurs at the centre line of the 15cm-wide substrate at a fixed point within the 18cm-long PECVD zone, located 13cm from the entry point of the substrate as shown in Fig. 7. The emphasis of this discussion is the topmost Si:H *p*-layer, because of the need to carefully control its thickness (at ~100Å), optical properties and phase in the solar cell in order to optimize the open-circuit voltage and blue response. The goal of this investigation is to monitor the growth of the *p*-layer at high hydrogen dilution ratio R ($R = [H_2]/[SiH_4]$) versus thickness after plasma ignition over the leading end of the substrate roll, in a test-run as the layer progresses through the a-Si:H (or so-called 'protocrystalline' Si:H), mixed-phase amorphous+nanocrystalline (a+nc)-Si:H and single-phase nanocrystalline (nc)-Si:H growth regimes.

After *p*-layer deposition, the leading end of the roll has been measured across its full width using ex situ mapping SE (AccuMap-SE, J.A. Woollam Co.) over the range of 0.75 to 6.5eV, with a 1 × 1cm^2 grid in order to characterize the *p*-layer uniformity before deposition of the final indium-tin oxide top contact. From the leading end of the roll, the *p*-layer exhibits an approximately linear thickness gradient over the start-up length (i.e. the length of the PECVD zone), because increasing distances along the substrate from this end have spent an increasing amount of time within this zone. Thus, using ex situ mapping SE, the spatial phase diagram of the *p*-layer can be identified across the 15cm width and 18cm start-up length of the roll. Such a spatial phase diagram identifies the regions of the roll where protocrystalline Si:H, mixed-phase (a+nc)-Si:H and single-phase nc-Si:H appear at the near surface of the *p*-layer. The phase diagram allows one to develop the deposition process and substrate speed to ensure a uniform high-quality protocrystalline Si:H *p*-layer over the entire area of the flexible substrate, as desired for optimization of *n-i-p* solar cell performance in the substrate/BR/*n-i-p* configuration [15].

To achieve this level of understanding of the deposition process, the *p*-layer was deposited on Cr/Ag/ZnO/*n*/*i*-layer at a slow web speed and monitored by real-time SE. A slow speed is used such that the *p*-layer initially evolves through the desired protocrystalline phase, but then transitions first to mixed-phase, and finally to single-phase nc-Si:H in the time that it takes the web to cross the full deposition zone. In contrast, an optimized process requires a higher web speed, ensuring that the maximum *R* value is used while avoiding nanocrystallite nucleation for an ~100Å *p*-layer [15]. In fact, after the initial leading end is coated at the slow web speed for *p*-layer analysis purposes, the web can be accelerated to a higher speed and the *R* value can be adjusted as needed to achieve their optimum values. The phase diagram for a slow web speed is identified through the roughness evolution from the real-time SE analysis, which can be confirmed in a subsequent comparison with the mapping results obtained along the centre line of the substrate roll.

For the fabrication of an *n-i-p* solar cell, several deposition steps were performed before the critical *p*-layer. First, the polyethylene naphthalate (PEN) plastic was fully coated with Cr metal, which acts as an adhesion layer. On top of the Cr, an opaque Ag metal film was sputter deposited, followed by a 3000Å ZnO:Al layer to form the back reflector. Next, a 200Å-thick a-Si:H *n*-layer and a 3000Å-thick *i*-layer were deposited by PECVD. As the last silicon PECVD step, which was the focus of this study, the thin *p*-layer was deposited at a substrate temperature of 110°C, with an RF power of 40W, a pressure of 1.5Torr, and flows of 2sccm SiH_4, 300sccm H_2 (resulting in R = 150) and 0.5sccm dopant gas (5% B_2H_6 in H_2; resulting in $D = [B_2H_6]/[SiH_4] = 0.0125$). Both the pressure and the RF power were fixed, starting from plasma ignition and continuing throughout p-layer growth. At the slow web speed of 0.015cm/s, the effective *p*-layer thickness reaches ~800Å after the web traverses the full 18cm deposition zone, as determined by the mapping SE measurement. The real-time SE measurement can observe at most only a fraction of ~0.7 (13cm/18cm)

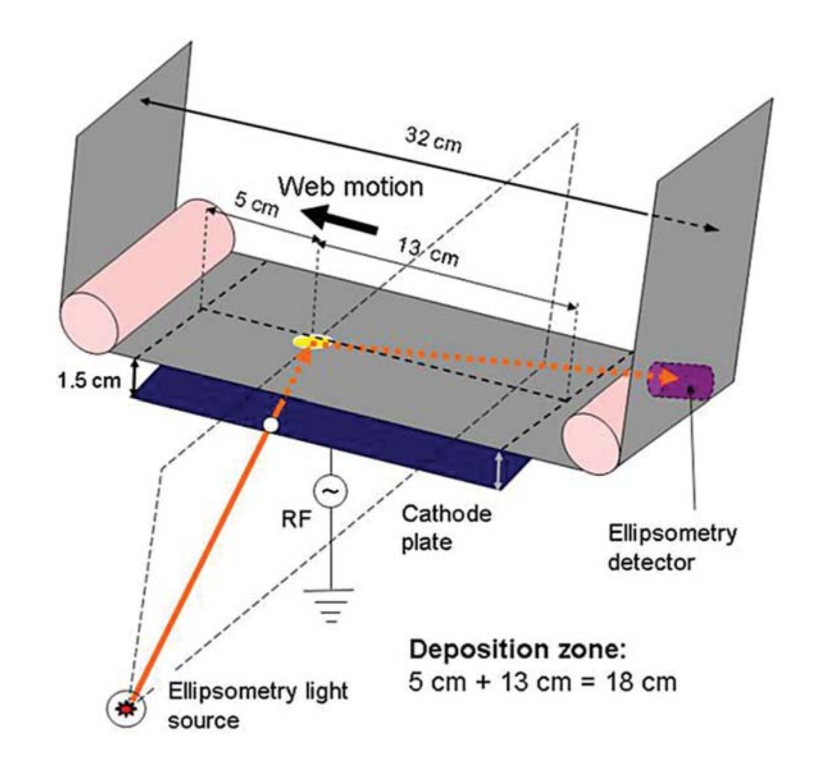

Figure 7. Schematic of the monitoring configuration used for real-time spectroscopic ellipsometry (SE) of a-Si:H *n-i-p* solar cells fabricated by plasma-enhanced chemical vapour deposition (PECVD) in a cassette roll-to-roll cluster tool. For deposition of the *p*-layer, the plasma is ignited (at t_0) while the substrate is moving at a constant rate v. Under ideal growth conditions, the thickness at the monitoring point increases linearly from 0 at the rate $d(t) = (R_o/v)x(t)$; $0 \leq x(t) \leq x_0$, where R_o is the deposition rate and $x(t)$ is the distance of a point fixed on the substrate, as measured from the edge of the plasma zone at time t, defined so that $x(t_0) = 0$. Under ideal conditions, after a time $t = x_0/v$, the thickness saturates at $d = R_o x_0/v$, where x_0 = 13cm, the distance between the monitoring point and the edge of the plasma zone where the substrate first enters.

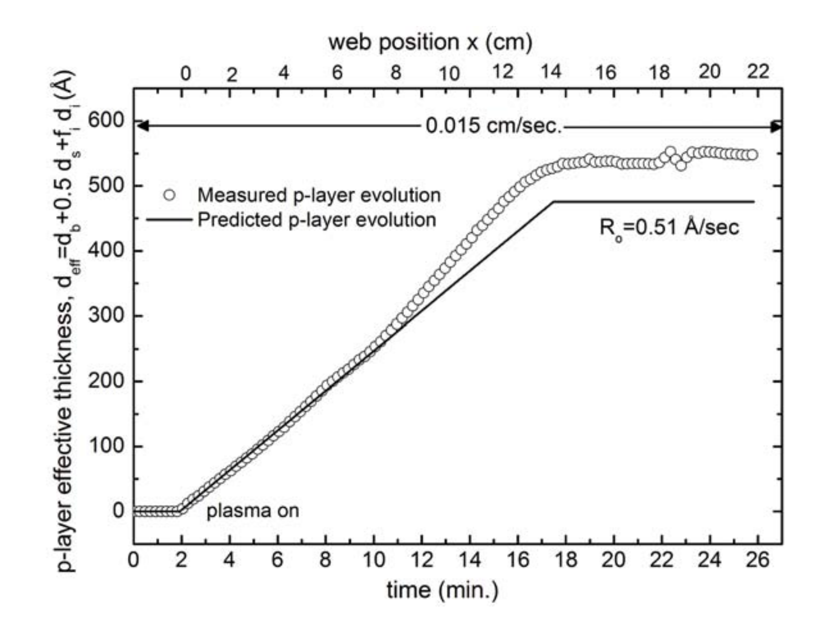

Figure 8. Evolution of the effective thickness as measured by SE during roll-to-roll deposition of a thin hydrogenated silicon (Si:H) *p*-layer at a web speed of v = 0.015cm/s on an underlying a-Si:H i-layer; also shown is a prediction (solid line) assuming a time- and position-independent deposition rate R_o within the plasma zone. The assumed rate of R_o = 0.51Å/s is that associated with an amorphous phase as measured in the early stages of growth.

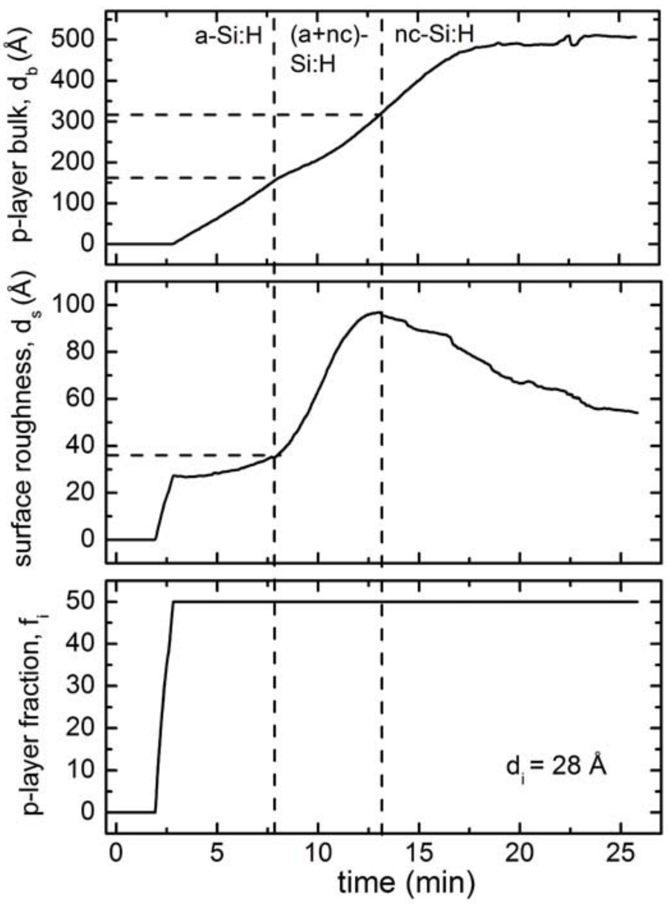

Figure 9. Evolution of bulk layer thickness (top), surface roughness layer thickness (centre) and interface filling fraction (bottom) during roll-to-roll PECVD of a thin-film Si:H p-layer at v = 0.015cm/s web speed on an underlying a-Si:H i-layer. In the bottom panel, a transition from *i*-layer surface roughness to *i*/*p* interface roughness occurs when the *p*-layer filling fraction reaches 50 vol%.

of this effective thickness development, or ~580Å, the deficit from 800Å being due to the deposition that occurs over the 5cm length beyond the monitoring point.

The optical properties of the underlying layers are needed to analyze the structural evolution of the *p*-layer and are obtained from analyses of data collected after depositing each layer in succession. The techniques used leading to these results are reported elsewhere in the paper. The opaque Ag and the ZnO:Al optical properties are generated by least-squares regression analysis [8], using a parameterization that includes a Drude component in the low-energy, near-infrared region and one or more critical point oscillator components in the high-energy, ultraviolet region [3]. The amorphous *n*, *i* and *p*-layer optical properties are generated using the same approach, but with the type of parameterization shown in Fig. 6. Fig. 8 shows the evolution of the *p*-layer effective thickness, which consists of interface, bulk and surface roughness thickness components, respectively, according to the expression $d_{eff} = 0.5d_i + d_b + 0.5d_s$. Also shown is a prediction (solid line) based on the assumptions of a constant deposition rate over time, starting from plasma ignition, and also uniformity of that rate along the centre line in the first 13cm of the deposition zone. Significant deviations from the prediction can be understood by considering the time evolution of the three individual components as shown in Fig. 9.

Before *p*-layer deposition, a microscopic roughness layer exists on the *i*-layer surface, as a 50/50 vol% mixture of *i*-layer/void. At the onset of deposition, the void component is filled in by the *p*-layer material in a time of ~1 minute, as shown in the bottom panel in Fig. 9 [16]. After 1 minute, the onset of bulk *p*-layer growth is observed on the resulting i/*p* interface roughness layer (top panel in Fig. 9). The surface roughness and bulk layer thickness evolution for the *p*-layer suggests that the *p*-layer grows initially in the amorphous phase. The layer undergoes an amorphous to mixed-phase (a+nc) transition at ~8 minutes, occurring after ~155Å of bulk *p*-layer deposition and at which point the surface roughness shows an abrupt increase. Thus, the acceleration of the *p*-layer deposition rate in Fig. 8 starting from ~8 minutes can be attributed to a higher growth rate for the nc-Si:H phase compared with the protocrystalline Si:H phase [17].

After the mixed-phase growth regime, the *p*-layer undergoes a mixed- to single-phase nc-Si:H transition at ~13 minutes when the surface roughness reaches its maximum and begins to decrease. This transition occurs after ~320Å bulk *p*-layer thickness. The decrease in surface roughness is attributed to the coalescence of inverted conical crystallites that protrude above the surface; the result is single-phase nc-Si:H [17]. The thickness saturates at 17 minutes, at which time the moving web has fully crossed the deposition zone. For later times, all film characteristics should stabilize at the values obtained at 17 minutes; however, the continued decrease in roughness suggests a temporal non-uniformity such that crystallite nucleation and coalescence is favoured with increasing duration after the plasma ignition.

"Optimizing the deposition process and ensuring that the web is uniformly flat by maintaining constant tension across the width can improve the p-layer thickness uniformity at the desired final thickness."

The ex situ mapping result of the *p*-layer deposited at 0.015cm/s is shown in Fig. 10. Here, the surface roughness evolution (Fig. 10(a)) along the central line is in good agreement with that of the real-time SE result. The mapping result also demonstrates that the *p*-layer film initially grows in the a-Si:H (or protocrystalline) phase, transitions to mixed-phase (a+nc), and finally coalesces into single-phase nc-Si:H. The mixed-phase transition occurs when the surface roughness layer is ~30Å; above that thickness, there is a sharp increase in the roughness thickness as indicated in the real-time SE result of Fig. 9 (centre panel). Thus, the amorphous- to mixed-phase transition line is drawn on the surface roughness thickness map where this abrupt increase is observed (left broken line). By superimposing this transition line onto the bulk layer thickness map (Fig. 10(b)), the amorphous- to mixed-phase transition is observed to occur at bulk layer thicknesses from 30 to 200Å, depending on the substrate location. Similarly, the transition from the mixed-phase (a+nc) to single-phase nc-Si:H occurs where the surface roughness thickness reaches a maximum (right broken line). By superimposing this transition line onto the bulk layer thickness map, the transition is

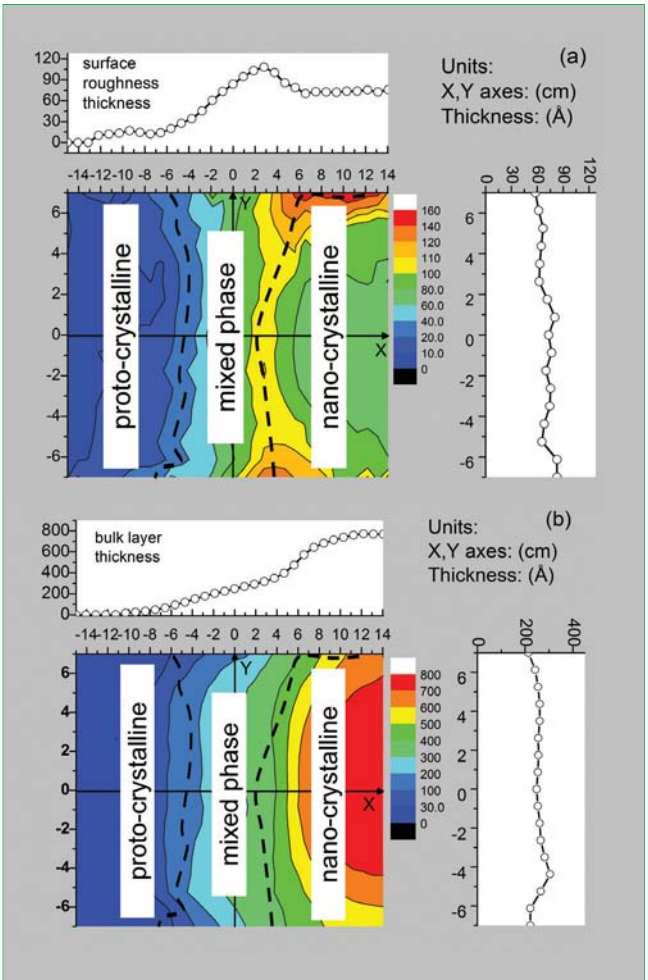

Figure 10. Maps of (a) *p*-layer surface roughness and (b) *p*-layer bulk thicknesses deposited at a web speed of $v = 0.015$cm/s on PEN polymer coated with a Cr/Ag/ZnO/*n*/*i* layer. The broken line on the left indicates the locations at which the amorphous to mixed-phase amorphous+nanocrystalline (a+nc) Si:H transition occurs at the top of the deposited *p*-layer. The broken line on the right indicates the locations at which the mixed-phase to single-phase nanocrystalline (nc) Si:H transition occurs at the top of the *p*-layer.

observed to occur at bulk layer thicknesses over the range of 300 to 600Å. The lines on the bulk layer thickness map establish the spatially dependent phase diagram for $R = 150$.

The thickness maps enable one to evaluate the uniformity along the width of the flexible substrate. From Fig. 10(b), it is clear that the bulk *p*-layer thickness is greater in the central region than at the edges. The effect is enhanced in the nc-Si:H growth regime, possibly due to the higher growth rate of the nc-Si:H phase, coupled with the apparent lower nanocrystal nucleation density near the edges, as noted below. A thicker layer at the centre may also occur if the plastic is slightly warped so that the central portion of the plastic is closer to the cathode plate than the edges. Below the transition to single-phase nc-Si:H, the surface roughness layer tends to be larger near the centre of the substrate; however, near and above this transition, the situation is reversed. The net effect of the observed behaviour is that, near the edge of the substrate, nucleation occurs at a lower thickness and the density of these nuclei appears to be lower since the coalescence occurs at a somewhat greater bulk layer thickness [17]. Since the web speed determines the time during which the substrate resides in the deposition zone, the desired final thickness can be obtained by choosing the web speed proportionately. Optimizing the deposition process and ensuring that the web is uniformly flat by maintaining constant tension across the width can improve the *p*-layer thickness uniformity at the desired final thickness.

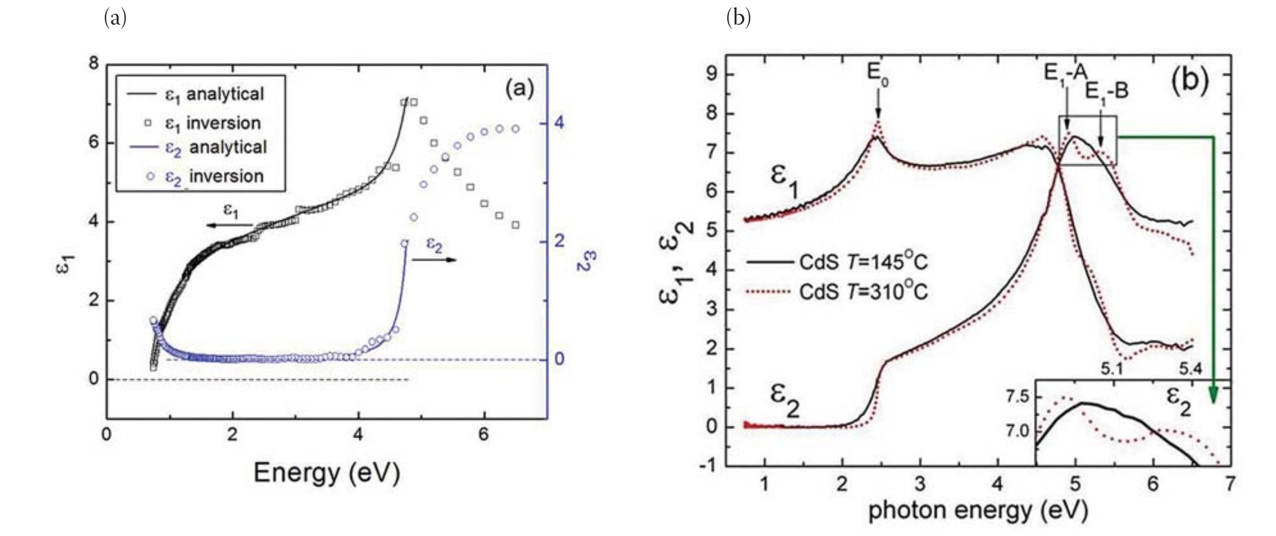

Figure 11. (a) Room temperature dielectric function of the topmost SnO_2:F layer of NSG-Pilkington TEC-15 glass; both methodologies of exact inversion (points) and analytical fitting below 4.8eV (lines) are shown and are in good agreement; (b) room temperature dielectric functions of two cadmium sulphide (CdS) thin films prepared by magnetron sputtering at substrate temperatures of 145°C and 310°C.

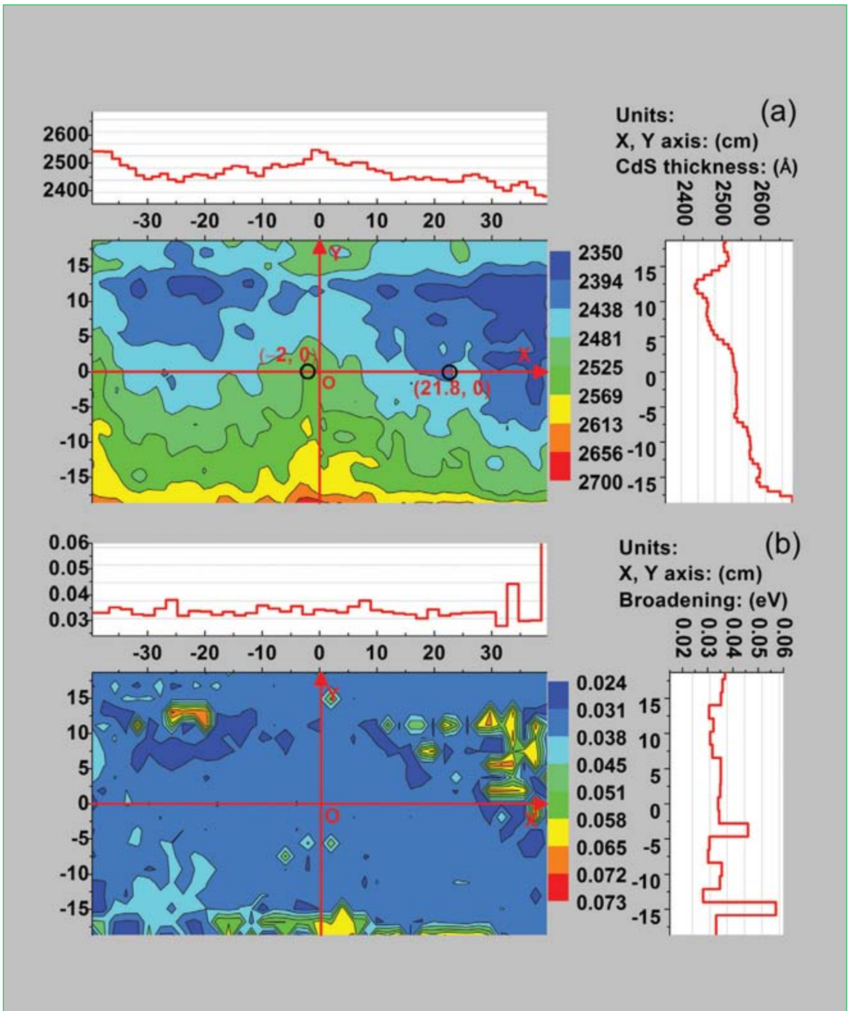

Figure 12. Maps of (a) CdS bulk layer thickness and (b) E_0 critical point (CP) broadening parameter over an ~40 × 80cm² region of a PV plate consisting of coated glass. The CdS film was deposited by atmospheric pressure vapour deposition on NSG-Pilkington TEC-15 glass for demonstration purposes (hence the large thickness). The plots in (a) and (b) (above and to the right of the maps) show the parameter variations along the X and Y axes. The experimental spectra and best-fit results for the two indicated points in (a) are given in Fig. 13.

CdTe photovoltaics

Optical properties

Application of SE and polarimetry methods for the characterization of the optical structure of CdTe-based thin-film PV requires a database of optical properties [18]. The semiconductor layers of the solar cell are deposited on soda-lime glass substrates coated with transparent conducting oxide (TCO). PV modules typically incorporate 60 × 120cm² glass panels and operate in the superstrate configuration, meaning that the solar irradiance passes through the coated glass on which the semiconductor layers are deposited. Standard coated glass (such as TEC-15 by NSG-Pilkington) consists of thin layers (~300Å) of undoped SnO_2 and SiO_2, and a thicker layer (~3000Å) of doped SnO_2:F.

The complex dielectric function spectra ε of the thicker SnO_2:F is the most critical among those associated with the TCO multilayer stack, and must be obtained in the completed stack using the ε spectra of the three underlying materials (glass, SnO_2, SiO_2) and the thicknesses of the thin SnO_2 and SiO_2 layers. To obtain the SnO_2:F dielectric function, a procedure was used that first applied mathematical inversion to the (ψ, Δ) spectra. To perform the inversion, the real and imaginary parts, ε_1 and ε_2, of ε were extracted in the analysis procedure simultaneously with the bulk and surface roughness layer thicknesses. The latter were selected by trial and error in an attempt to eliminate interference-related artefacts in ε_1 and ε_2 that appear in the semitransparent regime of photon energy (i.e. < 4.8eV) when the thicknesses are incorrectly selected [19]. Once the best results are obtained,

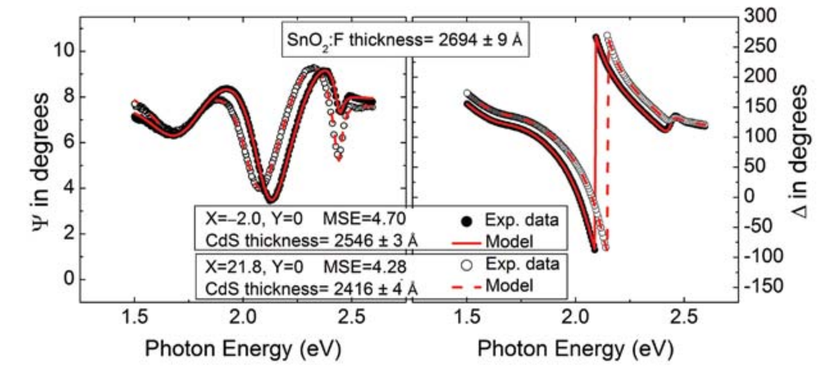

Figure 13. Experimental (points) and best-fit (lines) (ψ, Δ) spectra at positions (X = −2.0, Y = 0) and (X = 21.8, Y = 0) in Fig. 12(a), showing the effect of the CdS thickness on the data and fits. The SnO_2:F thickness was almost the same for the two positions and within 2694 ± 9Å. Confidence limits and mean square errors (MSEs) for the two best fits are also given.

an analytical model can then be used to smooth the inverted dielectric function and eliminate any residual artefacts that generally occur due to inadequacies in the optical model of the sample.

Fig. 11(a) shows the comparison of the inversion results for the topmost TEC-15 layer with the best-fit analytical expression below 4.8eV. Good agreement provides support for the overall analysis procedure. Above 4.8eV the inversion results were artefact free, so an analytical model was not needed. The analytical expression used a Drude free electron component due to free carriers in the SnO_2:F [20], a Sellmeier component to model the normal dispersive behaviour in ε_1, and a Lorentz oscillator to model the high energy absorption onset as evidenced by the increase in ε_2 above 4eV [3]. The Drude expression is given by:

$$\varepsilon(\omega)=\varepsilon_{0s}-\frac{N_{ec}e^2/\varepsilon_0 m_0}{\omega[\omega+i(2\Gamma_m/\hbar)]} \qquad (1)$$

where ω is the optical frequency, ε_{0s} is a constant contribution ($\varepsilon_{0s}\geq 1$), N_{ec} is the free electron concentration, e is the electron charge, ε_0 is the free space permittivity, m_0 is the optical effective mass and ħ is Planck's constant. The Drude amplitude A and broadening energy Γ_m are given by $A^2 = N_{ec}e^2\hbar^2/m_0\varepsilon_0$ and $2\Gamma_m = \hbar/\tau$, respectively, where τ is the free electron relaxation time. These relationships can be used to deduce the electrical properties of the film, such as the optically extrapolated DC resistivity ($\rho = 2\hbar\Gamma_m/A^2\varepsilon_0$). From the thickness d of the SnO_2:F, the optically extrapolated DC sheet resistance is given by $R_s = \rho/d$.

It is also critical to parameterize ε of the cadmium sulphide (CdS) and CdTe layers that form the solar cell [18]. In this case, high-accuracy complex dielectric functions are obtained from films that are free of oxide overlayers via in situ measurements of thin films, followed by cooling and measurement at room temperature. Thicknesses in the 500–1000Å range are used for greater uniformity versus depth into the film. By monitoring the deposition by real-time SE during film growth, accurate bulk and surface roughness layer thicknesses are also obtained; these are not expected to change upon cooling to room temperature. Inversion in order to extract (ε_1, ε_2) of the thin film uses these accurate layer thicknesses.

As an example, the focus will be on the CdS layer, which is analogous to the top p-layer in the a-Si:H device to the extent that it serves as a window layer, and its optical properties and thickness have a significant effect on the blue response and thus short-circuit current of the solar cell. Fig. 11(b) shows the complex dielectric functions obtained in situ at room temperature for 500Å-thick CdS films prepared by magnetron sputtering at substrate temperatures of 145°C and 310°C with a fixed Ar pressure and flow of 10mTorr and 23sccm, and an RF target power of 50W [18]. The complex dielectric function spectra can be parameterized using an expression of the form as shown in Equation 2 [3], where the sum is over the three critical points (CPs), including the bandgap E_0, and E_1-A and E_1-B. The function f describes a broad background given as a Lorentz oscillator versus photon energy E with a well-defined energy onset E_g. For the nth critical point,

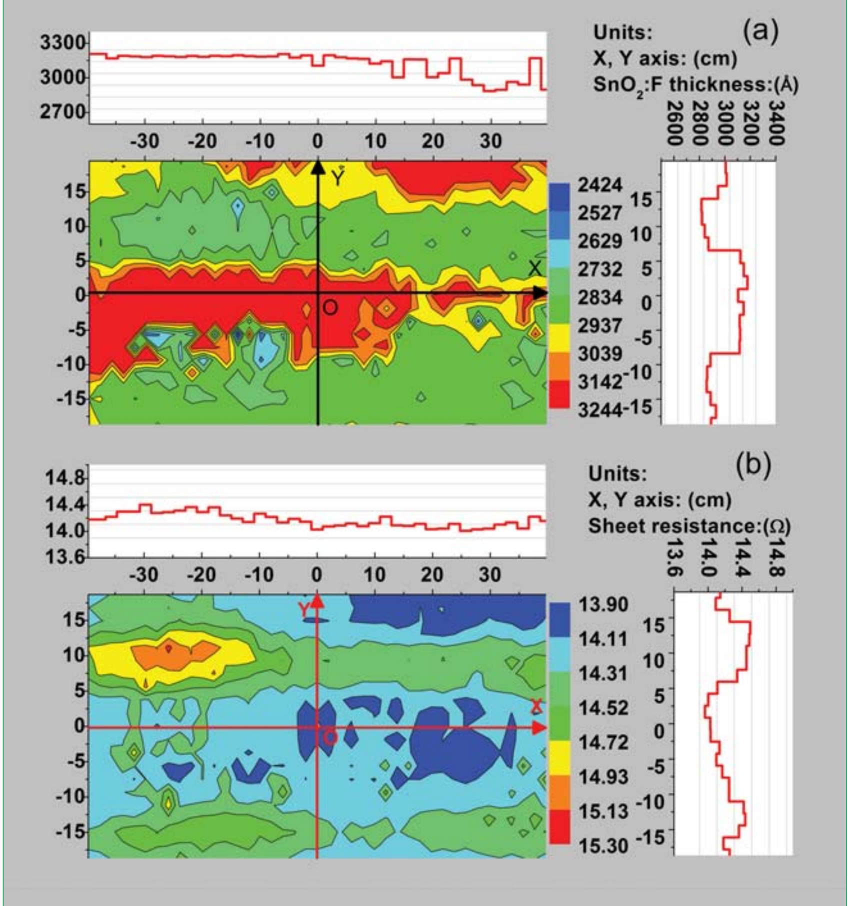

Figure 14. Maps of (a) SnO_2:F bulk layer thickness on the TEC-15 glass panel and (b) optical sheet resistance of the SnO_2:F layer. The plate in this case is the same as the one in Figs. 12 and 13; thus the SnO_2:F layer lies beneath the CdS layer. The plots in (a) and (b) (above and to the right of the maps) show the variations in the deduced parameters along the X and Y axes.

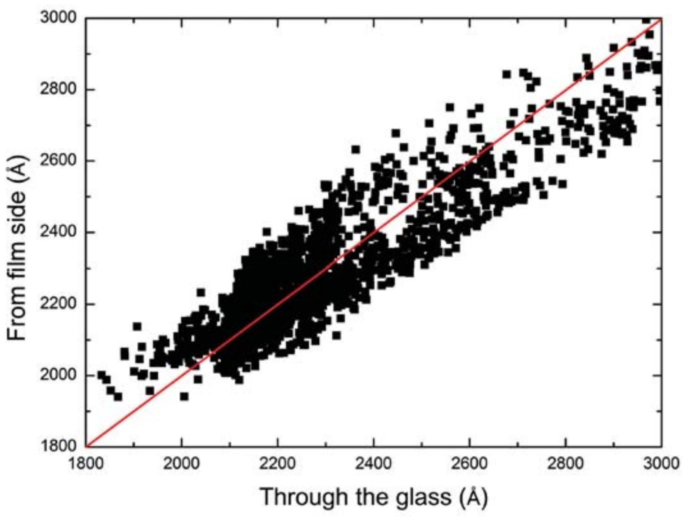

Figure 15. Correlation between the CdS thickness determined in a film-side measurement and the corresponding results obtained at the same position but through the glass. The scatter plot is obtained from individual measurements over the 40 × 80cm² region of the CdS-coated TEC-15 glass plate of Figs. 12–14.

A_n, E_n, Γ_n, μ_n and ϕ_n are the amplitude, energy, broadening parameter, exponent, and phase of the *n*th CP. For the Lorentz oscillator A_L, E_L and Γ_L are the amplitude, resonance energy and broadening parameter. In the parameterization of Equation (2), the exponents are fixed at the values obtained in the best fits to the single-crystal CdS complex dielectric function.

The most significant difference between the two spectra in Fig. 11(b) is in the widths Γ_n of the CP features, as shown in the inset for ε_2 of the two high-energy CPs labelled E_1-A and E_1-B. This difference can be attributed to variations in the average radius *R* of crystalline grains in the material. In addition, the CP energy positions can also vary due to stress in the films. Both effects can be quantified through the expressions:

$$\Gamma_n = \Gamma_{bn} + \hbar v_{gn}/R \qquad (3a)$$

$$E_n = E_{bn} + C_{Xn} X \qquad (3b)$$

where Γ_{bn} and E_{bn} are the broadening parameter and energy position for the single crystal in the limit of large *R* and zero stress. In Equation (3a), ħ is Planck's constant and v_{gn} is the group velocity associated with the *n*th CP; in Equation (3b), C_{Xn} is a stress coefficient. For a collection of samples fabricated under different conditions, the other parameters in Equation (2) can be either fixed or linked to the dominant parameters *R* and *X*. In this way, the number of variable parameters can be reduced from a total of 17 in Equation (2) to three which describe the physical properties of the sample, namely grain size *R*, stress *X* and void fraction f_v, the latter introduced independently through an effective medium theory.

Thus, the approach is similar to the one used to simplify the analysis of amorphous semiconductor films. The reason for this approach is clear. In fitting optical data for multilayer stacks, although all points in the 17-dimensional parameter space defined by Equation (2) are physically possible, only a small fraction of this space is accessible to CdS. By restricting the volume of accessible parameter space, the global minimum in the error function and the solution to the analysis problem can be located more easily and quickly. Furthermore, as a larger collection of materials with a wider range of properties is fabricated, the database can be modified to expand the parameter space and accommodate the new materials. As a result, optical property database development is a continuous 'work in progress.'

Off-line mapping

Off-line SE data have been collected from the film side over an ~40 × 80cm² area of a TEC-15 glass panel coated with CdS. These data have been analyzed using a five-layer model with free parameters that include the bulk and surface roughness layer thicknesses of the CdS and the three layer thicknesses of the TEC-15 glass substrate, including the SnO_2, SiO_2 and SnO_2:F [10]. The optical property parameters that are also incorporated in the modelling include the set of CdS CP broadening values which are linked to a single grain-size parameter *R*, and the Drude amplitude *A* and broadening Γ_m for the SnO_2:F layer that enables determination of the resistivity and sheet resistance of the layer.

Fig. 12 depicts maps of the CdS bulk layer thickness and the E_0 broadening parameter over the 40 × 80cm² area. The bulk layer thickness is observed to range from 2350 to 2700Å. These thickness values are much larger than those used in modules (typical values in modules are ~1000Å); thus, this plate is used for evaluating the SE mapping capabilities only. The effect of a 150Å difference in the CdS thickness appears clearly in the fringe patterns of the spectra in Fig. 13, and the difference is well described by the model. A larger broadening value in Fig. 12(b) is an indication of a smaller grain size *R*, or, more generally, a larger concentration of centres that scatter excited carriers. Smaller grain sizes in turn can result from a higher nucleation density in the deposition process. Regions with a larger E_0 broadening parameter in Fig. 12(b) appear to be correlated with reduced thickness or the presence of the plate edge.

Fig. 14 shows maps of the underlying SnO_2:F thickness and its sheet resistance, the latter obtained from the Drude parameters of the optical model as an extrapolation of optical frequency data. From the map in Fig. 14(a), the thickness of the topmost SnO_2:F layer of the TEC-15 stack is observed to vary between 2500 and 3250Å. In Fig. 14(b), only small variations in the optical sheet resistance are observed, ranging between ~14 and 15Ω/sq, with 15Ω/sq being the nominal value for TEC-15-coated glass panels.

The results in Figs. 12–14 are obtained from an analysis of SE data collected from the film side of the glass. This is preferable when the film stack is relatively thin (which generally implies that it is also relatively smooth) and when no single layer becomes optically opaque over a large part of the spectrum, which is the case for the plate studied here, consisting of glass/SnO_2/SiO_2/SnO_2:F/CdS. More often, however, in on-line applications it is more important to analyze the complete film stack, consisting of the TEC-15 glass and the CdS/CdTe heterojunction. Because the CdTe film used in PV modules is deposited to ~2–5μm, the resulting surface exhibits extensive microscopic, macroscopic and even geometric optics scale roughness, as well as being opaque at energies above 1.5eV, the CdTe bandgap. In this case, higher sensitivity to the underlying layers of CdS and SnO_2:F is obtained by directing the light beam through the glass.

In this optical configuration, various steps must be taken to optimize the measurement and analysis [21]. First, it is best to eliminate the ambient/glass reflection and measure

$$\varepsilon = \varepsilon_0 + \{\sum_{n=1}^{3} A_n[E - E_n - i(\Gamma_n/2)]^{\mu_n} \exp(i\phi_n)\} + f(E, A_L, E_L, \Gamma_L, E_g)$$

Equation 2.

only the glass/film-stack reflection; this is possible due to the relatively large thickness of the glass (~3.2mm) that leads to spatial separation of the two beams. Isolating the reflection from the glass/film-stack interface can be facilitated also by focusing the incident beam on that interface. Second, one must incorporate into the optical model a layer of different optical properties on the Sn bath side of the soda-lime glass, as well as stress in the glass. On its way from the source to the detector, the light beam makes two passes through the ambient/glass interface and through the glass itself, and the polarization modifications that occur in these passes differ from those predicted for a uniform slab of isotropic glass.

> "Among the features that may need to be incorporated for an improved correlation is an interface roughness layer between the SnO_2:F and the CdS, and an oxide-modified layer on the surface of the CdS."

In Fig. 15, the correlation between the CdS thickness as measured through the glass and from the film side is observed to be good; however, there is significant scatter. Among the features that may need to be incorporated for an improved correlation is an interface roughness layer between the SnO_2:F and the CdS, and an oxide-modified layer on the surface of the CdS. Thus, the optical model for the sample, and for PV multilayers in general, is a work in progress that must be improved over time along with the optical database.

Future directions in instrumentation for on-line SE

For the mapping ellipsometer used to obtain the results of Figs. 10 and 12–15, typical high-accuracy measurements are taken every ~5 seconds, including time for translating the ellipsometer, autofocusing and multiple optical cycle averaging. This relatively low measurement speed for mapping motivates future instrumentation development based on imaging [22–24]. A promising new approach developed by Fried and co-workers is to image the PV panel along a line across its width using an expanded light beam [11,23–24]. One dimension of a two-dimensional detector array is used for line imaging, and the second dimension is used for spectroscopic analysis. As a result, the data across the width of the panel are collected in parallel, significantly increasing the speed. Such instrument development is not without its challenges and, ultimately, limitations; however, the goal of future

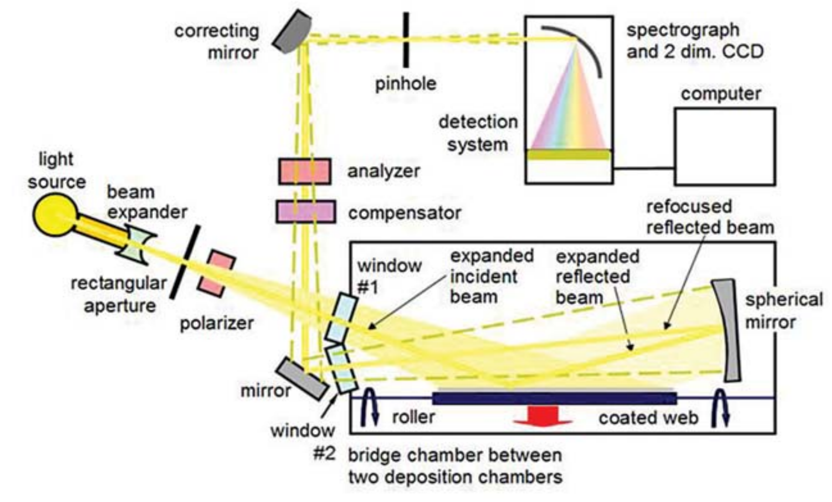

Figure 16. Simplified schematic of instrumentation for on-line SE imaging across the substrate width in conjunction with mapping along its length made possible by translation of the substrate on the production line. Although the design is shown for analysis of the coated substrate in roll-to-roll deposition, it can also be used in mapping moving glass panels.

efforts is to approach the high accuracy of the lower speed point-by-point approach in on-line applications.

Significant progress has been made starting from the original concept [11]. Characteristics of the instrument include an ~10-second measurement time for an image with 30 spatial points across the width of a 15cm wide panel, for a spatial resolution of ~0.5–1cm. Thus, in the current configuration, three to six line images can be generated at a substrate speed of 2–4cm/s. Two selectable spectral ranges from 350 to 650nm and from 650 to 1000nm have been used; the full range of 350 to 1000nm can be collected with a doubled line-image acquisition time of ~20 seconds. A total of 50 points are obtained over each range for a spectral resolution of 6–7nm. Consequently, each readout of the two-dimensional array leads to ~1500 spatial/spectral points. To reach the full potential of such an instrument, a 4× beam expansion to 60cm must be possible for on-line monitoring of CdTe PV panels, upscaling from the current width of 15cm, which is suitable for in situ analysis of roll-to-roll deposited materials as demonstrated in Figs. 7–10. Upscaling will require a brighter source and a more sensitive camera in order to maintain the current 0.5–1cm spatial resolution. Another expansion in instrument capability involves widening the spectral range with a single measurement cycle. This will require advanced polarizing optics (polarizers and compensators), along with multiple sources, and two-dimensional array detectors.

The current version of the line-imaging multichannel ellipsometer uses the rotating polarizer configuration of Fig. 1(a), in which case the rotations are performed step-wise rather than continuously [23,24]. In future developments of this expanded-beam imaging instrument, the step-wise rotating polarizer configuration should be replaced by the continuously rotating compensator, primarily to achieve improved performance for a wider variety of sample types, but also for a polarimetric capability critical for rough-surface applications.

An advantage of the point-by-point measurement approach is the ability to autofocus on the sample, maintaining a small spot size, and therefore to separate out the ambient/glass reflection in superstrate applications in which measurements are performed through the glass. In addition, an autoalignment capability enables determination of angle/plane of incidence corrections that are necessary for high accuracy when dealing with non-planar glass or flexible foil substrate surfaces. With the current expanded-beam instrument, line imaging is performed with a large depth-of-field pinhole camera, and angle of incidence and internal mirror calibrations are performed using planar wafer Si standard samples [24]. Advanced approaches must be developed for self-calibration as a component of data acquisition, which is possible to a limited extent with the rotating compensator configuration [25]. Corrections to calibration parameters may also be possible in data reduction, given sufficiently comprehensive models and optical property databases. The application of the imaging instrument for measurements through the glass is expected to be particularly challenging due to the incoherent superposition of ambient/glass and glass/film-stack interface images. With the depolarization information provided by the rotating compensator configuration, it may be possible to address these challenges.

As shown by the simplified schematic of Fig. 16, the expanded-beam ellipsometer has a critical advantage in that the full width of the PV panel can be probed with a single beam that enters and exits through individual viewports. In fact, no moving optical components are needed. This approach enables in situ monitoring of PV panels under vacuum, in particular in roll-to-roll systems, utilizing bridge chambers between successive deposition chambers for the purposes of in situ monitoring of each critical thin-film fabrication step, before the next step is performed. This capability is expected to assist in optimizing and troubleshooting processes during equipment installation, enhancing yields during production and identifying equipment maintenance issues that require shutdown.

Summary

This paper has reviewed the current state of the art in polarization spectroscopy for in situ, real-time and off-line analysis of the uniformity of thin-film PV materials, including multilayers on rigid glass as well as on flexible metal and polymer foil substrates. The example given for in situ, real-time spectroscopy comes from process development and optimization of roll-to-roll fabrication for thin-film hydrogenated amorphous silicon (a-Si:H). In this example, the flexible substrate/film is probed at a single fixed point along the centre line of the substrate as it moves through the deposition zone. The critical topmost *p*-type layer of the *n*-*i*-*p* solar cell has been studied, since a very thin amorphous film having the more ordered protocrystalline structure is desired. The first large-area off-line mapping example is demonstrated in this *p*-layer study, in which the uniformity across the width of the substrate/film stack is evaluated. A second example is shown, in which the uniformity in the properties of a partially completed CdTe PV panel of CdS-coated glass is evaluated. The thickness and properties of the critical CdS layer have been obtained; a very thin polycrystalline film with low defect density is desired in this application. In general, a significant component of the methodology development effort occurs in the research laboratory through the construction and verification of optical models, in particular approaches for working with very rough surfaces; the accumulation of optical property databases; and the evaluation of new instrument design concepts.

The construction of optical models involves incorporating non-idealities such as graded optical properties in bulk layers, interdiffusion at interfaces and substrate-related artefacts (for example ambient/glass reflections) as well as the features of surface and interface roughness for a wide range of in-plane scales. Substrate-related artefacts become even more significant when measurements are performed through the glass. It is important to note that optical model development evolves over time, as previously unaccounted-for deviations between measured and best-fit ellipsometric spectra can be understood in terms of new optical features. There is also a close interrelationship between improvements in the optical model and improvements in the optical property database. The optical properties (n, k) of the materials that make up a thin-film PV stack can be parameterized using very general physics-based optical models; however, for polycrystalline semiconductors, the number of parameters in these expressions approaches 20 or more, depending on the number of band structure CPs in the studied spectral range. Optical property database development involves relating the optical property parameters to a much smaller number of parameters that describe basic physical properties of the materials. It is important to note that optical database development evolves as improved correlations between optical property parameters and basic materials properties are established.

This paper has demonstrated that useful information can be extracted in reflection from surfaces that exhibit roughness on a wide range of in-plane scales. Within scalar scattering theory, macroscopic roughness (having an in-plane scale of the order of the wavelength of the probe light) suppresses r_p and r_s equally, so its effect on (ψ, Δ) can be neglected. The resulting macroscopic roughness enables one to deduce a spectroscopic haze parameter for the film stack, which is inherently useful; however, the required irradiance calibration is challenging, especially in on-line environments. For geometric optics scale roughness, with an in-plane scale much larger than the wavelength, a key component of polarimetric analysis is the ability to separate out the depolarization that accompanies this roughness scale. An important future direction is to integrate and apply these capabilities in a wider variety of real-time applications, and in off-line and on-line mapping tools. Also, future research must be performed in the laboratory to evaluate the applicability of the scalar scattering theory under a wider range of conditions.

Future directions in adapting off-line mapping instrumentation to in situ and on-line applications have been identified. The off-line mapping examples demonstrated in this article employ relatively slow point-by-point measurement, in which the ellipsometer is translated over the surface of the sample. A solution to this problem, implemented by Fried and co-workers, is similar to that developed in transitioning to high-speed spectroscopy – namely, to incorporate parallel detection for the different spatial points across the width of the moving PV panel. As a result, the light beam is expanded to form a line over the width of the panel, and that line is imaged through a spectrograph onto one dimension of a two-dimensional array detector. The spectrograph disperses the image across the second dimension of the array for parallel spectroscopy performed simultaneously. Although challenges must be overcome to achieve the accuracy of the existing point-by-point mapping methods, the potential pay-off in terms of speed justifies further development of this approach.

References

[1] Ellison, T. et al. 2006, "Inline diagnostic systems for the characterization of multi-junction solar cells", *Proc. IEEE 4th World Conf. PVE Conv.*, p. 1736.

[2] Collins, R.W. et al. 2005, "Multichannel ellipsometry", in Tompkins, H.G. & Irene, E.A. (eds.), *Handbook of Ellipsometry*, William Andrew, Norwich, New York, p. 481.

[3] Collins, R.W. & Ferlauto, A.S. 2005, "Optical physics of materials", in Tompkins, H.G. & Irene, E.A. (eds.), *Handbook of Ellipsometry*, William Andrew, Norwich, New York, p. 93.

[4] Collins, R.W. et al. 2006, "The ultimate in real-time ellipsometry: Multichannel Mueller matrix spectroscopy", *Appl. Surf. Sci.*, Vol. 253, p. 38.

[5] Woollam, J.A. et al. 1999, "Overview of variable angle spectroscopic ellipsometry (VASE), Part I: Basic theory and typical applications", *SPIE Proc.*, Vol. CR-72, pp. 3–28.

[6] Johs, B. et al. 1999, "Overview of variable angle spectroscopic ellipsometry (VASE), Part II: Advanced applications", *SPIE Proc.*, Vol. CR-72, p. 29–58.

[7] Johs, B. et al. 2001, "Recent developments in spectroscopic ellipsometry for in situ applications", *SPIE Proc.*, Vol. 4449, pp. 41–57.

[8] Jellison, Jr., G.E. 2005, "Data analysis for spectroscopic ellipsometry", in Tompkins, H.G. & Irene, E.A. (eds.), *Handbook of Ellipsometry*, William Andrew, Norwich, New York, p. 237.

[9] Dahal, L.R. et al. 2010, "Application of real time spectroscopic ellipsometry for analysis of roll-to-roll fabrication of Si:H solar cells on polymer substrates", *Proc. 35th IEEE PVSC*, Honolulu, Hawaii, USA, p. 631.

[10] Huang, Z. et al. 2010, "Optical mapping of large area thin film solar cells", *Proc. 35th IEEE PVSC*, Honolulu, Hawaii, USA, p. 1679.

[11] Fried, M. et al. 2011, "Application of a dual-spectral-range, expanded-

beam spectroscopic ellipsometer for mapping large-area, laterally-inhomogeneous, photovoltaic multilayers", *Proc. Mater. Res. Soc. Symp.*, Vol. 1323, p. C3.12.
[12] Azzam, R.M.A. & Bashara, N.M. 1977, *Ellipsometry and Polarized Light*, North-Holland, Amsterdam.
[13] Fujiwara, H. et al. 2000, "Assessment of effective-medium theories in the analysis of nucleation and microscopic surface roughness evolution for semiconductor thin films", *Phys. Rev. B*, Vol. 61, p. 10832.
[14] Beckmann, P. & Spizzichino, A. 1963, *The Scattering of Electromagnetic Waves*, Pergamon, Oxford.
[15] Koval, R.J. et al. 2002, "Maximization of the open circuit voltage for hydrogenated amorphous silicon *n-i-p* solar cells by incorporation of protocrystalline silicon *p*-type layers", *Appl. Phys. Lett.*, Vol. 81, p. 1258.
[16] Koh, J. et al. 1995, "A real time spectroellipsometry study of hydrogenated amorphous silicon *p-i-n* solar cells: Characterization of microstructural evolution and optical gaps", *Appl. Phys. Lett.*, Vol. 67, p. 2669.
[17] Stoke, J.A. et al. 2008, "Optimization of Si:H multijunction *n-i-p* solar cells through the development of deposition phase diagrams", *Proc. 33rd IEEE PVSC*, San Diego, California, USA, pp. 413: 1–6.
[18] Li, J. et al. 2009, "Spectroscopic ellipsometry studies of thin film CdTe and CdS: From dielectric functions to solar cell structures", *Proc. 34th IEEE PVSC*, Philadelphia, Pennsylvania, USA, pp. 1783–1788.
[19] Aspnes, D.E., Studna, A.A. & Kinsbron, E. 1984, "Dielectric properties of heavily doped crystalline and amorphous silicon from 1.5 to 6.0 eV", *Phys. Rev. B*, Vol. 29, p. 768.
[20] Stjerna, B., Olsson, E. & Granqvist, C.G. 1994, "Optical and electrical properties of radio frequency sputtered tin oxide films doped with oxygen vacancies, F, Sb, or Mo", *J. Appl. Phys.*, Vol. 76, p. 3797.
[21] Chen, J. et al. 2009, "Through-the-glass spectroscopic ellipsometry of CdTe solar cells", *Proc. 34th IEEE PVSC*, Philadelphia, Pennsylvania, USA, p. 1748.
[22] Chegal, W. et al. 2004, "A new spectral imaging ellipsometer for measuring the thickness of patterned thin films", Jpn. *J. Appl. Phys.*, Vol. 43, p. 6475.
[23] Major, C. et al. 2008, "Wide angle beam ellipsometry for extremely large samples", *Phys. Stat. Sol.* (c), Vol. 5, p. 1077.
[24] Fried, M. et al. 2011, "Expanded beam (macro-imaging) ellipsometry", *Thin Solid Films*, Vol. 519, p. 2730.
[25] An, I. et al. 2004, "Calibration and data reduction for a uv-extended rotating-compensator multichannel ellipsometer", *Thin Solid Films*, Vols. 455–456, p. 132.

Acknowledgements

The authors would like to acknowledge the contributions of Chi Chen, Jie Chen, Andre Ferlauto, Zhiquan Huang, Christoph Ross, Carl Salupo and Christopher Wronski to this research and development. Support of this work was provided by the U.S. Department of Energy, Solar Energy Technologies Program, University Processes and Products Development Support Projects (Grant Nos. DE-FG36-08GO18073 and FG36-08GO18067), and by the State of Ohio Department of Development under the Wright Centers of Innovation Program.

About the Authors

Robert W. Collins is a distinguished university professor and NEG endowed chair in the Department of Physics and Astronomy at the University of Toledo, Ohio, USA. He co-directs the Center for Photovoltaics Innovation and Commercialization and has been involved in research and development of thin-film photovoltaics since 1976.

Lila Raj Dahal is a senior graduate student in the Department of Physics and Astronomy at the University of Toledo, Ohio, USA. He has been involved in research and development of thin-film Si:H photovoltaics since 2007. Lila has presented papers at several conferences in materials research and photovoltaics and authored a number of articles in conference proceedings.

Kenneth R. Kormanyos is the president and a senior research fellow of Calyxo USA. He is a co-inventor of the atmospheric pressure thin-film deposition technology employed by Calyxo GmbH for its manufacturing of CdTe photovoltaic modules. He has been involved with CdTe photovoltaics since 1998. Kenneth has nineteen US patents and six publications in the technical areas of PV manufacturing, tempering of low-ε glasses, natural gas-fired forced convection glass tempering systems, and compact systems for vitrification of hazardous or radioactive wastes.

Nikolas Podraza is an assistant professor in the Department of Physics and Astronomy at the University of Toledo, Ohio, USA. His research interests include optical characterization of materials, correlations between electrical and optical properties, and thin-film devices. Nikolas has authored more than 50 papers in peer-reviewed journals and conference proceedings.

Sylvain Marsillac is an associate professor in the Department of Electrical and Computer Engineering at Old Dominion University, Virginia, USA. He specializes in the science and engineering of the fabrication and characterization of solar cells. Sylvain has authored more than 100 papers in peer-reviewed journals and conference proceedings.

Enquiries

Center for Photovoltaics Innovation & Commercialization and Department of Physics & Astronomy
University of Toledo
Toledo, OH 43606
USA
Tel: +1 419 530 3843
Email: robert.collins@utoledo.edu

Calyxo USA
12900 Eckel Junction Road
Perrysburg, OH 43551
USA

Department of Electrical & Computer Engineering
Old Dominion University
Norfolk, VA 23529
USA

Fab & Facilities

Materials

Cell Processing

Thin Film

PV Modules

Power Generation

Market Watch

Industry–academia partnership helps drive commercialization of new thin-film silicon technology

Subhendu Guha, United Solar Ovonic, Auburn Hills, Michigan; **David Cohen**, University of Oregon, Eugene, Oregon; **Eric Schiff**, Syracuse University, Syracuse, New York; **Paul Stradins**, National Renewable Energy Laboratory (NREL), Golden, Colorado; **P. Craig Taylor**, Colorado School of Mines, Golden, Colorado, & **Jeffrey Yang**, United Solar Ovonic, Auburn Hills, Michigan, USA

ABSTRACT

The low material cost and proven manufacturability of thin-film silicon has made this material very attractive for low-cost photovoltaics (PV). It is widely recognized that increasing the light-to-electricity conversion efficiency will play a critical role in expanding the acceptance of these products. The first commercial thin-film silicon solar cell consisted of a single-junction structure using amorphous silicon; multijunction cells incorporating amorphous silicon and silicon germanium were later used to further improve efficiency. An even later development was the incorporation of nanocrystalline silicon as an active layer. This very interesting material, which consists of nanocrystallites embedded in an amorphous tissue, has already given rise to a significant increase in the performance of these multijunction cells. Most recently, some very innovative light-trapping concepts have been suggested that can improve the efficiency further. Both these topics, however, have required expertise not readily available within one organization. A thin-film silicon team has been established under a US Department of Energy's Solar America Initiative programme to address the material, device and manufacturability issues for this technology. United Solar Ovonic is the team leader, with Colorado School of Mines, University of Oregon, Syracuse University and the National Renewable Energy Laboratory (NREL) as members. The collaborative effort has resulted in a new understanding of the material and devices; innovative light-trapping ideas were developed, and world-record initial efficiencies of 16.3% for small-area cells and 12% for large-area encapsulated cells were reached. Of equal importance is United Solar's decision to introduce this technology into production. This paper presents the important technical results obtained under this programme and will discuss future directions.

Introduction

Hydrogenated amorphous silicon alloys (a-Si:H) have received a great deal of attention as a material for the low-cost manufacture of solar cells and panels. Silicon is non-toxic and abundant in nature. The lack of long-range order in the material allows absorption of sunlight in a very thin film, thereby reducing material costs. a-Si:H alloy is also being extensively used for large-area flat panel displays, proving that the deposition of solar cell material over a large area should not be a limiting issue. Cells can also be deposited on flexible substrates, allowing laminates to be incorporated in building-integrated photovoltaic structures (Fig. 1). The production of solar panels using thin-film silicon technology has grown steadily over the years. It has been reported that production of solar panels using this technology increased from 198MW in 2007 to 1.3GW in 2010 [1].

The challenge, however, is to increase the light-to-electricity conversion efficiency. The material a-Si:H is very intriguing: the absence of long-range order facilitates efficient photon absorption and also causes tailing of the conduction and the valence band edges. The material also contains defects such as dangling, strained and weak bonds that act as recombination centres for the electrons and the holes. The efficient operation of a solar cell depends on a two-step process: 1) photon absorption for the generation of the carriers and 2) subsequent carrier transport and collection. Even though the photon absorption is efficient, the presence of the recombination centres arising from the defects and the band tails impedes the transport of carriers and lowers the efficiency. The other challenge is the phenomenon of light-induced degradation [2]. Exposure to light increases the defect density in the material, and the cell efficiency decreases. While there has been tremendous progress in the understanding of the problem, it still persists. The degradation, of course, is lower when the cell thickness is small, since the photogenerated carriers do not have to travel a large distance. But that results in less absorption.

Figure 1. World's largest rooftop system (11.8MW) in Zaragoza, Spain. The system uses flexible thin-film silicon PV laminates.

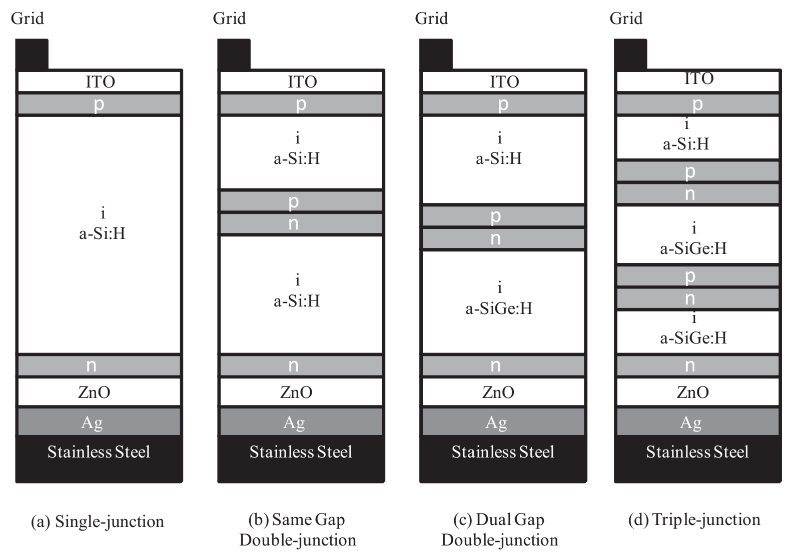

Figure 2. Schematic of different cell structures.

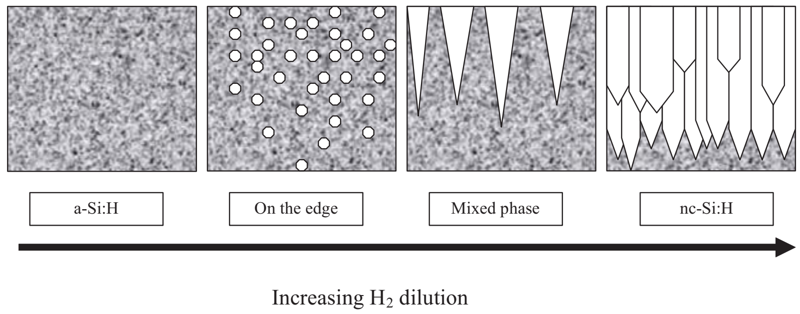

Figure 3. A schematic drawing of material structure changes with increasing hydrogen dilution.

In the early days, single-junction cells were used to make solar panels; Fig. 2a shows a schematic of a cell on a metal substrate, although many researchers and manufacturers use glass substrates. As the limitation of the single-junction cells became apparent, double- or tandem-junction cells with or without different bandgap materials (Figs. 2b and 2c) and triple-junction cells with multiple bandgap alloys (Fig. 2d) were developed. These cell structures allowed a wider spectrum of light to be absorbed in the cell and also reduced light-induced degradation, since the individual component cells were thinner. Until very recently, the highest cell efficiency was achieved with a triple-junction structure, in which the top cell employed a-Si:H of about 1.8eV bandgap to capture the blue photons, the middle cell employed an amorphous silicon-germanium alloy (a-SiGe:H) of about 1.6eV bandgap to capture the green photons, and the bottom cell employed a-SiGe:H of about 1.5eV bandgap to capture the red photons. Any light that has not been absorbed bounces back from the back reflector (BR) to enhance absorption. During the last several decades, many innovations have been made to improve the quality of a-Si:H and a-SiGe:H alloys. Hydrogen dilution of the active gas during deposition was found to improve the quality of the intrinsic layers; bandgap profiling of a-SiGe:H improved the built-in field, thus facilitating superior carrier collection. Another area of development was the use of BR for light trapping. Use of textured BR and incorporation of the improved alloys resulted in world-record initial cell efficiency of 14.6% using a triple-junction structure [3]. The technology is also used for large-volume manufacture of solar panels [4].

> "The efficient operation of a solar cell depends on a two-step process: 1) photon absorption for the generation of the carriers and 2) subsequent carrier transport and collection."

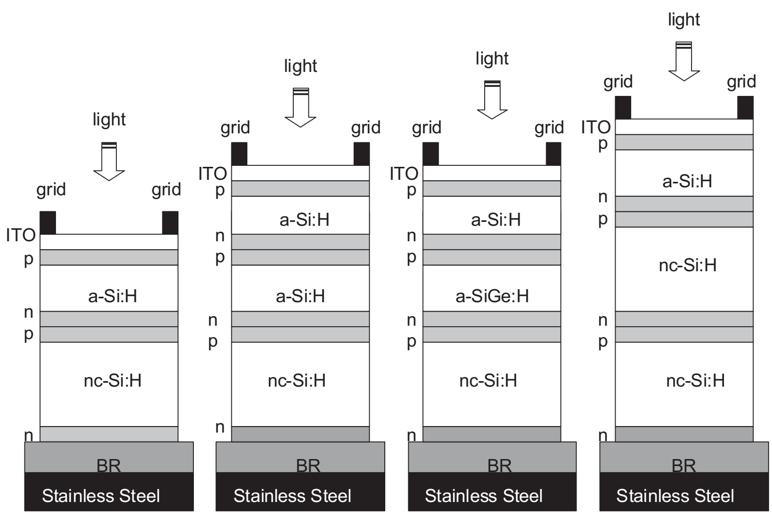

Figure 4. Different cell structures incorporating nanocrystalline silicon.

While the use of a-SiGe:H led to significant increases in performance, incorporation of Ge in a-SiGe:H generally reduces the quality of the material; therefore, a new class of materials named nanocrystalline silicon (nc-Si:H) or microcrystalline silicon alloys emerged [5] to replace a-SiGe:H in the bottom cells of a multijunction structure. The best quality a-Si:H uses hydrogen dilution of the active gas (silane) during plasma deposition, which improves the order in the film. As the hydrogen dilution increases, the transition to the nanocrystalline phase takes place. The material is characterized by formation of nanocrystallites embedded in an amorphous matrix; the volume fraction and the size of the nanocrystallites grow with increasing hydrogen dilution. Fig. 3 shows a schematic of nanostructure evolution as hydrogen dilution increases.

The tiny crystallites grow with increasing hydrogen dilution, forming cone-shaped structures as the hydrogen dilution further increases. For a very dilute mixture, columnar growth starts taking place and cracks develop in the film with adverse effects on material quality. The best material is thus grown just above the edge of hydrogen dilution for the amorphous to nanocrystalline transition.

The alloy nc-Si:H has been found to have superior long-wavelength absorption, which, coupled with the fact that it does not show degradation under long-wavelength light, makes this alloy an attractive candidate to be used in the bottom cells of a multijunction structure, with the promise of increasing the efficiency of multijunction cells further. Different cell structures have been investigated (Fig. 4) to determine the highest efficiency.

Research challenges

It was apparent that, in order to improve small-area cell efficiency beyond 14.6%, a clearer understanding of nc-Si:H was needed. A BR that can result in better light trapping than obtained with the conventional random texture also needs to be developed. The complexity and breadth of the issues demand that a multidisciplinary approach be used. The programme needs expertise in materials research, optics and device physics. Under the DOE's Solar America Initiative programme, United Solar formed a team drawn from industry, a national lab (NREL) and academia (Colorado School of Mines, Syracuse University and University of Oregon) to address the complex issues that will result in further increase in cell efficiency. Some highlights of the collaborative work are given below.

Back reflector for light trapping

One approach to increasing the effective harvesting of long-wavelength photons, thus enhancing current generated in thin-film silicon solar cells, is to use textured and highly reflective substrates or BRs. The conventional light-trapping method uses a randomized texture in which maximum light trapping has been shown to be limited by $4n^2$, where n is the refractive index of the absorber material. Commonly used BRs are Ag/ZnO-coated stainless steel (SS) substrates [6]. The desired texture of the Ag and ZnO layers can be obtained by optimizing deposition conditions. The texture has a wide distribution of features of different sizes.

Using near-infrared quantum efficiency spectra, a collaboration with Syracuse University was undertaken to calculate the enhancement factors for the cells. It was found that the very best enhancement factors are ~25 [7]. This is much less than the classical limit of ~50, and as seen in Fig. 5, one can have an additional gain of ~3mA/cm^2 when the classical limit is reached.

To further increase the efficiency, advanced light trapping with a gain in photocurrent exceeding the classical $4n^2$ is needed. In recent years, several advanced light-trapping approaches have been investigated, including BRs with periodic gratings, photonic structures, and plasmonic scattering by metal nanoparticles [8]. A theoretical analysis showed that, by using metal nanoparticles embedded in the BRs, the gain from plasmonic light trapping could exceed the classical limit of $4n^2$. Schiff has recently derived a non-resonant limit of light-trapping enhancement (E) with plasmonic scattering for weakly absorbed light in a solar cell of thickness d [9]:

$$E = 4n^2 + \frac{n\lambda}{d} \tag{1}$$

where λ is the wavelength of the light. For a 1μm-thick solar cell at the long-wavelength region of 1000nm, the additional gain from the surface plasma polaritons is n, and the increase in short-circuit current density, J_{sc}, is predicted to be about 0.6mA/cm^2. It is clear from Equation 1 shown above that the additional gain is more pronounced in thinner cells. For a 0.25μm-thick cell, the additional gain is $4n$, which is equal to about 16 for Si. In principle, even larger gains are possible using resonant enhancement, for which the surface plasmon resonance is matched to the semiconductor bandgap.

With an increase in J_{sc} in the bottom cell as a result of superior light trapping, one has to worry about increasing the current density in the other cells to obtain proper current matching. The cell thicknesses cannot be increased, since that will result in higher light-induced degradation. Reflection from intermediate layers between the cells has been suggested using different materials. A dual-function nc-SiO_x:H layer made with proper hydrogen dilution and doping with P has been shown to be effective in increasing the top cell and middle cell currents in a-Si:H/nc-Si:H double-junction and a-Si:H/a-SiGe:H/nc-Si:H triple-junction solar cells [10].

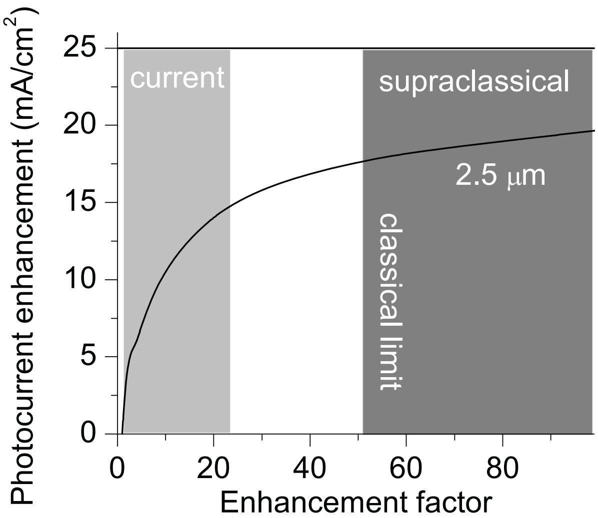

Figure 5. Enhancement in photocurrent with multiple reflections.

Materials research

Structure

The nc-Si:H films show a profound inhomogeneity in the growth direction, as can be seen by transmission electron microscopy (TEM) and atomic force microscopy (AFM) micrographs. We start with an amorphous zone, followed by a layer consisting of a mixture of amorphous and nanocrystalline silicon. Our collaboration with NREL showed that cone-shaped structures containing large numbers of nanometre-sized grains appear as the growth continues [11]. These composite cones result from the nanocrystalline phase growing faster than the amorphous phase, as shown by the 'cone kinetics model' developed at NREL [12].

> "By optimizing the profiling parameters, such as the amount of hydrogen and the rate of change in hydrogen dilution ratio, the nc-Si:H solar cell performance was significantly improved."

To overcome the negative effect of the nanocrystalline evolution on solar cell performance, a hydrogen dilution profiling technique was designed to control the growth of the nanocrystalline phase [13,14]. A very high hydrogen dilution was used to deposit a seed layer to reduce the thickness

Thin Film

of the incubation layer, and then a hydrogen dilution profiling was used, with decreasing hydrogen dilution ratio over time to keep the material close to the transition from the nanocrystalline phase to the amorphous phase. By optimizing the profiling parameters, such as the amount of hydrogen and the rate of change in hydrogen dilution ratio, the nc-Si:H solar cell performance was significantly improved.

In order to understand the nature of hydrogen bonding, hydrogen-effusion mass-spectroscopy measurements on a series of nc-Si:H cells with different degrees of crystallinity and hydrogen content were carried out in collaboration with NREL[15]. Fig. 6 shows corresponding hydrogen-effusion time profiles taken at a fixed temperature–time ramping rate, with the area under the curves representing hydrogen content. Samples A and C were grown under conditions in which the crystalline volume fraction of the nc-Si:H cell absorber layer was only about 30%, while B and D were highly crystalline at about 75%. The latter films have lower overall hydrogen content, since most of the hydrogen resides in the amorphous phase. Importantly, however, low-crystallinity cells show strong low-temperature hydrogen-effusion peaks at 400°C, signifying that the nc-Si grain boundaries are well passivated by hydrogen. Indeed, these cells A and C show significantly better performance: an increase of 80mV in open-circuit voltages, and efficiencies higher by 2.5% absolute. Thus, the low-temperature hydrogen-effusion peak serves as a good metric for cell absorber optimization.

Several techniques were used, in collaboration with the Colorado School of Mines, to probe the nanostructure of nc-Si:H thin films [16]. The x-ray diffraction data (XRD) reveal crystallites of approximately 11 to 24nm in length with a preferred <220> orientation in the film growth direction. Small-angle x-ray scattering (SAXS) experiments show crystallite sizes four times smaller than those revealed by XRD, demonstrating that crystallites are elongated along the growth direction (Fig. 7). Based on 10 to 14% atomic hydrogen measured in the a-Si:H phase, the SAXS and nuclear magnetic resonance results indicate that the crystallite interfaces are up to 35% hydrogenated.

Defect density

In collaboration with the University of Oregon, detailed measurements have been carried out to examine the defect density of nc-Si:H with varying crystalline volume fraction, using drive-level capacitance profiling (DLCP) as well as transient photocapacitance and transient photocurrent spectroscopy techniques [17,18]. In general, defect density is lower than in a-Si:H; moreover, deep defects lying about 0.4eV below the conduction band

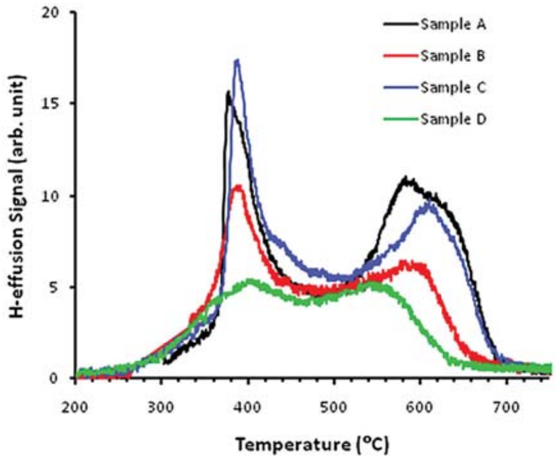

Figure 6. Hydrogen-effusion time profiles for four different nc-Si:H solar cells. Samples A and C have low crystalline volume fraction, while B and D are highly crystalline.

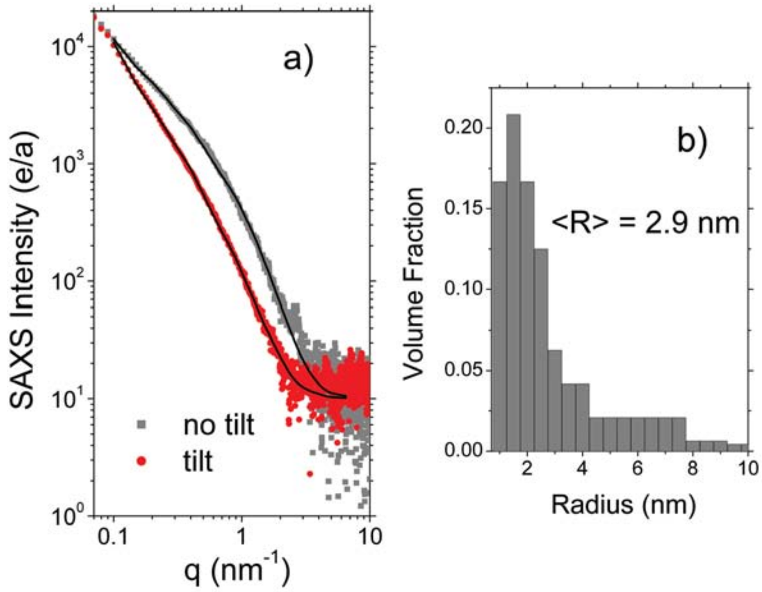

Figure 7. SAXS measurement on nc-Si:H films showing elongated crystallites.

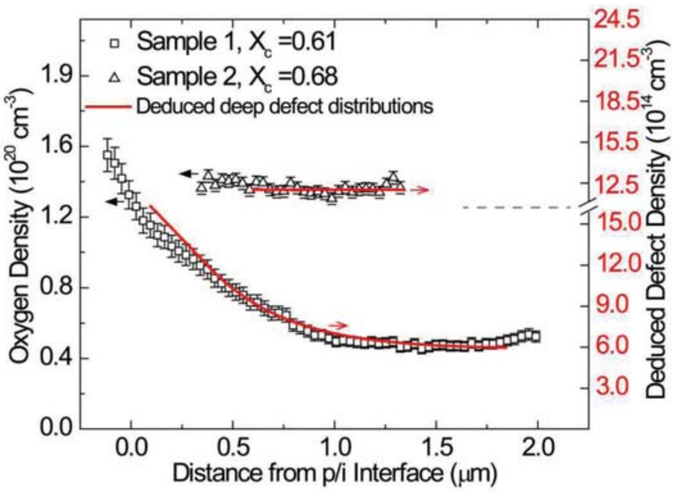

Figure 8. Correlation between oxygen content and deep defect density for two samples with different volume crystalline fraction X_c.

edge (E_c) were correlated with the presence of Si crystallites. The work was later extended to examine the effects of oxygen impurities on the electronic properties [19]. Because the DLCP measurements allow spatial distributions of defects to be mapped, these could be compared with secondary ion mass spectrometry (SIMS) concentration profiles of impurity species within the film. In this manner, a clear correlation was established between the oxygen content and a prominent deep defect band located about 0.7eV from E_c (Fig. 8). These findings are corroborated by photoluminescence measurements performed in collaboration with the Colorado School of Mines.

Device performance

Based on the understanding gathered from the research work as outlined above, United Solar has been steadily increasing the cell efficiency over the past few years [20]. Improvements have been made in hydrogen dilution profiling, design of seed and buffer layers, optimization of pressure and cathode-to-substrate distance, cathode design and gas flow dynamics, random BR, and interlayer. Two world-record efficiencies have been reported: a small-area ($0.25cm^2$) initial cell efficiency of 16.3% (Fig. 9) and a large-area ($400cm^2$) encapsulated initial cell efficiency of 12% (Fig. 10). The large-area efficiency has already been confirmed by NREL, and the small-area cell is being sent to NREL for efficiency confirmation.

Future directions

Significant improvements in the efficiency of multijunction cells have been made in recent years by incorporating nc-Si:H in the cell structure. United Solar has already initiated a programme to modify one of its existing deposition machines to incorporate the new structure into production. Our understanding of nc-Si:H is in its infancy. Further improvements in efficiency can be made; Table 1 shows the highest efficiencies that can be reached using different structures [21], with calculations being based on realistic cell parameters of the component cells. Module efficiencies approaching 20% using low-cost thin-film silicon technology will have a big impact on module and system cost. Innovation has to continue and

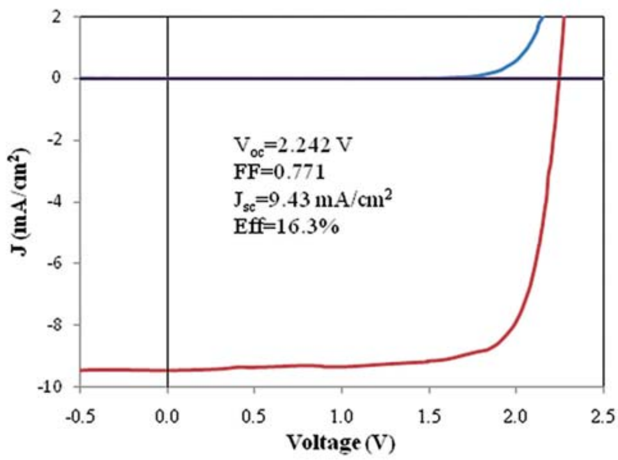

Figure 9. Initial small-area cell efficiency using a triple-junction structure incorporating nc-Si:H.

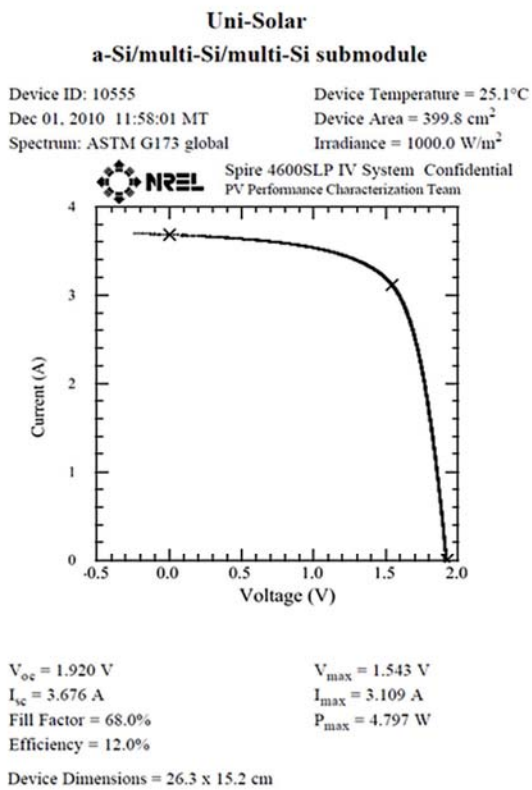

Figure 10. Initial large-area encapsulated cell efficiency using a triple-junction structure incorporating nc-Si:H, as measured by NREL.

Cell structure	Current status a-Si/a-SiGe/nc-Si	Option 1 a-Si/a-Si/nc-Si	Option 2 a-Si/a-SiGe/nc-Si	Option 3 a-Si/nc-Si/nc-Si
V_{oc} (V)	2.24	2.50	2.30	2.15
J_{sc} (mA/cm^2)	9.13	11.8	12.3	12.6
FF	0.75	0.85	0.85	0.85
Efficiency (%)	15.4	25.1	24.0	23.0

Table 1. Highest cell efficiencies obtainable with different structures [21]. Note that since the publication of [21] in 2010, a 16.3% efficiency has now been achieved.

sustained collaboration between industries and academia will facilitate the progress.

Acknowledgements

We would like to thank the many colleagues in our organizations who collaborated with us in this research to advance the technology. This work was supported by the US Department of Energy under the Solar America Initiative Program Contract No. DE-FC36-07 GO 17053.

References

[1] Mehta, S. 2011, "27th annual data collection results", *PV News*, Vol. 30, No. 5, p. 3.

[2] Fritzsche, H. 2001, "Development in understanding and controlling the Staebler-Wronski effect in a-Si:H", *Annu. Rev. Mater. Res.*, Vol. 31, p. 47.

[3] Yang, J., Banerjee, A. & Guha, S. 1997, "Triple-junction amorphous silicon alloy solar cell with 14.6% initial and 13.0% stable conversion efficiencies", *Appl. Phys. Lett.*, Vol. 22, p. 2975.

[4] Yang, J., Banerjee, A. & Guha, S. 2003, "Amorphous silicon based photovoltaics – from earth to the 'final frontier'", *Solar Energy Mat. & Solar Cells*, Vol. 78, p. 597.

[5] Shah, A. (ed.) 2011, *Thin Film Silicon Solar Cells*, EPFL Press, Switzerland.

[6] Yue, G. et al. 2009, "Optimization of back reflector for high efficiency hydrogenated nanocrystalline silicon solar cells", *Appl. Phys. Lett.*, Vol. 95, p. 263501.

[7] Zhao, H. et al. 2011, "Classical and supraclassical light trapping in thin film solar cells", Solar Am. Initiative Rev. Meet., April [unpublished].

[8] Zeman, M. et al. 2010, "Advanced light trapping in thin-film silicon solar cells", *Mat. Res. Soc. Symp. Proc.*, Vol. 1245, p. 65.

[9] Schiff, E.A. [unpublished].

[10] Yan, B. et al. 2011, "Effect of dual-function nano-structured silicon oxide thin film on multi-junction solar cells", *Proc. 37th IEEE PVSC*, Seattle, Washington, USA.

[11] Jiang, C.-S. et al. 2008, "P-induced nanocrystallite dispersion in amorphous-nanocrystalline mixed-phase Si:H thin films", *J. Appl. Phys.*, Vol. 103, p. 063515.

[12] Stradins, P., Teplin, C.W. & Branz, H.M. 2009, "Phase evolution in nanocrystalline silicon films: Hydrogen dilution and the cone kinetics model", *Phil. Magazine*, Vol. 89, pp. 2461–2468.

[13] Yan, B. et al. 2004, "Hydrogen dilution profiling for hydrogenated microcrystalline silicon solar cells", *Appl. Phys. Lett.*, Vol. 85, p. 1925.

[14] Guha, S., Yang, C.C. & Yan, B. 2011, "Method for depositing high-quality microcrystalline semiconductor materials", US Patent 7902049 B2.

[15] Su, T. et al. 2010, "Effects of grain boundaries on performance of hydrogenated nanocrystalline silicon solar cells", *Mat. Res. Soc. Symp. Proc.*, Vol. 1245, p. 113.

[16] Kiriluk, K.G. et al. 2010, "A SAXS study of hydrogenated nanocrystalline silicon thin film", *Mat. Res. Soc. Symp. Proc.*, Vol. 1245, p. 271.

[17] Hugger, P.G. et al. 2008, "Properties of light-induced degradation and the electronic properties of nanocrystalline silicon solar cells grown under functionally graded hydrogen dilutions", *J. Non-Cryst. Sol.*, Vol. 354, p. 2460.

[18] Hugger, P.G. et al. 2009, "Insights and challenges toward understanding the electronic properties of hydrogenated nanocrystalline silicon", *Phil. Magazine*, Vol. 69, p. 2541.

[19] Hugger, P.G. et al. 2010, "Relationship of deep defects to oxygen and hydrogen content in nanocrystalline silicon photovoltaic materials", *Appl. Phys. Lett.*, Vol. 97, p. 252103.

[20] Guha, S., Yang, J. & Yan, B. 2011, "Amorphous and nanocrystalline silicon solar cells and modules", in Bhattacharya, P., Fornari, R. & Kamimura, H. (eds), *Comprehensive Semiconductor Science and Technology*, Vol. 6, Amsterdam, Elsevier, pp. 308–352.

[21] Guha, S. & Yang, J. 2010, "Thin film silicon photovoltaic technology – from innovation to commercialization", *Mat. Res. Soc. Symp. Proc.*, Vol. 1245, p. 3.

About the Authors

Subhendu Guha is chairman emeritus of United Solar Ovonic, the world's largest manufacturer of flexible solar laminates. An international authority in the science and technology of thin-film silicon-alloy solar cells, Dr. Guha has received much recognition for his work, including the World Technology Award in the Energy category in 2005 and the PVSEC Award in 2009 for outstanding contribution to the science and technology of photovoltaics.

David Cohen is a professor at the University of Oregon. He received his Ph.D. degree from Princeton in 1976, and his interest in disordered semiconductors relevant to photovoltaic technology began 32 years ago while at Bell Labs. Professor Cohen joined the University of Oregon in 1981, where he has been pioneering new experimental methods for characterizing the defect physics of amorphous semiconductors.

Eric A. Schiff is a professor at Syracuse University and has been researching solar cells and thin-film semiconductors for 25 years. He has published more than 100 papers and has been granted several patents. Professor Schiff has a Ph.D. in semiconductor physics from Cornell University.

Paul Stradins is a scientist at the NREL. He has made key contributions in understanding light-induced defect creation and electronic transport in a-Si:H, in particular the Staebler-Wronski effect (SWE) at liquid helium temperatures, as well as the cone kinetics growth model and suppression of SWE in mixed-phase a-Si:H/nc-Si:H.

P. Craig Taylor is a Professor at the Colorado School of Mines and Director of Renewable Energy Materials Research Science and Engineering Center. He received the Ph.D. degree from Brown University in 1969, and was employed at the Naval Research laboratory from 1969 to 1982, after which he joined the Physics Department at the University of Utah. Professor Taylor is a Fellow of the American Physical Society.

Jeffrey Yang is the Senior VP of Technology at United Solar Ovonic. He has worked in the thin-film silicon photovoltaics field for more than 30 years, and published more than 250 papers. Dr. Yang has co-organized IEEE Photovoltaic Specialist Conferences and Materials Research Society symposia and workshops.

Enquiries

Subhendu Guha
United Solar Ovonic LLC
3800 Lapeer Road
Auburn Hills
Michigan 48326
USA
Email: sguha@uni-solar.com
Website: http://www.uni-solar.com

PV Modules

Q-Cells launches independent production of its Q.Peak module on its new 130MW production line

Ten years to the day that Q-Cells manufactured its first solar cell, the company revealed that it is independently launching production of its Q.Peak high-performance module at its Solar Valley Thalheim headquarters. The new production line was commissioned on July 25, 2011 holding a 130MWp production capacity and will produce the Q.Peak modules from monocrystalline solar cells made in Germany.

At its full capacity, the production line will produce 1,400 solar modules per day and 511,000 modules a year. The monocrystalline Q.Peak modules will be available with an output rating from 245Wp to 260Wp.


Source: -Cells SE

Q-Cells' Q-Peak modules will be available with an output rating from 245Wp to 260Wp.

Business News Focus

Seraphim modules bankable with Unicredit Leasing

Seraphim Solar System's PV modules are now bankable with one of Europe's largest solar project financiers, Unicredit Leasing Group. The agreement with the Italian banking organization will improve customer confidence in Seraphim's products and in turn boost European sales.

Before signing off on the agreement, Unicredit Leasing sent a team to Seraphim's Changzhou site to carry out a thorough audit of the facility. Seraphim is also looking to establish similar agreements with other European banks.

Suntech offers two new technologies to US solar market

Suntech Power Holdings is targeting a greater share of the rapidly growing commercial and utility-scale PV markets in North America with the launch of two high-performance modules. Suntech introduced its 'HiPerforma' 245W module using its advanced 'Pluto' cell processing technology, and a module using its 'SuperPoly' multicrystalline wafers, also developed in-house using advanced silicon ingot casting techniques, dubbed the 290W Vd-Series.

Already released into the European market, the 'HiPerforma' modules are expected to generate 2%–5% more power per watt peak (kWh/kWp) over time, due to a superior spectral response and high shunt resistance.


Source: Suntech

Suntech's Pluto Technology modules.

Suntech offers a 25-year power output warranty, with 0/+5% positive power tolerance that is claimed to deliver 6.7% more power than the standard industry warranties. The product meets or exceeds UL1703, IEC 61215, and IEC 61730 standards.

Suntech's new 290W Vd-Series multicrystalline module utilizes a laboratory silicon casting technology that produces high-quality multicrystalline wafers using modified multicrystalline casting equipment. In addition to higher power output, the technology achieves lower oxygen content for multicrystalline wafers leading to strong resistance to light-induced degradation.

It comes as a 72-cell module with a 25-year power output warranty, with 0/+5% positive power tolerance, that warrants 6.7% more power than the standard industry warranty. The product meets or exceeds UL1703, IEC 61215, and IEC 61730 standards.

ReneSola ships 54.8MW of 'Virtus' wafers and 20MW of 'Virtus' modules in June

Having established pilot production of its new higher efficiency cells, dubbed 'Virtus,' earlier this year, ReneSola has said that it shipped 54.8MW of Virtus wafers and 20MW of Virtus modules in June, 2011. Shipments were made to European customers, according to the company. ReneSola expects to discontinue approximately 200MW of monocrystalline wafer production this year to focus on Virtus wafer production.

ReneSola noted that Virtus wafer production was operating at an annual capacity of 900MW with a target to reach 1.8GW by the end of 2011, which will be entirely dedicated to Virtus wafer production.

Management had said in March 2011 that ReneSola planned to spend US$350 million in 2011 to increase wafer capacity 1.9GW, up from 1.3GW in 2010. The company also said it was still at 100% utilization, despite a downward revision to shipping guidance for the second quarter.

ReneSola claims that the higher grade V-Grade Virtus wafer achieves cell conversion efficiency rates of 17.5%-18.2%.A lower-grade wafer, dubbed, M-Grade achieves cell conversion efficiency rates of 16.7%-17.0%. These high rates of efficiency are said to be established at the wafer level prior to the cell manufacturing.

ReneSola noted that 54.8MW of Virtus wafer shipments comprised approximately 22.7MW of V-Grade wafers and 32.1MW of M-Grade. In respect to module shipments in June, all of the 20MW of modules were using V-Grade Virtus wafers. ReneSola's Virtus modules were said to generate up to 250 watts of power. ReneSola is in the process of applying for 10 patents related to the Virtus wafer and module, and is also applying for trademark protection in several countries.

Westinghouse Solar sees module shipments rising

Westinghouse Solar reported revenue for the second quarter of 2011 up 38% quarter-on-quarter and expects revenue to accelerate further from the third quarter onwards as its new modules gain traction in the market.

The company reported revenue of US$2.8 million compared to US$2.2 million in the second quarter of 2010 and US$2.0 million in the first quarter of 2011. The company said the growth was due to the expansion of its distribution network and strategic partners, on the back of more competitive pricing.

The PV module manufacturer noted that two of its strategic partners were gaining momentum with projects. The company said that Lennar had standardized on its modules for their new homes in several Texas communities, while Lowe's Home Improvement has started to sell complete Westinghouse Solar systems through its website.

PV Modules Order Focus

REIL places order for Spire module manufacturing line

India's Rajasthan Electronics & Instruments (REIL) has placed an order for a 12MW semi-automated module manufacturing line with Spire. REIL will use the line to ramp up production at its Jaipur facility in an attempt to gain a larger share of the module market in India's rapidly-growing solar industry.

The news of REIL's decision to expand its manufacturing capacity came soon after reports surfaced that the Indian Government is preparing to increase the size and number of projects that can be awarded to developers during the next round of license bidding.

Canadian Solar reaches India in 33MW PV module supply deal for 2011

An India-based solar engineering, procurement and construction (EPC) company, Cirus Solar Systems has secured a 33MW PV module supply deal with Canadian Solar for several key projects, some of which have begun module shipments. The supply deal will last through the fourth quarter of 2011. Canadian Solar said that the PV modules would be used in projects undertaken by Cirus Solar Systems for 'two prominent Indian conglomerates,' without disclosing specific identities.

The deal marks Canadian Solar's move into the Indian market, which it expects to become one of the largest solar markets in the world, according to Dr. Shawn Qu, Canadian Solar's chairman and CEO.

LDK Solar signs module supply contract for 14.1MW project

LDK Solar has signed a contract to supply 58,803 modules for Advanced Solar Products' new 14.1MW project in East Windsor, New Jersey. When completed, the system, which is located on the McGraw-Hill Companies' campus, will be the largest privately-owned, net-metered PV project in the Western Hemisphere.

NJR Clean Energy Ventures (NJRCEV), a subsidiary of New Jersey Resources, is to invest US$60 million in developing and installing the system. Construction began on July 22 and the plant is expected to be fully operational by spring 2012.

LDK Solar signs module supply contracts with Chinese companies

LDK Solar has signed module supply contracts with two major electric power companies in China. The first contract is worth 30MW and was scheduled for shipment to an unnamed firm in the Qinghai province in August of 2011, while the second, totalling 5MW, will be delivered in the first half of 2012 to a company in the Jilin province.

Phono Solar extends module supply agreement with Sybac

Sybac Photovoltaics has placed an order with Phono Solar for 10MW of its mono- and polycrystalline silicon solar modules. The order, which will be delivered before the end of 2011, is the latest step in a strategic partnership between the two firms to install utility-scale projects throughout the US.

Aide Solar to supply Folium Energy with 150MW of PV modules for California PV projects

Folium Energy signed a deal with Aide Solar, a subsidiary of Panjit Group, to buy 150MW of its solar PV modules for use in 710 ground-mounted solar projects throughout California. The agreement was signed under California's PPA for small renewable generation feed-in tariffs program, which allows each solar site in the program to generate a minimum of 100kW, but not surpass 1.5MW of solar power.

Folium will install the 710 solar projects in locations located throughout 35 different counties in California. Work will begin in the fourth quarter of 2011, with the project expected to be complete in one year.

Gross profit for the second quarter of 2011 was reported to have reached US$194,000 or 7% of revenue, compared to US$342,000 or 15.4% of revenue for the second quarter of 2010, and US$278,000 or 13.9% of revenue for the first quarter of 2011.

SunPower to manufacture solar modules in Mexico for North American market

Citing the need to meet demand for the rapidly expanding North American solar market, SunPower said it will lease an existing building in Mexicali, Mexico to build its E18 series, E19 series and world-record-setting E20 series solar panels as well as its T5 solar roof tiles.

SunPower did not disclose any timelines for the new manufacturing facility nor the expected target capacity and production levels. Depending on the design and previous use of the building, it would typically take six to 10 months before tool installation and initial production ramp.

Various market research firms are forecasting the US PV market installations to more than double in 2011, from under 1GW installed in 2010 to over 2GW in 2011. Unlike key markets such as Germany, ground-mounted utility-scale PV power plants are a key part of the reason for the strong growth. SunPower has previously highlighted it has a significant project pipeline, specifically in the US.

Mage Solar signs sponsorship deal with German Bundesliga team SC Freiburg

Another PV company has jumped on the sports team sponsorship bandwagon, as Mage Solar has signed a long-term premium partnership deal with German Bundesliga side SC Freiburg. Mage Solar said the goal of the agreement is the sustainable continuing development and establishment of its photovoltaic brand in public.

Pilot Sport of Munich, a sports marketing firm, acted as facilitator and service provider for Mage and negotiated on the solar company's behalf with Infront Sports and Media, the marketing partner for the football club.

Other solar companies partnering with Bundesliga teams include Yingli Green with powerhouse Bayern Munich, Q-Cells with defending champions Borussia Dortmund, Jinko Solar with Bayer Leverkusen, and Suntech with 1899 Hoffenheim. The first sponsorship between a PV firm and a German side, SolarWorld with Cologne, kicked off in 2009.

Markus Feil, CEO of Mage Solar (left), and Fritz Keller, chairman of SC Freiburg (right), celebrate the signing of the sponsorship deal.

JinkoSolar signs sponsorship deal with Bayer Leverkusen football club

German football club Bayer 04 Leverkusen has signed a three-year sponsorship contract with solar giants

JinkoSolar. The deal not only provides Jinko with advertising space at the club's BayArena but also grants it exclusive rights to install solar panels on the stadium itself. Last season, Bayer finished as runners-up in the Bundesliga and consequently Jinko will not only gain exposure during domestic matches but also in the Uefa Champions League.

Jinko will not be the only solar company gaining exposure courtesy of the Bundesliga next season; Yingli Green and Q-Cells have signed sponsorship deals with Bayer's Bundesliga rivals Bayern Munich and Borussia Dortmund respectively.

Suntech unveils new module for Israeli solar market

Suntech Power has released a new PV module for the Israeli solar market. The 300W Vd series module is available immediately and is being targeted at the rapidly-maturing Middle Eastern rooftop solar industry.

Suntech developed the 72-cell modules using its hybrid wafer manufacturing process, which combines the high efficiency of a monocrystalline wafer with the cost-effectiveness and reliability of its polycrystalline equivalent; the final product boasts a cell efficiency of 15.5%, a figure considerably higher than the industry average of 13–14%.

Suntech has also released two modules for the US, Canadian and Latin American markets: the 245W HiPerforma multicrystalline module for residential, commercial and utility scale installations and the 290W Vd Series specifically for utility scale application.

Testing and Certification News Focus

Moser Baer Solar extends PV modules mechanical warranty to 10 years

Moser Baer Solar (MBSL) revealed that it has doubled its mechanical warranty for its MBVP Max Series, Model CAAP BB and higher PV modules to 10 years. The modules will continue to carry a 25-year performance warranty on top of the 10-year mechanical warranty.

The decision to extend its mechanical warranty came after in-house R&D activities over the past few years, which aimed to execute rigorous process control in the manufacturing process and end-of-life (EOL) testing, prompted MBSL to offer this new standard.

LDK Solar joins Intertek's 'Satellite' service to speed module certification

With lead times on module certification continuing to be an issue for PV module manufacturers, LDK Solar's Module Test Lab, based in Nanchang City, China, has become officially recognized by Intertek as a qualified and authorized 'Satellite' laboratory in an attempt to reduce certification times and costs.

Intertek's Satellite program enables module manufacturers to conduct required tests within their own labs; however, Intertek conducts compliance tests that can lead to certification such as ETL based on UL1703 standards.

Enfoton Solar fits production lines with MBJ Solutions' inspection system

Enfoton Solar has fitted its module production lines with MBJ Solutions' electroluminescence inspection equipment. The high-resolution inspection systems will provide rapid feedback on module output quality, thus enabling Enfoton to optimize its manufacturing performance.

Source: MBJ Solutions

MBJ Solutions' standalone high speed inspection system for electroluminescence imaging.

The system's automatic image processing software combines high image quality with easy operation, which in turn enables easier and more accurate module quality assessment. MBJ has expanded its product portfolio with the launch of its SolarModule EL-quickline LEL and the SolarModule EL-inline SEL systems.

Suntech doubles warranty period for solar panels

Suntech Power has extended the limited warranty for it solar panels from five to 10 years. The new warranty covers defects concerning materials and workmanship and is applicable for all standard panels shipped out after April 1.

In addition to the limited product warranty, all of Suntech's standard modules come with a 25-year power output warranty that guarantees 6.7% more power than the typical industry warranty. The panels also feature 0%/5% positive power tolerance, which means that they will meet or exceed their nameplate power capacity, compared to the industry standard of -3%/+3%.

Source: Dunmore

Fraunhofer CSE has joined Dunmore's FastCert project.

Fraunhofer joins Dunmore's 'FastCert' project to reduce backsheet R&D and module assembly costs

PV module backsheet material specialist Dunmore has recruited Fraunhofer USA's Center for Sustainable Energy Systems (CSE) to consult with its 'FastCert' customers on reducing the cost of producing solar modules by increasing performance and lowering material and manufacturing costs. By providing its backsheet material customers access to a network of research and development knowledge, Dunmore hopes that PV module manufacturers gain greater success in the certification processes.

Fraunhofer USA established a specific group within the CSE to focus on PV modules. The PV Module Group is said to work with materials suppliers, equipment vendors and module manufacturers to increase module efficiency, improve product lifetime and reliability, boost manufacturing output, and minimize installation barriers.

The FastCert program is designed to streamline product development management, certification and material supply management throughout all phases of the program.

CNPV details its linear power module warranty

Module manufacturer CNPV Solar Power has stated that its linear power warranty is guaranteeing 7% more power than a 'traditional power warranty,' that is normally a 'two-step' approach with trigger points at 10-12 years and 25 years.

The CNPV's linear power warranty assurance specifically creates a definitive linear continuous underwriting of the power curve with provision for the module output to change by no more than 0.67% per year, after the first year of installation. CNPV had previously offered a 'two-step' power warranty of 25 years.

The linear power warranty is expected to be made available on module deliveries from Q3'11. CNPV said that the new warranty terms are improvements on existing assurance, with no downgrading of fine detail to allow risk reduction.


A key test
of a PV module
is when the sun
isn't shining.
3M™ Scotchshield™ Film Backsheets
Real world performance against the elements.
Moisture can seriously degrade a photovoltaic module. Engineered with innovative fluoropolymer technology, 3M™ Scotchshield™ Film backsheets offer excellent moisture protection to weather the storm. Plus outstanding heat resistance and UV stability when the sun beats down. No other solar partner can match our more than 30 years of Renewable Energy solutions, powered by a century of 3M innovation.
Proven performance. Global reach.
Unbeatable value. The power of 3M.
www.3M.com/ScotchshieldFilm
3M and Scotchshield are trademarks of 3M.
© 2011, 3M. All Rights Reserved.
3M

Q-Cells first to produce multicrystalline modules with above 18% efficiencies

Verified by Fraunhofer ISE in Freiburg, Q-Cells has beaten its own record module efficiencies for multicrystalline-based wafers. The new world record efficiency rating is 18.1%, which beats its recently established record of 17.8%. Q-Cells claims to have the first multicrystalline-based modules that have efficiencies above 18%.

The Q.ANTUM cell technology used to achieve record module performance, is based on 180µm-thick multicrystalline wafers, which were metallized on the back side and passivated with functional nanolayers. Dielectric layers combined with local contacts are used to form a new type of structure for the back side that can accommodate a range of silicon qualities and thin wafers thicknesses. In April 2011, a cell produced on the basis of the Q.ANTUM technology marked a record efficiency of 19.5%.

Bosch Solar takes module warranty conditions to a new level

Bosch Solar Energy has removed clauses related to customer compensation for lost earnings in the event that a module's output is too low, resulting in lower customer costs and administration related to claims. Inline with some of its competitors, Bosch Solar has also doubled the product quality guarantee from five to 10 years and offers a 25-year performance warranty for modules that were delivered before July 2011. The new warranties apply from July 2011 onwards.

Bosch Solar said that for all future warranty claims, it would replace the module with a correctly working model of the same type or possibly eliminate the fault. Alternatively, lost earnings would be compensated, with Bosch providing an alternative in the event that the module type is no longer produced.

Other important changes introduced include dropping the need for the customer to obtain a measurement report by an accredited expert or an institution before a claim would processed. Furthermore, Bosch Solar has dropped the clause requiring the customer to bear the cost of transport and installation of a replacement module(s).

Bosch Solar said the changes are based on the view that customers have calculated the earnings to be expected from a PV system installation in advance of the purchase and expect a close correlation between correct calculations and actual earnings.

Source: Bosch

Bosch Solar has also improved the product quality guarantee from five to 10 years and offers a 25-year performance warranty for modules that were delivered before July 2011.

Product Reviews

IMA Automation

IMA Automation offers compact modustringer with adhesive dispensing option

Product Outline: IMA Automation Berlin has developed a significantly enhanced and upgraded model of its well-known modustringer series. The new modustringer has been reduced in length by one third and is offered at a lower price than the original system introduced two years ago. According to IMA Automation, the new system features a simplified process flow, increased service friendliness and delivers a single-track throughput of 1,200 cells per hour.

Problem: Key requirements for module assembly are productivity while ensuring careful handling of solar cells to minimize breakage rates.

Solution: The new, shorter modustringer system variant comes without an integrated electroluminescence inspection stage for incoming cells. This significantly reduces the complexity of its transport logistics yet keeps in place all subsequent basic process steps. Incoming cells continue to be checked in regard to outbreaks, fissures, etc. A key advancement to the system has been the functional decoupling of tasks within its incoming process stations. Due to its autonomy in cell feeding, the modustringer keeps running for one hour without operator intervention. Its new flux station with piezo-based valves allows jet fluxing with adjustable fluxing areas in the front and back of the cells for selective soldering. The in-line ribbon preparation is carried out in parallel, simplifying handling and enabling automatic adjustment to various busbar distances. The stretch forming of the ribbon material can be defined as a path or load-dependent option.

Applications: Silicon cell module stringing.

Platform: The modustringer allows for versatile modular configuration of many solutions due to the functional separation of ribbon and cell preparation.

Availability: Currently available.

MBJ Solutions

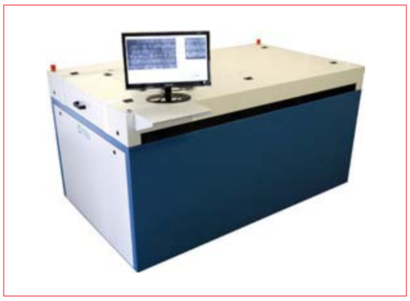

MBJ Solutions completes electroluminescence inspection product line-up

Product Outline: MBJ Solutions has expanded its product portfolio to complete its line-up of electroluminescence inspection systems. Two new products have been launched, which include the SolarModule EL-quickline LEL and the SolarModule EL-inline SEL. The high-performance product family SolarModule EL-inline and the mid-performance product family SolarModule EL-quickline are now both available for short-edge and long-edge leading production lines.

Problem: Hidden defects like micro-cracks are invisible to the human eye, which present a significant risk of decreasing the module's performance. Detection of micro-cracks is therefore required throughout the production process to ensure non-defective operation of modules in the field.

Solution: Electroluminescence imaging identifies hidden defects. Integrating EL inspection in the module production provides helpful information about the production process before lamination, after lamination and after flashing. Contacting for the 'testing before lamination' and 'testing after lamination' versions can be fully automated or performed manually.

Applications: Solar modules at different stages of the production process can be inspected by the system, e.g. panels before lamination, after lamination or framed modules. The system is designed for both mono- and multicrystalline silicon solar modules. Module sizes handled include minimum of 400 × 600mm and maximum of 1050 × 2000mm (W × H). Thin-film module applications are also available.

Platform: The system is available as short-edge leading and as long-edge leading configuration, so the SolarModule EL-inline can be integrated in both types of conveying systems.

Availability: Currently available.

Schmid and Lauffer

Schmid and Lauffer co-develop fast cycle-time laminator

Product Outline: A joint collaboration by Schmid Group and Maschinenfabrik Lauffer has led to the launch of a new fast cycle-time two-level stacking laminator. Employing membrane-free technology patented by Schmid, the laminator draws on the knowledge and experience in press and lamination technology by Lauffer.

Problem: Lengthy process cycle-times have often been seen as a longstanding issue for module lamination steps, while optimizing the process for consistently high-high yields to minimize defects that ultimately can impact the lifetime of the module in the field.

Solution: The multi-level design of these new laminators allows temperature to be steadily introduced to glass-glass and glass-film solar modules from both sides with a +/- 1°C temperature homogeneity. This significantly shortens the process times in comparison to standard membrane laminators; as a result, process times of less than 7.5 minutes have become the new standard in glass-film module production with immediate effect. The new lamination process also opens up further potential for the significant reduction of process times using suitable, innovative film types. Lauffer is the exclusive supplier of the custom-designed laminator systems. Membrane-less lamination of modules allows savings in operating and maintenance costs of several thousand euro per annum.

Applications: Module lamination of glass-glass and glass-film.

Platform: The new laminator adds to Schmid's module assembly equipment offerings and turnkey range of complete semi- and fully-automated lines. The first system available is a two-level laminator using membrane-free technology patented by Schmid.

Availability: Currently available.

Product Reviews

Solar Gard Photovoltaics

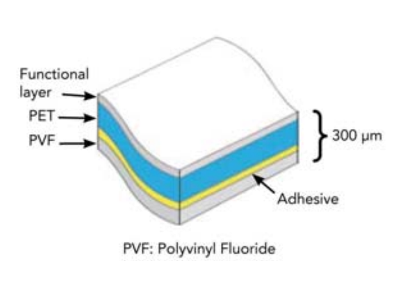

Solar Gard Photovoltaics' PV T10f backsheet claims superior performance

Product Outline: Solar Gard Photovoltaics, part of Bekaert Specialty Films, has introduced the PV T10f to its line of high-quality backsheets for photovoltaic modules. Solar Gard is a global leader in the development and manufacturing of flexible films and PV T10f leverages the Company's more than 30 years of expertise in coating and laminating to improve EVA adhesion and peel strength. Solar Gard PV T10f is UL recognized and performance tested at TÜV, and outperforms third-party testing criteria.

Problem: Backsheets can be extremely costly elements in the PV module manufacturing process. Products that display performance levels similar to those of TPT can provide significant cost savings.

Solution: The innovative Solar Gard PV T10f backsheet represents the new standard in PV backsheet technology. With a combination of a tried and tested Tedlar weather resistant outside layer, benchmark hydrolysis resistance and a proprietary functionalized surface that dramatically enhances adhesion to EVA, Solar Gard PV T10f claims to deliver excellent results. Solar Gard's proven film success and commitment to innovation has led to the development of new coating combinations to deliver a backsheet that is cost effective and meets high performance objectives.

Applications: PV module encapsulation.

Platform: Designed to meet a range of panel sizes and configurations, Solar Gard PV T10f is manufactured in ISO-certified facilities in the United States. Available worldwide, additional PV production capacity will be added in Qingdao, China in 2012.

Availability: Currently available.

Somont

Somont offers new tabletop cell soldering system that bridges lab to fab requirements

Product Outline: Somont, a company within the Meyer Burger Group, has developed a new soldering table for the semi-automatic connection of solar cells. The new tabletop system is claimed to allow module manufacturers to save valuable time and costs, enabling effective verification of solar cells, soldering strips, flux and pastes without having to interrupt production for evaluation and testing.

Problem: Development departments are often faced with the challenge of having to test the solderability of new solar cells for the market directly on the stringer in a company's production line. This results in the loss of valuable production time for testing purposes.

Solution: Somont's new soldering table allows fast and cost-effective verification of new developments and products without the need to interrupt production. The potential conflict of interest between development and production departments will be reduced and large amounts of material will be able to be tested without any time pressure. Another important advantage is a reduction in ramp-up time due to the availability of exact parameter measurements. Newly developed technologies and/or materials can be tested and subsequently verified quickly on the stringer.

Applications: Cell soldering for 5" and 6" cells as well as two and three busbars with fast changeover times; minimum cell thickness of 160µm.

Platform: Somont's new table is suitable for use in any laboratory or development unit and uses Somont's 'Soft Touch Soldering' technology that is claimed to provide excellent peeling forces and high-quality reproduction results. Soldering head temperature range: 300°C; heating plate: (no pre- and post heating) 200°C.

Availability: Currently available.

Yamaichi Electronics

Yamaichi Electronics' Eco-Si junction box uses hermetic sealed over-molding technology

Product Outline: Yamaichi Electronics has developed a new photovoltaic junction box for crystalline solar modules for the Y-Sol product family. The new Eco-Si junction box uses hermetic sealed over-molding technology to provide greater sealing and long life, even in extreme conditions.

Problem: Crystalline solar modules are becoming increasingly more cost-effective to manufacture, requiring lower-cost components to take advantage of module manufacturing price declines.

Solution: The Eco-Si junction box is the first junction box for PV modules with an IP protection class of IP68, thus allowing safe operation of the module even under the harshest of conditions. This high protection class was achieved by the consistent use of the hermetic sealed technology introduced by Yamaichi Electronics. With this technology, the cables and electronic of the junction box are over-molded in a single highly-efficient work step, ensuring absolute freedom from leaks. The Eco-Si is also designed for system voltages of 1500V and comes standard with three SMD safety diodes to protect the module efficiently in case of shadow. The diodes are hermetically enclosed by the housing of the Eco-Si junction box, discharging their heat optimally to the UL-listed plastic of the socket, thus avoiding overheating.

Applications: Photovoltaic module junction box for crystalline-based modules. The flat design, only 22mm in height, is easy to stack in production and permits very flat installations.

Platform: Part of the Y-Sol product family, the junction box has now been extended to the point that its TÜV- and UL-certified components permit the complete cabling from the photovoltaic module to the power inverter.

Availability: Currently available.

Snapshot of spot market for PV modules – quarterly report Q2 2011

pvXchange, Berlin, Germany

ABSTRACT

Solar enterprises will each be faced with the occasional surplus or lack of solar modules in their lifetimes. In these instances, it is useful to adjust stock levels for modules at short notice, thus creating a spot market. Spot markets serve the short-term trade in different products, where the seller is able to permanently or temporarily offset surplus, while buyers are able to access attractive offers on surplus stocks and supplement existing supply arrangements as a last resort.

Introduction

Demand in the German PV market initially saw a significant increase in May, driven by ongoing price reductions for all module types, as well as an urgency to connect to the grid before the new feed-in tariffs came into effect in July. This surge in demand has created shortages of some products, such as the SMA Tripower-Series inverter.

However, the German government decided not to reduce the feed-in tariffs, mainly because of fewer than expected PV power installations since the beginning of the year. This sent the German PV market down sharply, because installers are now waiting for a further price reduction, which will not be until January 2012. However, there is expected to be a resurgence in demand come September.

In Italy, demand declined in May as a result of the disclosure of the new Conto Energia IV. Lack of clarity on various issues, such as restrictions on the use of agricultural land, as well as a provision for higher tariffs for PV plants built with European modules, contributed to increased uncertainty. Although the cornerstones are still not very clear, the market demand showed a mild recovery due to a reduction in prices.

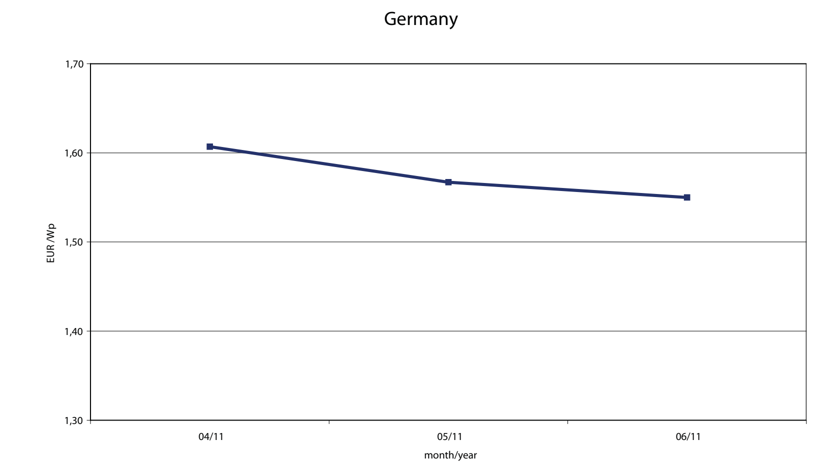

Figure 1. Development of module prices for modules produced by German manufacturers from April 2011 to June 2011.

The booming residential and commercial sectors in the USA have contributed to increased demand on the spot market. The Obama administration is trying to make PV power more affordable: the US Department of Energy's SunShot Initiative, worth US$27 million, is aimed at reducing installation costs (especially approval procedures and grid connections, which make up as much as 40% of the system price of a PV installation) through simplification and standardization of the administrative process. Vermont is the first state to introduce a simplified process that will allow installations to be connected to the grid within 10 days.

> "The booming residential and commercial sectors in the USA have contributed to increased demand on the spot market."

The decline in feed-in tariffs in Germany and Italy for ground-mounted installations, in which thin-film modules are especially successful, will lead to increased competition for roof-mounted systems of all sizes. First Solar, the world's most successful thin-film module producer, has announced plans to develop a strategy especially for small roof-mounted systems. On the other hand, thin-film producing companies are benefiting from the development of new PV markets in countries such as Malaysia, Thailand and the Philippines.

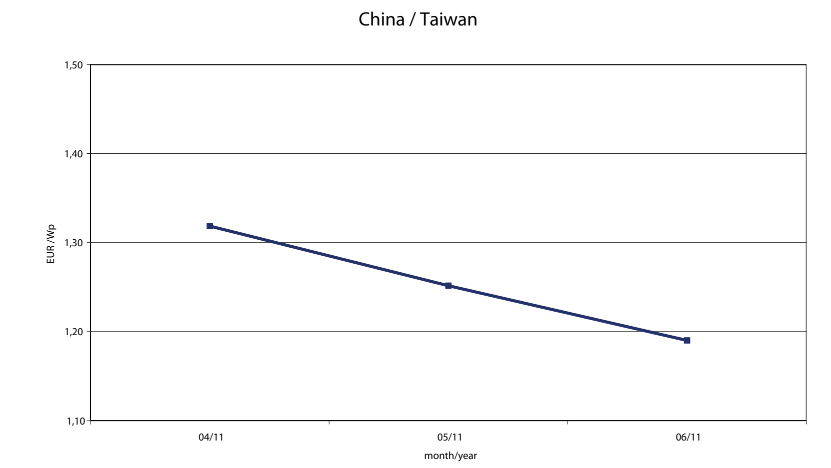

Figure 2. Development of module prices for modules produced by Chinese or Taiwanese manufacturers from April 2011 to June 2011.

For the first time, crystalline modules were offered below €0.90/Wp in June on the B2B exchange pvXchange. Prices of Chinese brands have fallen more than 15% from January to May, and the cost of CdTe First Solar modules decreased by 16% during the same time period.

"For the first time, crystalline modules were offered below €0.90/Wp in June on the B2B exchange pvXchange."

PV Modules

On the spot market, module prices from all regions continued to fall in June. The largest price drop occurred in Japan and was caused, to some extent, by the yen depreciation against both the euro and the US dollar. Further price reductions in the coming weeks are expected. First- and second-tier manufacturers from China will continue to put enormous pricing pressure on all manufacturers.

Meanwhile, inventory levels are still very high and pvXchange estimates that globally there are ~8GW of solar modules in stock. Nevertheless, Chinese manufacturers remain optimistic about their capacity expansion plans, but rumours during the last few months indicate that Chinese banks are becoming more restrictive with granting further credit lines to manufacturers.

About the Authors

Founded in Berlin in 2004, **pvXchange GmbH** has established itself as the global market leader in the procurement of photovoltaic products for business customers. In 2010, the company procured solar modules with an output of around 180MW. With its international network and complementary services, pvXchange is constantly developing its position in the renewable energy market, a market which continues to grow on a global scale. Based in Europe, pvXchange also has a presence in Asia and the USA.

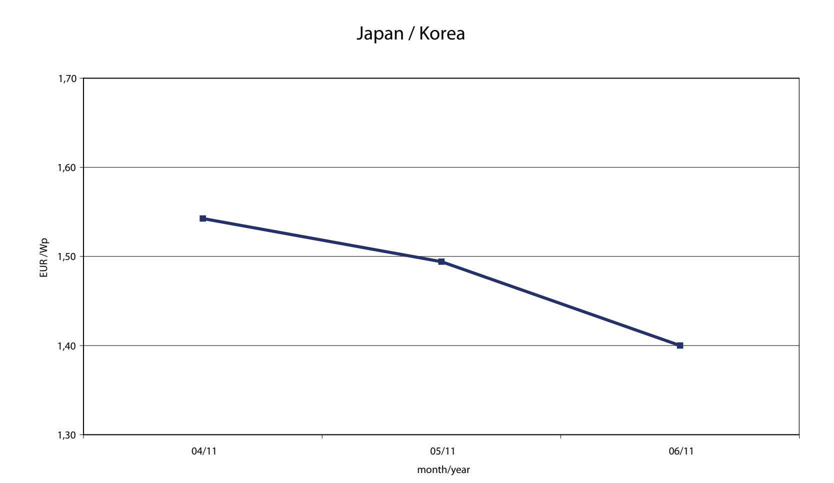

Figure 3. Development of module prices for modules produced by Japanese or Korean manufacturers from April 2011 to June 2011.

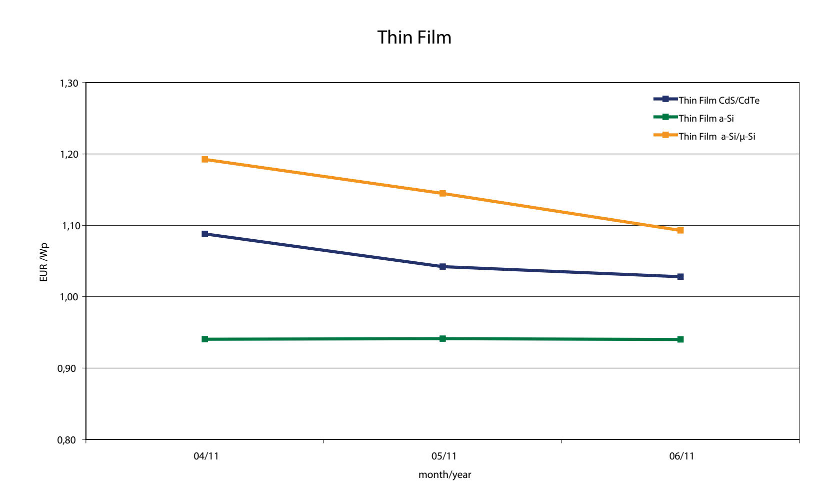

Figure 4. Development of module prices for thin-film modules from April 2011 to June 2011.

Enquiries
pvXchange GmbH
Tempelhofer Ufer 37
10963 Berlin
Germany

Tel: +49 (0) 30 236 31 36 0
Fax: +49 (0) 30 236 31 36 23
Email: info@pvxchange.de
Website: www.pvxchange.com
www.pvxchange-international.com

PV module testing – how to ensure quality after PV module certification

Alexander Preiss[1,2], **Stefan Krauter**[1,4], **Michael Schoppa**[1] & **Ilka Luck**[1,3]
[1] Photovoltaik Institut Berlin (PI-Berlin) AG, Berlin, Germany
[2] University of Technology Berlin, Berlin, Germany
[3] PICON Solar GmbH, Berlin, Germany
[4] University of Paderborn, Paderborn, Germany

ABSTRACT
By definition, PV module certification is simply based on conformance to standards. The IEC norms for PV modules are considered to be adequate quality requirements for guaranteeing initial quality. However, it is commonly understood that two products A and B may meet the standard's requirements, but overall quality – considering long-term stability, performance and safety – can still be quite different. PV module testing should therefore be carried out more frequently and beyond IEC requirements. A factory inspection once a year – as suggested by most certification bodies to ensure continuous quality of certified crystalline modules – may not be sufficient. The need for additional control is demonstrated in this paper, with reference to our experience from PV module testing and quality assurance activities for wholesalers and project developers. We present the necessity of additional measurements under standard test conditions (STC) and advanced testing methods, which are becoming essential for reliability.

Introduction
Solar panels are expected to have a guaranteed service time of 20 to 30 years with typical degradation rates of 0.3–0.5%/a of STC power output for crystalline modules. Because of the introduction of Germany's PV feed-in tariffs (regulated by the Renewable Energy Sources Act), PV systems became attractive for long-term investments, based on a thorough calculation of return over their lifetime. The first plants have actually reached the designated service lifetime and have shown that a service time exceeding 20 years is possible without major losses of performance. However, recent failures in the open field have indicated that theoretical and actual service lifetime can differ significantly, with failures already occuring a few weeks after installation in some cases. In this paper we will report four years of experience within the accredited PI-Berlin laboratory, beginning with an overview of the results of the tests carried out, including major fail criteria for certification. The results of studies that focused on peel-off, gel content and potential induced degradation (PID) tests, as well as the results of quality assurance actions, are presented. In the studies only IEC-certified module types were investigated.

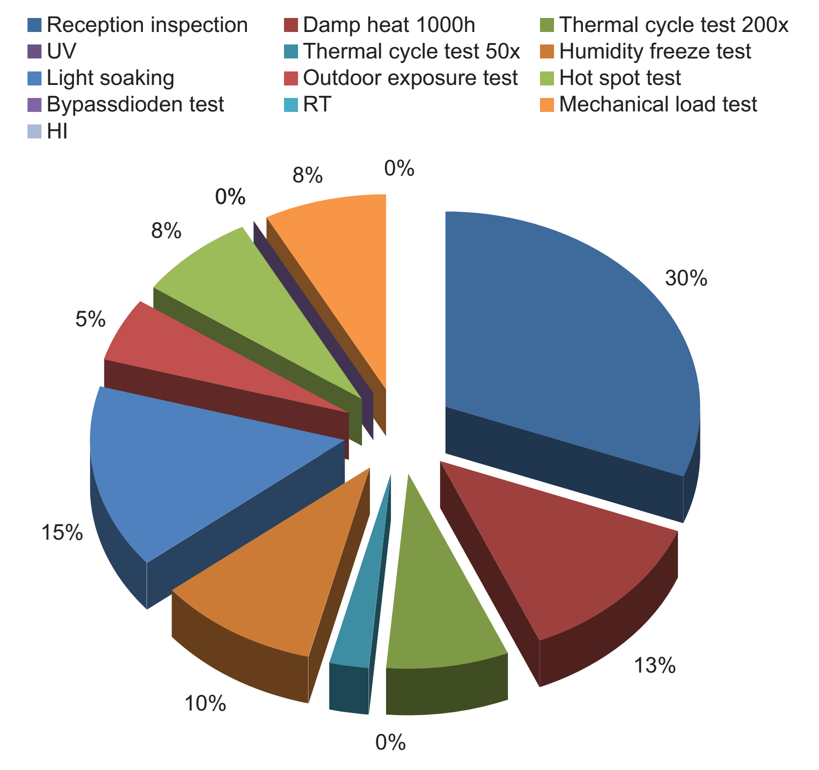

Figure 1. Distribution of fail criteria during the certification process for all tested modules.

IEC-certification, quality assurance and field-test analysis
We have tested PV modules at every stage of product life – certification for product launch, production process quality assurance, incoming quality, etc. – as well as acting as expert for legal actions after product installation. All these tasks were able to be carried out in house, since the PI-Berlin group consists of a comprehensive range of subsidiaries involved in all aspects of a module's lifetime: certification (PI-Berlin), quality assurance (PICON), planning of large-scale PV projects (PI-Experts).

Certification according to IEC
Since 2008 the PI-Berlin AG test laboratory, acting as CBTL (certification body test laboratory) in the CB scheme of the IECEE (IEC System for Conformity Testing and Certification of Electrotechnical Equipment and Components), has worked on 140 cases with TÜV-Süd as a certification body for PV modules.

A total of 32% of certifications have been aborted due to major problems, and

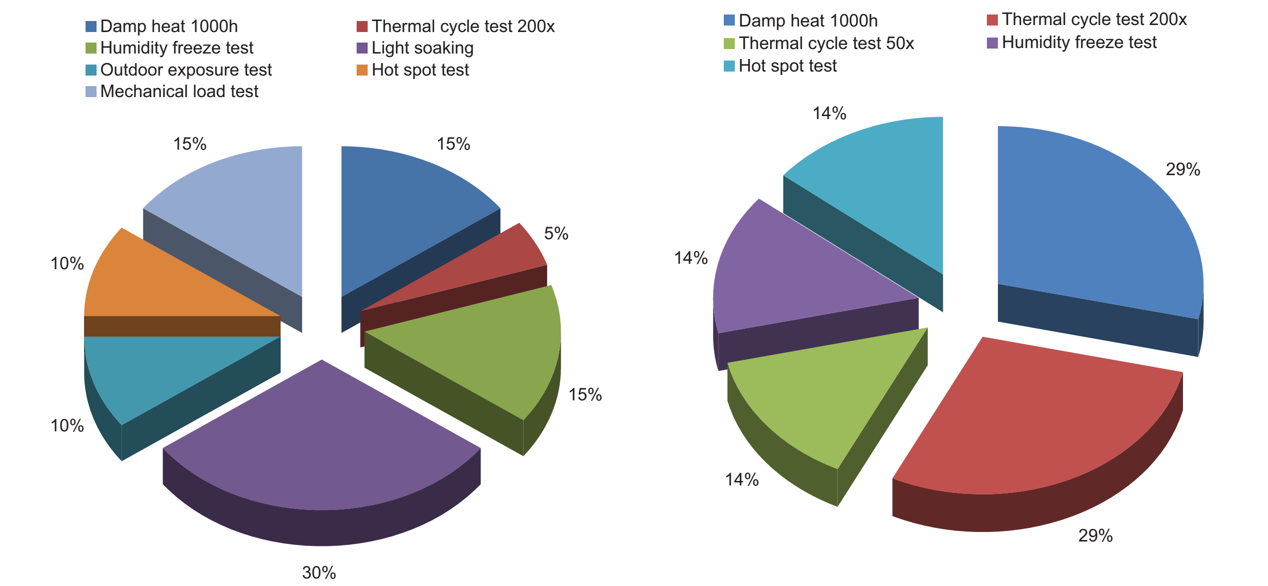

Figure 2. Comparison of failures during the certification processes for thin-film technology modules (left) and c-Si technology modules (right).

a breakdown of the tests involved in those failures is shown in Fig. 1. Often obvious problems such as insufficient initial STC power output, deficient insulation and visual defects have caused premature termination of the testing and certification process.

"The hot-spot test is problematic for both thin-film and c-Si technologies."

Fig. 2 shows a comparison of the reasons for the aborts, in terms of the cell technology applied (thin film vs. c-Si). The main reasons for aborts for thin-film technologies have been the mechanical load test, insufficient STC power output (in stabilized conditions) and environmental tests (outdoor exposure test, measurement of NOCT (nominal cell operation temperature)). For c-Si modules, 86% of failures are due to climate chamber tests (damp heat, humidity-freeze and thermal cycle tests). The hot-spot test is problematic for both thin-film and c-Si technologies. Initial aborts (visual inspection, initial insulation test) have been excluded from the statistics.

Quality assurance

For quality assurance tests, randomly chosen modules are taken either from the free market or from a delivery at the customer site, such as a specific PV power plant project. The number of tested modules depends on the scale of the power plant (e.g. 10 STC/MW_p). These modules are tested according to IEC standards and also beyond these standards by performing several repetitions of standard tests or special tests – laminate peel-off, EVA gel content, EL, etc.

Upon inspection of the STC power output of the modules shown in Fig. 3, it is evident that there is a tendency for STC power output to be deficient. Only a few cases lie outside the range –5% to +2%. Because of the primacy attached to profit,

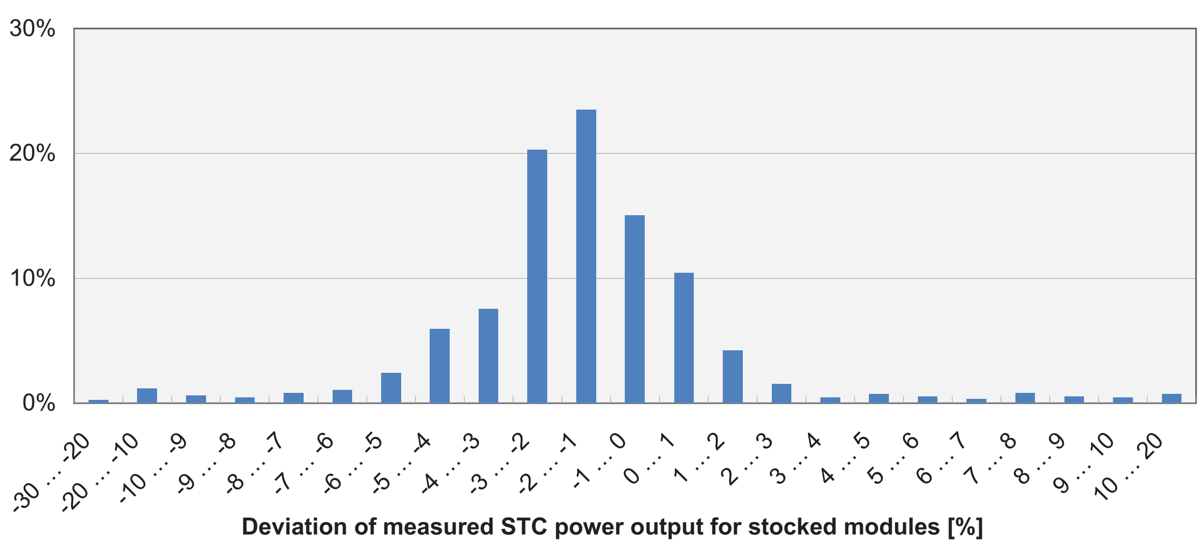

Figure 3. Frequency distribution of deviations of the independently measured STC power output from the labelled power for ex stock modules.

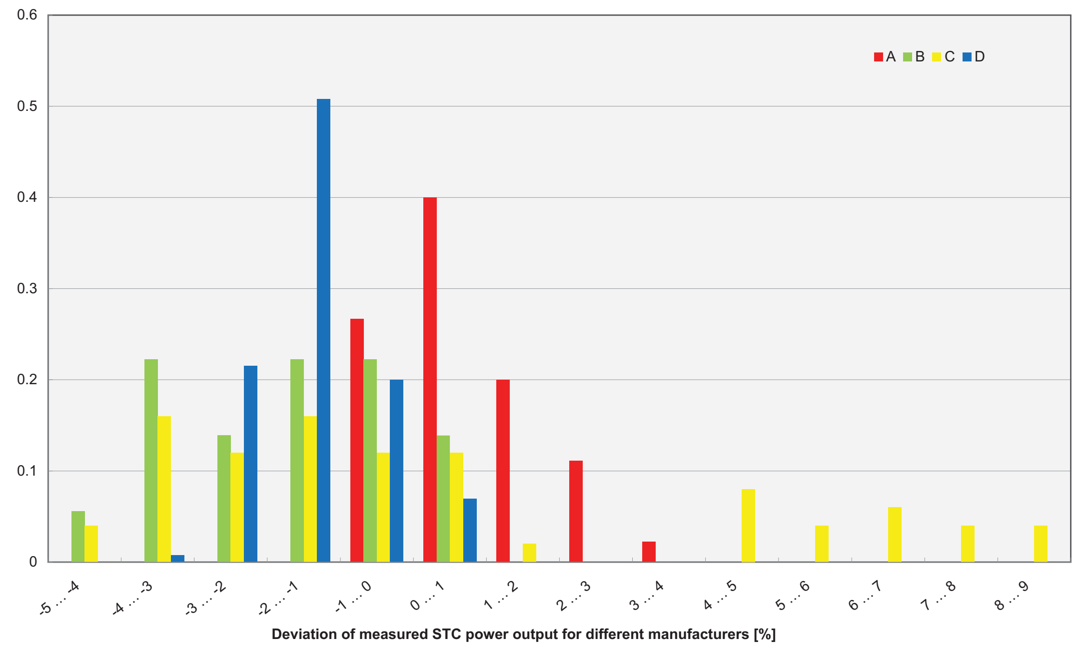

Figure 4. Frequency distribution of deviations of the independently measured STC power output from the labelled power for modules from four different manufacturers A, B, C and D.

positive deviations are in general caused by imprecise calibration of manufacturer's equipment. However, recently, 'plus tolerances only' are becoming a new marketing feature for some manufacturers.

As Fig. 4 shows, manufacturers have different attitudes towards quality control. Producer A has a tendency to overstate the power on the label, while D has a tendency to underestimate actual power output. Producer B has the same tendency as A, but with a broader distribution. Producer C apparently has two factories with different tendencies.

Lamination quality

EVA gel content test

Another quality attribute is the gel content of the encapsulation material. Generally an encapsulate material made of ethylene vinyl acetate (EVA) is used in PV modules. This encapsulate is produced as a film and delivered and stored in rolls, which are protected against humidity and light. The length and the width of the rolls may vary. Most EVA producers recommend storage at a temperature below 30°C (optimum 22°C) and a relative humidity below 50%, for a maximum period of 6 months after production. The rolls should not receive direct sunlight and should always be wrapped tightly in their original packaging. A cut piece of EVA should be stacked and used within 8 hours.

The film is composed of the co-polymer EVA. Initially, the polymer is a thermoplastic, but the manufacturer of the film adds a curing agent and other chemicals (e.g. UV stabilizer). The curing agent is peroxide, which decomposes with increases in temperature and starts a chemical reaction, namely the curing process in the laminator. When the curing process is over, the original thermoplastic has become an elastomer, which can no longer be melted. The material is then irreversibly cured.

The known problems of EVA are:

- **Evaporation of the curing agent before curing:** there may not be enough curing agent left for the curing process due to incorrect storage or mistakes made on the producer side.
- **Too short a curing time:** an insufficient curing time may have been selected in order to achieve process optimization and increase the production. This results in inhomogeneous curing across the modules, or homogeneous but only partial curing.
- **Incorrect curing parameters:** too high or too low a temperature for curing may have been chosen. As in the case of an inappropriate curing time, a partial curing could result, or the material may be irreversibly damaged.
- **Non-uniform curing:** since the development of ultra-fast, fast-curing or similar curing sheets, in combination with the increase in module sizes, the curing process might not be completed across the whole module. The curing level has been found to deviate up to 20% within the area of a single module. The problem is the time difference between the curing temperature

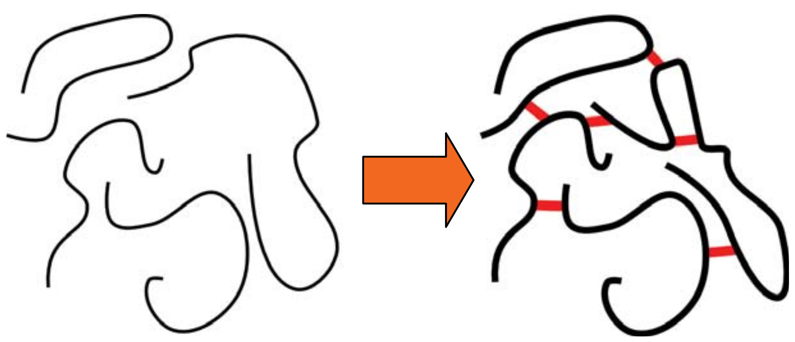

Figure 5. Schematic of the EVA curing process.

reaching the centre and the corner of a module. In addition, thermal stress might result in bending of the module, which lifts parts of the module away from the laminator surface and reduces heat transfer and temperature development.

- **Error made by supplier:** it could happen that the supplier does not put enough peroxide in the EVA, stores it for too long or just mixes different qualities of EVA to improve profit. Non-uniformly distributed curing agents and other chemicals in the foils may cause different properties within the module area. In highly optimized processes this may lead to partial curing.

The *gel content* is a ratio describing the actual proportion of cured EVA in a sample and is a satisfactory quality indicator for the lamination process parameters and the materials used. Results of EVA gel content tests by PI-Berlin are presented in Fig. 6. Typically, the EVA manufacturer recommends a gel content > 75%, but about 60% of tested modules do not in fact reach this value. As shown in Fig. 7, a wide distribution of gel contents is possible within the same manufacturer. Therefore, the quality of processing deviates not only among manufacturers but also within one producer.

"Typically, the EVA manufacturer recommends a gel content > 75%, but about 60% of tested modules do not in fact reach this value."

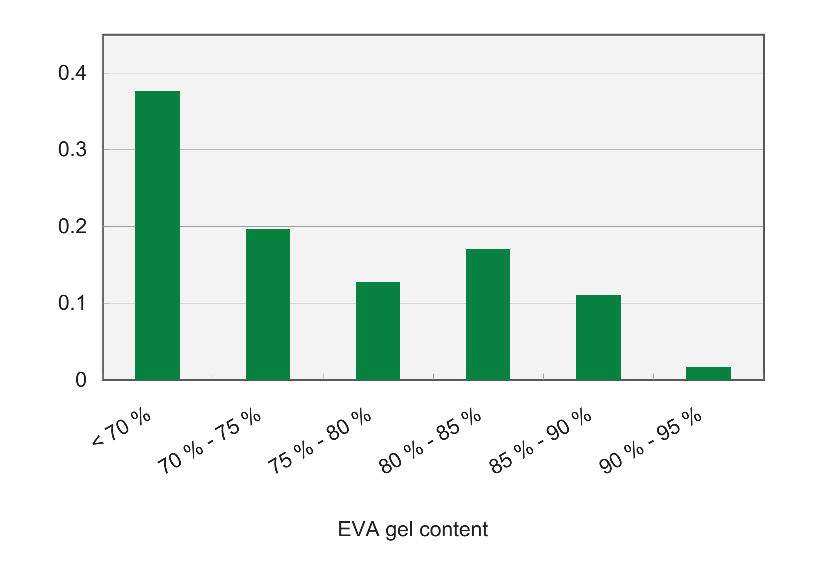

Figure 6. Frequency distribution of EVA gel content of 120 analyzed PV modules.

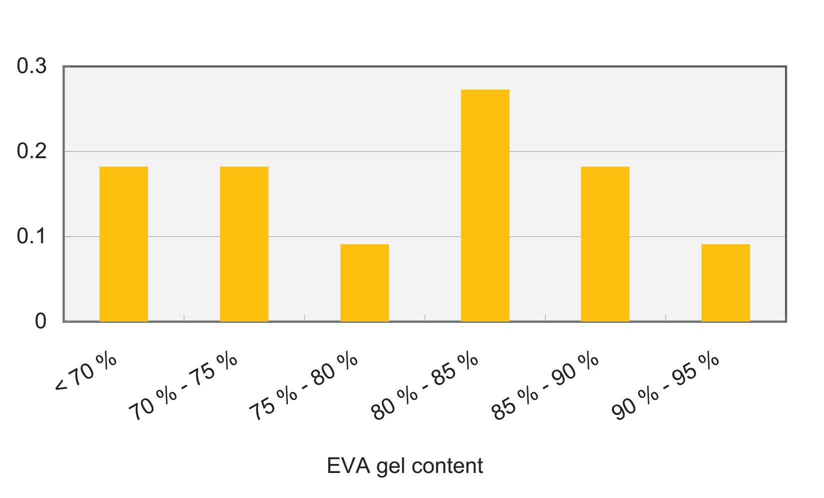

Figure 7. Frequency distribution of EVA gel content of analyzed solar modules from manufacturer A.

Peel-off test

A proper sealing of the modules is important for ensuring a long service time. The peel-off test checks adhesion and consists of measuring the force required to separate the module layers. Typically, it is possible to test the adhesion between:

- encapsulant material (EVA and back sheet) and the back side of the solar cells;
- encapsulant material (EVA and back sheet) and the bus bars;
- encapsulant material (EVA and back sheet) and the front glass;
- layers within back-sheet material (or back-sheet laminate).

Preparation of the module consists of preliminary cuttings of 1cm-wide strips

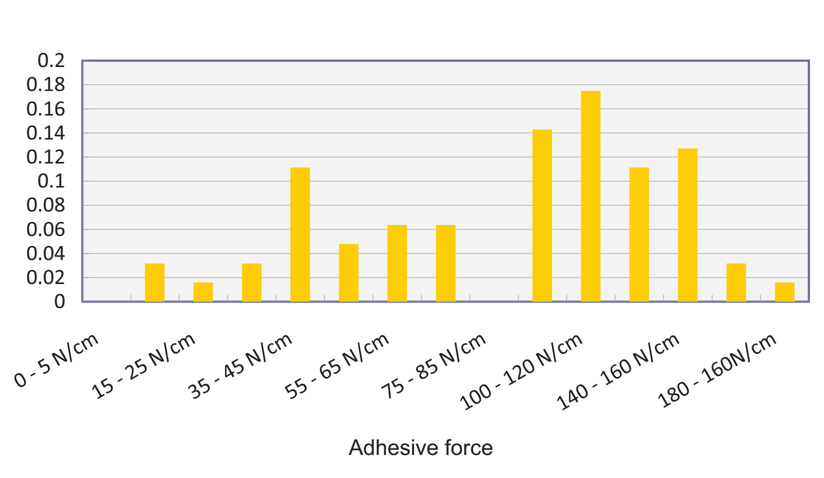

Figure 8. Frequency distribution of the measured adhesive force between EVA and glass.

Note: If cleanliness of the surface of the laminated components is not considered, the EVA gel content test (see above), carried out as the only laminator quality indicator, may be misleading. The gel content test may give acceptable results, but the adhesion of the laminate components (and the service time of the module) may be significantly less than the gel test alone would suggest.

at the centre of the back sheet of the module. The peeling test has to be initiated manually in order to have a 1cm-long free strip, which can be clamped in the wedge grip. An increasing force is applied to the wedge grip, and the specific force is recorded (in N/cm) at the point when the strip starts to separate from the module. As seen for gel content measurements of EVA, a broad distribution of the adhesive strength between EVA and glass can be observed. Fig. 8 shows the results of the peel-off test: in some cases EVA can be easily peeled off from the glass of the module, with little force involved. For other test samples, the back-sheet material breaks before separation occurs. Some clustering of test results can be observed for forces above 95N/cm, but there is no standard defined for this test yet.

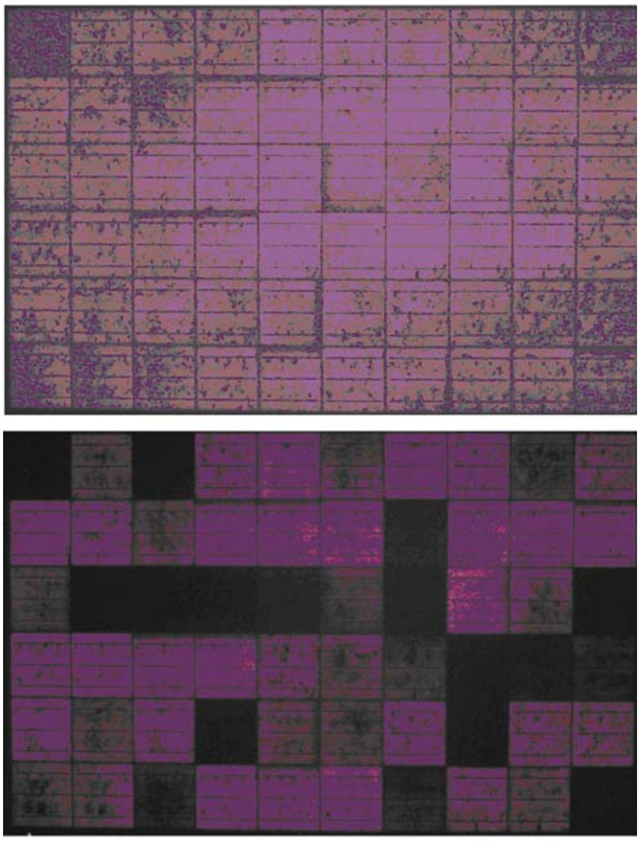

Figure 9. Results of an accelerated PID test (48h at –1000V) in a climate chamber (damp heat: 85°C, 85% r.h.). Top: module in initial state. Bottom: same module after treatment, with a loss of 40% of initial STC power output.

Potential-induced degradation (PID)

It has been known for several years that the STC power output of PV modules may degrade, due to electrical potential between the frame and the cells, and this effect is known as 'potential-induced degradation' (PID). The results of this power-reducing process can be detected via an electroluminescence analysis. In PV systems, PID can be detected by a reduced fill factor (FF), but in advanced stages of the process the I_{sc} (short-circuit current) decreases as well. The affected cells (or some areas on the cells at the beginning of

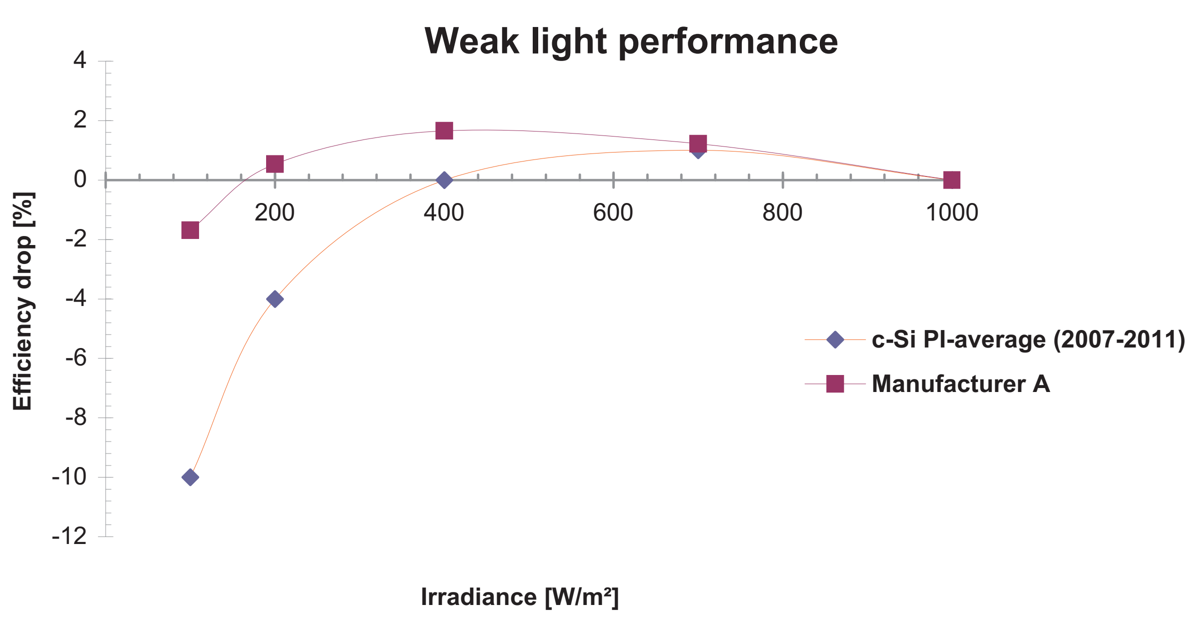

Figure 10. Weak light performance curve of a module with a 'positive' weak light behaviour. An efficiency drop of 30% is also possible.

the process) no longer contribute to power output and are recognized as 'black-cells' in electroluminescence images. For installed modules, PID first affects modules with the highest electrical potential and those located in humid environments (near to the ground, or frame parts with water inside). Precautions taken in the design of the power plant (reduction of potentials) may counteract this effect, or a preliminary filtering of modules with PID affinity is also possible. For the majority of c-Si modules, the PID effect is almost completely reversible.

> "For installed modules, PID first affects modules with the highest electrical potential and those located in humid environments (near to the ground, or frame parts with water inside)."

The sensitivity of a module or of cells to PID can be detected in accelerated damp-heat climate chamber tests, as shown in Fig. 9. The modules were treated for 48 hours in a damp-heat chamber (85°C and relative humidity of 85%), with a potential of –1000V at the terminals. The results for a large number of tests range from a total power loss (–100%) to no effect on STC power output (–0%).

Weak light behaviour

In addition to the temperature coefficient, the efficiency of modules at low irradiation levels is a crucial factor for the energy yield of a PV system. At PI-Berlin, weak light behaviour is measured in a Pasan IIISb flash light sun simulator. Using diverse absorption filters, it is possible to reduce irradiance without spectral changes to almost any value between 50 and 1200W/m^2. The change in electrical efficiency relative to STC efficiency is evaluated. The behaviour is often quite specific to a technology, but has been measured for multicrystalline Si (m-c-Si) technology modules, with a wide variation of the results. PI-Berlin's internal criterion for a 'positive' weak light behaviour at an irradiance level of 100W/m^2 is a maximum efficiency loss of 10%. Fig. 10 illustrates the measurements of one manufacturer's module compared to PI-Berlin's average data. In the average data, the worst performers have shown a decrease in relative efficiency of 30%.

Field data

An unexpected low energy yield of a PV system is often the reason for testing already installed modules. This may be true for single modules, as shown in Fig. 11, but equally for entire strings of modules in a PV power plant, as shown in Fig. 12. The beginning of the degradation process can be detected by adequate monitoring of a photovoltaic system. The reasons for less power output cannot be determined by simple power output measurements; further analysis requires removing the modules and transferring them to the laboratory environment (e.g. to check for PID). This process is quite time consuming and expensive, but can often be prevented by performing quality checks before mounting (e.g. using the tests mentioned earlier).

> "The beginning of the degradation process can be detected by adequate monitoring of a photovoltaic system."

Conclusions

Based on PI-Berlin's experiences in module damage, low energy yields and quality assurance actions, it has become clear that certification according to IEC and all follow-up actions are not sufficient for ensuring a service time of 20 or more years. It is remarkable that – even for IEC-certified modules – there is a significant variation in quality not only between manufacturers but also within the delivered charge from a specific manufacturer. For already installed modules, it is difficult to ascertain later whether impairments are degradations due to unsatisfactory design of the solar power system or inherent problems of the modules themselves.

In the setting up of large-scale PV projects, it is possible to prevent these problems and confirm the long-term stability of modules by quality check-in

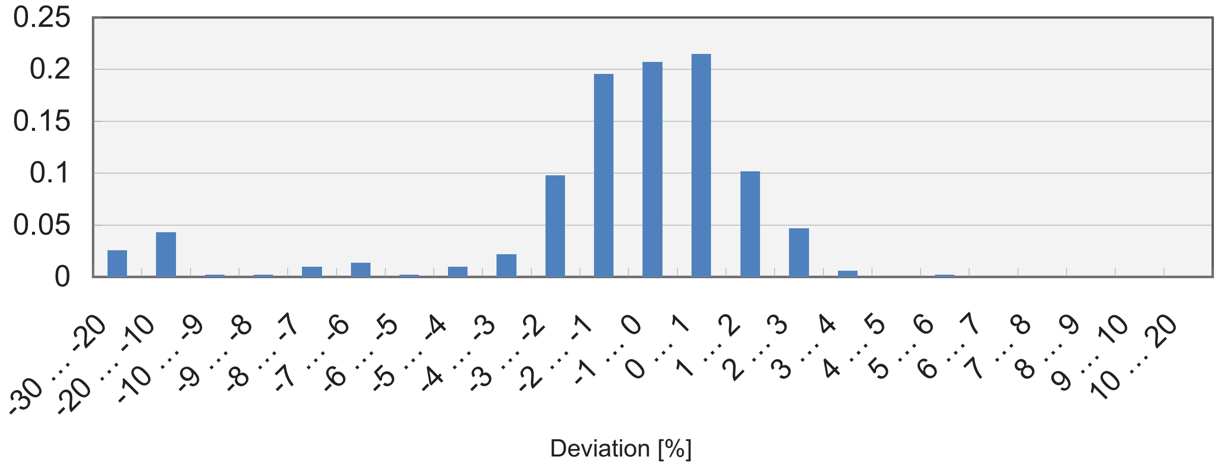

Figure 11. Deviation between measured and labelled STC power output of unmounted photovoltaic system modules.

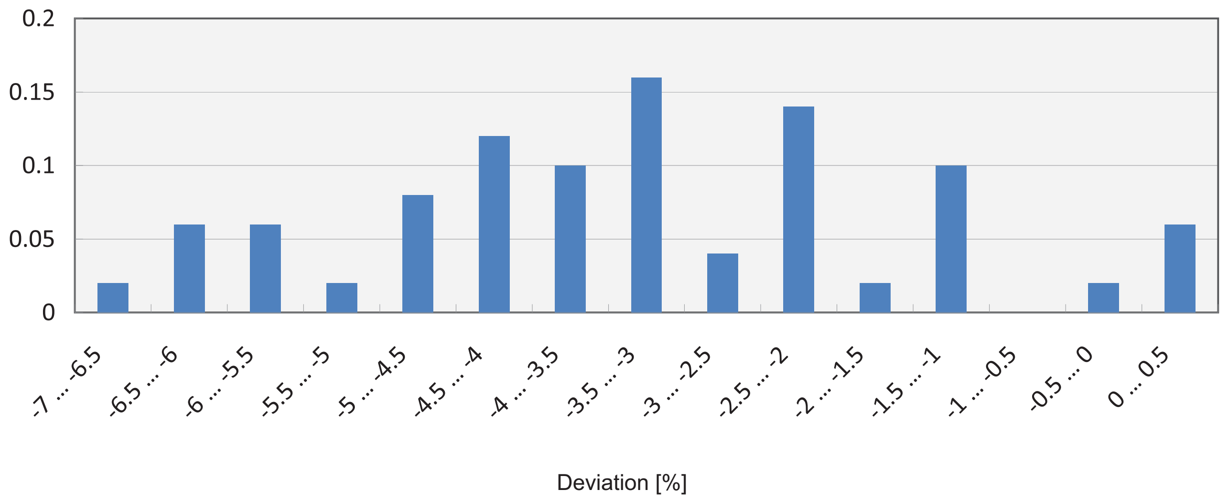

Figure 12. Deviation of measured and labelled STC power output of separate strings of modules in operating photovoltaic systems.

tests, which include factory inspections, climate chamber tests beyond IEC standards, advanced visual inspections, electroluminescence analysis, UV treatments, hot-spot tests, EVA gel content tests and peel-off tests. Moreover, the knowledge of the implemented quality assurance actions triggers an educative effect on the part of the manufacturer.

About the Authors

Alexander Preiss is responsible for the PV outdoor laboratory of PI-Berlin AG, which he set up in 2007. He also works as a project engineer for the accredited PI-Berlin laboratory. From 2000 to 2007 he studied physics at the Humboldt University in Berlin and received a master's degree in experimental solid-state physics. For his thesis he carried out a feasibility study for the optimization of CIS solar cells at the Hahn Meitner Institute. Alexander started his Ph.D in 2007 on yield simulation of PV generators in the Department of Electrical Drives at the University of Technology Berlin (TUB).

Stefan Krauter is a professor at the University of Paderborn and head of the Department of Sustainable Energy Concepts. He received his Ph.D. in electrical engineering for work on performance modelling of PV modules from the University of Technology Berlin (TUB) in 1993. He co-founded Solon in 1996, and in 1997 received a visiting professorship for PV systems at UFRJ-COPPE in Rio de Janeiro, and later at UECE in Fortaleza. During his stay in Brazil he set up a series of congresses and fairs (RIO 02/3/5/6/9/12 – World Climate & Energy Event, together with the Latin America Renewable Energy Fair), to promote the global use of renewable energy. Professor Krauter has been back in Germany since 2006 and co-founded PI-Berlin AG, participating on the board of directors and acting as a senior consultant.

Michael Schoppa is head of the accredited and internationally accepted PV-testing laboratory of PI-Berlin AG, which specializes in quality and material control of PV modules and components. In 2004 he worked on long-term stability for new solar concepts as a research associate at the Monash University in Melbourne, Australia, and later as a graduate at the Hahn Meitner Institute in Berlin. From 2006 to 2007 he was a project engineer in the area of international certification for TÜV Rheinland and in charge of customer support and supervision. Michael participated in the formation of PI-Berlin's PV-testing laboratory and quality management, and under his direction the laboratory gained national accreditation in 2008 and admission to the international CB Scheme (NCBTL) in 2009.

Ilka Luck has a Ph.D. in physics and an MBA. She worked on international R&D projects in the areas of CIGS and international industry cooperation as a scientist at the Hahn-Meitner-Institut Berlin (now the Helmholtz-Center Berlin) from 1998 to 2001. She is the co-founder of several companies in the renewable energy sector, notably Sulfurcell Solartechnik GmbH (now Soltecture) in 2001 (managing director 2001–2006) and PI-Berlin AG in 2006. From 2007 to 2008 she was the managing director of Global Solar Energy Deutschland GmbHand and in that position was responsible for setting up the 30MWp production facilities. Dr. Luck founded PICON Solar GmbH as an operating partner in 2008, to provide a wide range of consulting services focused on PV.

Enquiries

Photovoltaik Institut Berlin AG
Wrangelstr. 100
10997 Berlin, Germany

University of Technology Berlin
Sek. EM 4
Einsteinufer 11
10987 Berlin, Germany

PICON Solar GmbH
Fehrbellinerstr. 84
10119 Berlin, Germany
E-mail: luck@picon-solar.de

University of Paderborn
Electrical Energy Technology
Pohlweg 55
33098 Paderborn, Germany

PV Modules

Assessing the real quality of PV modules

Thibaut Lemoine, STS-certified Ltd., Shanghai, P.R. China

ABSTRACT
With new industrial challenges faced by the PV industry – such as the striking development of Chinese manufacturers, and ever more demanding investors and financial institutions – the quality of PV modules has never been as important as it is today. Because normative requirements are not matching the buyers' expectations, the questions of what the real quality of a PV module is and how to assess it still remain. This paper analyzes the current situation in terms of quality and the causes of problems, and proposes some ways of addressing the issues in order for the industry to progress on the long path to excellence.

Introduction

Given the continuous FiT cuts in almost all the major markets, the demand for lower prices has led the PV industry to relocate to developing countries, in particular to China, which today accounts for more than 50% of the worldwide production of PV modules. With over 700 manufacturers in the country to choose from, ranging from family-owned businesses making a few hundred kilowatts of modules per year to huge stock-listed companies producing over a gigawatt in a year, it can be difficult to make a decision when it comes to selecting the right partner. In this context, distributors, EPC, installers and end-users are witnessing a flood of products of varying standards of quality. The reality of the situation is that there is apprehension with every purchase made from Chinese manufacturers, and the same question comes to mind each time: "What is the real quality of the products I am buying?"

This question has been around in the PV industry for many years, but there has so far not been any universally accepted answer. Quality remains subjective depending on the buyers' expectations. We can say that buyers generally expect a PV module to provide the right power output and to continue to do so for several decades. But on top of these basic specifications, there are some implicit requirements, such as safety for users and installers. Some new considerations have also been added with the evolution of the industry and the emergence of residential installations, in which respect end-users are more demanding in terms of the aesthetic aspect of products that are integrated into their homes. Of course, the monetary question is of utmost importance, as the industry is turning to investors who insist on a risk analysis of their investments.

The limitations of the IEC/ISO standards and accelerated aging tests

Nowadays, it is almost impossible for a manufacturer to sell their products without a certificate of compliance with IEC standards. However, all the experts, including certification bodies such as TUV, agree that IEC61215 for crystalline modules and IEC61646 for thin films do not cover all the aspects of quality for PV modules. In order to better understand why, it is important to understand the typical behaviour of a population of products – namely PV modules – and the related defect trend of this population over time.

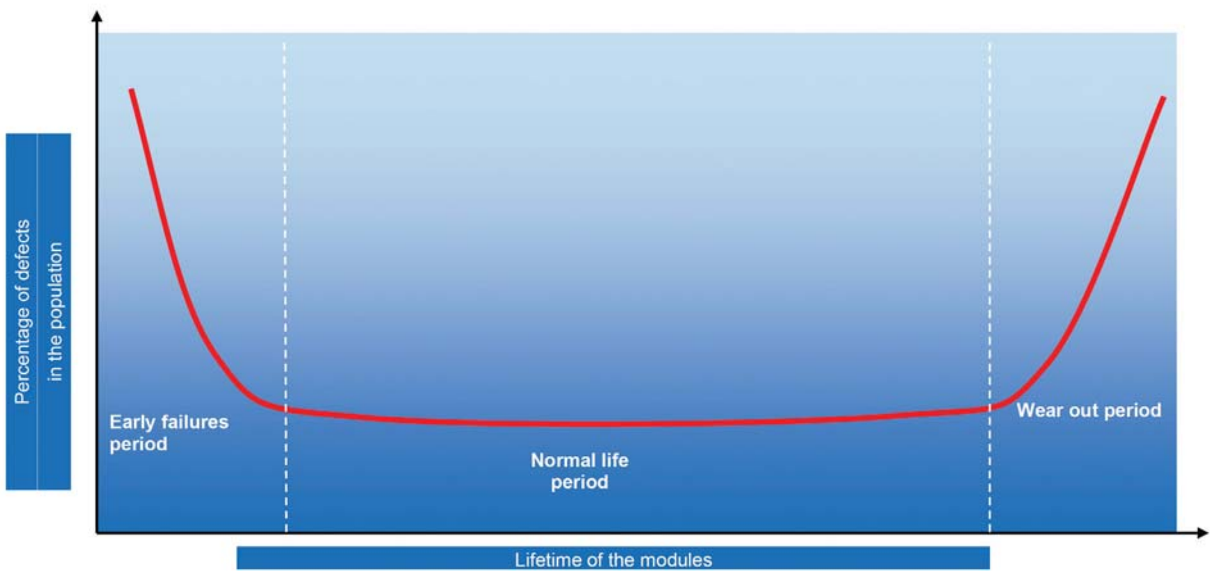

Figure 1. The bathtub curve.

“Nowadays, it is almost impossible for a manufacturer to sell their products without a certificate of compliance with IEC standards.”

As in the case of populations of other products, PV module populations follow the ‘bathtub curve’ as shown in Fig. 1. A population of products (for instance a quantity of modules used to complete a 20MW project) will go through three different behaviours over three consecutive periods of time:

- An **early failure** period, during which the defect rate will be high and will decrease with time.
- A **normal life** period, during which the defect rate will be low and constant.
- A **wear out** period, during which the defect rate will increase with time and become high.

Typically, a lot of defects will occur during the early life of the modules due to poor design (causing epidemic failures), some modules not being manufactured according to the required design and correct process settings, or defective components being used. During the normal life of the modules, some defects will appear randomly at a very low rate. This is part of the normal behaviour of the population of any product. Finally, when the components start wearing out because they have reached the limit of their intrinsic endurance, the failures will increase until the whole population is worn out. To each of these periods correspond different types of defect and different causes, and consequently different ways of detecting and preventing failures.

The IEC standards do not address all the different periods of life of the products and their associated failures, and there are many reasons why:

- **Design qualification:** the standards have been developed for the qualification of the design of the PV modules. The tests performed are able to determine if modules produced in the same environment, with the same processes and with the same components, will have a ‘normal’ life. Due to time constraints and costs considerations, a single module will not be subject to the complete set of tests required by the standards. It is therefore difficult to assess the behaviour of the modules under real conditions.

- **Life expectancy:** it is specifically mentioned in the standards that the actual life expectancy of the modules will depend on the conditions under which they are operated. The tests are not truly representative of actual outdoor exposure for 25 years or more, because of the difference in climates, sun irradiance and various other conditions.

- **Sampling:** all the tests performed are based on samples of typically 8–10 modules. These samples are considered to be representative of the mass production, but in reality this is not necessarily the case. Modules sent to the laboratory for testing are carefully selected and prepared by the manufacturers, which biases their representativeness. In some cases, there is even malicious intent, which is highlighted by the example of a large manufacturer that, at the beginning of its operations, sent some modules from another company to take the tests.

To address the first two points above, a series of new tests have been developed in order to come as close as possible to the real operating conditions of the modules. However, due to the equipment and time necessary to perform these kinds of tests, and notwithstanding the fact that the modules come to the end of their life expectancy after testing, it is practically impossible to perform the tests on all the products. So there remains the problem of sampling and its representativeness of the whole population.

What are the real quality risks?

While most of the modules sent to the laboratory to obtain certificates of compliance pass these tests successfully nowadays, feedback from the field is indicating a high percentage of failures. Some investors were a bit disappointed in 2010 when they discovered that after one year in the field, over 90% of the modules from their 1MW project began to delaminate and ended up on the ground! In another case, a module set on fire, causing damage to part of the house on which it was installed. What is the common link between these products? – they were both certified compliant with IEC standards.

“While most of the modules sent to the laboratory to obtain certificates of compliance pass these tests successfully nowadays, feedback from the field is indicating a high percentage of failures.”

These examples, although of dramatic proportions, are still characteristic of the uncertainty regarding the performance and behaviour of products in the field. Indeed, whether or not these extreme situations make the news headlines, installers, users and investors are confronted everyday with issues related to the quality of their modules. As a result, confidence is undermined in the products and the whole industry suffers from those issues in terms of disparagement from rival industries. As of today, the industry still lacks reliable and statistically usable data to better understand what the problems are and to predict the future of the gigawatts of modules already installed. However, with industrial quantities of modules already installed for over a decade, some results and trends are now starting to take shape.

Fig. 2 shows the distribution of field failures according to data collected from 21 major manufacturers as presented during the NREL forum on quality assurance

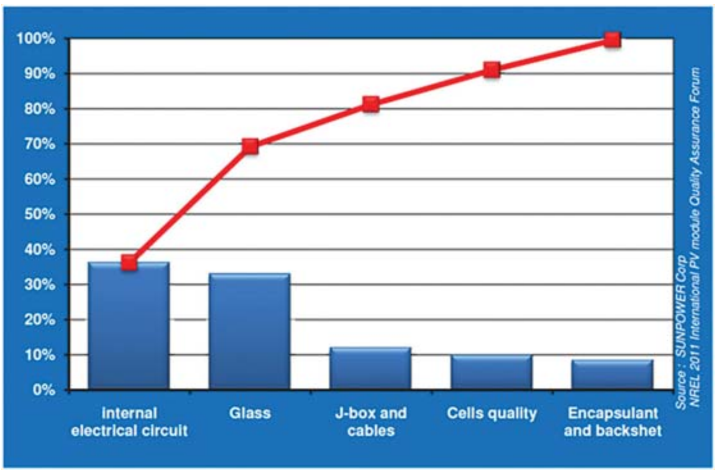

Figure 2. Distribution of field failures among 21 major manufacturers.

in San Francisco in July 2011 [1]. The feedback covers 8 years on average, but an extrapolation of the defect rate shows that at least 4% of the modules will fail after only 15 years. Different conclusions can be drawn from an analysis of the data. First of all, the data coverage of 8 years is less than a third of the life expectancy of the modules and did not take into account the DOA (dead on arrival) factor; the percentage of failed modules is therefore understated. Second, the data shows the distribution of failures at a particular age of the modules, but this distribution will evolve over time, as some defects such as those related to the quality of the cells are likely to appear later in the lifetime of the modules. All in all, it is unlikely that the expected reliability will be met.

In parallel to this field feedback, some manufacturers and third parties such as STS have started to report statistical analyses of the defects seen during inspections and quality control of large quantities of modules. The data that was used to predict the percentage of early failures of the modules and the period over which this will occur show the lack of maturity of the industry. The PV industry today is comparable to some extent to an industry such as consumer electronics as it was 25 years ago. Containers are filled with a percentage of defective modules that will not fulfil their function for even one day. Those defects, which could easily be avoided, range from damaged packaging and performance issues to cosmetic and workmanship issues, and account for up to 15% the modules inspected by STS.

What are the causes of failure?

The analyses conducted by the manufacturers and STS reveal that one important aspect of those failures, with consequences for both reliability and early failure rate, is that the vast majority of them are not linked to the module design itself but rather to the manufacturing processes and changes to the components.

While some efforts have been made recently in the industry towards the automation of processes, the main part of PV module production, including some critical steps of the process, remains highly reliant on manual operations. It is no surprise, then, that a lot of problems originate from human errors. On the other hand, automation has also led to some difficulties for manufacturers in setting up some increasingly complicated processes to satisfy the ever more demanding technology of modules.

Remarkably, since some manufacturers are still not equipped with reliable measuring equipment or not using it properly, measurements are misleading them into unknowingly producing defective products while convinced that the opposite is true. Finally, in tense economic situations, the temptation to reduce costs by using cheaper materials, despite the prohibition by certifying bodies, has played a significant role in the emergence of defects. A lot of new materials – such as encapsulation material, frames with different cross-sections or even solar cells of different grades – are being used in production without proper certification for mass production.

"Remarkably, since some manufacturers are still not equipped with reliable measuring equipment or not using it properly, measurements are misleading them into unknowingly producing defective products while convinced that the opposite is true."

How to assess and prevent the risks?

The next logical question is, of course, how to prevent these risks. While manufacturers have put some effort into increasing the quality level of their products in the last couple of years, the greed for short-term profit and the imbalance between supply and demand often prevail against quality: hence the importance of independent assessments of quality by third parties. Even if compliance with

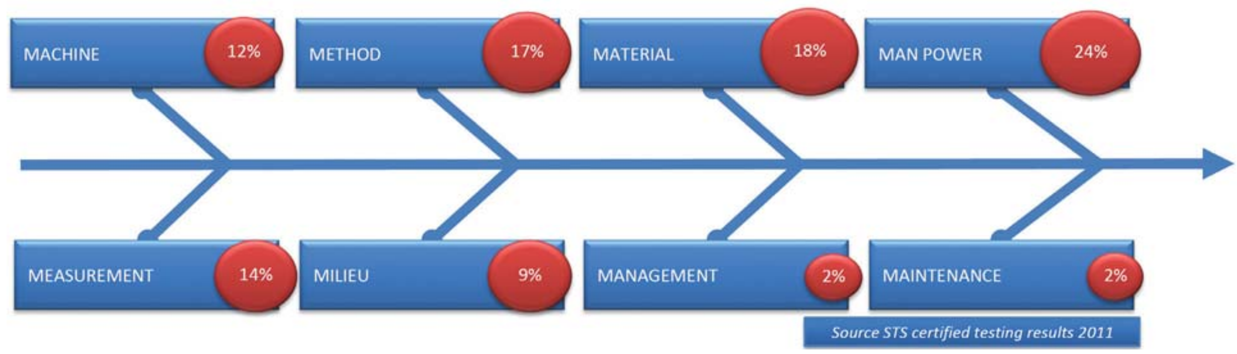

Figure 3. A breakdown analysis of the causes of failures (also known as 8M analysis) showing, in the form of a fishbone diagram, the distribution of the causes attributed to the defects detected during STS inspections and testing activities.

IEC and UL standards has shown their limits in guaranteeing the quality level of the products, the standards should not of course be ignored, and purchasing PV modules that are not duly certified puts the buyers at risk. There is a continuing debate on whether to perform sampling inspections and what sampling levels to use, or whether to simply control everything and, if not, what to control.

In theory, if manufacturers perform most of the relevant tests to determine the quality level of a PV module, then why perform a 100% inspection of the modules? The question of maturity in the industry is raised again. Even though sampling provides a good confidence rate for a stable process, it is not really adapted to processes involving a lot of manual operations and unstable manufacturing processes as implemented today in the industry. In any case, sampling may address design issues and prevent epidemic failures, but the process and human errors, which are random by definition, cannot be entirely detected by this inspection method. Thus, a full quality control by an independent company seems to be, in theory, the best choice. However, because of economic and time constraints, some tests cannot be conducted on a large number of modules. The choice of tests to be performed must therefore be relevant to creating a correct balance of cost, lead time and quality.

Performance assessment

With current progress in technology, the assessment of performance (including performance under non-standard conditions) has become affordable in terms of investment. It is important to use as reliable a sun simulator as possible, meaning that conditions as close as possible to natural light are reproduced in a controlled manner. Even if the IEC 612215 standard requires only the use of class B sun simulators to assess the output power, it is highly recommended to use the class of sun simulator as defined in the IEC 60904-9 standard.

Cell quality

Since solar cells are the main components

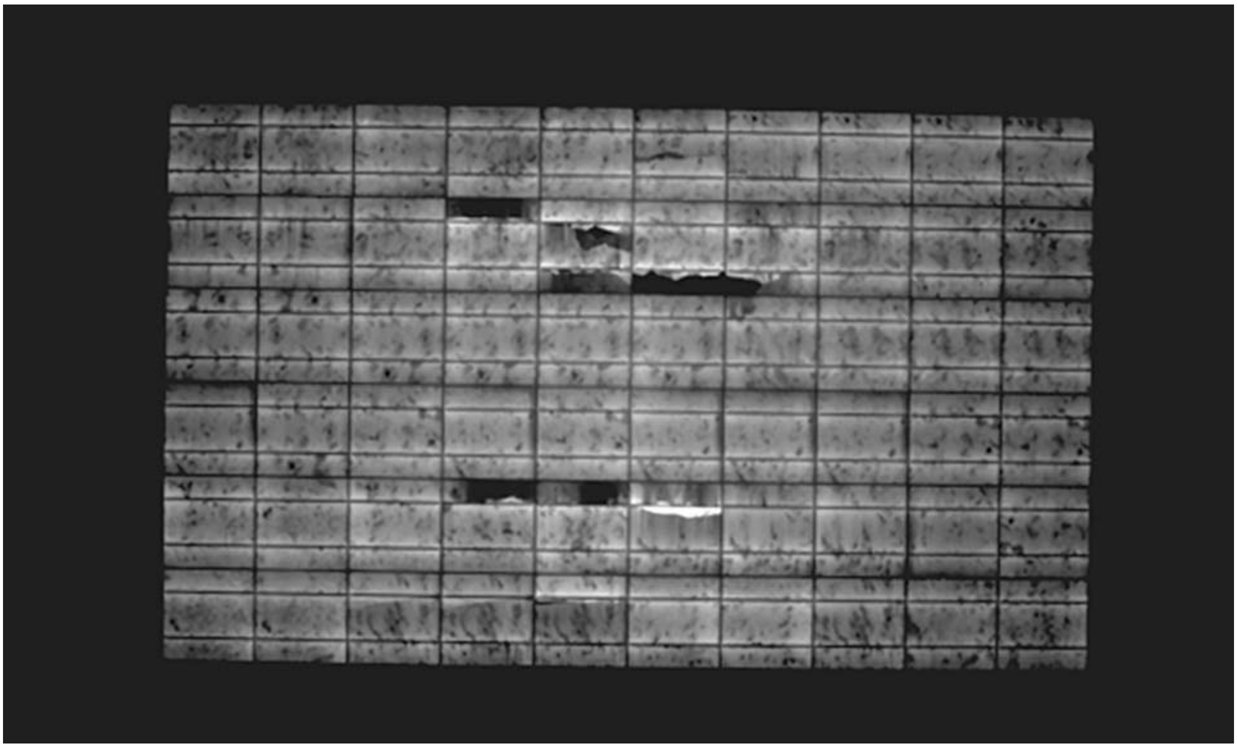

Figure 4. Electroluminescent imaging of a multicrystalline module.

of a PV module, it is mandatory to inspect them carefully. An easy-to-use and non-destructive way of assessing the quality of the cells is to check them under electroluminescent light (Fig. 4). This method uses a property common to all semiconductors that is the opposite of the normal use of solar cells. While a solar cell produces electricity when irradiated by light photons, the opposite reaction is also true. An electrical load is applied to the cell, which will then emit some radiation that can be captured by a camera, and the more efficient the cell, the higher the radiation. Areas such as cracks, which are not emitting radiation, indicate a lower efficiency than elsewhere and therefore a problem in this area of the cell. The different defects observed provide an indication of the future behaviour of a cell and consequently of its reliability.

Workmanship

A careful visual inspection of the products can also reveal some serious defects. These could be dimension or connection issues that can cause problems during installation; sealing defects that may not ensure adequate protection of the cells in harsh environment conditions; or sharp edges that can lead to injuries to installers. The list of problems is a long one.

Production monitoring

An expertly carried out monitoring of the production process completes the testing aspects, in order to guarantee a total quality approach focusing on continuous quality improvement.

The financial aspect

Quality has of course some direct consequences for the return on investments made for any PV project. Since all manufacturers provide warranties on products for at least five years, and on performance for over 20 years, there should be no concern about costs incurred due to quality issues. The fact is that warranties normally do not cover shipping and installation costs or loss of profit related to defective modules. In the end, the cost of a claim is often much higher than originally anticipated, and claims should be avoided as much as possible. Product defects can have a significant impact on profits, hence the need for improved quality assurance. In a recent study of a 12.5MW project [2], it was demonstrated that an increase of 1% in yield can increase the project profitability by 10%.

Another aspect of the financial issue is from the point of view of the manufacturer. On the one hand, the cost of a claim is at least as high for manufacturers as for buyers. On the other hand, there are also some indirect consequences for manufacturers, such as the loss of business opportunities, which can be very costly in a small industry such as PV. In this regard, some third parties have already recognized that the assessment of quality should be cost effective and have made some efforts to support the buyers and the manufacturers with services that do not exceed 1% of the cost of the products.

"In this regard, some third parties have already recognized that the assessment of quality should be cost effective and have made some efforts to support the buyers and the manufacturers with services that do not exceed 1% of the cost of the products."

Conclusions

Even if most stakeholders have clearly understood the importance of providing quality modules, the question of what is a good quality product still remains unanswered. There are obviously some gaps in the current definition of IEC standards; compliance may be necessary for manufacturers to sell their products, but it is not sufficient to ensure the quality level of the product up to the buyers' expectations. On the one hand, tests are being developed to estimate the true reliability of products; on the other hand, screening of large quantities with simple and relevant tests remains necessary to separate the grain from the chaff. Third parties have to play an important role in helping both manufacturers and buyers to collaborate in the common goal of developing the industry for a brighter future.

References

[1] De graaf, D. 2011, "How do qualified modules fail – what is the root cause?", NREL Intl. PV Module Quality Assur. Forum, San Francisco, California, USA.

[2] Williams, D. 2011, "Financial investors' perspective on quality assurance", NREL Intl. PV Module Quality Assur. Forum, San Francisco, California, USA.

About the Author

Thibaut Lemoine received a master's degree in mechanical engineering from the French National Engineering School of Belfort (ENIBe) and a master's degree in international industrial business management from the University of Technology Belfort Montbeliard (UTBM). He has more than 12 years' experience in both the manufacturing field and quality control, having worked for major French groups in industries ranging from automotive and stationery to consumer electronics and PV. Thibaut has been in China for 10 years, working in partnership with major manufacturers, and is a co-founder of Senergy Testing Solutions Ltd, where he is currently the General Manager.

Enquiries

STS-certified Ltd.
2606-26/F BM Intercontinental Center
100 YuTong Road
Shanghai 200070
P.R. China
Tel: +86 21 32221065
Fax: +86 21 63816576
Email: thibaut.lemoine@sts-certified.com
Website: www.sts-certified.com

European Office
Feldchenstr. 32a, D-63743
Aschaffenburg
Germany
Tel: +49 15111238726
Email: europe@sts-certified.com

Power Generation

Desert Sunlight solar project gets go-ahead from Department of Interior; construction to begin soon

Joshua Tree National Park, California.

US Secretary of the Interior Ken Salazar has greenlighted the Desert Sunlight Solar Farm, a 550MW (AC) solar power project to be developed, built and operated by First Solar on 4100 acres of public lands in the California desert outside Joshua Tree National Park. Construction on the site is due to begin shortly.

Desert Sunlight is the beneficiary of a conditional loan guarantee commitment of US$1.88 billion, which was announced in June by the US Department of Energy.

Frank De Rosa, First Solar's senior VP of North American project development, has claimed the project will be the largest PV project on federally managed land in the US and one of the two largest PV solar projects in the world. Although he could not provide any detail on the timeline of the construction phases planned at the project or any update on a potential buyer/owner for the site, De Rosa did say that nearly nine million of the company's Series 3 cadmium telluride thin-film PV panels will be deployed.

First Solar has two signed power purchase agreements for the project, one for 250MW with Southern California Edison, the other for 300MW with Pacific Gas & Electric.

An onsite substation and a 230kV generation tie line will connect the project to the Red Bluff substation, which will convert the power from 230kV to 500kV for transmission on SCE's regional grid. De Rosa also noted that in regards to eventual interconnection of the power plants' output to the two utilities' grids, the solar company is not planning on energizing one off-taker before the other.

The PV farm will create more than 630 jobs at peak construction and pump an estimated US$336 million into the local economy. When built, Desert Sunlight will produce enough electricity to power over 165,000 homes. The project, located about six miles north of Desert Center, will also generate about US$27 million in sales and property tax revenue to Riverside County.

First Solar's 550MW system will be located in California's Joshua Tree National Park.

Asia News Focus

LDK Solar, Datang announce 20MW solar project in China

LDK Solar and Datang International Power Generation are planning to build a 20MW solar power plant in Qinghai, China. Work on the first 10MW installation phase is scheduled for August, with the entire project scheduled to be completed by the end of September. LDK will carry out engineering, procurement and construction on the site.

Indian solar projects secure financing

India's National Solar Mission has taken a major step forward by approving 35 new systems. The projects will contribute 610MW towards the government's goal of generating 20GW through solar by 2022.

Each project signed a power purchase agreement (PPA) with NTPC Vidyut Vyapar Nigam (NVVN) in January and was given six months to secure financial backing. All bar two of the 37 developers entering the auction were able to submit evidence they had arranged funding; the two rejected projects had capacities of 5MW.

Seven of the successful applicants are solar thermal projects – totalling 470MW – while the remaining 28 are regular PV systems, totalling 140MW. Among the companies building the larger thermal projects include billionaire Anil Ambani's Reliance Power and Lanco Infratech. They both faced forfeiting as much as INR1.89 billion (US$42 million) in bank guarantees if they failed to secure financial backing.

The PV developers have until January 2012 to install the systems, while the solar thermal projects have until 2013.

Schott Solar to supply 16MW of modules to Phoenix Solar projects in Thailand

Phoenix Solar Singapore has placed an order with Schott Solar for 67,000 PV modules, with a capacity of 16MW, for two projects near Bangkok, Thailand since June, 2011. The contract on supplying these modules was said to have been negotiated at this year's Intersolar Europe. The two installations are expected to go into operation by the end of 2011.

Schott Solar is supplying Phoenix Solar Singapore with polycrystalline modules from its 'Perform Poly 2xx' series to Thailand between June and September. The two system PV power plants are expected to achieve peak output of 9.7 and 6.2MW, respectively. From December, the plants are expected to supply an annual electricity yield of around 25,000MWh.

The project owner is Solarta, a joint venture between Yanhee Solar Power and the independent power supplier Ratchaburi Electricity Generating Holding.

Schott Solar module.

Canadian Solar reaches India in 33MW PV module supply deal for 2011

Cirus Solar Systems, an India-based solar engineering, procurement and construction company, has secured a 33MW PV module supply deal with Canadian Solar for several key projects. Module shipment has already begun and the agreement will last until the end of Q4. Canadian Solar said that the PV modules would be used in projects undertaken by Cirus Solar Systems for two prominent, but unnamed, Indian conglomerates.

Europe News Focus

Work begins on solarhybrid's 40MW Fürstenwalde park

Construction work has begun on one of Germany's largest solar parks. The 40MW system, located on the site of a former military airport in Fürstenwalde, is being built by solarhybrid at a total cost of €76 million.

Suntech is supplying the 173,712 modules for the installation, while SMA is providing the accompanying 46 inverters and Gestelltechnik the mounting systems. Grid connection has been pencilled in for

Source: solarhybrid

Building work at solarhybrid's 40MW Fürstenwalde project.

late October. When complete, Fürstenwalde is expected to produce around 36.5 million kWh of electricity per annum.

Fürstenwalde is the latest system solarhybrid and Suntech have collaborated on after forming a strategic partnership in May. The partnership will help solarhybrid fulfill a project pipeline totalling 81.5MW.

Activ Solar completes first phases of 80MW Ukrainian solar plant

Activ Solar has completed the first two phases of its record-breaking 80MW PV project in Ukraine. When all four stages are completed, the power station, located on 160 acres of land in Ohotnikovo, Crimea will be the fourth largest development in the world.

Source: Activ Solar

The first phase of Activ Solar's 80MW Ohotnikovo system.

Each installation phase will add 20MW to the system; the first has been connected to the grid and the second is expected imminently, while the remaining two are due to come online before the end of 2011. The finished park will be comprised of 360,000 modules, generating around 100,000 MWh of energy every year.

Acciona Energy activates 50MW Palma del Río CSP system

Acciona Energy has activated its new Palma del Río I solar thermal plant in Cordoba, Spain. The 50MW system is comprised of 792 solar collectors spanning 135 hectares and takes Acciona's CSP portfolio in Spain to 200MW.

The new system and its twin plant, Palma del Río II – which was connected to the grid in December 2010 – will generate enough electricity to meet the energy requirements of 70,000 homes in southern Spain. Around €500 million has been invested in the two plants.

Acciona has two other 50MW CSP plants in Spain and is building a fifth at Orellana in Badajoz, which has a penciled-in completion date of late 2012. Mitsubishi has a 15% stake in the four systems.

Enel Green Power to build to CSP plants in southern Europe

Enel Green Power (EGP) is to continue the diversification of its energy portfolio by building two concentrated solar power (CSP) plants in southern Europe.

Source: Torresol

An aerial view of Torresol's 19.9MW CSP plant in Spain.

The first of these developments, a 30MW standalone parabolic-trough plant, will be in Sicily, Italy, while the second, a 25MW system linked to a water desalination project, is to be located in a yet-to-be-identified Mediterranean country, according to Sauro Pasini, the head of engineering and innovation research at Italian utility Enel.

Until recently, the majority of EGP's 6.2GW renewable portfolio was made up of wind (44%) and hydro (41%) projects, with solar accounting for less than 2%. However, this looks set to change, with the two CSP plants being the latest sign that the company is looking to establish itself as a prominent figure in Italy's solar industry; last week Enel opened a 160MW thin-film module manufacturing facility in Sicily alongside co-owners Sharp and STMicroelectronics.

EGP's decision to invest in CSP represents a significant vote of confidence for the fledgling technology, which has come under scrutiny from some industry analysts who feel rapid price declines for PV components may soon make it uncompetitive.

But unperturbed by the question marks surrounding its future, several developers have moved ahead with CSP ventures, including Torresol's 19.9MW Gemasolar project in Spain, which recently become the first plant to feed an uninterrupted 24-hour supply of electricity into the grid.

US & Canada News Focus

BrightSource submits certification application to CEC for 500MW CSP solar power plant in California

BrightSource Energy has submitted an Application for Certification (AFC) with the California Energy Commission (CEC), which calls for the construction of a 500MW solar project in Inyo County, California. The Hidden Hills Solar Electric Generating System (SEGS), located on 3,280 acres of privately owned land next to the California and Nevada border, will consist of two 250MW solar thermal power plants, which will each have its own solar field and solar power tower. The two CSP plants will generate power for Pacific Gas & Electric (PG&E) under two PPAs that were approved by the California Public Utilities Commission in 2010.

The company stated that its plans to use its LPT solar thermal energy system at the Hidden Hills SEGS project will minimize the impact to the area's surrounding environment, with each plant utilizing a taller tower so that a greater concentration of heliostats can be achieved. BrightSource also plans to place mirrors on individual poles that will then be positioned directly into the ground, which the company claims gives the solar plant the ability to be built around the natural forms of the land. Given that the project will be constructed in a desert region, BrightSource advised that it would use an air-cooling system to convert steam back into water in a closed-loop cycle using only 140-acre feet of water per year and therefore conserving water for the region.

Commercial operation begins at NRG Solar, Eurus Energy America's 45MW plant

Commercial operation has begun at California's largest solar power project after NRG Solar and Eurus Energy America activated their 45MW Avenal Solar Generating Facility in Kings County.

Source: PR Newswire

Avenal Solar Generating Facility is the largest completed solar park in California.

The facility was developed by Eurus and the electricity produced will be sold to Pacific Gas & Electric (PG&E) under separate 20-year power purchase agreements. When operating at full capacity, the three systems that make up Avenal – Avenal Park, Sun City and Sand Drag – will use 450,000 Sharp tandem-junction amorphous silicon modules and generate enough electricity to cater to the energy requirements of 36,000 Kings County homes. The total cost of the project is approximately US$220 million.

US DOE fronts US$50 million for PVMI Part II, SUNPATH

A US$50 million fund from the US Department of Energy is up for grabs for any domestic PV manufacturer wanting to take solar technology from the lab to the fab. The funding program is the second solar Sunpath Photovoltaic Manufacturing Initiative (PVMI) initiative launched by the DOE and is designed to support companies with pilot level commercial production facilities to rapidly scale up their manufacturing capabilities.

The key criterion for funding is the demonstration of innovative, low-cost solar technologies, which are in certain areas already being supported via the PVMI initiative. The DOE said that its national laboratories were stepping up their validation facilities to ensure that the technologies developed and manufactured in PVMI Parts I and II are tested at scale in multiple locations and climates in the United States.

The DOE is seeking applicants with industrial-scale demonstrations of PV modules, cells, or substrates that offer lower-cost solutions in line with the SunShot goals. The deadline for applications is October 28.

PG&E decides on project developers for its 50MW Californian solar portfolio

US utility giant Pacific Gas & Electric (PG&E) has chosen the three project developers charged with installing its 50MW Californian solar portfolio. Building work on the systems is scheduled to begin in February 2013 and when completed they will contribute towards PG&E's five-year effort to add 250MW of utility-owned generation.

The successful bidders – selected through the utility's 2011 solar PV solicitation – were Recurrent Energy, Fotowatio Renewable Ventures and Westlands Solar Farms; they will build projects in Kings County (20MW), Kern County (12MW) and Fresno County (18MW) respectively.

Each system has a 20-year power purchase agreement with PG&E and will help the utility meet California's 33% 2020 renewable portfolio standard by 2020.

Source: First Solar

With a capacity of 48MW, Copper Mountain is the largest completed project in the US.

Rest of the world News Focus

Sistema de Energia Renovavel to install 600MW of solar capacity in Brazil by 2020

A new green initiative in Brazil, titled Sistema de Energia Renovavel (SER), is planning to install 600MW of solar capacity throughout the country by 2020. SER hopes that within six years, the new systems – the first of which is scheduled to come online next year – will provide electricity at prices comparable to rival energy sources.

Despite Brazil's high irradiance levels, solar accounts for a tiny percentage of the country's energy portfolio. However, falling equipment prices and increased government support means this is all set to change, and SER is putting itself in position to capitalize. Its first project will have a capacity of 5MW and be located in one of the northeastern states of Bahia, Paraiba, Rio Grande do Norte and Ceara.

SER is projecting that the systems in its portfolio will generate up to 6.5kWh of electricity per square metre every day – figures that have already attracted interest in Brazil's PV potential from further afield.

One possible panel supplier to emerge is Arizona-based First Solar, which has a partnership with Spanish solar company and SER stakeholder Assyce Fotovoltaica Sociedad.

Donauer Solartechnik installs solar system at health centre in Gambia

With a third of its population below the international poverty line and many more living without access to electricity or clean water, Gambia is one of the world's poorest nations. It is also one of the world's great untapped solar resources.

And with these two facts in mind, module supplier Donauer Solartechnik has taken on the role of philanthropist by donating a rooftop PV system and solar powered water pump to River Boat Doctors International's (RDI) health centre in Buniadu.

Originally the off-grid system was not intended to be a charitable donation. However, Donauer Solartechnik owner Rudolf Donauer was so convinced of the worthiness of RDI's work in Gambia that he offered to install the system free of charge.

Archimede Solar Energy, Chiyoda to develop CSP plants in Middle East and North Africa

Japanese engineering and construction firm Chiyoda has signed a cooperation agreement with Italy-based Archimede Solar Energy (ASE) for the development of CSP projects in the Middle East and North African (MENA) regions. This will be Chiyoda's first venture in the CSP plant market with its experience mainly found in developing petroleum and petrochemical industrial plants.

Chiyoda plans to become an IPP developer using ASE's proprietary molten salt CSP technology. ASE maintains that it is the only global producer of commercially available solar receiver tubes, which use solar thermodynamic plants that run with parabolic trough technology using sodium and potassium nitrate as their heat transfer fluid.

Although a development timeline was not released, the companies advised that they are dedicated to realizing CSP plants using the molten salt receiver tubes in the MENA region.

Soitec, Schneider Electric to promote CPV in Morocco

Soitec and Schneider Electric have signed a memorandum of understanding (MOU) with the Moroccan Agency for Solar Energy (Masen) to develop concentrated photovoltaics (CPV) technology in the North African country.

The MOU is part of the Moroccan Solar Plan and will focus on creating a CPV sector capable of catering for Morocco's rising domestic energy demand. Among its core aims is the construction of two 5MW pilot plants; the first will be located in Ouarzazate and is set to be completed in early 2012, while the second is still awaiting approval from the partners.

The MOU's three other key goals are: an in-depth research and development initiative; the creation of a local supply chain for CPV system components; the establishment of a CPV-trained workforce.

Source: Wikipedia

Old town of Ouarzazate (Medina) in Morocco.

Product Reviews

Suntech

Suntech's 250W BlackPearl module offers 10% more power than conventional modules

Product Outline: Suntech Power's STP250S-20/Wd+ BlackPearl high-efficiency module is powered by a new generation of crystalline silicon cells. The BlackPearl modules achieve up to 15.2% conversion efficiency, approximately 10% more power than conventional polycrystalline products.

Problem: There is an ever-present need to offer cost-competitive conventional polycrystalline modules at higher efficiencies to meet residential rooftop rates of return on investment, especially in a period of declining feed-in tariff rates. Advanced cell and module designs give higher performance but are more expensive to produce and increase the up-front purchase cost for consumers.

Solution: The BlackPearl 250W product is a 60-cell module comprised of six-inch black square cells that delivers one of the highest power-per-weight ratios in the industry. The module features a +0 to +5% positive power tolerance and low oxygen content, which gives it strong resistance to light-induced degradation. All Suntech BlackPearl modules feature an anti-reflective surface that traps the sunlight into the cells, as well as a hydrophobic self-cleaning surface structure. In addition, the modules are built to withstand all weather conditions including 3,800N/m^2 (~270km/h) wind load and 5,400N/m^2 (~55kg/m^2) snow loads.

Applications: The product is ideally suited to rooftop installations where weight, power and aesthetics are key customer considerations.

Platform: Utilizing technology different from that of the company's Pluto products, the BlackPearl module is comprised of six-inch square cells that contain minimal oxygen content and achieve 18% conversion efficiency at cell level.

Availability: Currently available in Europe.

Advanced Energy

Advanced Energy's Solaron 500kW PV inverters achieve 98% efficiency

Product Outline: Advanced Energy Industries has improved the performance of its 500kW Solaron PV inverters, which have achieved a 98% efficiency rating from the California Energy Commission (CEC), a record-breaking efficiency rating that is between one and three percentage points higher than comparable commercial and utility-scale solar PV inverters in this power class.

Problem: Inverter efficiency determines the amount of energy converted from a solar array to power that is delivered to the system owner, financier or utility. Each percentage increase in efficiency leads to additional kilowatt-hours of energy produced, resulting in more cash and RECs generated from a solar PV system. When properly balanced with cost and long-term reliability, incremental gains in efficiency can lead to a significant improvement in project profitability.

Solution: Advanced Energy's new Solaron 500 HE inverters are claimed to be able to generate more cash-flow for project developers, owners and financiers via the improvement of peak energy efficiency to 98.7% and weighted efficiency to 98%. The CEC is the leading North American agency for reviewing, compiling information and approving inverters for commercial use.

Applications: Commercial- and utility-scale PV power plants.

Platform: Solaron and PV Powered inverters are said to be easy to install and are accompanied by SiteGuard whole-site O&M services.

Availability: Currently available.

Unique Solutions

Unique Solutions offers mobile module testing unit for PV large-scale installations

Product Outline: Unique Solutions, a division of Unique Solar Bremen, has launched its new module inspection system, the LazySusan. The inspection unit can be used to check complete modules for damage, as in damaged fingers or busbars, cracks and ineffective cell areas. Unique Solutions has constructed a mobile testing unit called which can be transported by mini van to any required location.

Problem: Importers or insurance companies can never be sure whether the modules bought locally or overseas are of the requisite quality, and there is therefore a need to check for damages before installation, especially large-scale PV projects.

Solution: The modules are inserted into the testing device, connected to the power unit and checked using the EL process. High resolution cameras take a picture of all cells, the result of which is displayed on a computer screen, making cracks, inactive fingers, structural damage and cell defects visible. The LazySusan is lightweight, flexible and is equipped with a scanning unit to scan the bar codes of the modules. All information is displayed on a touch screen and can be traced back to each single module. Information can be saved on an external hard disc, printed out or sent by email to the office for further handling. The unit can be set up within 15 minutes and the scanning process only takes seconds. Evaluation of the module must be carried out by the human eye in the basic version. Advanced- and Profi- versions allow defect are indication by colour marking.

Applications: Inspection of modules for cracks, imperfections and defects..

Platform: Size: approx. 1400 × 990 × 1910mm; weight approx. 65kg, 230V. The system is available in three different formats: LazySusan Basic, LazySusan Advanced and LazySusan Profi.

Availability: Currently available.


Q.CELLS
YIELD SECURITY
ANTI PID TECHNOLOGY (APT)
HOT-SPOT PROTECT (HSP)
TRACEABLE QUALITY (TRA.Q™)
3 × SAFE! FOR HIGHER YIELDS
Our new product generation not only offers highest efficiencies – thanks to the Q.CELLS Yield Security, our cells and modules are also the safest and most reliable on the market.

Diversified Technologies

Diversified Technologies' micro-grid power distribution system handles 1MW of power transfer

Product Outline: Diversified Technologies has introduced a new micro-grid power distribution system for the simple integration of solar power generators by transmitting DC power along a cable suitable for up to 1MW of power transfer. The PowerMod Micro-Grid Power Distribution System features direct solid-state switching and includes a DC power supply, DC cable and down converter for providing AC or DC power at the load end point. This new power distribution system is said to offer a link cost as low as US$1.00 per Watt, depending upon configuration.

Problem: A generator or load can be placed anywhere along the system's cable, thus eliminating the common issue of the limitations displayed by AC point-to-point installation.

Solution: DTI's universal high-frequency power converter architecture can be used for a wide range of applications requiring AC-to-DC and DC-to-DC power conversion. The higher control bandwidth provided by high-frequency switching allows the output power to be highly regulated into nonlinear and transient loads. This technology can also be applied to variable frequency power converters. The system can provide a constant 10kV DC transmission at up to hundreds of kilometres for wind turbines and solar power generators.

Applications: Micro-grid power distribution suitable for up to 1MW of power transfer.

Platform: The PowerMod Micro-Grid Power Distribution System uses PowerMod High Voltage Solid-State Switch Modules that provide over one million hours of predicted reliability per MIL-HDBK-217F. The system includes a DC power supply, DC cable and down converter that enables AC or DC power at the load end point.

Availability: Currently available.

Enphase Energy

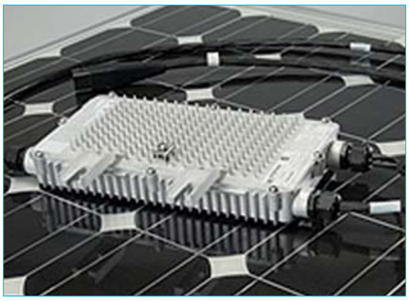

Enphase Energy's 215-Series microinverter comes with 25-year limited warranty

Product Outline: Enphase Energy's new 215-Series microinverter comes with a 25-year limited warranty and an electrical interconnection system – the Engage System – for streamlining solar installations.

Problem: As they are relatively new to the market, microinverters have so far been used mainly as a bolt-on additional product. Simplifying system integration costs while improving conversion efficiencies could significantly reduce installation costs and make microinverters more cost competitive.

Solution: The M215 is claimed to be the only microinverter to achieve a weighted power conversion efficiency of 96% (CEC). All 215-Series microinverters incorporate Enphase's third-generation technology, which, with an output 13% higher than previous generations, was specially developed to maximize the performance of 60-cell PV modules. The Engage System incorporates the Engage Cable, which comes with built-in connectors that can support an entire 4kW system on a single branch. The Engage Cable can be cut to length and also comes with additional cable termination and splice kits to further reduce BOS requirements. The Engage Port is designed to replace the standard DC junction box on a module, enabling module manufacturers to easily integrate the microinverter technology into their product portfolio.

Applications: Integrated AC modules for residential and commercial applications.

Platform: The 215-Series microinverter delivers a platform for ACM or solar modules with integrated microinverters. The platform offers a simple connector that replaces the junction box and allows easy integration of this technology into new ACM product lines.

Availability: Currently available in North America with CSA certification; soon to be available in Europe with VDE certification.

Power-One

Power-One's 1.4MW PV inverter offers greater reliability and shorter maintenance cycles

Product Outline: Power-One has introduced its new Aurora Ultra-1400 central inverter with an output power of up to 1.4MW. The central inverter – the largest product in the Power-One RE offering – is liquid-cooled and has been designed for large commercial and utility-grade installations.

Problem: Maximizing yield from large commercial and utility-scale PV power plants requires improved uptime and energy harvesting through a reduction in downtime caused by the failure at the inverter level or the photovoltaic field.

Solution: The Aurora-Ultra inverter has power conversion efficiencies of up to 98.7% combined with an extra wide input voltage range and multiple MPPT channels, which optimize energy harvesting across a wide array of operating conditions. The main feature of the new system is represented by its IP65 enclosure with passive liquid cooling and total segregation of internal compartments that extends the maintenance cycle and reduces the cost of maintenance. The product is equipped with an internal recombiner compartment with up to 24 individually fused inputs. Due to the circuit topology, the output voltage is 690V (AC) which allows a significant reduction of AC losses and the possibility of direct coupling with LV/MV standard transformer used in the large wind industry.

Applications: Large commercial and utility-grade installations.

Platform: This large inverter system can be monitored via Ethernet communication and two independent RS-485 communication interfaces for inverter and intelligent string combiner monitoring. It is compliant to BDEW (German Federal Association for Energy and Water) and FERC 661 (Federal Energy Regulatory Commission) specifications.

Availability: Currently available.

Product Reviews

National Semiconductor

National Semiconductor's SolarMagic chipset and firmware detect arc faults in PV system

Product Outline: National Semiconductor has introduced the SolarMagic arc detection reference design, comprised of analog front-end integrated circuits (ICs) and multi-band dynamic filtering firmware. The company claims that this is the first commercially available chipset to detect hazardous DC arc faults in PV systems.

Problem: Intermittent connections or insulation deterioration (faults) can cause DC circuits to generate arcs of considerable energy in PV systems, which can pose safety risks to surrounding infrastructure and personnel.

Solution: A sophisticated signal processing approach is required to reliably detect the entire range of dangerous arcing events without false alarms when the PV array is operating under safe conditions. National Semiconductor has developed a patent-pending signal processing approach. The MBDF firmware uses a state-of-the-art abstracted pattern recognition approach that does not require the arc signature to match a rigid, pre-described, absolute shape.

Applications: Arc detection for solar modules.

Platform: National's SolarMagic chipset is an analog front-end (AFE) featuring three highly integrated ICs. The SM73201MM 16-bit, 50 to 250kSPS, differential input, micropower ADC digitizes the arc signal after the AFE gain and filtering stage, and sends the digital signal to the microcontroller. The SM73308MG low offset, low noise, RRO operational amplifier provides the V_{ref} mid-point for the arc-detect AFE. The SM73307MM dual precision, 17MHz, low noise, CMOS input amplifier provides gain and filtering of the arc signature signal.

Availability: Currently available; SolarMagic arc detection chipset is available in a variety of industry-standard electronic packages.

SolarEdge

New power optimizers and unique string monitoring combiner box from SolarEdge

Product Outline: SolarEdge Technologies has launched its next generation of module power optimizers and a unique string monitoring combiner box with ground fault detection and interruption (GFDI) per string. The optimizers boast record efficiency of 99.5% (98.8% EU weighted efficiency), and are claimed to enable production of up to 25% more energy and faster ROI in residential, commercial and large-scale PV systems through module-level MPPT and monitoring.

Problem: The ongoing focus on conventional PV inverter performance and reliability is a result of the need to offer the maximum IRR on projects, regardless of size. Module power optimizers are becoming increasingly sophisticated to offer improved efficiencies and higher reliability.

Solution: With a new, highly efficient ASIC chipset and 32% lower part count, the new power optimizers are more efficient and 40% smaller in size. A selection of cutting-edge components and improved dynamic control are combined with an enhanced per-module MPPT algorithm that dynamically tracks the global maximum operating point for both module and inverter. Ground leaking strings are automatically alerted and isolated through up to 64 individual string disconnects, and are controlled and monitored locally and remotely.

Applications: Various models will support residential, commercial and large-scale installations.

Platform: Warranted for 25 years, the new power optimizers are enhanced with SolarEdge's 'SafeDC' features: automatic electric arc detection and termination, and automatic module shutdown in case of inverter or grid shutdown. The SolarEdge inverters (98% maximum efficiency) are specifically designed to work with power optimizers.

Availability: Currently available.

Solyndra

Solyndra offers non-penetrating easy mount system for commercial metal roof market

Product Outline: Solyndra has launched the Solyndra 200 Series Metal Roof Solution, a non-penetrating adjustable mounting system that is designed to meet the additional solar installation challenges posed by metal roofs. Metal roofs make up a significant and growing portion of the large, low-sloped, commercial, industrial and agricultural rooftop markets.

Problem: Attaching conventional racking to metal roofs often damages the structure and could compromise the integrity of the roof. Therefore, a lightweight, non-ballasted and non-penetrating PV system design is required for metal roofs.

Solution: Adapted from Solyndra's 200 Series mounting system, the new metal roof mounts require no tools in the assembly process and are adjustable to meet the majority of low-slope metal roof configurations supplied by the industry's metal roof manufacturers. The innovative adjustable mount design has no attachments and uses no tools, enabling fast and easy installation. The low, 2.8lbs-per-square-foot distributed load allows for simple installation without ballast or penetrations in winds up to 130mph when installed in accordance with Solyndra's installation guidelines.

Applications: Large, low-sloped, commercial, industrial and agricultural rooftop markets.

Platform: Although not essential to the system, customers can maximize power from Solyndra's cylindrical solar modules by choosing white or reflective 'cool roofs,' conserving energy and reducing ambient heating caused by rooftops while generating more power.

Availability: Currently available.

Grid connection requirements and test procedures: Experiences in the certification process of PV inverters

Dominik Geibel, **Dr. Gunter Arnold** & **Dr. Thomas Degner**, Fraunhofer Institute for Wind Energy and Energy Systems Technology (IWES), Kassel, Germany

ABSTRACT

The new German BDEW MV guideline demands static and dynamic functionalities from distributed energy resource (DER) units in order to support network operation and stability. Initial indications show that, in general, photovoltaic (PV) inverters are able to fulfil both the static and the dynamic requirements. Besides the new requirements of the guideline, an extensive certification process for DER units and plants has also been introduced. During initial certification processes, a significant need for PV-specific test procedures and test equipment has been determined. This article describes the developments within this area from the perspective of a measurement institute.

Introduction

The strong increase in installed distributed energy resources (DERs) has a major influence on network behaviour. By the end of 2010, more than 55GW of renewable generation had been installed in Germany, of which 17.3GW fell upon PV. At the end of 2009, more than 23% of all PV systems with an installed capacity of 2279MW were connected to medium- and high-voltage grids [1]. The share of 'large' PV systems above 100kW rated power is showing a strong increasing trend.

Due to the large growth in the numbers of DER units, the adaptation of interconnection requirements has been under discussion, at the national and international level, between network operators, manufacturers, DER plant operators and research institutes. A paradigm change of the role of DER units is occurring. Commonly, in the past, DER units were not permitted to take an active role, but nowadays all DER technologies are asked to support the network in terms of static and dynamic issues [2].

In Germany, since January 2009 the new BDEW guideline [3] for interconnection of DER units to the MV network has been in force. From the beginning of August 2011, advanced interconnection requirements for the LV networks also come into operation.

In addition to the release of the new BDEW MV guideline, a certification process for all kinds of DER units and plants has been introduced. This procedure is already familiar for wind turbines, but had to be extended to all other DER technologies with all the

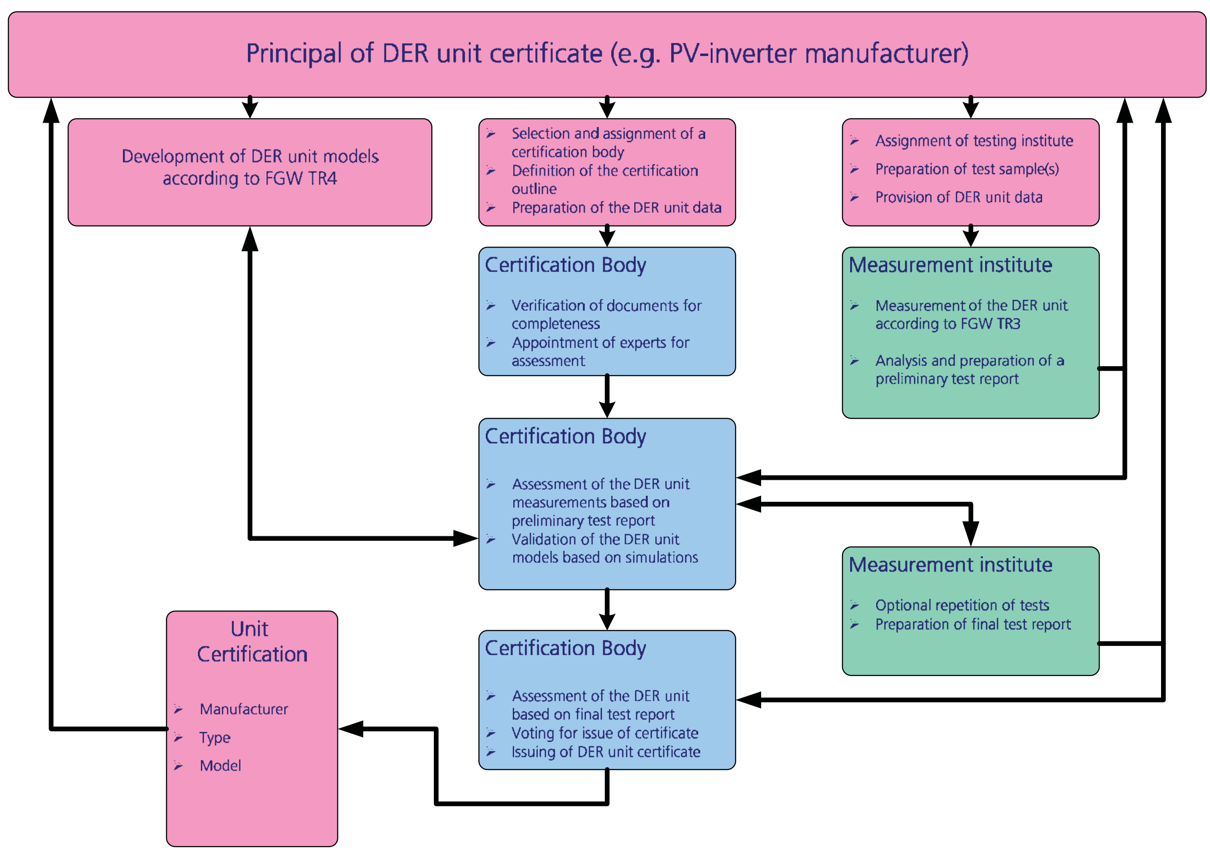

Figure 1. Flow chart of the process of unit certification.

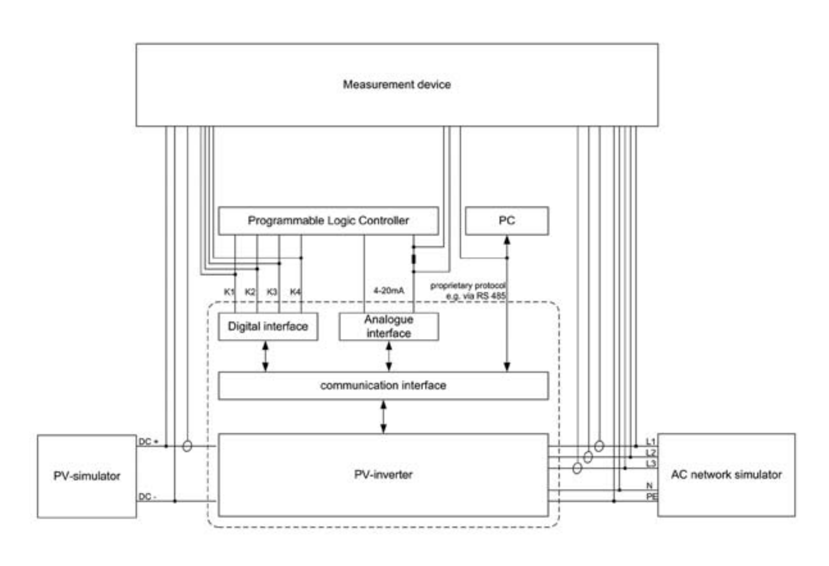

Figure 2. General measurement set-up of a PV inverter for measurements according to FGW TR3.

associated implications. This has resulted in several temporary regulations since, on the one hand, the development of the new inverter functionalities required a lot of time and resources from the manufacturers and, on the other hand, adapting the existing certification guidelines of wind turbines to other DER units with different primary energy sources posed a challenge.

This article concentrates on testing issues arising within the certification process. A short overview of the general certification procedure is given first, followed by a description of new test procedures especially developed for PV inverters. Additionally, requirements for testing PV inverters regarding laboratory infrastructure are discussed. The new functionalities of the BDEW MV guideline are explained by presenting measurements achieved during certification processes carried out by Fraunhofer IWES.

Procedure of unit certification according to FGW TR8

As evidence of compliance with the new BDEW MV guideline, it is mandatory to obtain unit and plant certificates. Therefore the procedure of certification according to FGW TR8 will be briefly described as follows.

Since January 1st 2009, the grid-conformance behaviour of distributed generating systems (such as a solar or wind farm) connected to the public MV network must be validated by a so-called unit certificate. Additionally, for plants above 1MVA rated power, a plant certificate based on the unit certificate is required. The temporary regulation allowed PV units to delay the fulfilment of the static requirements stated in the BDEW MV guideline until July 1st 2010, and of the dynamic requirements until April 1st 2011.

By nature, the principal of the unit certificate (typically the manufacturer of the DER unit) plays a decisive role within the certification process. Fig. 1 shows the significant steps of the procedure and the participants – the manufacturer, the certification body and the measurement institute. For achieving conformance with the BDEW MV guideline, measurements according to FGW TR3 [4] and validation of simulation models according to FGW TR4 [5] have to be carried out. Based on these results a certification body is allowed to issue a unit certificate guaranteeing that the requirements of FGW TR8 [6] have been fulfilled.

Laboratory infrastructure for measurements according to FGW TR3

General measurement set-up for a PV inverter

Fig. 2 shows a general set-up of a PV inverter for taking measurements according to FGW TR3. Besides the acquisition of voltages and currents on the DC and AC sides of the PV inverter inputs and outputs, the set points supplied to the communication interface of the PV inverter have to be recorded synchronously. Since several kinds of set point signals are commonly used – e.g. RS 485 (for internal farm communication), digital signals from a ripple control receiver or analogue signals – the measurement equipment should provide various flexible inputs for the acquisition of set point signals.

Usually, RS 485 signals are generated via manufacturer-specific software commands and sent from the PC to the PV inverter. If digital or analogue interfaces are used, the set point signals can be easily generated in the laboratory via a programmable logic controller (PLC).

Requirements for the DC source

Using a PV generator is not mandatory for the supply of the PV inverter at the DC terminals, since FGW TR3 states that module-independent tests are sufficient for the determination of the behaviour on the AC side. Instead of a PV generator, it is possible to use a variable DC voltage source which fulfils the requirements of Annex E of FGW TR3 regarding power and voltage range, control mode and dynamics. This simplification is especially meaningful with regard to high-power applications, since a real PV generation in this power range proves to be quite costly. For testing string inverters, the use of PV simulators is quite common. This ensures that the characteristic curve of a PV array is provided to the PV inverter, even during transient events such as radiation changes or network faults.

Requirements for the AC network simulator

If the power rating of the DER unit is of the order of a few kilowatts, it makes sense to use a network simulator for the measurements instead of connecting the DER unit to the public network. This procedure offers advantages, especially for the test of power quality parameters and of low-voltage ride-through (LVRT). Of course, the network simulator has to fulfil certain requirements in order to achieve a behaviour comparable to a public network. A basic requirement is that each phase of the simulator be controlled independently in amplitude and phase angle; controlling the frequency should also be possible. Furthermore, the usage of a physical impedance network for emulation of a network connection point with certain parameters – short-circuit power S_k and network impedance angle ψ_k – is mandatory.

For DER units with power ratings up to 90kVA, the laboratory at Fraunhofer IWES offers a network simulator with the aforementioned requirements. This 4-quadrant AC network simulator, consisting of linear amplifiers, provides the possibility of reproducing any desired network behaviour.

Test infrastructure for high-power applications

For economic reasons, it is nearly impossible to provide such high-class test equipment for DER units with higher power ratings. A balance has to be struck as to which kind of test infrastructure is used for certain power levels. It is obvious that a general solution cannot be given. However, Fraunhofer IWES has set up a reference laboratory for testing DER units in the higher power range; the developed concept is shown in Fig. 3 and will be briefly described below. The reference lab is integrated within the new test centre IWES-SysTec of Fraunhofer IWES for Smart Grids and Electro mobility (see Fig. 4).

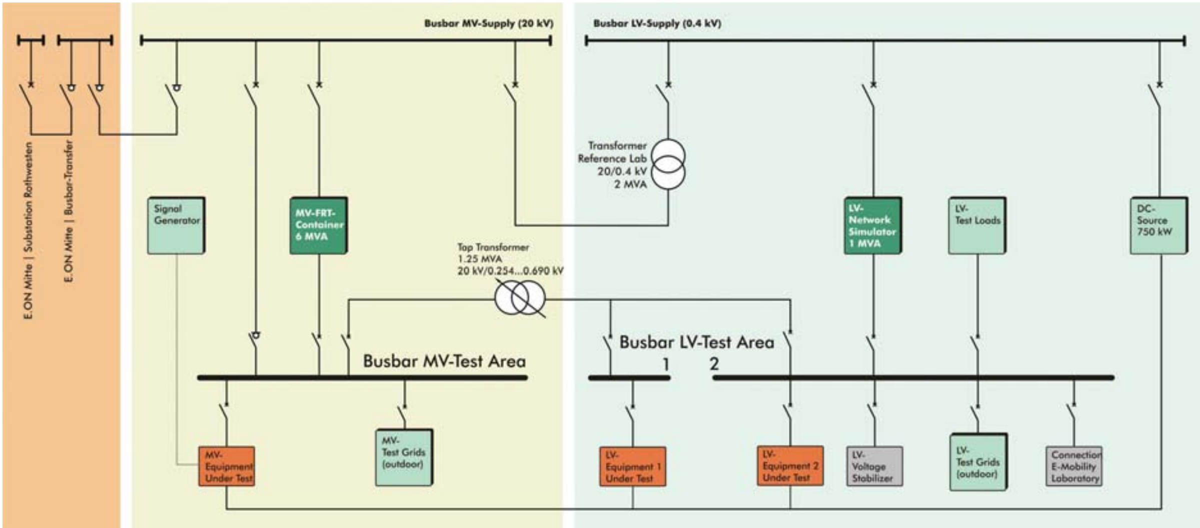

Figure 3. Schematic of the new reference laboratory of Fraunhofer IWES at IWES-SysTec for testing DER units in the higher power range.

Source: Fraunhofer IWES, Frank Hellwig

Figure 4. IWES-SysTec: new test centre of Fraunhofer IWES for Smart Grids and Electromobility.

The IWES reference lab offers the possibility of testing DER units rated up to 1.25MVA on an LV level and up to 6MVA on an MV level. The testing possibilities are not limited to PV inverters; moreover, new network elements such as voltage stabilizers or controllable transformers can be integrated as equipment under test into the reference lab.

> "The IWES reference lab offers the possibility of testing DER units rated up to 1.25MVA on an LV level and up to 6MVA on an MV level."

Different test beds on the LV and MV levels for static and dynamic requirements have been developed and set up. At the LV level, the static requirements are covered by using an LV network simulator with a nominal apparent power of 1MVA. At the MV level, for testing static requirements, a signal generator is connected to the secondary systems (controller, protection, etc.) of the DER unit. The dynamic requirements are tested by using a so-called

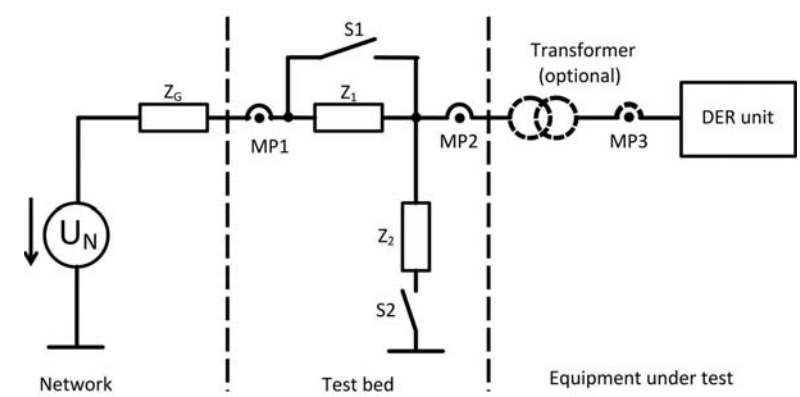

Figure 5. Simplified schematic of the LVRT container according to FGW TR3.

Nominal network voltage Rated power of the EUT	10/20kV 0.25–6MVA
Short-circuit power of the connection point	80–350MVA
Ambient temperature	–25 to +60°C
Operating temperature	0 to +50°C
Humidity	≤ 70% average per day
Test bed assembly	40-foot Maritime High Cube container

Table 1. Technical details of the mobile LVRT container developed by Fraunhofer IWES.

LVRT container. This mobile container is connected in series between the DER unit and the public MV network and generates network faults on the MV level without disturbing the public network. The simplified schematic of the developed system is shown in Fig. 5 and technical details are given in Table 1. For DER units with LV outputs, a step transformer with a wide voltage range (from 254V to 690V) is used for connecting these units to the LVRT container.

Development of PV-inverter-specific test procedures

As a basis for obtaining the unit certificate, measurements have to be carried out in order to prove compliance with the BDEW MV guideline. The measurement institute has to be accredited according to DIN EN ISO/IEC 17025. The applied test procedures are described in FGW TR3 and, although they were originally developed for wind turbines, nowadays all kinds of DER units (wind, photovoltaic and biomass) have to be tested according to these procedures. Therefore a combination of adapted existing test procedures and newly developed procedures for each kind of primary energy source has to be used. The reasons for this are that primary energy sources (sun, wind, etc.) behave differently, and the units to be certified have widely varying power ratings, ranging from a few kilowatts (e.g. string inverters) to several megawatts (e.g. central inverters).

Several committees within the FGW association are responsible for the adaptation and development of the PV-inverter-specific test procedures. Through the collaboration of certification bodies, measurement institutes and manufacturers, achieving a target-oriented approach for modification of the FGW guidelines should be ensured. In particular, during the first certification processes for PV inverters, a lack of clarity in existing test procedures was identified and brought to the attention of the corresponding committees. As a result of this, several new test procedures for PV systems were created.

Test procedure for LVRT

According to IEC 61400-21 [5], LVRT tests have to be carried out by generating network faults at the MV level, but these test procedures are not meaningful for PV inverters with low-power ratings (≤ 100kW). Therefore FGW TR3 also allows testing LVRT behaviour by providing network faults at the LV level (according to Annex F.2). However, it must be ensured that the faults have the same behaviour as if they were generated at the MV level. The vector group of the MV/LV transformer has to be considered, especially for unbalanced faults. Fig. 6 shows the difference during the fault for a Dd and a Dy transformer.

If LVRT tests are conducted with a network simulator, it must be possible to control the voltage amplitude and the phase angle of each line independently, with very high slew rates (> 30V/µs for the network simulator used). In order to provide realistic network conditions, a physical impedance network for setting up the short-circuit power and the network impedance angle

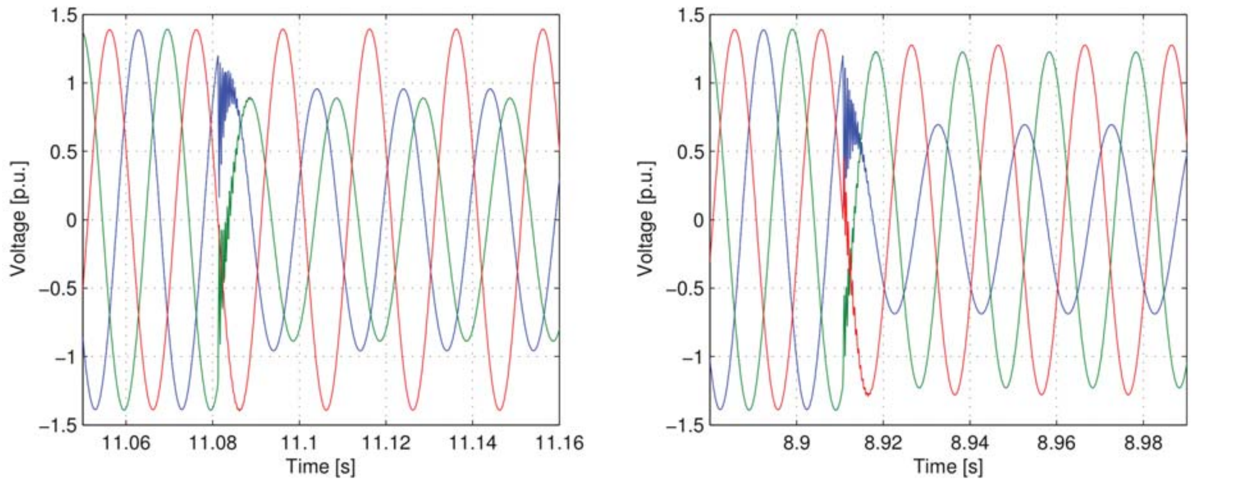

Figure 6. Measured voltages during unbalanced faults. Left: Dd MV/LV transformer. Right: Dy MV/LV transformer.

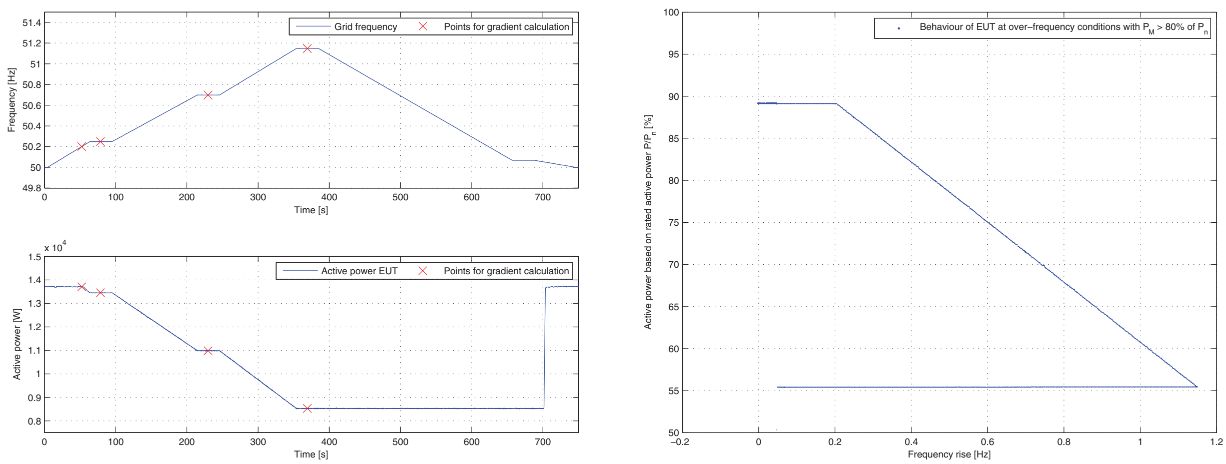

Figure 7. Measurement results for active power reduction corresponding to the over-frequency behaviour of the STP15000TL string inverter.

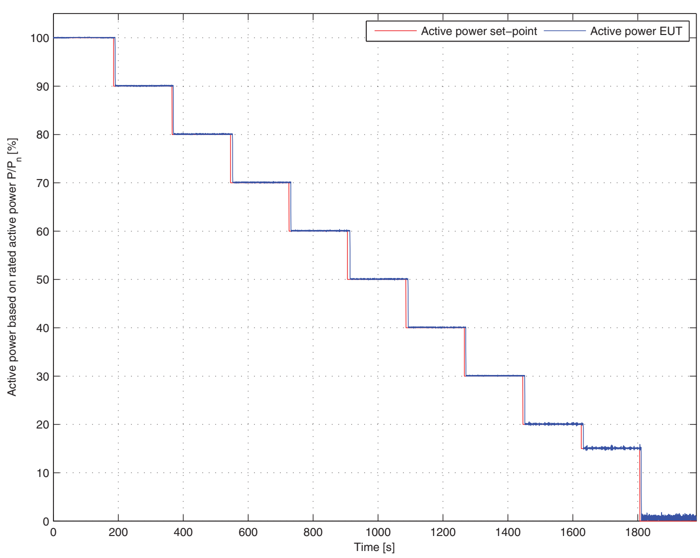

Figure 8. Measurement results for the STP15000TL string inverter with active power reduction by the network operator.

is used. Besides the network impedance, the impedance of the transformer and the cables of the DER unit should be taken into account in the impedance calculation.

Confirmation of electrical properties of PV inverters according to German BDEW MV guideline

In the BDEW MV guideline, several requirements concerning static and dynamic behaviour of DER units are described. They can broadly be grouped as follows:

- Active power provision, including set point control and power reduction in an over-frequency condition
- Reactive power provision by set point or characteristic curve (Q(U), cosφ(P))
- Power quality issues such as switching operations, flicker, harmonics, interharmonics and higher frequency components

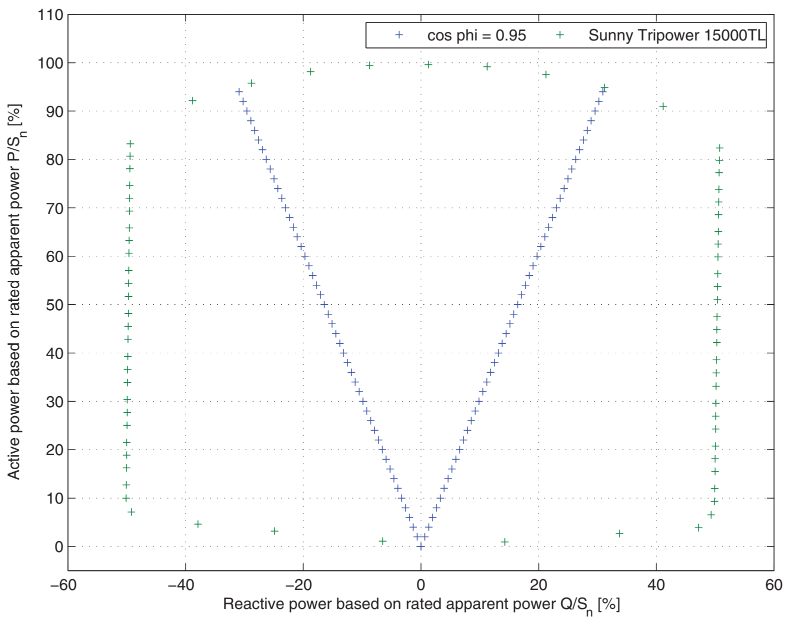

Figure 9. Measured reactive power capability of the STP15000TL string inverter.

- Grid protection
- Connection conditions
- Response to voltage drops (LVRT)

The most important new functionalities concerning grid integration issues, namely active power and reactive power provisions as well as LVRT, are described below. The mode of action of these functionalities is clarified by presenting the measurement results obtained at the Fraunhofer IWES laboratory for the certification process of the SMA Solar Technology string inverter Sunny Tripower STP15000TL.

Active power

The new functions for active power control enable the DER unit to reduce the actual power output in case of network congestion. This power reduction is either done locally, and automatically if there is an over-frequency situation in the network, or done remotely by the network operator.

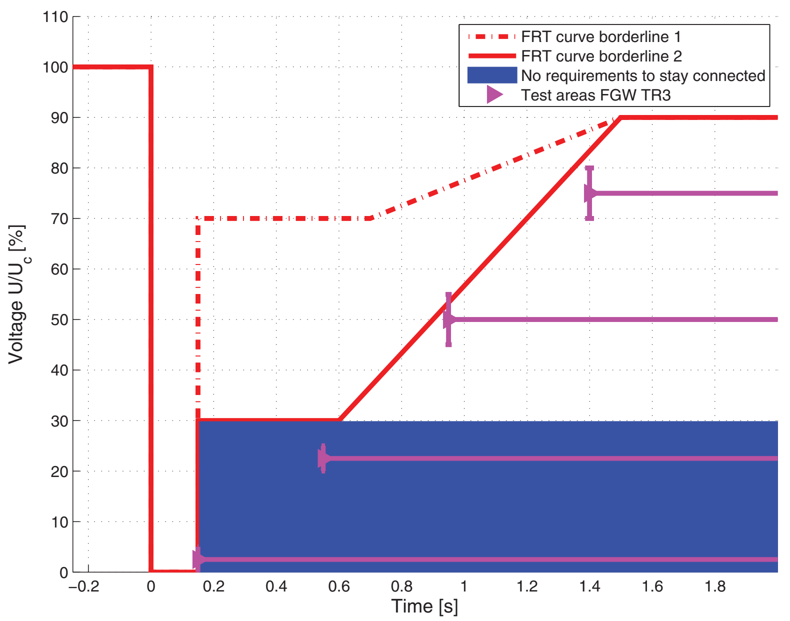

Figure 10. German LVRT curve for type 2 generators, according to [3] and FGW TR3 test areas.

Power reduction in an over-frequency condition

A surplus of power generation capacity in the network leads to a frequency rise. If frequency control of the network is no longer capable of keeping the frequency within acceptable limits, DER units can support the network by reducing active power injection. The BDEW MV guideline asks for an active power reduction of 40% per Hz, starting at 50.2Hz, but an increase of active power injection is allowed when the frequency falls below 50.05Hz.

To comply with FGW TR3, six different specified frequency points in the range 50.00–51.20Hz have to be set for testing purposes, and the active power reduction of the inverter is evaluated for these points. Using a network simulator for the tests offers the advantage of being able to continuously vary the grid frequency. The frequency profile used at Fraunhofer IWES for testing the DER units is shown in Fig. 7 (left). In accordance with FGW TR3, when a specified frequency point is reached, the frequency is held constant for at least 30s. Between these specified points, the frequency is changed at a rate of 0.225Hz/min. The power reduction behaviour as a function of frequency is then determined from the measurement data, based on average values over 200ms, and shown in Fig. 7 (right).

Power reduction by the network operator

In contrast to the autonomous reduction of active power in over-frequency conditions, power reduction by the network operator occurs remotely and is selective. The network operator is allowed to reduce the active power injection of DER plants in order to secure network operation in the event of, for example, network transmission capacity shortages or overloading of network equipment.

The DER units must be able to reduce the active power output to set points given as percentages of the rated active power, the most common values being 100%, 60%, 30% and 0%. However, according to FGW TR3, different steps of active power must be tested. The set points and measurement results for the STP15000TL string inverter are given in Fig. 8.

Besides the set point accuracy, the response time of the unit has to be measured. The response time – defined as the time taken until the active power enters and stays within the tolerance band around the set point – should not exceed 1 minute. This time range is considered to cover the whole communication line, beginning from the receipt of the set point signal at the plant controller up until the alignment of the reduced active power output at the DER unit. Experiences with different kinds of PV inverters have shown that this requirement can be met quite readily and is not difficult to implement in the software of the inverter.

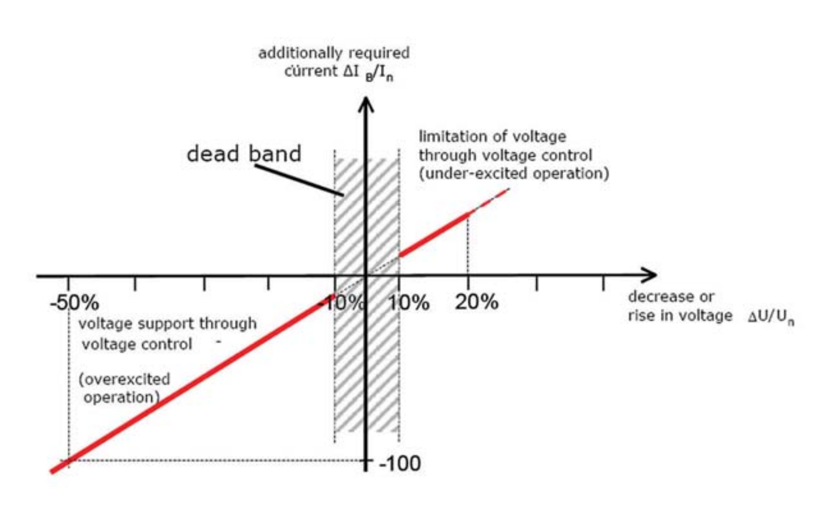

Figure 11. Reactive current injection from DER units during balanced network faults, according to [7].

Reactive power

Nowadays, because of the rising deployment of DER units, voltage control is becoming an important issue. In the past, DER units did not inherently provide reactive power, but with extended reactive power control functionalities, they are now able to support the network and thereby increase the capacity of their integration into the network.

The BDEW MV guideline demands a power factor of 0.95, leading and lagging at the point of common coupling (PCC). In order to fulfil this requirement, inverters should be capable of delivering a power factor lower than 0.95, since the reactive power demand of internal network equipment, such as cables and transformers, must also be considered.

The limiting factor for reactive power provision of inverters is the current-carrying capacity of semiconductors. An over-dimensioning of the inverter is necessary if a simultaneous injection of reactive power at rated active power is desired. Otherwise, the maximal active power injection has to be limited.

To determine the reactive power capability, at least three 1-minute average values based on 200ms average values have to be recorded for every 10% power band, i.e. 0–10%, 10–20%, and so on. This ensures that the reactive power behaviour of the inverter over the whole active power range is known. Fig. 9 shows the reactive power capability of the measured PV inverter. As it can be seen from the image, the PV inverter fulfills the requirement of a power factor of 0.95 from the BDEW MV guideline.

> “During the certification, it is necessary to determine: 1) the accuracy of the set point alignment and 2) the time duration for the set point adjustment.”

Besides the functionality of pure reactive power provision, the network operator has the possibility of providing a set point according to the actual system needs. The BDEW MV guideline allows several possibilities:

- Fixed power factor cosφ
- Fixed reactive power in Mvar

- Characteristic curves:
  - Power factor and active power cosφ(P)
  - Reactive power and voltage Q(U)

During the certification, it is necessary to determine: 1) the accuracy of the set point alignment and 2) the time duration for the set point adjustment. Clearly, if an inverter provides several interfaces for receiving set points, all of them are to be tested. At the moment, the characteristic curve test is not mandatory for unit certification, but has to be considered for plant certification.

Measurement results of dynamic requirements - LVRT

Network faults cause voltage dips, the magnitudes of which depend on the distance to the fault location and the network topology and parameters. In the past, because of grid protection settings, DER units had to disconnect from the network very quickly in the event of under-voltage conditions. Due to the rising number of DER units, transmission network operators are particularly afraid of a sudden loss of a large number of distributed generating capacities. Therefore, DER units should technically be able to ride through faults in order to continue active power injection immediately after a fault clearance. Fig. 10 shows the LVRT curve according to the BDEW MV guideline and the test areas of FGW TR3 used for the measurements of the DER unit.

Voltage support through reactive current

A further requirement of DER units is voltage support during network faults. Depending on the magnitude of the voltage dip and the k-factor characteristic (Fig. 11), an additional reactive current has to be injected by the DER unit, and this must be least its rated current. In the calculation of the reactive current set point, reactive power injection and voltage deviations before the fault have to be taken into account.

The influence of the injected reactive current on the network voltage is shown in Fig. 12. Here, the same voltage dip is applied to the PV inverter by a network simulator with a physical impedance network, but different settings of the k-factor are used. During the first voltage dip, the k-factor is 0, which means that the PV inverter simply rides through the fault but does not inject any reactive current. For the second voltage dip, the k-factor is set to 2, which leads to a reactive current injection in the range of the nominal current of the PV inverter, at a voltage drop of about 50% of the nominal voltage. The rise of the measured voltage in the grid simulator can be clearly seen.

During the procedure of taking measurements for certification, LVRT tests have to be performed using different parameters and the results evaluated. Adjustable parameters, according to FGW TR3, are the type of fault (balanced and unbalanced), the active power injection before the fault (10–30% and > 90%) and the k-factor. A sampling rate of at least 5kHz is required for the transient measurements. Furthermore, it has to be ensured that the length of time recording before and after the fault is sufficiently long to determine all necessary parameters, e.g. the voltage and current before the fault,

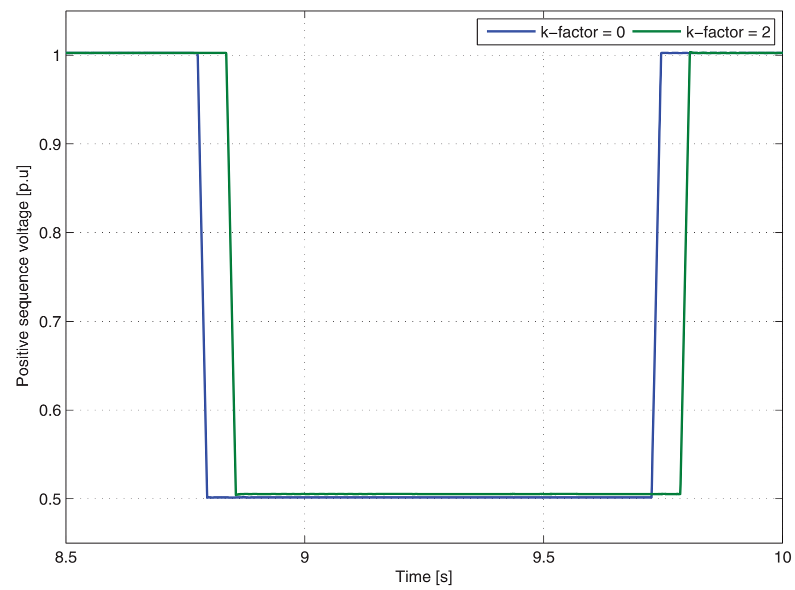

Figure 12. Influence of reactive current injection during network faults. The same voltage dip is applied to the PV-inverter (STP15000TL) in both cases.

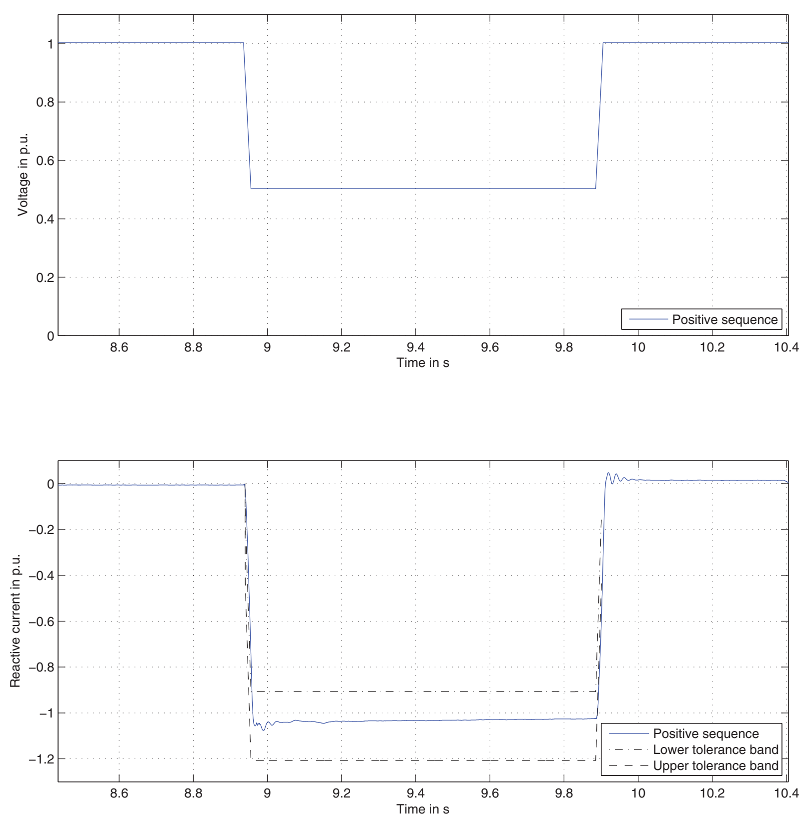

Figure 13. Measurement results for the STP 15000TL, when a balanced voltage dip to 50% of the nominal voltage U_n is applied.

which are used to calculate the reactive current set point, and the active power behaviour after the fault clearance.

Different parameters characterizing the behaviour of the DER unit during the fault have to be calculated from the transient recordings and documented in the test report, e.g. half- and full-period RMS and peak values of the short-circuit current contribution at different points in time during the fault; the time to reach 90% of the active power before the fault occurred; and the determination of the k-factor and the control response time. Observations from different measurement campaigns have indicated that the requirement of achieving a control response time of 20ms according to TC2007 [7] is the most challenging.

Fig. 13 shows a typical measurement of the reactive current injection during a fault, using the STP 15000TL. The reactive current injection of the PV inverter starts very quickly and stays within the tolerance band of –10% and +20% of the rated current around the reactive current set point. The control response time requirement is also satisfied because of the fast reaction of the inverter.

Conclusions and outlook

Initial tests have revealed that PV inverters are generally capable of satisfying the static as well as the dynamic functionality requirements of the new German BDEW MV guideline, in terms of supporting network operation and stability. The extensive certification process for DER units and plants that has been introduced, in addition to the new guideline, has highlighted a particular need for PV-specific test procedures and test equipment. Therefore it has been necessary to develop specific features, such as laboratory infrastructure and test procedures, required for the confirmation of the electrical properties of PV inverters, according to the test guideline FGW TR3. This guideline, developed primarily for wind turbines, has been successfully adaptated for PV inverters during the last two years.

With particular regard to LVRT tests at the LV level, Fraunhofer IWES has been able to develop, validate and successfully apply a new method of testing, using a network simulator with a physical impedance network, for several certification procedures. However, it is recognized that there is a lack of laboratory capacity, not only for testing but also for the development and validation of new test procedures. This is particularly true for high-power applications and so, in September 2011, Fraunhofer IWES set up a reference laboratory for inverters rated up to 6MVA, to support future development in the field of PV inverters.

Acknowledgements

The authors would like to thank the German Federal Ministry for Environment, Nature Conservation and Nuclear Safety for the support of the project 'PV-EMS' (FKZ 0325028), and the German Federal Ministry of Economics and Technology for the support of the project 'Erprobung Neuer Netze – Aufbau eine Referenzlabors für neue Netzkomponenten und Netzbetriebsmittel' (FKZ 03KP203). Only the authors are responsible for the content of this publication.

References

[1] Federal Network Agency 2010, *EEG-Statistikbericht 2009*, Bonn, Germany.

[2] Degner et al. 2009, "Utility-scale PV systems: Grid connection requirements, test procedures and European harmonisation", *PVI*, 4th Edition, p. 135.

[3] Bundesverband der Energie- und Wasserwirtschaft e.V. (BDEW) 2008, *Technische Richtlinie für Anschluss und Parallelbetrieb von Erzeugungsanlagen am Mittelspannungsnetz*, Berlin, Germany.

[4] Fördergesellschaft Windenergie e.V. 2010, *Technische Richtlinie für Erzeugungsanlagen*, Teil 3, Rev. 21, Kiel, Germany.

[5] Fördergesellschaft Windenergie e.V. 2010, *Technische Richtlinie für Erzeugungsanlagen*, Teil 4, Rev. 3, Kiel, Germany.

[6] Fördergesellschaft Windenergie e.V. 2010, *Technische Richtlinie für Erzeugungsanlagen*, Teil 8, Rev. 5, Kiel, Germany.

[7] Verband der Netzbetreiber –VDN e.V. beim VDEW, *Transmission Code 2007*, Berlin, Germany.

[8] Arnold, G. et al. 2011, "Erfahrungen mit der Prüfung und Zertifizierung von PV-Erzeugungseinheiten/-anlagen gemäß BDEW-Mittelspannungsrichtlinie", 26. Symposium Photovoltaische Solarenergie, Bad Staffelstein, Germany, March.

About the Authors

Dominik Geibel is a member of the Electricity Distribution Networks Group at Fraunhofer IWES. His main areas of interest include control of power converters, grid integration and testing of DERs. Dominik received his diploma in electrical engineering and information technology from the University of Karlsruhe in 2006 and is currently working towards a Ph.D. degree at the University of Kassel.

Thomas Degner is a senior researcher at Fraunhofer IWES in Kassel and leads the Electricity Distribution Networks Group. He is also the coordinator of the European Network of Excellence of DER Laboratories (DERlab) and active in the CENELEC working group WG03 of TC8X. His research topics include micro-grids, ancillary services, interconnection requirements, testing procedures and network protection concepts for distribution networks. Thomas holds a diploma in physics and received his Ph.D. for work concerning the layout and control of wind–diesel hybrid systems.

Gunter Arnold has been a member of the Electricity Distribution Networks Group at Fraunhofer IWES since 2008. His main research topics focus on power plant features of PV inverters and testing procedures for grid integration of DER generators, as well as power quality characteristics of DER plants. Gunter has a diploma degree in electrical engineering from the Technical University of Darmstadt and received his Ph.D. from Kassel University in 2004.

Enquiries

Fraunhofer Institut für Windenergie und Energiesystemtechnik (IWES)
Königstor 59
34119 Kassel
Germany
Tel: +49 561 7294 211
Fax: +49 561 7294 200
Email: dominik.geibel@iwes.fraunhofer.de
Website: http://www.iwes.fraunhofer.de

Market Watch

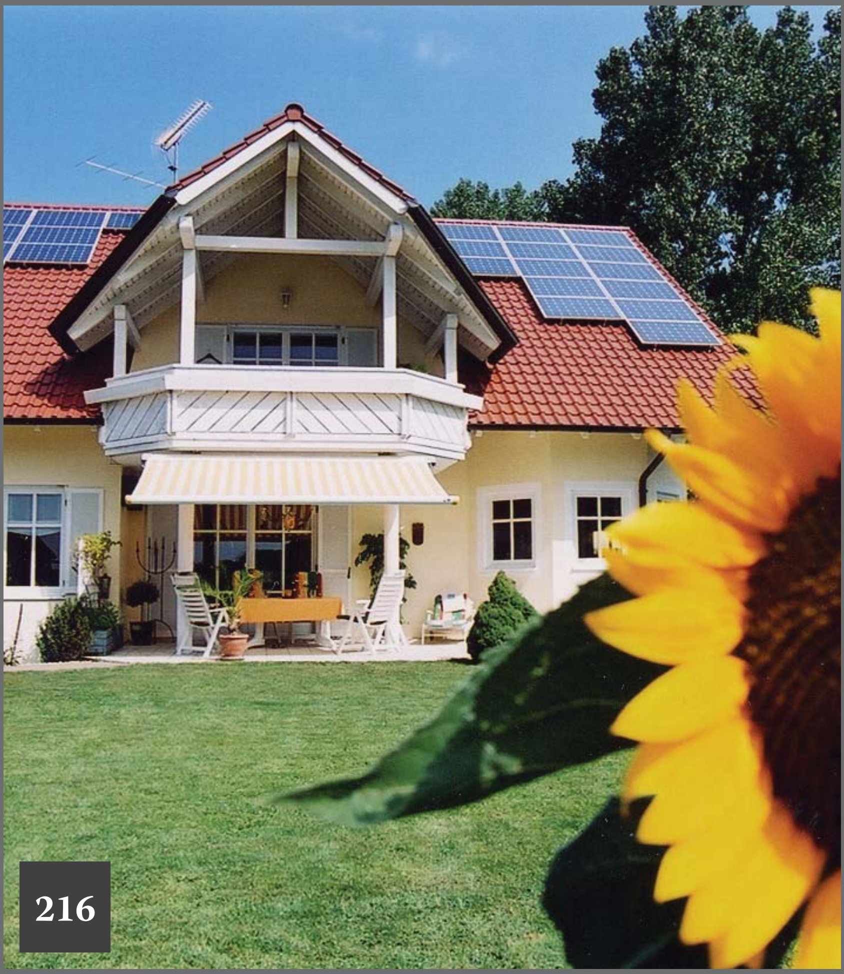

First Solar quarterly sales continue downward trend: capex cut over US$200 million

First Solar manufacturing plant, Perrysburg, Ohio, USA.

Ion implant market leader Varian Semiconductor Equipment First Solar has reported second-quarter 2011 net sales of US$533 million, a decrease of US$34.5 million from the first quarter, as well as a decrease of US$42.5 million from the fourth quarter of 2010. The CdTe thin-film leader noted that the sales decline was primarily due to lower average selling prices, which in turn were due to policy uncertainties in Italy, Germany and France, leading to weaker-than-expected demand.

However, First Solar revised downwards its 2011 guidance across most areas. Net sales were lowered to between US$3.6 billion and US$3.7 billion, compared to previous guidance in the first quarter of between US$3.7 billion and US$3.8 billion. Operating income was tweaked to between US$900 million-$960 million, compared to US$900 million-US$970 million.

Capital expenditure was also not immune to the downward revisions. First Solar had previously guided capex in the range of US1.0 billion to US$1.1 billion in 2011. Capex is now expected to be in the range of US$800 million to US$900 million.

First Solar reported module production in the second quarter of 483MW, with annualized run rate per line dipping 2MW quarter on quarter to 62.1MW, but cost-per-watt production costs and module efficiencies remained the same as the last two quarters, at 75 cents per watt and 11.7%, respectively. The company said during the conference call that costs at its low-cost Malaysian plants had dropped to 69 cents per watt.

Capacity expansions in Malaysia for lines 5 and 6 are now completed and the lines fully ramped, while its Frankfurt-Oder 2 facility is ramping earlier than previously expected in the third quarter of 2011. With revenue falling in the first two quarters of 2011, First Solar management highlighted in the conference call the company's efforts to diversify its pipeline further on a geographical basis.

Financial and Business News Focus

MEMC and SunEdison to acquire Fotowatio Renewable Ventures' US unit

MEMC Electronic Materials and its SunEdison unit have reached a definitive agreement to buy privately-held Fotowatio Renewable Ventures, the 100%-owned US subsidiary of solar project developer/operator/owner, Fotowatio Renewable Ventures. When the deal closes, MEMC will pay US$112 million plus repayment of approximately US$22.9 million in intercompany loans and capital contributions.

The final purchase price is subject to adjustment based on the actual amount of intercompany loans and capital contributions at closing. The agreement also includes an additional deferred payment of up to US$103.6 million should FRV US achieve certain performance targets. The acquisition is expected to close in the third or fourth quarter, subject to customary closing conditions, including the receipt of regulatory approvals.

The FRV US PV portfolio features 42MW in operation in the US, including the 14MW power plant at Nellis Air Force Base. The company's solar portfolio also includes 28 projects in various stages of development, which could provide SunEdison with up to 1.4GW of solar projects in the US. The FRV US staff of 50 employees will remain in Northern California and will report into MEMC's SunEdison subsidiary.

GE Energy to invest US$40 million in eSolar

GE Energy is to consolidate its business partnership with eSolar by investing US$40 million in the concentrated solar thermal power technology developer. As part of the agreement, Paul Browning, GE Energy's president and CEO of Thermal Products, will join eSolar's board of directors.

GE has recently launched its Integrated Solar Combined Cycle (ISCC) power plant solution, which couples eSolar's innovative solar thermal technology with GE's fleet of combined cycle products. When combined with GE's FlexEfficiency 50 Combined Cycle Power Plant technology, the ISCC is capable of delivering fuel efficiencies of more than 70%.

eSolar has signed an licensing agreement with GE for the exclusive use of its modular technology with ISCC in every country bar China and India. The two companies are targeting Europe, Africa, the Middle East and the US, and are already working alongside investors to develop a 530MW project in Turkey. eSolar is also planning further projects that are due to be unveiled in the near future.


eSolar's Sierra SunTower.

Source: eSolar

Losses nearly halved at Conergy as sales increase almost 40%

A strong boost to sales in the second quarter helped Conergy to reduce losses from the previous quarter to €6.7 million, down from €12.3 million in the previous quarter. The company increased sales by almost 40% to €225.2 million, compared to €163.3 million in the prior quarter, but down from €239.4 million reported in the same period of 2010. The dramatic fall in module prices impacted gross profit margin, which fell to 19.1% from 24.6% at the beginning of the year.

As is the case with many of its competitors, Conergy noted that sales efforts were being focused on expanding business outside Germany, which saw international business sales increase by 36% to €157.2 million on the previous year. Highlighting that 70% of the company's total sales are now coming from outside Germany, Conergy was able to more than double its sales (€63.1 million) in the Asia-Pacific region in a year. Strong EPC business and project pipeline in Thailand and India were noted.

Source: Conergy

Conergy has increased its sales by almost 40% to €225.2 million, compared to €163.3 million for the previous quarter.

Though the North American market is expected to double to over 2GW in 2010, Conergy sales to the region were €13.4 million, up 7.2% compared with the prior quarter. Sales in Europe (excluding Germany) were impacted by a halt in the Italian market in the second quarter. The company also noted that business in the UK had increased by over 600%, with growth of over 62% in Greece and 25% in Spain.

Munich Re, KKR team up to buy 49% equity stake in Grupo T-Solar

Insurance group Munich Re, through its asset management division MEAG, and investment firm Kohlberg, Kravis Roberts & Co. (KKR), partnered up to buy a 49% equity stake in the existing operating assets of Grupo T-Solar, which holds a total capex to date for the assets of €1.073 million. In the acquisition, MEAG and KKR obtained 34 PV plants located in Spain and eight PV plants located in Italy, which were said to hold a collective installed capacity of 168MW and a generation capacity of more than 250GWh per year.

The assets bought by MEAG and KKR will be contained under a new company named T-Solar Global Operating Assets, while Grupo T-Solar will continue to hold a 51% equity stake while also providing management services. Additionally, MEAG and KKR came to an agreement with T-Solar Global, which allows it to buy new solar plants developed by Grupo T-Solar once they are in full operation. The investment was completed under Munich Re's Renewable Energy and New Technologies (RENT) program as Grupo T-Solar was restructuring its concession business.

Market Trends & Developments

IMS Research: PV installations to more than double in 2H11

Photovoltaic system installations are set to show a transformation in the second half of the year and more than double over first half-year figures, according to IMS Research's latest 'Global PV Demand' report. The market research firm has even revised its forecast to cater for the strong demand expectation, fueled by a recovery in the German market and strong growth in the US and Asia. IMS Research expects PV installations to reach more than 22GW this year, 1GW higher than its previous forecast.

Although German PV installations are projected to fall in 2011, compared to last year, Europe overall is forecasted to be only 1% down in 2011. The UK and Slovakia were said to have helped fill the void, according to IMS Research.

The new report revealed that 11 countries in Europe will install at least 100MW this year, with 20 countries globally installing the same or more, which is up from just 13 in the previous year. IMS Research projects that China will be a key installation market in the future, becoming one of the top three global markets in 2015.

Solarbuzz cites expected collapse in PV manufacturing equipment spending

On the back of a small 3% decline in PV capital equipment spending in the second quarter of 2011, market research firm Solarbuzz believes the drop is the forerunner to a collapse in equipment spending by tier 2 and tier 3 module and cell suppliers. This is due to overcapacity in the market and an expectation of a wave of consolidation or 'fall-out' of smaller players. PV equipment spending for c-Si ingot-to-module and thin-film modules is expected to decline sharply in 2012 to US$7.6 billion, down 47%, compared to a record level forecast of US$14.2 billion in 2011.

Coupled with market oversupply and strong inventory build through the second half of 2011, Solarbuzz expects the capacity-demand imbalance to usher in a significant cell manufacturer shakeout phase during 2012 to 2014. Finlay Colville, senior analyst at Solarbuzz, cites the fall of the PV book-to-bill ratio below parity in the second quarter of 2011 as an inflection point, highlighting a slowdown in manufacturing capacity increases planned for 2012. He said that this is the first negative growth rate for PV equipment spending since the second quarter of 2009.

According to Colville, the c-Si cell and module manufacturing equipment suppliers will feel the full force of the collapse in capital spending. The market research firm is projecting quarter-on-quarter revenue declines of 21%, 12% and 37% forecast from the fourth quarter of 2011 through to the second quarter of 2012, respectively.

However, Colville believes that only c-Si equipment suppliers with an established upstream product portfolio and strong market shares, such as GT Solar, Meyer Burger, Applied Materials and Jinggong would be 'sheltered' from the 'drop-off' in equipment bookings during the first half of 2011.

Local governments offer further support to China's FiT

Only days after China's National Development and Reform Commission set up a new feed-in tariff (FiT) for PV project tenders, worries have arisen about its financial viability for some PV companies.

Western China's solar radiation level of 5519.46MJ/m^2 per annum is higher than that of eastern China, which averages 4836.23MJ/m^2. Taking into account government subsidies, operation costs, utilization rates in different provinces, VAT, loans, corporate income taxes, surtaxes and interests, Sicheng Wang, a researcher from the Energy Research Institute of NDRC, noted that CNY1 (US$0.16) per kilowatt-hour could only profit four out of nine western provinces if the IRR is set at 8% and the investment return time at 15 years (both at the average levels of the industry). However, all 17 eastern provinces are likely to suffer losses at that price.

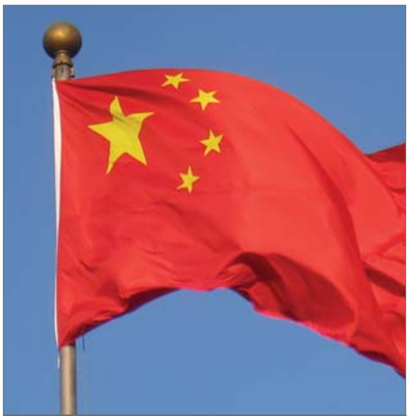

Many eastern provinces of China are on the cusp of introducing a local FiT to help local projects.

Many eastern provinces are on the cusp of introducing a local FiT to help local projects. Yun Ling, the deputy director of Zhejiang Economic and Information Technology Commission, said recently that Zhejiang province is to set the provincial FiT at the price of CNY1.43 (US$0.22) per kilowatt-hour, which is currently with the NDRC pending approval. The difference between the CNY1.00 and CNY1.43 rates will be funded by local governments.

Solar power in developing countries: will PV-supported micro-grids provide the next wave of demand?

Andy Skumanich & **Shannon K. Fulton**, SolarVision Co., Los Gatos, California, USA

ABSTRACT
Traditional markets for PV will be scaling back on the level of demand for PV, but there are already signs that the developing countries will be stepping in to pick up the slack. This will be a combination of both standard grid-connected and micro-grid types of installation. Micro-grids present the opportunity for countries to develop a cell-phone type of model for power distribution whereby regions without electrification can have a regional power source that allows for local access. This market is projected to become significant in the next several years, as the access to lower cost PV makes this option more easily implemented. This paper evaluates the market size of what has been an overlooked 'niche' for PV and describes the key considerations for a micro-grid installation, the developing conditions favouring installation, and some of the specifics of a micro-grid case study. The point is made that the grid-connected market will be increasingly assisted by the micro-grid segment as the latter becomes a significant source of PV demand and energy provision. Contrary to common notions, the micro-grid and hybrid off-grid segments will play an increasing role, even in areas with a grid in place.

Introduction

The beginnings of new market dynamics are becoming apparent in the PV industry. The trend to reduce incentives is already gaining momentum and the elimination of feed-in tariffs is likely in the next few years. This will certainly have an impact on the demand from the traditional demand sources. In the past decade it has been mostly Europe that has driven the demand for PV, but this is rapidly changing as country by country the surges begin to decrease. Spain came and went, Italy was big last year but is backing off, the Czech Republic is no longer mentioned, and now there is even the unthinkable – Germany may be approaching 'saturation.' In the meantime, Greece and Portugal – while they are awash in sun – have a very cloudy economic future to support any significant PV implementation. The US is engulfed in a race to cut spending, and Japan is still recovering and rebuilding its economy.

So where are the drivers for the next wave of PV adoption? The global PV market cannot depend on the bellwether countries to increase their PV demand and expand the market. Developing countries are in a unique position to step in and pick up the slack, and it may well be in the context of the micro-grid that this will happen. Bottom-up electrification initiatives are happening in the developing world, and are proving to be efficient and cost-effective entry-level strategies. Micro-grid applications for rural electrification represent a major opportunity. While many systems have historically featured diesel-distributed energy generation, the largest growth sector opportunity is for PV, in some hybrid power generation type of mode, as PV steadily replaces carbon-based power generation [1–5].

Developing countries with growth opportunities

Because energy is a requirement for economic growth, there is an increased focus by the various developing countries on addressing this need. Recently, many countries have established rural electrification programmes and national electrification agencies. The UN Millennium Development Goals (MDGs), adopted in 2000, contain no targets specifically related to energy; however, Richenda Van Leeuwen [6] of the UN Foundation points out that 2012 has been declared by the UN as the International Year

	Population without electricity (millions)	Electrification rate (%)	Urban electrification rate (%)	Rural electrification rate (%)
Africa	587	41.9	68.9	25.0
North Africa	2	99.0	99.6	98.4
Sub-Saharan Africa	585	30.5	59.9	14.3
Developing Asia	799	78.1	93.9	68.8
China and east Asia	186	90.8	96.4	86.5
South Asia	612	62.2	89.1	51.2
Latin America	31	93.4	98.8	74.0
Middle East	22	89.5	98.6	72.2
Developing countries	1438	73.0	90.7	60.2
Transition economies & OECD	3	99.8	100.0	99.5
World	1441	78.9	93.6	65.1

Source: International Energy Agency (IEA) 2010 [7]

Table 1. Summary of the extent of the need for rural electrification among different developing regions: regional aggregates of electricity access as of 2010.

of Sustainable Energy for All, and the goal of universal energy access by 2030 is one of the three goals of the Initiative and the Year. Citing the World Energy Outlook 2010 on energy poverty [7], the focus of which is to expand energy access at the household level, Van Leeuwen emphasizes that over 1.4 billion people, 85% of whom live in rural areas, have no access to electricity. Sub-Saharan Africa remains the biggest challenge, where nearly 70% of the people are without energy access. Van Leeuwen corroborates that there is a sizeable market for micro-grid and off-grid electrification projects, consistent with the International Energy Association's illustration that, in order for those 1.4 billion people to achieve access to energy by 2030, 70% would have to be supplied by micro-grid (75%) or off-grid installations (25%) [7].

The SolarVision analysis sees the growth opportunity for developing regions as significant, especially starting in the next few years as a few key elements fall into place: the lowering of the price for solar PV, the continued rise in diesel fuel costs, the increasing need to address developing countries' desire for local energy, the growing focus by governments, and the increase in urgency for pollution reduction from carbon-based sources. Grid extension will of course play a role, but the decentralized options will have a major contribution as the extension will be too expensive in some cases.

The SolarVision forecast for micro-grid growth indicates that the levels of micro-grid/partial-grid PV demand could grow to nearly 10GW in the next decade, and then approach a significant fraction of the levels of grid-connected PV demand in subsequent decades. Fig. 1 shows some of the details behind this visionary forecast – namely the drivers and relative investment potential. This chart presents the mix of developing countries and the PV micro-grid opportunity. The level of micro-grid

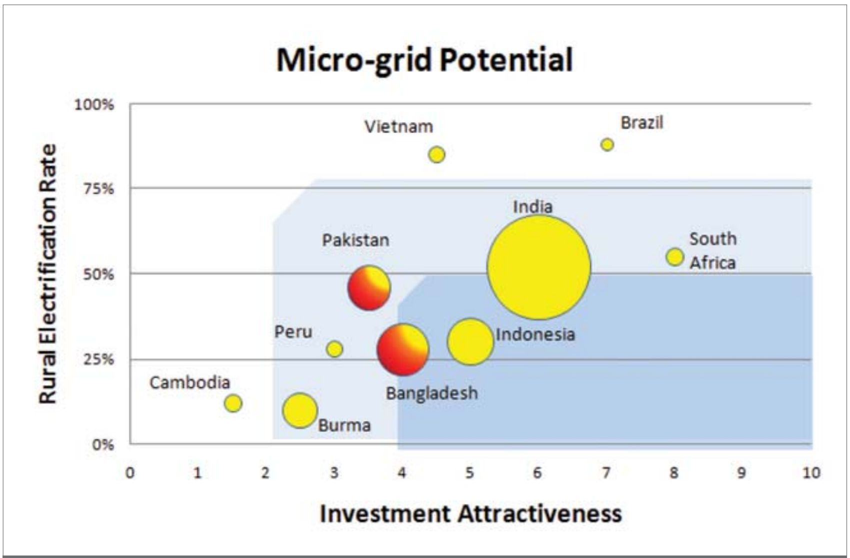

Source: SolarVision

Figure 1. The PV micro-grid opportunity based on IEA 2010 assessments.

viability increases (blue tones) to the right, as does the investment attractiveness in general terms. The vertical axis is the rate of rural electrification. Note that for some of the developing countries, the urban electrification is nominally high, but there is still a driver for micro-grid adoption in a partial- or auxiliary-grid mode, as will be further discussed below. The solar potential is the degree of 'yellow,' and the size represents the number of people in that country without direct access to electricity. For clarity and illustrative purposes, only a select subset of countries is presented.

As an example of some of the development financing, one source is coming from the Asia Development Bank (ADB). This organization has pledged US$9 billion, including projected private sector funds, for support of on-grid and partial-grid developments to the level of 3GW in the next two years – a very aggressive strategy. While the majority is grid connected, there will still be micro-grid deployment for rural electrification.

At present, less than 0.25% of Asia's overall electricity production comes from solar power, but the aim is to increase that contribution to 3% to 5% in the near future with financial support using seed money. Seethapathy Chandler, chairman of the ADB Energy Committee, has indicated that there is significant potential for solar energy; he has also highlighted that "solar is already cheaper in [various] places where they have to use diesel generators" [8].

What is a micro-grid and how is PV a part?

Solar PV plays a vital role in meeting the basic energy needs for such services as lighting and clean water in the developing world; however, those needs are growing quickly while resources remain few. These conditions are perfectly suited to a PV micro-grid solution, which provides reliable, comparatively low-cost power in a more amenable timeframe than a traditional grid. An example of rural electrification solutions with mixed sources is shown in Fig. 2.

A micro-grid (or mini-grid) is a village- or district-level concentrated web of distributed energy sources, energy storage and loads of up to 500kW that normally operate connected to an electricity grid. The various energy sources are tied together on their own feeder, which is then linked to the grid at a single point of common coupling. A micro-grid may be viewed as peer-to-peer transmission of energy, which is more networked and symmetrical, without a master controller or central storage unit that is critical for operation. Its reliability hinges on its diverse generation sources and ability to function and be controlled independently as needed (i.e. during a brownout or blackout). Micro-grid energy sources may consist of an evolving mix of standard and renewable options. In a manner similar to

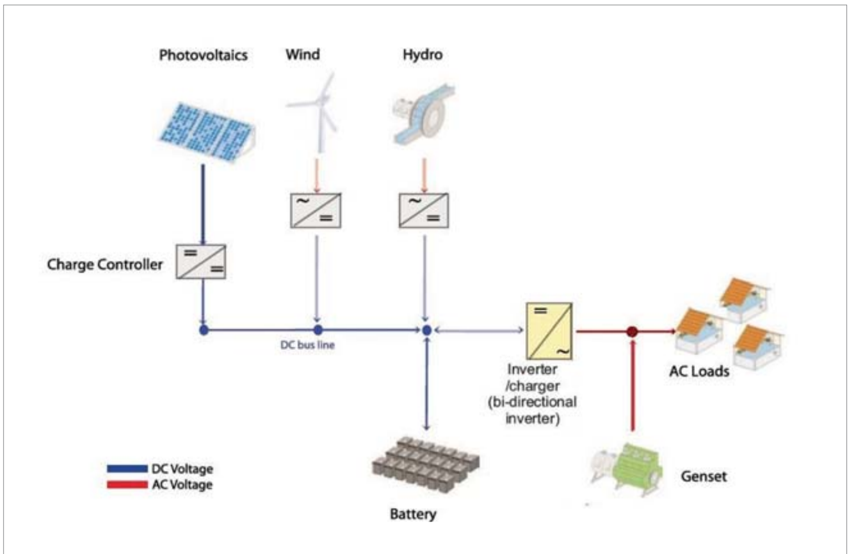

Source: Alliance for Rural Electrification (ARE)

Figure 2. Examples of mixed-source rural electrification solutions.

Source: ARE

Figure 3. Micro-grid in Tibet.

the early hybrid cars, the beginning stage may have more fossil fuel utilization, but this would decrease with time. Standard power-supplying sources in a micro-grid may also utilize novel equipment such as a microturbine to maximize efficiency while being augmented by PV. Over the course of time, the energy mix would become dominated by PV and possibly other renewables such as small wind, micro-hydro and biogas. Figs. 3 and 4 show examples of a micro-grid in Tibet, and rural off-grid PV in a small village in Cuba and in South Africa.

Micro-grids can be similar to the cell-phone model

The cell-phone model for micro-grids is a low-cost, limited-resources approach to energy delivery on a limited scale and which targets small localities. Original implementation of cell-phone technology and subsequent expansion of coverage occurred very rapidly, at comparatively low cost, with limited infrastructure and without overburdening the existing telecom infrastructure. In fact, in developing countries more people own cell phones than refrigerators. Just as cell phones are helping to lift the poor out of poverty, micro-grids could help shoulder developing countries' growing thirst for electricity without overburdening aging transmission lines or investing massive amounts of capital and time in constructing traditional power plants to meet this demand.

The technological development that distinguished the early cell phones was the use of multiple cell sites and the ability to transfer calls from one site to the next without the need for costly landline infrastructure and maintenance. Similarly, a single micro-grid or aggregate of localized micro-grids may operate independently of a centralized grid by switching between diverse power sources. This is especially important in developing countries such as Lebanon and India where the population endures episodes of prolonged power outages. Not only is the grid unreliable, but grid transmission can cost upwards of US$1 million per mile, making grid extension to rural villages or other areas with low population densities too expensive. As an alternative to grid extension, the cell-phone model allows for staged implementation of energy provision.

Key issues: affordability and reliability

The affordability of PV is improving as module costs drop and the incentive increases with volatile oil prices. Further module price decreases will come, and as new modes of energy storage become viable, the PV-integrated micro-grid becomes increasingly realizable by the developing countries with resources that must be prioritized.

Van Leeuwen [6] views increasing global recognition, supportive and predictable government policies, and workable payment structures as being critical to facilitating a reimbursement environment that would be attractive to private interest in rural micro-grid projects in developing countries. SolarVision has been providing guidance to a range of rural electrification customers in developing countries, including India and Latin American countries (such as Panama, Cuba and Chile), as well as Azerbaijan, Indonesia and some clients in Africa. Customers are trying to understand not only the various renewable energy technologies of micro-grids, but also the complexities of short- and long-term financing. Many different sources of financing and creative pricing strategies can and must be used to meet diverse electrification needs throughout the developing world. Some of these include microfinance loans, public/private cooperatives, international funds, standard bank loans and targeted subsidies.

Simon Rolland, secretary general of the Alliance for Rural Electrification (ARE), asserts that easier access to finance and the capacity of business and/or government to institute an easily applicable and replicable business model are integral to the success of rural micro-grid electrification projects. Rolland [9] also points out that developing a business model for a project involving rural electrification with renewables can be difficult due to the complexity of the technology involved; varying resource and load requirements; and questions of who owns, operates and maintains the system.

The key advantage of a micro-grid is its use of dispersed generation sources and its inherent reliability – the ability during an electricity grid outage to isolate itself from the grid seamlessly, with little or no disruption to the loads within the micro-grid. In India, where electricity is subsidized, the intermittency of the grid is so common that wealthier consumers who can afford it over-invest in backup off-grid systems. These households often have two switches – one flipped on when the grid is up and the other when the grid is down. In a more extensive configuration this arrangement acts as a partial auxiliary-grid.

At the other end of the spectrum, small villages exist in India where, although the grid may pass overhead, the expense of tying in the village is viewed as too great when compared to the limited income generated by villages with low consumer density. The micro-grid concept is a well-

Source: A. Skumanich

Source: ARE

Figure 4. Micro-grids deployed in Cuba (left) and South Africa (right).

Location	Application	Average energy output	Maximum daily peak load	Microgrid electricity generating resources					Battery storage	Funding sources
				PV	Small wind	Small hydro	Genset(s)	Gas turbine cogen		
Naperville, IL, USA	Substation operation	4,500kWh/yr	1.31kW	(5kW)						Local government, private
UCSD, CA, USA	University (small city)	221,000MWh/y	42MW	(1.2MW)			(Diesel)	(30MW)		State government, private
Bellavista, Jambeli Archipelago, El Oro province, Ecuador	Households, school, naval station	97,090kWh/yr	26kW	(35kW)	(20kW)		(Diesel)		✓	N/A - model only
Padre Cocha, Peru	Households, commercial, industrial, institutional	109,500kWh/yr	22kW	(28kW)			(Diesel)		✓	International, local government, private
Lao PDR	Households	57,488kWh/yr	8kW	(2kW)		(12kW)	(Diesel/ Jatropha)			Private–public partnership

Table 2. Comparison of various micro-grid configurations.

suited strategy for electrification of these rural villages. Combining a variety of distributed resources enables a community to generate sufficient electricity in the event of a prolonged power outage in order to operate emergency services, such as a police station or hospital, and ensures that citizens have sufficient power to meet their essential needs. Likewise, when the electricity grid disruption ceases, the micro-grid reconnects flawlessly to the grid, without adversely affecting the quality of power. Micro-grids are completely compatible with a centralized grid and serve as purposeful, more affordable components of grid expansion [4]. Again, this constitutes a partial-grid mode.

> "The key advantage of a micro-grid is its use of dispersed generation sources and its inherent reliability – the ability during an electricity grid outage to isolate itself from the grid seamlessly, with little or no disruption to the loads within the micro-grid."

The selection of a particular micro-grid technology can have far-reaching consequences for the sustainability of the services. Technical failures of even the most perfectly matched micro-grid system may result from an absence of indigenous capability. Community involvement (of both men and women) is necessary for successful operation, whether the system is locally or regionally maintained. Locally trained staff members often migrate to urban areas to exploit their new skills. In view of this, a consistent, reliable source of power from any micro-grid system depends on selection of trainees, particularly women, who are likely to remain in the area. Rolland [9] suggests that the best scenario is where a micro-grid project is community initiated but privately managed. This relationship strikes an ideal balance between community, government and private business.

Implementation: working systems in different contexts

Hybrid power systems typically rely on renewable energy to generate 75–99% of total supply [10]. The dominance by renewables empowers these systems with independence and lower energy prices over the long term. In many cases, a diesel generator is used as a backup to assist during periods of high loads or low renewable power availability. The battery backup size can be lower and suffers less stress than in a 100%-renewable power system, prolonging battery lifetime significantly and reducing replacement costs. Thorough site and community surveys are a basic foundation for any mini-grid project, regardless of the technology selected. Oversizing certain components, such as wiring and inverters, can accommodate future demand growth and facilitate micro-grid expansion.

Implementing sustainable hybrid micro-grids involves complex technical, financial and organizational issues which must address the end-users and their needs, capacity building and training, financing, and institutional strength [11]. Table 2 summarizes the technical aspects of several case studies of hybrid micro-grid installations in the US and developing countries.

Case study: City of Naperville, Illinois, USA

Very few examples of micro-grids exist in the US; however, interest continues to grow. The city of Naperville, Illinois, has made significant efforts over the last two decades to update its power grid and incorporate smart grid technology to improve reliability, cost competitiveness and efficiency. The city is partnering with the Galvin Electricity Initiative, a non-profit initiative to build smart micro-grid projects based on its 'Perfect Power' system architecture. While much of the city's focus is on utilizing smart grid technology to improve efficiency and reliability, it has also expanded its use of renewable energy by adding a 25-module, 5kW solar array to one of its substations. The array generates solar energy to offset the substation building's common energy requirements. The solar array's estimated yearly energy production is 4500kWh.

Case study: University of California at San Diego (UCSD), California, USA

UCSD's campus-wide micro-grid is recognized as one of the most technologically advanced in the world. It serves a 1200-acre, 450-building campus with a daily population of 45,000, running two 13.5MW gas turbines, one 3MW steam turbine and a 1.2MW solar-module installation that together supply 221GWh/yr, which is 86% of the campus's annual power [12]. UCSD recently began demonstrating the integration of smart grid technology with onsite renewable energy production to provide the power system optimization and energy market optimization capabilities necessary to ensure the reliability, energy efficiency and cost efficiency of the school's micro-grid. The smart grid improvements will also manage the response of the micro-grid to market energy prices on an hourly basis. This case is an example of a partial-grid connection in that, although the UCSD system is nominally a micro-grid, it operates in parallel with the grid – the latter supplying the remaining 14% of the needed energy.

Case study: Bellavista, Jambeli Archipelago, El Oro province, Ecuador

Hybrid micro-grids are, under most scenarios, the cheapest long-term option for rural electrification. Site-specific simulation of a PV and small-wind hybrid micro-grid system operating in a village on the island of Bellavista, located in the Jambeli Archipelago, El Oro province, Ecuador, was conducted by ARE using HOMER, a software tool developed by the US National Renewable Energy Laboratory and widely used in rural electrification planning. Modelling results demonstrate that a hybrid power system combining PV, small wind and a diesel generator set (genset) is the least expensive solution if small hydro is not an option. This combination has a low consumption of diesel fuel, and final costs determined by the model are 23% lower than hybrid PV, hybrid small-wind and 100% diesel generator systems. Of particular note from the modelling results is that, under the site-specific conditions presented in this case, diesel generator systems become prohibitively expensive when the fuel price per litre increases from $0.70 to $1.50 [10].

Case study: Padre Cocha, Peru

Padre Cocha is a small village of nearly 2500 people situated in the Peruvian Amazon, where almost 95% of the population has no electricity supply due to the expense of grid extension and diesel fuel. In July 2003, a remote area power supply (RAPS) hybrid micro-grid system serving 240 consumers began operation. The RAPS system consists of two solar arrays with capacities of 14kWp and 150kWh/day (totalling 300kWh/day), and a diesel generator of 128kW. Each solar PV array includes 180 solar PV modules of 80Wp each, 240 storage batteries of 375Ah, rectifier systems, a charger and a 40kW inverter. The system delivers electricity to the distribution grid at 240V (AC). The total daily average energy consumption is nearly 220kWh, 30% of which is produced by PV and the rest by the diesel generator [11].

The total cost of the system is estimated at US$577,000, but in 2004 the organization that implemented the system reported an expenditure of $2 million on administration, promotion, studies and equipment acquisition, mainly financed by a private donor, the International Lead and Zinc Research Organization, the Common Fund for Commodities, the Sandia National Laboratory and the Loreto Regional Government. The operation and maintenance costs, including purchase of fuel and provision for battery replacement, are US$37,704 per year. Since the RAPS was commissioned, a local community organization has been responsible for the system's administration, operation and maintenance [10].

The local community fully participated in this project; however, the community's technical and management capacity is limited and the system was incapable of generating its own revenues to cover the O&M costs. Based on regional socioeconomic studies, various tariff schemes have been considered in an effort to cover management, operation, and maintenance and replacement costs, but the current financial performance of the RAPS system is not sustainable and a higher tariff needs to be established [10].

Case study: Lao People's Democratic Republic (PDR)

Sunlabob, a private renewable energy provider based in Lao PDR, collaborated with a local non-governmental organization to involve the local community in bringing electricity into their homes. This particular hybrid micro-grid system combines a 12kW small hydro generator with a 2kWp PV system and a 15kVA diesel generator, which is also capable of operating on jatropha biodiesel. The three-phase grid mainly operates on the hydro generator. With a daily peak load of 8kW, the system meets nearly all of the village load demand, and since the energy from hydro and PV is large enough to cover these needs, the diesel genset is almost never used. Batteries are not an integral component of this system, since hydropower is available for night loads. Solar PV was added for the dry season, as well as the genset for emergency backup.

Sunlabob participates in a community-tailored private–public partnership, where public partners funded the fixed assets (public infrastructure and village grid), after which ownership was then legally transferred to the village. Sunlabob, as the private local energy provider, financed the moveable assets. Consequently, Sunlabob owns and is responsible for the power generation system and charges a fee to each household based on its consumption. The company employs two villagers to operate the system and collect the fees. Although the village officially owns the micro-grid, the maintenance is carried out by Sunlabob. The community also participated in the investment with in-kind work for the construction and therefore remains vested in the ongoing successful operation of the system.

Sunlabob plans to expand its local distribution network and connect it with a nearby grid in order to attract interest from the utility by highlighting the fact that small hybrid grids can supplement the main grid with added generation infrastructure and capacity, as well as social support. This provides a unique and seemingly effective organizational set-up, benefiting end-users, the utility and Sunlabob.

This project demonstrates the different challenges facing a private company looking to pursue a rural electrification project; high investment costs, low subsidies, obligation to collaborate with the utility, long-term collaboration and relations with local players were all issues that Sunlabob encountered. The project is running without any kind of public support, and this case study shows that long-term private sector involvement is possible if the right support schemes are set up, particularly in terms of regulatory flexibility [10].

Much has been learned, and is now being implemented

Several examples reflect some of the learning points. From a recent SolarVision engagement in Cuba [2,3], a key point highlighted was that high-level government support and commitment of the populace are necessary for a successful energy reinvention on any appreciable scale. Cuba created its own path towards a new energy paradigm by applying concepts such as distributed generation, efficiency, education and the gradual expansion of solar energy across the country.

India's long-view commitment for expanding its solar capacity is another key point. Such a strategy shows the intent of government support and specifically targets opportunities for entrepreneurial investment. India also intends to request both monetary and technological backing from developed nations in order to meet its Solar Mission objectives. Without such an ambitious plan, this type of support could not be won.

Financing of solar PV projects, whether micro-grid scale or large utility scale, remains a limiting factor. Limited financial resources from international non-profit-making organizations, private ventures and governments have created a pent-up demand for PV in the micro-grid context. However, the prices are dropping and the urgency for energy is increasing to the point where these developing countries are at a crossover point and seriously looking at how to implement some mode of micro-grid.

> "Financing of solar PV projects, whether micro-grid scale or large utility scale, remains a limiting factor."

The broader view is that these countries are interested in hybrids of solar with cogeneration. The hybrid mode combines a mix of PV, diesel and/or other elements such as micro-hydro. While the upfront costs of buying diesel generators may be dramatically lower, operational costs are increasing. Strictly diesel systems simply do not make sense when considering volatile oil prices; however, use of a diesel hybrid system can reduce the cost of batteries, which can be expensive and unreliable if not properly maintained [9]. Indeed, in some regions (e.g. Nepal) the cost of petrol is even higher because of transportation, and micro-grids are already financially viable and are being implemented.

A key area in which research is needed, according to Van Leeuwen [6], is smart grid technology applications with a focus on efficiency that may leapfrog into these newly electrified rural areas – again similar to the cell-phone model. Additionally, she would like to see more research and development of energy-efficient appliances for use in developing countries.

Conclusion

PV is well suited to being a key component in micro-grids. The global grid-connected PV capacity is rapidly approaching 30GW, with most of this growth taking place in the last 10 years. Micro-grid and off-grid segments are showing strong potential to become major components in the PV market. The estimated opportunity for micro-grid/partial-grid installations starting in the next several years could reach levels approaching 10GW in the next decade. Indeed, as the leading developed nations scale back on incentives, and even on the actual installations, it is likely that the micro-grid market will ramp up into a position that will provide a major demand market for solar. A noteworthy point is that even in countries with a grid, the intermittency of the grid itself is driving the consideration of micro-grids as support.

The worldwide movement away from fossil fuel energy sources to renewables is a trend based on the desire for energy independence, the reduction of greenhouse gas (GHG) emissions and limited fossil fuel resources. Karen Ward [13], HSBC's senior global economist, recently reported in a research note that there could be less than 49 years of oil supplies left, even if demand were to remain flat. Fossil fuel reserves are finite. Derived from this movement away from fossil fuels is recognition among industrialized and developing countries of the need for non-standard energy provision options. This is especially true in developing regions which lack the basic infrastructure.

The 'hot bowl of soup' metric needs to be added to the more standard ones of dollars per watt and levelized cost of energy. What is this metric? The amount of pollution coming from heating a bowl of soup. There is more air pollution coming from the heating of a bowl of soup in the developing countries than in the grid-connected countries, even with the carbon-based power plants in the latter. Micro-grid implementation is urgently needed to move rural populations away from burning wood and fossil fuels, which has a disproportionate impact on the global carbon levels and is ruinous for the physical and human landscapes exposed to such measures.

The electricity generated by PV and PV-integrated micro-grids is clean, renewable and reliable. The implementation of micro-grids is starting to show promise and is becoming a significant source of market opportunity as well as of energy for global consumption.

References

[1] Malik, I., Skumanich, A. & Ryabova E. 2010, "PV vs CPV and CSP: A comparative analysis of technologies and cost roadmaps", *Proc. 25th EU PVSEC*, Valencia, Spain.

[2] Skumanich, A. 2010, interview for a Cuban television station regarding the global view of PV and the implementation in developing countries, April 5.

[3] Skumanich, A. 2010, "Micro-grid considerations for rural electrification", invited talk at CubaSolar 2010, April 5–8, Bayamo, Cuba.

[4] Reddy, S. et al. 2011, "PV and storage for off-grid applications: Need for islanding even with grid access", *Proc. EU PVSEC*, Hamburg, Germany [in press].

[5] Skumanich, A. & Fulton, S. 2011, "Concentrated solar power: Are we there yet?", *EcoGeneration*, May/June.

[6] Van Leeuwen, R. (UN Foundation) 2011, interviewed by Shannon Fulton, July 20.

[7] International Energy Agency (IEA) 2010, *Energy Poverty: How to make modern energy access universal?*, special early excerpt of the World Energy Outlook 2010 for the UN General Assembly on the MDGs, September.

[8] Chandler, S. (Chairman of ADB Energy Committee) 2011, pers. comm. with A. Skumanich, August.

[9] Rolland, S. (Secretary General of ARE) 2011, interviewed by Shannon Fulton, July 19.

[10] Rolland, S. & Glania, G. 2011, *Hybrid Mini-Grids for Rural Electrification: Lessons learned*, ARE, Brussels, Belgium.

[11] Energy Sector Management Assistance Program (ESMAP) 2007, "Solar-diesel hybrid options for the Peruvian Amazon: Lessons learned from Padre Cocha", Technical Paper 111/07.

[12] Kleissl, J. (2011), pers. comm. with A. Skumanich, August.

[13] Ward, K. 2011, "Oil will be gone in 50 years: HSBC" [available online at http://www.cnbc.com/id/42224813/].

About the Authors

Andy Skumanich is founder/CEO of SolarVision Co., a boutique market and technology research company providing a wide range of support, guidance and analysis. The SVC client base ranges from investment companies requiring due diligence to global companies looking for guidance on solar and renewables. The firm provides support for clients in developing countries and is engaged with PV micro-grid installations activities. Prior to SVC, Andy was VP at Innovalight, a Silicon Valley solar start-up, and before that a senior technologist at Applied Materials Solar Division, which he joined after serving as a staff scientist at IBM Research. He holds a Ph.D. in physics from the University of California at Berkeley.

Shannon Fulton joined SVC in 2011 as a contributing consultant with a focus on energy concerns and renewables in developing countries. As a senior hydrogeologist at Environmental Management & Technologies, she is also actively studying the implementation of renewable energy in developing countries and how to accelerate this process. She is a director of the Illinois Solar Energy Association and chairs its policy committee. She graduated from Illinois State University with a B.S. in renewable energy technology, and also holds B.S. and M.S. degrees in geology/hydrogeology.

Enquiries

412 Los Gatos Almaden Rd.
Los Gatos
Silicon Valley, CA 95032
USA
Email: askumanich@solarvisionco.com
skfulton@solarvisionco.com

Can Germany's energy system cope with even more PV electricity in the future?

Jan Michael Knaack, German Solar Industry Association (BSW), Berlin, Germany

ABSTRACT
In recent years, Germany has seen impressive growth in its PV market. From a virtually non-existent market based on the 1,000 roof support program at the end of the 1990s, Germany now represents the world's biggest PV market and has created a strong PV industry base. With approximately 17GW of installed PV capacity at the end of 2010 – accounting for 2% of its electricity consumption, Germany has become a solar super power and triggered market growth and technology development worldwide. Nevertheless, the innovative scheme of feed-in tariffs (FiT), which provided incentives for solar PV installations and helped to ramp up an unknown cycle of innovation, will have to evolve towards more diversified ways of supporting system transformation of the electricity market and PV market integration until full competiveness of PV technology is reached in Germany, anticipated for 2017.

Current restrictions of the PV market in Germany

With 7.4GW of newly-installed capacity, Germany reached an all-time high of PV installations in 2010. Nevertheless, the notable production of PV electricity has sparked discussions about the grid's technical capacity to integrate large amounts of fluctuating PV electricity as well as the surcharge for the electricity consumer resulting from the FiT payments. Many responsible industry players in Germany have understood these constraints and have committed themselves to the German PV Industry Roadmap 2020, a strategy paper that has been developed in a process that began in mid-2010 by the German Solar Industry Association BSW-Solar. The paper was realized with the support of the strategy consulting companies Roland Berger and Prognos [1]. In accordance with the German government's national action plan, representatives of the industry agreed at aiming for the creation of a sustainable PV market growth of between 3 and 5GW per year until 2020 in order to enable Germany to at least attain the EU National Action Plan goal of 51GW of PV installations [2].

With that said, the industry is also committed to doing its share in the race towards halving the per-watt PV-system cost and to actively contribute to changing the electricity system to become more capable of absorbing at least 10% of solar electricity, while also distributing a significantly increased portion of electricity from other fluctuating sources, especially wind energy. In the long term, the macroeconomic balance of cost for ramping up this industry sector is overall very positive, and looks set to generate more than €50 billion in 2030 as a result of industry and job creation as well as energy savings in Germany.

Over a long duration, however, such a strategy often involves costly upfront investments. The PV market in Germany is stimulated by apportionment for producing electricity from renewable energy sources (RES-E), borne by the electricity rate payer. This apportionment, commonly known as feed-in tariffs (FiT), is a sensible issue as unnecessary expenses must be avoided for electricity rate payers in Germany. (The term 'feed-in tariff' is rather misleading, as it creates the impression among those unfamiliar with the industry that it is a form of tax or tariff, though it is, in effect, a bonus for the production and provision of clean electricity.)


Source: BSW-Solar/SunTechnics

Figure 1. In Germany, small PV systems play an important role in the transformation of the energy system towards a decentralized, competitive and environmentally-friendly system.

In addition, no industry player is interested in creating a boom-and-bust market spurred by investors aiming at excessive profits, as recent developments in Spain, the Czech Republic and Slovakia have shown. These countries, like many others in the world, had adopted their own version of Renewable Energy Legislations, working with FiTs or Production Premiums.

Evolvement and development of the German FIT

FiTs were first adopted in Germany in 1990's "Renewable Energy Feed-in-Act", with only a few different groups of tariffs for renewable technologies. Wind and solar electricity were in one tariff category. The new law also guaranteed privileged electricity grid access, which was an innovation in the then centralized and state-owned electricity sector. The system was further specified in the year 2000 within the Renewable Energy Sources Act (abbreviated to EEG in German). This new law differentiated between the FiTs with respect to the different renewable energy technologies, taking into account their specific costs as well as their cost reduction potentials.

Furthermore, the tariffs were set independent from the current electricity consumer prices which gave more investment security to the financing companies. In their original version, FiTs were paid for each kWh produced using renewable energies being fed into the grid. By setting a fixed price for the generation and distribution of renewable energy sourced electricity (RES-E) that is paid to the producer over a fixed period, these FiTs provide a stable investment option for technologies that still need time to become cost competitive, but which are needed due to other considerations such as climate change, scarcity of resources, etc.

Further noteworthy and vital aspects of the system are the fact that the producers are afforded priority access to the electricity grid and while there is a degree of obligation on the part of the conventional utilities to buy all RES-E, the electricity consumer is also obliged to pay an additional surcharge to refund the extra costs. In this way, a 'polluter-pays' system for excessive energy use is set up, which also incentivizes energy efficiency. A strong motivation for cost reduction is being provided by reducing the FIT for the different technologies by a specified percentage each year. In Germany, this base gradual decrease has been 9% for solar PV in the last few years.

This rather simple but clever legal framework has triggered the creation of the world's largest market for PV and greatly boosted R&D and industrial mass production. Furthermore, awareness of PV's potential has been raised among stock companies as well as domestic users, with the latter having financed and installed a large share of the currently-installed one million PV systems in Germany. The contribution of the integration of RES-E to increasing energy prices has been very limited during most of this period, and has even alleviated some of those increases due to merit-order effects of RES-E at the energy market. The strong increase in energy prices in Germany since the mid '90s is primarily a result of a failed market liberalization in 1998 that established oligopolistic market structure. Other factors for these price increases included rising coal, gas and uranium prices as well as increased energy taxation [3].

Development of a PV industry in Germany

In the early years of Germany's PV industry, many PV products were imported mainly from the then-leading nations of Japan and the USA. A thriving industry quickly emerged on the market in the form of Germany, ramping up its production to 3.2GW at the end of 2010. Since the PV market's shift from a supply to a demand model at the end of 2008, competition among producers and installers has been followed by steep cost reductions. Technological improvements and economies of scale had to be handed down to the private and institutional investors in order to guarantee the attractiveness of PV investments with ever-faster decreases in FiTs. Since mid-2006, the price of a typical crystalline-based PV solar rooftop system (<100kWp) has more than halved in Germany, currently (Q2 2011) coming in at less than €2,500/kWp. This decrease, coupled with lean administrative processes, bankability as well as experienced companies and installers, makes Germany one of the most competitive markets for PV in the world [4]. The strong price decrease for solar PV has obliged the German legislator to conduct unprecedented additional FiT cuts in the past two years. These measures aimed at framing the market size into a determined corridor-of-growth – still without a cap – as well as limiting investors' margins to reasonable levels and thus the surcharge for the energy consumer. A reasonable level of return on a PV investment is considered one above the market interest rate for safe options, such as that of a bank account but lower than more risky options such as stocks, etc. As a matter of political – though unwritten – consensus, a range of 4 to 7% is considered acceptable, with slightly higher rates for institutional investors. One of the strongest aspects of the EEG for many years has been its reliability for investors, making investments in RES-E both predictable and bankable. It is exactly this reliability aspect that is in danger of being threatened by fickle political decision-making.

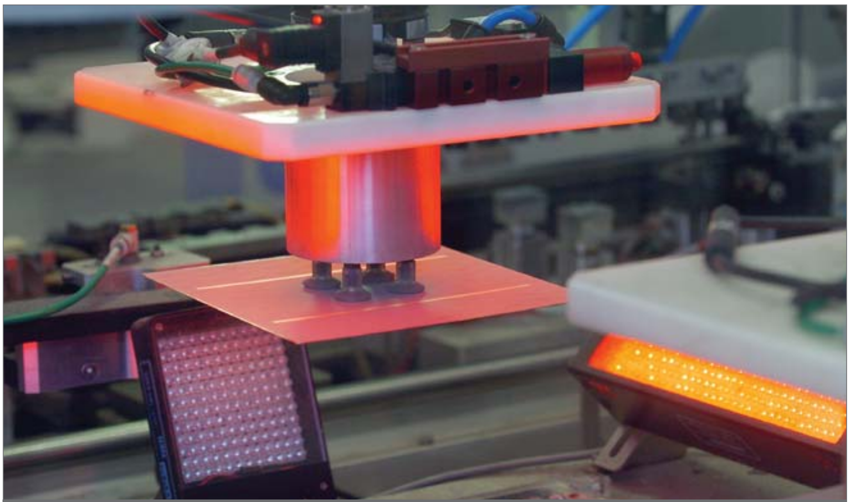

Source: BSW-Solar

Figure 2. Germany provides most of the machine equipment for PV systems production, and is also a leading producer of high-quality PV systems.

Market Watch

> "One of the strongest aspects of the EEG for many years has been its reliability for investors, making investments in RES-E both predictable and bankable."

These new insecurities are, on the one hand, the result of success from a grown-up industry and willing investors. Industry players have developed the capacity to quickly upscale production and massively reduce costs. Nowadays, professional installers and EPC companies can install MW parks within months. On the other hand, the traditional process of setting FiTs had to become more flexible and reactive due to those new production capacities threatening to undermine the intentions of the responsible politicians. Policy makers have come to understand this, and started to become more innovative in reforming the EEG with close support of the industry as of 2008.

Amendments to the EEG: 2009 to 2011

A first step for such an innovative policy was a more flexible and gradual decrease system with the 'corridor of growth' that was first introduced with the EEG amendment in 2009, but which had to be adjusted twice. Additional feed-in cuts in Germany were introduced to limit market growth. A bonus for direct consumption of electricity was newly introduced in 2009 for small systems below 30kWp and extended to systems up to 500kWp. A direct consumption bonus is a slight production bonus for PV electricity that is consumed at the site of production, diminishing the discrepancy between production and demand. This bonus makes it more attractive to directly consume electricity if the kWh rate for household electricity is above 19.49¢(€). In this way, incentives are being set to self-consume locally produced electricity and to adapt the size of the PV system to the actual size of the building as well as to integrate means of storage, especially e-mobility. Local production and consumption will avoid transportation costs and grid extension and provide incentives to construct systems according to electricity use in the future.

This 'direct consumption' approach was one way of reducing the grid load of the production of PV electricity in areas with little consumption, whilst creating incentives for approaching PV system size to local demand. An obligation for remote control applications for solar systems of more than 100kWp had been

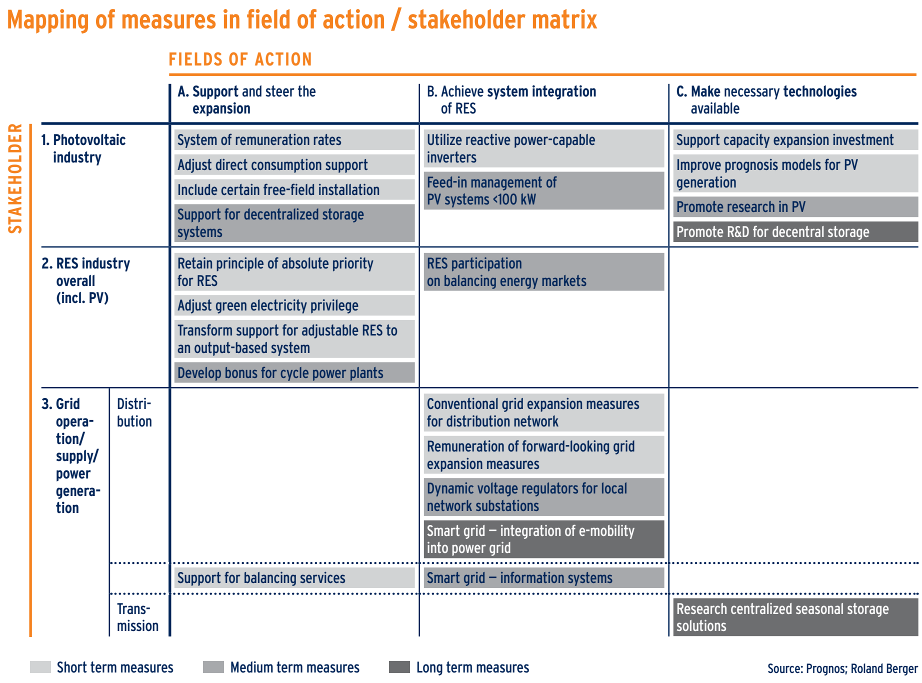

Figure 3. Mapping of measures in field of action / stakeholder matrix.

planned, but could not be realized due to inadequate technical specifications. In 2010, construction limitations for ground-mounted systems were also introduced, partly to avoid conflicts with agricultural land use and local rejection of such projects, but it also heavily limited market growth of this sector.

Some of these new approaches had been formulated with the support of the German Solar Industry Association with the aim of creating a sustainable market growth. Nevertheless, the further integration of fluctuating RES-E such as PV will have to go far beyond those first approaches and challenge Germany's electricity infrastructure, placing it and its companies in the first row of the future energy revolution.

How will the energy system have to change in the future?

In its industry Roadmap for 2020, the German Solar Industry Association identified a series of fields of action, whereby the support scheme for RES-E should be adapted in the short term to provide incentives to alleviate certain shortcomings of the existing regulations for a more even generation of PV electricity. It gives clear indications regarding which areas of the electricity system need to be restructured and where contributions to technology modifications of the PV and the RES-E industries and other stakeholders are required. The different measures have either short-, mid- or long-term perspectives; some of these have been implemented in the meantime since the November 2010 completion of the Roadmap.

A. Supporting and steering the expansion of RES-E

The objective of this first set of measures is to incentivize, through modified support schemes, a continued growth of fluctuating electrical energy production and their integration into the existing electricity grid from a market perspective. Such a modified support scheme should enhance decentralized RES-E production close to consumption, create an even regional distribution throughout Germany and establish a control infrastructure for the electricity grid through measures such as:

- Further expanding incentives for direct consumption of electricity to reduce the additional expenses for the electricity consumer and to reduce grid use, especially on the low voltage level.
- Integrating ground-mounted plants into the direct consumption incentive schemes in order to exploit bigger peak saving potentials at commercial and industry level.
- Enhancing regional distribution and production of PV electricity due to a geographically more diversified FiT scheme according to varying irradiation levels in Germany.
- Integrating a scheme to support combined power provision from multiple RES-E sources, which, as a whole, produce non-fluctuation electricity and make commercialization of such combined RES-E power provision easier, as these amounts are currently too small to be tradable.
- Furthering the development and use of decentralized electrical storage systems such as cheap but potent batteries in houses or electric mobility.
- Creating a regulatory control framework for RES-E power provision to control grid stability, e.g. by installations of compulsory power production measures and their connection to remote control tools.
- Legalizing and establish incentives for anticipatory planning and construction measures of the grid operators, who are obliged to adapt the electricity grid according to requirements deriving from EEG-electricity sources.
- Introducing incentives for the provision of storage capacity at regional level.

B. Improved technical integration of PV and RES-E into the electricity system

The expansion of PV and renewable energies leads to a system transformation, from the central power supply that has existed thus far to a decentralized supply structure. Up to now, power grids have been set up for centralized power supply. The increasing connection of fluctuating and de-centrally fed-in renewable energies leads to new technical challenges that require an adjustment of the supply system. Technical recommendations for enhancing the integration of RES-E into the electricity grid have the following aims:

- To provide grid system services through renewable energies, e.g. with inverters providing reactive power, remote control technology to reduce the power to ease peak load and develop appropriate communication technology.

- To replace local electrical transformers that change the voltage level with dynamic voltage controllers, which better cope with different voltage levels.

- To install remote control software for PV systems smaller than 100kWp, thus enabling grid operators to regulate electricity-producing systems in times of thread to the electricity system.

- To work on improvements of the European cross-border high-voltage interconnections to make use of varying RES-E sources across Europe.

- To develop more seasonal storage solutions such as pump storage, compressed air, etc.

C. Increased R&D support to develop new technologies

In order to make the quickest possible progress via approaches A and B, but also to limit the conversion costs and to remain competitive on the international market, new technologies must be made available at an early stage. These measures must focus on innovations that will be necessary in creating a 100% RES-E provision and have a rather long-term focus.

Such measures will include:

- Improved prognosis models for PV generation.

- Improved R&D in PV, decentralized and centralized storage.

The proposals made by the German Solar Industry Association have been widely acknowledged by policy makers as providing a comprehensive overview of goals, commitment of the industry and, for the first time, explicit measures detailing how to achieve those goals. Some of the proposals have been reconsidered to amend laws concerning the structure of the electricity grid and respective incentives, and go far beyond amendments of the EEG.

The new EEG for 2012 and perspectives for the future

With its July 2011 decision upon the amendment of the EEG, the German government has started to consider some of the aspects proposed in the Roadmap, though it is focusing mainly on reducing the costs of further PV plants by tight yet gradual decreases according to market size. (Acceptance of this new EEG 2012 has yet to become law by being published in the Official German Federal Law Gazette.) Nevertheless, remote control technology for newly constructed and existing PV plants will become compulsory at different stages in 2012 for eligibility for FiT payments. Direct consumption is being considered as a useful way to change the incentive structure of PV; as a result, its applicability period has been extended. Public programs to enhance R&D in the industry – such as the so-called "Innovation Alliance for PV" – were started in late 2010, while a program to develop energy storage has come to fruition in 2011. E-mobility is a big topic for Germany's government and car makers, and will give rise to a number of R&D programs in the near future. Further minor amendments of the legal basis of the energy grid are currently under discussion. Thanks to the PV-Roadmap, the technical discussions are on their way, although different interest groups require a degree of involvement in the process, leading to an extension of its duration.

The government's decision to fade out Germany's nuclear energy use by 2021, which was made in response to the Fukushima nuclear disaster, will have stimulating effects for developing a different energy infrastructure that is more appropriate to integrating RES-E. Germany's policies and innovative and committed RES-E industry has lent the country the opportunity to master these disruptive changes to the energy system. For the PV industry in Germany, as well as the entire economy, a change in the energy system holds the potential to develop entirely new technologies in one of Germany's core competencies – engineering complex systems and control technology processes. This process, although costly in the first instance, creates first-mover advantages and might well create generic knowledge for those participating companies – and possibly eventual benefits for the entire society.

References

[1] Wegweiser Solarwirtschaft – PV Roadmap 2020 (available online at http://www.solarwirtschaft.de/roadmap).

[2] National Renewable Energy Action Plans (available online at http://ec.europa.eu/energy/renewables/transparency_platform/action_plan_en.htm).

[3] BMU price report (available online at http://www.bmu.de/files/pdfs/allgemein/application/pdf/broschuere_strom_aus_ee.pdf).

[4] BSW price report (available online at http://www.solarwirtschaft.de/medienvertreter/infografiken.html?L=hmkufdbspc).

About the Author

Jan Michael Knaack has an M.A. in public policy & management, and has been working in the solar industry since 2006. In his role at the German Solar Industry Association he works as manager in charge of both research policy monitoring and the promotion of exports and international lobbying within the International Affairs Office. Prior to his work with BSW-Solar, he worked in the software business (web-based learning; business simulations) after having worked for a short period for the International Organization for Migration in Geneva, Switzerland as well as the German Development Service in West Africa.

Enquiries

Jan Michael Knaack
BSW – Bundesverband Solarwirtschaft e.V.
Quartier 207
Friedrichstraße 78
10117 Berlin
Germany

Tel: +49 (0) 3029 777 8837
Fax: +49 (0) 3029 777 8899
Email: knaack@bsw-solar.de

Revisions

In the 10th edition of *Photovoltaics International*, we featured a paper entitled "Every solar cell is an original: laser marking of silicon solar cells yields new opportunities in quality control" (pp. 16–22) authored by Peter Wawer, Uli vom Bauer, Jörg Müller & Daniel Paul Schreiter from Q-Cells SE in Germany. The publisher, after correspondence with concerned members of the industry, wishes to highlight some misleading statements in this paper. After much discussion, it has been decided that the marking of two sides of a wafer in combination with two readers without having control of the wafer orientation in the production line is sufficient to allow for reading to take place. Furthermore, compared to 2D data matrix marking, the brick marking technology allows a reduced information density that is still sufficient to offer a unique ID for every single wafer produced worldwide. In regard to claims made in relation to breakage rates and their relationship to brick marking, there is no current evidence published that brick marking increases breakage rates.

In the 12th edition of *Photovoltaics International*, we featured a paper entitled "Progression of n-type base crystalline silicon solar cells" (pp. 94–102) authored by L.J. Geerligs, N. Guillevin & I.G. Romijn of ECN Solar Energy in The Netherlands. Some data were provided in Tables 1 and 2 that were erroneous, and the authors have asked that we publish an updated version of both Tables 1 and 2 (amendments have been highlighted in both tables).

Type	Area (cm^2)	Metallization	V_{oc} (mV)	Efficiency (%)	References
bifacial BSF	239	screen printed	**641/-**	19.49/19.89	[33]/[34]
PERL, laboratory	4	evaporated front grid, rear full area evaporated	705	23.9	[2]
PERT, laboratory	4	evaporated front grid + plating, rear full area evaporated	695	21.9	[16]
Al-rear emitter, selective FSF	6" Cz	screen printed	639/641	18.5/18.5	*[45,46]/[49]
Al-rear emitter, Al_2O_3 passivated, laboratory	4	evaporated	649	19.8	**[43]

** Obtained 18.6% on a 5" FZ wafer.*
*** An efficiency of 20.0% was actually obtained with a-Si rear side passivation, but judging from the V_{oc} the potential of Al_2O_3 passivation seems to be better.*

Table 1. Results of the various n-type cell concepts (non-back contact).

Type	Area	Metallization	V_{oc}	Efficiency	References
MWT	239	screen printed	644	**19.65**	[61]
IBC	155		721	24.2	[12]

Table 2. Best results for n-type back contact cell concepts.

Photovoltaics International

Advertisers & Web Index

To advertise within Photovoltaics International, please contact the sales department: Tel +44 (0) 20 7871 0123

Advertisers & Web Index

Photovoltaics International

DON'T MISS: **PV inverter supply chain** | **Developments in p-type back-contact solar cells** | **Large-scale wafer production focus**

I would like to purchase a subscription.

Price: ☐ 1 x Issue **$59.00 USD** (includes international delivery)
☐ 4 x Issue **$199.00 USD** (includes international delivery) Please start my subscription with edition ....

Method of payment: ☐ Credit Card ☐ Bank Transfer

Name: ....
Job Title: .... Job Function: ....
Company: .... Div/Dept: ....
Street Address: ....
City: .... Post Code/Zip: ....
Country: ....
Telephone Number: .... Web URL: ....
E-mail: ....
For the purposes of our circulation audit, please indicate the last digit of your birth year (YYYY): ....

Company Activity (tick where appropriate):

☐ PV Manufacturer (inc. Thin Film & Module) ☐ Materials Supplier ☐ Equipment Supplier

If you ticked any of the above three options, please indicate the company technology type by ticking one or more of the boxes below:

☐ Si Cell ☐ Thin Film ☐ Module ☐ Concentrator ☐ Emerging ☐ Polysilicon ☐ Ingot/Wafer

☐ University ☐ Energy Utility Supplier ☐ Government Agency
☐ R&D Facility ☐ Financial Community ☐ Other (please specify ....)

In order to continually improve Photovoltaics International we require your feedback. We would be very grateful if you would answer the following questions:

(Q) Which section(s) of the publication are of interest to you? (please tick)

☐ Fab + Facilities ☐ Materials ☐ Cell Processing ☐ Thin Film
☐ PV Modules ☐ Power Generation ☐ Market Watch

(Q) What technical subjects do you wish to see in future editions?...

....

Signature:.. Date ....

Payment Details:

Fax on +44 (0) 20 7871 0101 or email info@pv-tech.org:

Type of credit card: ☐ VISA ☐ MasterCard ☐ American Express

Card Number: ....
Expiry Date: ....
3 Digit CVV Code (back of card): ....
Cardholder's name: ....

Post: Make cheques payable to **"Solar Media Ltd."**
Photovoltaics International, Trans-World House,
100 City Road, London EC1Y 2BP, UK
Online: PayPal - visit **www.pv-tech.org/shop**

To request an invoice please call on 020 7871 0148
or **email:** subscriptions@pv-tech.org

Bank Transfer Details:

Account Name:	Solar Media Ltd.
Account Number:	80686832
Sort Code:	20-39-53
Swift Code:	BARC GB 22
IBAN Number:	GB 42 BARC 203953 80 68 68 32
Bank:	Barclays Bank Plc, 10 Hart Street, Henley-on-Thames, Oxon, RG9 2AX.

All invoices are calculated in Pounds Sterling.

Any payments made in US$ must be made according to the appropriate exchange rate at the time of payment.

Helios Solar Works module factory brings 'Made in the USA' back to heart of Milwaukee

Helios Solar Works is a relatively new contributor to the 'Made in the USA' trend in photovoltaic manufacturing. The company manufactures its high-efficiency monocrystalline PV modules in the heart of a city better known for "beer and brats" than renewable energy – Milwaukee, WI. Helios's 40,000 sq ft headquarters, located inside an LEED-certified building constructed a few years ago as part of a redevelopment project in the old stockyards district, features a state-of-the-art automated production line.

Helios USA moved quickly from the close of financing in April 2010 to the manufacture of its first certified PV panel in early February 2011 – 10 months from money in to module out. The company has two product offerings so far: its 25-year warranted, fully certified 60- and 72-cell monocrystalline-silicon modules (240–255Wp and 280–305Wp, respectively), with a 96-cell, 410Wp panel coming to market in October, according to GM Brent Brucker.

The current factory capacity sits at 40MW, with plans to scale it to 80MW and then 120MW over the next 12 months, according to COO John Kivlin, a long-time Motorola hand. He believes the building could accommodate up to 200MW of production capability with some "goosing"; Helios is already actively investigating possible sites in the southeast and southwest US for a future production facility.

The first and second shifts at the plant are up and running after going through more than two months of training, Brucker said, with the hiring of the third shift planned by October. About a third of the 30-some employees are US military veterans (some of whom are disabled), a point of pride for CEO Steve Ostrenga, who also spoke highly of the quality of the workforce in Milwaukee, an area hard hit by cutbacks in the automotive, electronics, and power control industries.

The chief exec cited the company's participation in the 'Heliene Alliance' – a strategic confederation of several PV players in Canada, France, Spain, and the US – as a major reason for the company's rapid initial ramp-up. Although most of the other firms are part of the Heliene Energy family, Helios Solar Works remains independent while benefitting from the close cooperative interaction of the group.

Calling the alliance a "gentlemen's agreement," the former US Peace Corps volunteer and US Army Reserve vet turned solar entrepreneur explained that the companies have joined forces and pooled their resources to buy components and materials, ship spare parts to each other, educate their employees (Helios' first shift trained in sister facilities in Spain and Ontario, Canada), test and measure their products, bid on projects together, and research and develop next-generation technologies. The partnership represents a compelling alternative path to reducing costs through collective economies of scale.

On the manufacturing side, perhaps the most important alliance collaborator has been Spanish module equipment supplier SAP Solar, which designed and built the tools and layout for Helios's line. Kivlin gave a large part of the credit for the quick ramp to the systems provider's platform-based methodology, and believes that the next round of production expansion should take only six months.

Ostrenga added that SAP's soldering approach was a particular differentiator, with its lower spoilage rates and faster throughput than competitive solutions. He also listed another advantage of partnering with a company like the Badalona, Spain, concern and its proven turnkey production scheme: a constant upgrading of equipment, including a brand-new-to-market soldering tool that the Midwestern modco has just bought.

Image courtesy of Helios Solar Works

Another benefit of the alliance mentioned by the CEO is the deep understanding of, and nimble response to, their respective local and regional markets that each member brings to the family table. This homegrown flavor extends to how the companies seek out supply-chain vendor companies in their own specific global neck of the woods as much as possible.

On the testing side, the alliance's four modcos work in concert, Ostrenga explained, making strategic choices together on what components to modify or change in their modules. This incremental approach to recertification, done in concert with Intertek, keeps the process leaner, quicker – and cheaper.

As for Helios' own supply chain (albeit one in a constant state of evaluation), Ostrenga and Kivlin told me that the company sources its high-efficiency mono c-Si cells from a trio of reputable, internationally diverse manufacturers: US-based Suniva, Taiwanese market leader Motech, and German stalwart Bosch. The high-transmission glass comes from Saint-Gobain and AGC (plus a third, Midwest US-based outfit on board in November), CPP and Isovoltaic provide the backsheet materials, and the EVA rolls out from STR and Flexcon.

Module efficiencies are just below 16%, according to Kivlin, reaching >15.7% on the 72-cell model. He expects that number to get north of 16 by October, mainly through a module design tweak that will remove about 25mm of wasted space around the frame edge on the sunny side of the panel.

Guaranteeing on-time delivery of the contracted module wattage, Helios has already shipped megawatts to a growing number of high-efficiency PV-hungry projects. These include 1MW as part of a 5MW UK system developed by German firm Sunstroom (the other 4MW of panels came from Heliene Spain) as well as thousands of modules to US military bases such as Forts Drum and Polk and 2MW to an unnamed US Navy installation in San Diego (in case you hadn't guessed, the company's products qualify under all 'Buy America' provisions).

While production output may be capacity constrained for the moment – Kivlin said they're sold out – these new breed of Milwaukee's finest are anything but enthusiasm and national pride constrained. "We are tired of seeing manufacturing go overseas," explained Ostrenga. "We want to make a product that will change the world, and do it in the US."

This column is a revised/updated version of a blog that originally appeared on PV-Tech.org.

Tom Cheyney is North American editor for the *Photovoltaics International* journal and writes blogs and news for PV-tech.org.